Combustion Characteristics of Biomass Briquettes

by Joel Chaney, MSci Physics with French

Thesis submitted to The University of Nottingham
for the degree of Doctor of Philosophy

May 2010

"Though the fig tree should not blossom nor fruit be on the vines,
the produce of the olive fail and the fields yield no food,
the flock be cut off from the fold and there be no herd in the stalls,
yet I will rejoice in the LORD; I will take joy in the God of my salvation
God, the Lord, is my strength"
(Habakkuk 3:17-19a, English Standard Version of the Bible)

"The steadfast love of the LORD never ceases;
his mercies never come to an end;
they are new every morning;
great is your faithfulness"
(Lamentations 3:22-23, English Standard Version of the Bible)

To my Dad, Mum and Sister

Acknowledgements

Abstract

Nearly half the worlds population is dependent on wood as their primary energy source. Therefore with deforestation becoming increasingly prevalent in many regions of the developing world, there is an urgent need to improve combustion efficiency of stoves or to find alternative fuels. Densification of loose biomass residues into briquettes is a means of upgrading the feedstock material. Briquettes are easier to store, more convenient to use and burn at a more steady and controlled rate than loose biomass. This investigation focuses on understanding some of their combustion characteristics and the relationship to the briquette design and manufacture process.

The social context of the work is presented through an informal case study considering the potential of briquetting in Ghana. The initial experimental work focuses on developing a process to manufacture newspaper briquettes of consistent quality at low-pressures using a wet technique, and a method to burn them in a controlled way is suggested. These techniques were used to carry out a study on rectangular slab-shaped briquettes, looking at the effect of process variables (density, moisture content and size) on briquette burn-rate. An analytical expression for the normalised burn-rate (NBR) of a briquette in free-air, in terms of these of these variables, was found by numerical fitting. The effect of shape on combustion was also experimentally investigated using cylindrical briquettes with a central hole (holey briquettes) burning in free-air and an analytical expression was derived for their burn rate. The NBR behaviour of sawdust briquettes, rapeseed oil residue briquettes as well as slabs of pine wood was then studied. Rapeseed oil residue has a very different calorific value from that of newspaper, and a method was suggested for predicting the difference in rate as a function of difference in calorific value.

In the second phase of the work, a numerical model of pyrolysis was developed. The model assumed that heat transfer through the fuel limited the rate of pyrolysis. The thermal parameters (thermal conductivity, heat capacity and thermal diffusivity) were estimated using a heat probe method, and the kinetic parameters found by numerical optimization. The model was shown to predict, for newspaper briquettes, the experimentally observed size dependent behaviour of the normalised burn rate, and the trend observed for the effect of changes in density. The model was applied to predict the effect of changes in a briquettes thermal parameters on burn rate, and an analytical expression found by numerical fitting. This provides a means of estimating relative changes in burn rate due to changes in fuel properties, and forms the basis for a pyrolysis sub-model for use in stove optimisation. Such a model has the advantage of being able to vary key, easily quantifiable and easily controlled solid biomass briquette properties relative to the behaviour and properties of a well understood fuel such as wood. In the final part of the study, some of the limitations of the numerical model are explored by completing a sensitivity study investigating the relative effect of some of the key assumptions made.

Contents

List of Symbols

a	Empirical constant
A	Area [mm^2 and m^2]
Ash	The ash fraction
A/V	Briquette area-to-volume ratio [mm^{-1}]
ρ	relaxed density of the briquette [kgm^{-3}]
b	Empirical constant
c	Specific heat capacity [$Jm^{-3}K^{-1}$]
C	Carbon
cf	Friction coefficient
CO	Carbon monoxide
CO_2	Carbon dioxide
Cal	Calorific value [$MJkg^{-1}$]
C_1	Empirical constant
C_2	Empirical constant
C_3	Empirical constant
C_4	Empirical constant
C_5	Empirical constant
C_6	Empirical constant
C_7	Empirical constant
D_a	Effective diffusion coefficient of oxygen through the ash layer [m^2s^{-1}]
e	Empirical constant
E	Apparent activation energy in the kinetics equation [$Jmol^{-1}$]
ef_w	Effective moisture content [%]
Ei	Exponential integral
f	Empirical constant
F	Empirical constant
g	Empirical constant
GCV	Gross calorific value [$MJkg^{-1}$]
h	Convective heat transfer coefficient [$Wm^{-2}K$]

H	Height [mm]
H_{solid}	Latent enthalphy of devolatisation [$MJkg^{-1}$]
I	Intensity of radiation [Wm^{-2}]
ID	Internal diameter of a holey briquette [mm]
k_0	Kinetic rate constant (pre-expoential factor in the kinetics equation) [s^{-1}]
k_r	Reaction rate
L	Length [mm]
L_c	Characteristic length
$\dot{m}$	Rate of combustion [kgs^{-1}]
m	Mass [kg and g]
M	Briquette mass [g]
$\%M$	Percentage moisture content (dry basis) [%]
M_v	Mass flux of volatile gases [$gm^{-2}s^{-1}$]
M_∞	Free-stream mass flux [$gm^{-2}s^{-1}$]
n	Order of reaction
NBR	Normalised burn rate (normalisation is with respect to the samples initial mass) [s^{-1}]
NCV	Net calorific value [$MJkg^{-1}$]
Nu	Nusselt number
Nu_m	Modified Nusselt number (by blowing)
O_2	Oxygen
P	Compressive pressure [Mpa]
q	Input energy per unit length, per unit time [Wm^{-1}]
Q	Heat transferred [Js^{-1}]
r	Distance
S	Specific gravity
R	Ideal gas constant
Re	Reynolds number
S	empirical constant
t	Time [s]
T	Temperature [K]
T_m	Peak response temperature [K]
u_∞	Free-stream flow velocity
V	Volume [mm^3 and m^3]
VF	View-factor
w	Percentage moisture content [%]
W	Width [mm]
ϵ_{ash}	Porosity in the ash layer

α	Thermal diffusivity $[m^2 s^{-1}]$
β	Empirical constant
Γ	Empirical constant
δR	Change in burn rate $[s^{-1}]$
δT	Change in temperature $[K]$
δx	Thickness of control volume used in the solution of the numerical model $[m]$
ϵ	Flame emissivity
ζ	Empirical constant
λ	Thermal conductivity $[W K^{-1} m^{-1}]$
μ	Empirical constant
ν	Percentage concentration of hydrogen $[\%]$
Ξ	Exponential frequency factor
σ	Empirical constant
ς	Geometrical factor
τ_0	Shear boundary stress $[N m^{-2}]$
Υ	Blowing coefficient
χ	A model parameter
Ψ	Fraction of char
ω	Solid angle

Subscripts

n	Vector size
a	to the atmosphere
air	Air
ash	The ash layer
b	of the Biocoalbriquette
$convec$	Convective
f	Flame
$final$	Final
g	Gas phase
i	Element index
in	into the solid
j	Element index
NP	Newspaper
s	Surface of the briquette

rad	Radiation
RSO	Rapeseed oil
$solid$	Solid
uni	Uniform
w	wall
θ	to the atmosphere

Chapter 1

Introduction and Social Context

People have a basic need for energy to cook. Currently, in developing countries, this tends to be met by directly burning wood derived products in fires and stoves; in Sub-Saharan Africa, biomass provides about 75% of all people's energy needs [1]. It is important that the energy source used is provided in a sustainable way and is burnt efficiently, and these are key themes that form the basis for this thesis. In order to identify an appropriate focus for the work, a field study was completed in Ghana at the start of the project. This served as a context for the research that was subsequently carried out. What follows in this introductory section is a case study on Ghana, providing the social background for the work in the ensuing chapters.

1.1   Introduction to Energy Use in Ghana

Ghana is centrally placed amongst the West-African countries that lie along the shores of the Gulf of Guinea. It is bounded on the West by Cote d'Ivoire, on the north by Burkina Faso, and on the east by the Republic of Togo (see Figure 1.1). The 2000 Population and Housing Census of Ghana [2] estimated the total population to be approximately 18.5 million, comprising an almost equal number of men and women. The population can be divided into rural dwellers, who make up 67% of the total, and urban dwellers, representing the remaining 33% [3]. Ghana has a hydroelectric dam, know as the Akosombo Dam, located in the coastal plain at Kpong, approximately 80km from the capital Accra. It was made by flooding the Volta river basin and is now one of the largest man-made lakes in the world. In 2004 it was recorded to have supplied almost 90% of the country's electricity [4]. However, the electricity supplied by the Dam serves primarily the

Figure 1.1: A map showing the location of Ghana amongst the West-African countries, reproduced from [7].

urban areas where only a third of the population resides, while rural dwellers live with limited or no access to electricity [5]. Furthermore, even in the towns the electricity supply is often intermittent and unreliable [6].

Wood derived fuel (woodfuel), that is firewood and charcoal, is the dominant source of energy used for cooking amongst Ghana's population [5]; indeed it is the cheapest [6]. This leads to high consumption and dependency on these two wood-based fuels. Figure 1.2 shows a typical open three-stone fire used for cooking, and Figure 1.3 shows two common charcoal stoves. The use of woodfuel is not only limited to rural households, but is also predominant in the industrial and commercial sectors of the economy. The pressure exerted on Ghanaian forests is significant [3], and with a growing demand, this will, if energy use patterns are not altered and alternatives are not introduced, hamper economic growth [3].

There have been several initiatives in Ghana to encourage improved efficiency in household cooking, by using more efficient improved stoves, and switching to other fuels such as LPG. Improved stoves are carefully designed to reduce fuel consumption, primarily by improving heat transfer to the cooking pot. One success story is the introduction of the Gypa stove (see Figure 1.3), which is based on the

Figure 1.2: A Typical three-stone cooking fire [6].

Figure 1.3: Charcoal is commonly used as a cooking fuel especially in the urban areas. On the left we have the traditional charcoal stove, known as the coalpot and on the right a popular improved charcoal stove, the Gypa stove. The Gypa stove is more thermally efficient than the coalpot, and ash is collected in a compartment below the charcoal, making it cleaner to use [6].

Kenyan Jiko, a widely used improved charcoal stove from Kenya [6]. The Gypa was introduced by the Shell Foundation who trained several entrepreneurs in the manufacturing process. One of these trainees has now decentralised his business and is expanding very successfully across different regions of Ghana, especially in rural areas [6]. This is an example of how improved energy technology can not only reduce the amount of fuel needed, but also create small scale businesses generating local employment. However, with depleting wood reserves, a reliance on woodfuel alone will not address the energy challenges faced by the country. This situation is probably typical of many developing countries, and with the economic and environmental consequences that it brings, means additional fuel sources need to be considered.

This thesis considers the use of biomass[1] residues, a potential energy feedstock that is not currently being capitalised in Ghana. This work considers upgrading these residues by densifying them to form briquettes. Potentially, they might provide an appropriate alternative energy source that would displace direct and indirect (charcoal) wood consumption, and so reduce the dependency of the population on the forests for fuel.

However, for briquettes to be feasible on a practical level in a developing country context, there need to be sufficient, accessible and suitable residues in the right locations. Before considering the more technical aspects, this case study of Ghana gives an insight into woodfuel use, the quantities involved, and whether the amount of residues, with other competing uses, could make way for briquetting as a feasible alternative, something which is not currently considered in the recommendations of the Ghana Energy Commission [8]. This chapter provides an overview, rather than a detailed study, of the feasibility of briquetting in order to put the latter technical work of the thesis in its social context.

1.2   Woodfuel consumption in Ghana

In order to understand the feasibility of briquettes as an alternative fuel to wood in different parts of the economy, it is important firstly to appreciate the current demands for wood and who the consumers are. Secondly, the quantity, availability and location of residues needs to be taken into account, in order to determine whether there are sufficient biomass residues available to provide enough energy

---

[1]The term biomass is used in this thesis to describe the full spectrum of biomass materials that are produced from agriculture, forestry, everyday cooking, etc. For example cotton or millet stalks, groundnut shells, maize cobs, sawdust, rice husks, cassava peelings and stems.

to reduce significantly fuelwood demand where it is needed. Thirdly, social factors affecting the uptake of the fuel need to be taken into account, for example cultural and historical reasons for cooking in a certain way. In summary, it is necessary to identify where briquetting is practically, economically and socially viable, and thus identify to whom it would be most beneficial and marketable as an alternative energy source. In this study an overview is given of the first two steps in this process: the practical and economic viability.

1.2.1   Fuel use in Ghana

In Ghana, woodfuels account for more than 60% of the total energy consumed. Figure 1.4 illustrates how the share of woodfuel compares with the consumption by end users of oil products and electricity. Electricity, in contrast, supplies the smallest proportion of Ghana's energy requirements. To meet the demand for wood, a total quantity of approximately 18Mt is consumed per annum (with an uncertainty of 20% [8, 9]). Almost half of this wood is converted into charcoal in traditional earth kilns at an efficiency of only about 12.5%, that is 8kg of firewood yielding around 1kg of charcoal [3]. This is an inefficient use of timber as fuel. To understand the significance of the consumption of this annual quantity of wood, it needs to be understood in the context of what effect it has on the Ghanaian people, their environment and the economy. This is addressed in sections of this case study which follow.
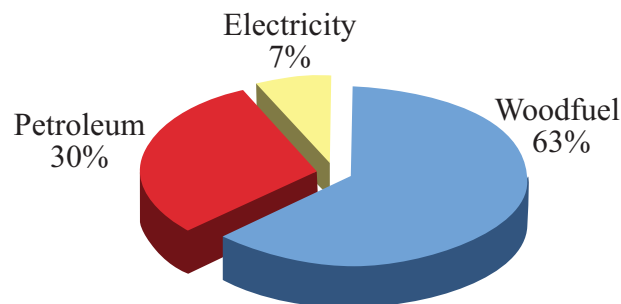
Figure 1.4: Composition of fuel use in final energy consumption for Ghana 2000 [8]

Figure 1.5 shows how the use of woodfuel is divided among different sectors of the economy. It clearly shows that households are the largest end users. Table 1.1 provides a more detailed breakdown of the total fuelwood use in residential, industrial and commercial sectors. Figures 1.6 and 1.7 present this in a graphical form, and a discussion of this data ensues in the sections that follow.

Demand Sectors	Consumers	Firewood usage (t/a)	Charcoal usage (t/a)	Equivalent fuelwood usage (t/a)	Overall woodfuel consumption (t/a)
Residential					
Urban	6,458,000	652,000	651,600	5,213,000	5,865,000
Rural	11,400,000	5,546,000	241,400	1,931,000	7,477,000
Industrial					
Fish smoking	71,000	767,000			767,000
Gari making	70,000	420,000			420,000
Palm oil	59,000	71,000			71,000
Bakeries	34,000	195,000			195,000
Potters	16,800	18,000			18,000
Others	53,690	268,000			268,000
Commercial					
Chop bars	12,916		93,800	750,000	750,000
Street sellers	64,580		106,600	853,000	853,000
Grills	6,458	21,300	170,000	170,000	191,300
Public		700,000			700,000
Total		**8,637,000**	**1,263,400**	**8,917,000**	**17,575,300**

Table 1.1: Woodfuel consumption in Ghana in tonnes/annum (t/a) for different sectors [9]
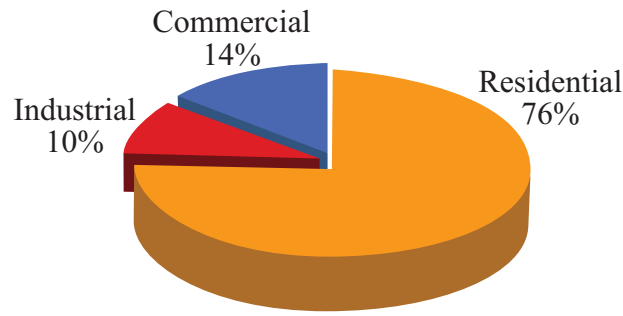
Figure 1.5: The share of fuelwood use in different sectors of the Ghanaian economy [9]
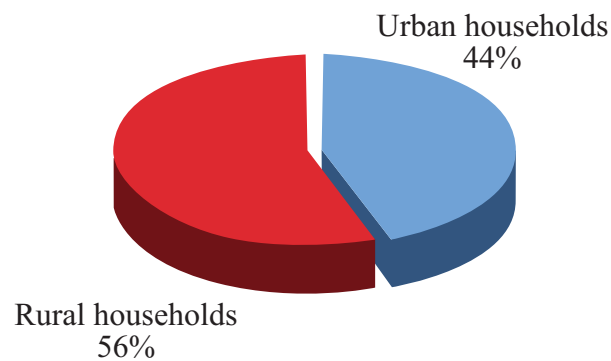
Figure 1.6: The share of woodfuel use in the household sector between rural urban areas [9]

The household energy sector

Figure 1.6 shows that there is an almost even split between woodfuel use in rural areas compared with urban areas. Urban households constitute 33% of the population and yet use 44% of the woodfuel in the household sector. This shows that although urban households might be expected to use cleaner forms of energy, such as LPG, kerosene or electric stoves, in fact wood is still heavily relied upon [10]; only about 6% have access to LPG and 1.1% have an electric cooking stove [2]. It is interesting to note that the form of woodfuel that predominates in households is closely linked to the users' location. Most households in urban areas cook predominately with charcoal (a form of woodfuel), which is purchased, whereas rural dwellers tend to use primarily firewood, harvested by hand. The nation's dependence on woodfuel means that any shortages and future restrictions on tree-felling, will have an impact not only on the rural dwellers, but also on the cost and availability of fuel for the whole household sector. Alternative fuels are thus of interest to both the urban and rural population.

It is worth noting that although there are significant residue streams from agriculture, the current use of crop residues as a fuel by households is low in almost all regions, with less than 1.7% using residues as a fuel for cooking. However, where wood is more scarce the use of crop residues increases, for example in the Upper Eastern region where woodland is very sparse, about 18% of people were recorded as using crop residues as a primary cooking fuel in the year 2000 [2]. This suggests that firewood is the fuel of preference when it is available, and informal discussions with villagers in the Kumasi region further confirm this [6]. Consequently, with crop-residues only currently being used where there are severe wood shortages, if their use is to be encouraged in other parts of the country, it will be necessary to find a means of upgrading their performance in cooking to at least as good as the woodfuels they are trying to replace.

Sector	Year 2000	Year 2003
Residential	90.4	90.3
Commercial and Services	77.4	78.9
Industrial	66	61

Table 1.2: Percentage contribution of woodfuel to total energy consumption by selected sector [10].

Industrial and commercial sectors

Figure 1.7 clearly shows that fish smoking uses the largest share of woodfuel in the industrial sector, followed by gari making (gari is roasted ground cassava) and then bakeries (Figure 1.8 shows a typical bread oven). The combination of other industries[2] also make a significant contribution to woodfuel use, for example brick making (Figure 1.9 shows wood being used to fire bricks). It is important to note that industry is region-specific and varies enormously across Ghana depending on resources and conditions. For example, palm oil processing occurs mainly in the Ashanti region of Ghana, and fish smoking mainly in the Volta region where the lakes are found.

Figure 1.10 shows the division of woodfuel use in the commercial sector. The statistics presented here demonstrate that, even within the commercial and industrial sectors, woodfuel still provides the bulk of Ghana's energy needs, as in fact biomass does in most developing countries [11]. Consequently, there are

---

[2]The 'other' section in the industrial section will include many, mainly informal, enterprises including brewing of local drinks, tobacco curing, traditional soap making and brick making.
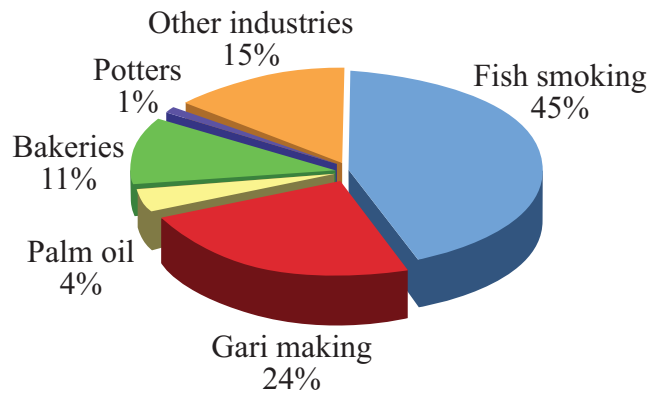
Figure 1.7: The share of woodfuels in the industrial sector of the Ghanaian economy [9]

Figure 1.8: A traditional baker's oven. Wood is purchased and used to heat the oven [6]

.

significant opportunities for briquettes as an alternative fuel in these sectors, a suggestion which was strengthened in discussions with a baker and a brick maker who suggested that they would consider using a well performing alternative fuel, provided it were financially competitive [6].

Currently, fuelwood is supplied to commercial businesses and industries primarily from the natural forests and the savannah woodlands; firewood collection and charcoal production is a source of income for the rural population. Indeed, 90% of woodfuel in the industrial and commercial sectors is obtained this way [8]. The other 10% is obtained from logging and sawmill waste. It is estimated that 65% of the people involved in such fuelwood businesses are women [8]. Commercialisation of any briquetting project to supply these sectors would certainly have to consider in detail and work with this fuel supply chain.

Figure 1.9: Traditional brick maker's fire their bricks using heat from burning firewood. The firewood is normally purchased from local suppliers

1.3   An Overview of Deforestation and its Effects on Energy Supply

In 1992 it was estimated that about 1.5 million hectares of forest remained in Ghana, with an annual rate of deforestation of about 22,000 hectares, or 1.5% (cited in [5, 12]). Timber logging for fuelwood and timber export is an important factor contributing to deforestation [13]. Firewood collection and charcoal production are major income earners for members of rural communities, and even if regulations and restrictions on tree-felling are in place, they are often not adhered to, and those who cut the trees and shrubs do not replace them [14]. This unsustainable forest management is commonplace [12] and has detrimental effects both on biodiversity and the environment as well as the producers themselves, who have to travel increasingly longer distances in search of their desired species of wood [8]. Furthermore, outside the controlled forest reserves, illegal logging has been increasing due to a lack of policing of timber operations [15]. Another chief contributor to deforestation is agriculture, which dominates land use in Ghana. An increasing population and a growing demand for cash crops (cocoa, coffee, palm-oil, tobacco), has led to increasing land requirements, which records suggest
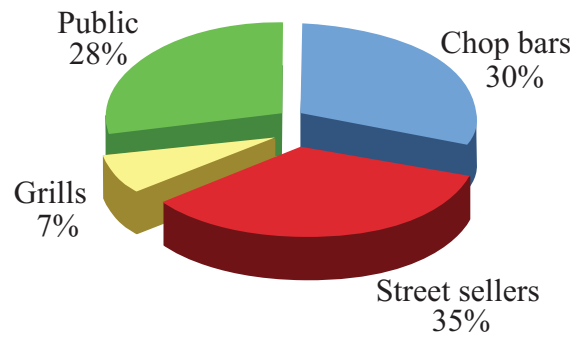
Figure 1.10: The share of woodfuels in the commercial sector of the Ghanaian economy [9]

are increasing every two years by about 9% . There are other pressures on Ghana's forests including annual bushfires in the dry season, open cast surface mining (e.g. for gold and diamonds, because the mineral belts are located in forestlands), and infrastructure development.

Ghana is heavily dependent on forest wood reserves for its energy supply, just as other countries are dependent on coal and gas. As already stated, woodfuel represents the largest source of energy consumed in Ghana [8]. For centuries, harvesting wood naturally from forests had been sustainable. However, with the increases in population, growing commercial woodfuel demands, and increased pressure on the forests for other commercial activities, resource utilisation has been reported to be beyond a critical point where the current levels are now exceeding the natural regeneration capacity of the forests [8]. The high dependancy of Ghana's population on the forests therefore means that deforestation has consequences, which significantly affect people's livelihoods, especially those who depend on woodfuel directly. For example, in the North of Ghana where land is becoming increasingly arid, and trees and shrubs increasingly sparse [14], limited forest resources are putting pressure on rural dwellers who largely depend on firewood as their principal energy source. They rely on harvesting firewood by hand for cooking, and depleting resources means they have to walk a greater distance to collect the day's supplies. In some regions women might spend between four to six hours travelling over seven to ten kilometres to collect only enough firewood for one day's cooking and heating needs for a household of four to five persons [10]. Although collecting fuelwood does not cost them any money, when long distances and time are involved in its collection, it denies the women the opportunity to be involved in any paid work, which would raise the family's income. This would provide money for alternative foodstuffs to enhance nutrition, for health care and for educating their children; it is reported that school attendance

wanes because of the burden of collecting fuelwood and the respiratory illnesses caused by cooking with it [10].

Alternative energy resources have the potential to reduce Ghana's dependence on woodfuel for energy, improve people's livelihoods and tackle one significant cause of deforestation. There are two issues that need to be addressed here: firstly to develop sustainable alternatives for the long term future of the country so that it is not so reliant on a single, currently depleting, fuel resource; and, secondly, to meet the current need of the rural poor who are forced to walk large distances to collect fuelwood. It is this group that does not buy its fuel and therefore is unlikely to be able to afford more high-tech and expensive future energy options. It is likely that a combination of technologies, rather than one solution, will be essential. One currently underutilised potential resource is waste residues from crops. These are often available both among the rural poor, who are commonly subsistence farmers, and from certain factories (such as the shells from cocoa production). An overview of the practical feasibility of using crop residues is presented in section 1.4 . Firstly though, in order to give an indication of future supply requirements, it is important to understand how the demand for wood is likely to increase with economic growth in the future. This will inform whether upgraded waste residues could indeed be considered a practical alternative.

1.3.1   Future projections of woodfuel demand

The Energy Commission of Ghana has made projections of the future demand for firewood and charcoal for different scenarios of economic growth. They are based on the 2000 National Population Census [2] and woodfuel data collected by the Energy Commission. If economic growth continues at the current rate, the Energy Commission predict that by 2020 about 30 million tonnes of wood will be required per annum. For a high economic growth scenario, it is anticipated that between 50-65 million tonnes of wood will be needed [8]. To meet these supply requirements by wood alone, the national wood stock would need to expand from its current 813 million tonnes to 1 billion tonnes for low economic growth, or 2 billion tonnes for high economic growth. Despite the current trend in deforestation, the Energy Commission suggest that it is possible to meet the requirements for low economic growth through plantations [8]. However, they believe that even this will be a struggle due to competition for land from other economic activities. High economic growth scenarios will put immense pressure on fuelwood supply, consequently leading to higher fuelwood prices and making fuelwood collection even harder for rural dwellers in certain areas. The Energy Commission believes

that importing fuelwoods is not a sustainable option, and therefore, if no action is taken, serious deforestation could result [8].

The Energy Commission suggests some strategies for meeting this requirement [8]:

- Expanding current wood plantations.

- Promoting the development of more sustainable forest management.

- Fuel substitution strategies, for example encouraging the industrial and commercial sectors to switch to LPG and using crop residues.

- Promotion of improved stoves designed to reduce firewood and charcoal consumption, both in informal industry and commercial sectors as well as for residential households; such stoves can be up to 10% more efficient.

- Improving charcoal production methods; overall, burning charcoal consumes significantly more wood than burning firewood because of the inefficiency associated with the charcoal production cycle. A simple calculation shows that only a 2% increase in yield would save around 1.2Mt of wood per annum.

The government has stated that it will support the introduction of technologies to improve efficiency in the consumption of woodfuels, as well as the introduction of substitute fuels [8]. The Energy Commission suggest the use of crop residues in larger scale power plants. However, upgrading residues by briquetting to use as a direct firewood replacement has not been considered. Briquetting, which can be achieved with very minimal equipment, is a technology that may be of great benefit to the rural poor, many of whom are unlikely to be able to afford an improved cookstove. It could also be done on a larger scale, for example using biomass waste from an industrial processing plant to produce briquettes for industries and businesses that currently rely on firewood, for example brick makers and bakers.

1.4   Biomass Crop Residues in Ghana

This study is focused on upgrading waste-crop residues. In assessing their potential, it is helpful to consider the scale of the feedstock from agriculture and logging that could supply briquette manufacture. Agriculture is very important in the Ghanaian economy. Indeed, in 2002, it was employing over 65% of the population and contributing about 42% to Ghana's GDP [5]. Crops generate large quantities of post-harvest residues. Table 1.3 provides some estimates of the potential of using residues from some of the stable foodcrops as a woodfuel

replacement. It is clear that Ghana is naturally endowed with a large energy potential in its biomass waste. For example, plantain residues could potentially reduce the pressure on woodfuel by 10%. Although it is clear from the table that there are insufficient residues available to completely replace woodfuel, it could potentially displace a maximum of one third of current woodfuel use, which would significantly reduce the current pressure on supply. For the rural poor it could be especially beneficial, because they are often the people with the most direct access to many of the residues.

Agriculture in Ghana varies enormously across the country and is distributed according to the local climatic conditions. Thus different residues will be most prominent in different regions. Table 1.4 gives a summary of the regions where the major crops of Ghana are grown, and of the residues left after harvesting [6]. It must be noted that many of the residues have competing uses, for example a proportion are used in soil reconditioning to sustain the agricultural cycle; others might be used for animal fodder. This is further discussed in Section 1.4.2.

In a report on energy supply to the economy, the Ghana Energy Commission discusses some of the limitations of the current available estimates of bioenergy resources: there is limited availability of data, and difficulties in assessing data reliability, because of lack of clarification of the data acquisition methods [8]. The crop-residue data given in this work must, therefore, be treated with caution, and considered only to provide a rough estimate.

1.4.1 Logging and wood processing residues

In addition to a large agricultural economy, Ghana also has a significant timber industry located in the Ashanti region, which annually produces considerable quantities of logging and wood-processing residues. In 2004 it was reported that Ghana earned £170 million from the export of 455,000m^3 of wood products [24]. Both logging and the industrial waste from wood processing, produce huge quantities of residues. The wood extracted from the forest in logging constitutes about 50% of the total volume of the tree. The other 50% is made up of the stump, off-cuts, and branch wood. This is considered waste and often left in the forest after logging [5], which of course, has some benefit for the regeneration of the forest. The logged wood is processed, for example into lumber, veneer and plywood. This processing produces a large amount of waste. For example, in 1993, out of 806,000m^3 of log equivalent processed, 518,000m^3 went to waste. This is equivalent to approximately 0.4 Mt, about 2.2% of the current woodfuel use of 18Mt [8]. The waste can be roughly classified into two groups: solid and

Crop	Crops [t][a]	Residue	Ratio r:c[b]	Residues [t]	LHV [$MJkg^{-1}$][c]	Wood equiv [t][d]	p.c.u.[e]	Refs
Rice	150,000	Straw and husks	1.75	262,500	16.14	2.49E+05	1.4	[8, 16]
Maize	1,189,000	Cobs and husks	1.5	1,783,500	16.03	1.68E+06	9.3	[16, 17]
Groundnut	520,000	Shell and haulms	2.5	1,300,000	13.79	1.05E+06	5.9	[6, 17]
Sorghum	315,000	Stalk	1	315,000	14.27	2.64E+06	1.5	[16, 18]
Cowpea	167,000	Foliage	1	167,000	16.00[f]	1.57E+05	0.9	[16]
Millet	165,000	Straw	2	330,000	16.77	3.26E+05	1.8	[16, 19]
Oil palm	429,000	Shell	0.45	193,050	13.87	2.03E+05	1.1	[6, 17]
Cacao	20,000	Coco hull	0.12	2,400	17.90	2.54E+03	0.01	[6][g]
Plantain	1,932,471	Skin and leaves	0.9	1,739,224	18.89	1.93E+06	10.7	[20] (cited in [3]) [21]

Table 1.3: A summary of national estimates of crop production. It includes estimates of the potential of each particular crop residue to meet the current woodfuel demand, assuming all of the residue was available and accessible for burning.

[a] Crop Production. The estimates are for the year 2006, except for the Plantain and Oil palm residues which are for 2001.

[b] Ratio of residue:crop. These are broad estimates based on [8], [6], [22] and [23], (the 1:1 estimate for cowpea is probably an underestimate).

[c] LHV stands for Lower Heating Value (Lower Calorific Value), units $MJkg^{-1}$.

[d] Wood fuel equivalent. The woodfuel equivalent was estimated from $LHV_{residues} * Mass_{residues}/LHV_{wood}$ where LHV_{wood} was taken as 17 $MJkg^{-1}$, the average calorific value found by a study on random samples of commercial firewood in Ghana (cited in [8]).

[e] p.c.u.=percentage of current use. The percentage of the latest approximation of woodfuel consumption in the literature of 18Mt/annum (made in 2001) [8] that each residue could potentially replace.

[f] The lower heating value of cowpea waste could not be found and was estimated, this is satisfactory because there are large uncertainties in the estimates for crop quantities, and the purpose of this calculation is a rough approximation of their energy potential. Furthermore, it is in fact unlikely that cowpea residues would be available as an alternative fuel because of its nutritional benefit to the soil and use as animal fodder (see [23] for details).

[g] The LHV was estimated from the higher heating value given in [21] using the method cited in [17].

fine waste [25]. Solid waste includes bark, edgings and off cuts, whereas fine waste includes sawdust and shavings. To give an idea of the relative percentages, in 1994, sawdust represented about 27% of all the wood-waste generated, whereas 67% was accounted for by off-cuts [5]. The large solid waste has some economic value and is sold as a domestic or industrial fuel in the form of firewood or charcoal, as a construction material, and for the manufacture of products such as flooring, tool handles and wooden pallets [5]. On the other hand, the fine waste, predominantly sawdust and wood shavings, are usually considered to be of little economic value and normally pose disposal problems at the sawmills [5]. They are either burned on site or transported to disposal sites; burning causes a great deal of pollution and is a nuisance to the general public. In this situation, briquettes could potentially offer a means of waste management, while providing a new fuel business avenue for the local economy.

1.4.2   Some considerations on the use of waste residues as fuel

Even if there are sufficient residues for briquetting to be considered feasible, there are other factors that must be considered, and problems that need to be overcome before the widespread adoption of these wastes as a fuel substitute becomes possible [26]. In this section an overview and discussion of some of the important issues is given.

Residues vary widely in their form and characteristics, which determines how well they can be used as fuel. In their unprocessed form, woody residues make the best fuel for cooking as they tend to burn well. Other crop residues are considered to make poorer fuels [6, 27]. For example, cereal straw and low density stalks are considered to burn too rapidly, with fluctuating power output, in their unprocessed form. Furthermore, their high bulk volume makes them difficult and uneconomical to transport and store. For these reasons, although they might be produced in large quantities, in their unprocessed form they are far from being the fuel of preference, both on a village level and in artisan cottage industries. In order for these residues to become a more attractive alternative fuel, either the residues themselves have to be upgraded to improve their burning performance (the technology of briquetting is one effective way of doing this), or better methods/technologies for cooking with the waste residues in their loose form need to be introduced.

Crops	Region	Residue	Notes on availability of residues
Maize	all regions, but over 100,000 Hectares in Central,Eastern, Ashanti, and Brong Ahafo	cob,husk, stalk	gathered during harvest, stalks left on field as fertiliser, waste husks generally burnt.
Rice	all regions, but over 15,000 hectares in Western, Volta, Upper East and 45,000H in Northern	straw,husk, bran	available at rice mills
Millet	Northern,Upper West and Upper East only	straw, bran	
Sorghum	Northern,Upper West and Upper East	straw,bran	stalks used as barriers to prevent errosion of soil
Cassava	all regions except Upper East and Upper West	peal	not available in bulk in one place
Yam	all regions excep Greater Accra and Upper East	peal	not available in bulk in one place
Plantain	all regions except Greater Accra, Upper West and Upper East	peal	not available in bulk in one place
Cocoyam	all regions except Greater Accra, Upper West, Upper East and Northern region	peal	not available in bulk in one place
Groundnut	Ashanti, Northern, Upper West and Upper East	shell,stalk, leaves	
Cowpea	Northern, Upper West and Upper East		
Cacao		hull,fibre	In processing factories in Accra large quantities are found.
Palm oil		nuts fibre, shell, fruit bunches	In the Ashanti region palm shell are bought by large-scale palm-oil producers as fuel to produce heat for their processing. They are therefore unavailable for briquetting. However, palm fibers are removed from the palm nut to make palm oil and are available in the villages.
Soya bean	Northern, Upper West and Upper East	stem	
Cashew nut		shell	processing plants soon to be starting in Greater Accra

Table 1.4: A summary of the major crops in Ghana and the residues that are generated from them during harvesting and processing. Source of data: [6, 16]

The worldwide quantities of agricultural residues are vast, but it is the location of waste generation that will largely determine their potential to be used as a fuel substitute. Most agricultural residues have a low bulk density and even transporting them a short distance can make their use financially unattractive [26]. This is especially true if the residues are scattered over a number of farms, and so would have to be collected in order to achieve sufficient quantities for briquette production to be worthwhile and competitive in the local woodfuel market. Furthermore, residue availability is often seasonal, and so a single source might not be reliable for the whole year. The most reliable potential sources of residues for supplying the urban population might be large food processing factories, such as chocolate manufacturers who dehusk cocoa beans, but again these would have to be situated near the fuel processing locations. Perhaps existing transport links used to deliver food to markets, for example, could be shared for transportation of briquettes to the same markets. On the village level, where people are producing briquettes to use on a more individual basis for cooking, also important is the question of access to the residues. This is often dependent on individual circumstances. For example a prosperous farmer with several hectares of farmland and a large herd of cattle might produce excess residues, whereas a farm labourer might only have access to much lower quantities [27].

Another important aspect to consider is the implications of a shift away from using agricultural residues for soil fertility, which could have an adverse effect on crop production and the environment [27]. In traditional farming methods, agricultural residues are the main source of organic matter in the soil; they supply the nutrients for next year's crop growth and help bind other nutrients, preventing them being washed away when it rains. They also reduce the water lost to the atmosphere from the soil, increasing the soil's water retention capacity. In addition, they improve soil structure by helping hold soil particles together, improving drainage and reducing the soil's susceptibility to erosion. For these reasons, they are a critical component to the farmers' livelihood, especially when artificial fertilisers are not used. If organic matter in the soil does become diminished, the soil is likely to become unstable and unable to support crop growth [27]. There are, however, many circumstances where agricultural residues would not be routinely reintroduced into the soil as organic fertilisers. These might be residues that could be theoretically collected and organically recycled, but due to the inconvenience, time or cost they are not. On the other hand they may, for example, be used for other purposes such as building materials or fodder for animals. Other crop waste is routinely burnt, such as maize husks in Ghana [6], and there are residues such as coconut shells, millet stalks and coffee leaves, which cannot be organically

recycled because their rate of decomposition is too slow. Some residues, such as cotton stalks, tend to attract pests if left in the fields [27]. Diverting such residues to be used as fuel therefore has no direct effect on the soil. The local use of residues needs to be considered on a case by case basis, and only after any other important uses have been taken into account, can an accurate picture be formed of the quantities of residues realistically available for the local situation.

On an industrial level, there are many sources of residues generated at large crop processing facilities that are currently considered waste. High transportation costs would inhibit such residues from being organically recycled in the fields. These wastes often mount up outside the factory, as was observed with cocoa shells in Ghana [6]. This is an untapped source, and there is much potential for these resources to be used as fuel without having an effect on people's livelihoods.

1.5   Summary: the Potential of Briquetting

Fuelwood is the dominant energy source both in the home and in many industries in Ghana, and this, alongside other causes, is putting pressure on woodlands resulting in increasing deforestation. Sparse forest resources then put pressure on rural dwellers who, as discussed earlier, depend on firewood as their principal cooking fuel. The principal firewood collectors, normally the women, then have the daily pressure of long journeys for its collection. On a national level, as the Ghanaian economy expands, there will be immense pressure put on fuelwood supplies, and further serious deforestation could be the result. It is clear, from the previous section that alternative fuel sources need to be identified, both for the livelihood of rural dwellers and for sustainable economic growth. One approach to helping this situation could be improving the efficiency with which the fuel is burnt so that more of the heat is usefully used, for example, by introducing more fuel efficient cookstoves (as previously discussed). Another aspect, often not so frequently considered, is that such an initiative might be combined with an appropriate method of fuel substitution, either a complete replacement, which can be burnt alone, or something which can be co-fired with the wood.

It has been revealed that there are currently large quantities of under-utilised waste biomass residues in Ghana. These are an untapped potential resource which, with appropriate technology could be upgraded to become a sustainable alternative to firewood. Considering the agricultural-based economy of much of the developing world, it is likely that this situation is typical in many developing countries. One possible means of making more efficient use of the biomass residues

is by briquetting. This involves collecting biomass materials that are not normally considered a useful fuel, due to their low density, and compressing them into a solid fuel of a convenient size and shape that can be burned in the same way as wood or charcoal. Briquetting increases the bulk density of the biomass material, increasing its energy density, which in turn reduces transport costs and makes it much easier for the end user to handle. Indeed, agricultural residues in their raw state are often bulky and difficult to handle and in combustion they often burn fast and are smoky [28]. Densification of the material results in marked improvement in combustion characteristics compared with loose biowaste [29]. Thus this simple technology might provide a practical means of upgrading the loose residues and providing a wood substitute that could potentially be used in existing stoves. Compared with other types of technology such as biogas digesters and gasification, briquettes do not impose significant changes in the way people cook their food. They are very low-tech and provide a low-cost method which can be made at a village level to upgrade fuel, even using a hand-operated press. Moreover, small village enterprises can be set up for their production, creating employment and generating income.

Briquette production can be on different scales, from small village producers making briquettes for themselves and other local families, to larger scale briquette manufacturers, producing sufficient quantities for local industries and commercial businesses. On the small scale, there have been a number of successful briquetting rural cottage industries established around the globe in developing nations, notably by the Legacy Foundation in America, who have designed a rural briquetting system and trained up entrepreneurs to set-up small scale businesses. They give details in a set of manuals [30–33]. These enterprises have multiple benefits: they generate rural employment and income, eliminate disposal problems sometimes associated with large quantities of waste agro-residues and provide an alternative to woodfuel, thereby reducing the impact on forests. Some of the important barriers to the use of crop residues have been highlighted, and these would also need to be carefully considered before the introduction of a biomass briquetting programme in a particular location. The simplicity, and therefore, accessibility of this technology, with the benefits it could bring to people's lives, gives it huge potential as an alternative energy source for developing nations.

Despite the potential for briquetting to provide an alternative to woodfuel, and the potential social and environmental benifits that it might have, it is not currently (in 2010) commonplace either in fires or in improved cookstoves in the developing world. In the case of Ghana, the Energy Foundation, in a document looking at future energy supply to the economy [8], does not even mention briquettes

as a potential woodfuel substitute. Rather, the focus is on reducing woodfuel consumption by improved stove methods. The academic literature also has this bias, and there is much work on studying the thermal and emission related performance of improved cook-stove design [34–40] (For example, a detailed study by Burham-Slipper looked at optimising stove performance by using a genetic algorithm in combination with computational fluid dynamics (CFD) [41]). There has, however, been little discussion on briquettes as a viable fuel substitute, and few studies to this end, as the literature review in Chapter 2 reveals. In terms of the practical use of briquette fuel, the ability to manufacture a consistent size and shape is advantageous for stoking a fire and for storage. However, in terms of stove optimisation for a specific fuel, one complication of using briquettes is the large variety of materials from which they can be made, and the different shapes, sizes, densities and moisture contents that a briquette can have. Furthermore, to design a briquette fuel that is able to replace wood, it is necessary to characterise the combustion behaviour of briquettes in terms of these fuel properties, in order to allow performance and power output of a particular wood-burning cookstove, for example, to be matched. Currently, there is little published work on the combustion of briquetted biomass and the effect of different properties on its combustion behaviour. What studies are available together with aspects that need to be addressed are discussed in more detail in Chapter 2.

1.6   Thesis Aims and Overview

The aim of this thesis is to better understand the effects on briquette combustion of key parameters. These can be grouped into two sub-catagories: material properties, which includes briquette density, moisture content; and briquette geometry, which includes its size and shape. This was achieved by completing the following objectives:

- The development of a method to manufacture briquettes in a controlled reproducible way, from a particular material, with a given density and moisture content.

- Development of a methodology to compare the burn-rate of different briquettes that allows relative trends in the behaviour to be observed and quantified.

- To use the combustion methodology to identify the influence of density, moisture content, geometry and material properties on the burn rate.

- Development of a numerical model of pyrolysis which is able to predict observed behaviour, and infer the effect of important material properties that are difficult to test experimentally, for example, the effect of a sample's heat capacity and thermal conductivity on its burn rate.

- To use the knowledge gained from the experimental study and numerical model to inform the manufacture of briquettes.

This work is set out in subsequent chapters as follows:

Chapter 2: Literature Review: A review of the manufacture of briquettes is given, which informs the methodology in Chapter 3. This is followed by an overview of solid fuel combustion, focusing on the effects of different fuel properties. Finally, a review of modelling pyrolysis of large solid fuel samples is presented. It is concluded that whilst there is a lot of work concerning the manufacture and testing of the mechanical behaviour of briquettes, there is little work concerning their combustion as a function of material properties: how the rate of combustion varies with briquette density, for example. Furthermore, for practical stove design in the field, many of the large particle solid fuel models that attempt to take into account material properties are computationally complex (necessitating prohibitive computing resources) and often have limited experimental validation. In order to understand how and to what degree the performance of cookstoves is affected by fuel properties an appropriate, more accessible and computationally low-cost model is required taking into account the key briquette parameters, such as fuel density, which can be varied as part of the manufacturing process.

Chapter 3: Experimental Methodology: A description is given of the experimental procedure used in Chapter 4 for the reproducible manufacture of briquettes and for investigations into their pyrolysis behaviour. The methodology provides a means by which the burn rate of different compressed biomass materials can be compared.

Chapter 4: An Experimental Study of Process Dependent Properties: The first part of the experimental study looks at the effect of feedstock moisture content on briquette final density. The section that follows describes experimental work on the effect of variables that can be controlled during briquette manufacture (process variables) on burn rate; that is the briquette geometry, moisture content and dry compressed density. Finally, the influence on the rate of having a central hole in a cylindrical briquette is investigated. The understanding of the effect of the different factors on the burn rate gained in this chapter, helps identify key factors that need to be described by an analytical model of briquette pyroysis.

Chapter 5: A Simple Model for The Pyrolysis of Compressed Biomass and The Determination of Thermal Model Parameters: A simple heat conduction model of the pyrolysis of solid fuels is presented. Details are then given of two experimental methods to determine the necessary parameters for the model. In the first, a dual heat probe method is used to determine the thermal conductivity, heat capacity and thermal diffusivity of a briquette. In the second, an experiment is described for estimating the heat transfer from a flame to a slab.

Chapter 6: Evaluation of the numerical model: This chapter provides details of how the Arrhenius kinetic parameters of the model, developed in Chapter 5, are determined. The model is then used to predict the burn rate of briquettes burning in free air, and to model the variations in the key parameters identified in Chapter 4. A better understanding is gained of how the rate changes as a function of the thermal conductivity heat capacity and thermal diffusivity of the material (which are difficult to vary experimentally). The model is used to generate an analytical briquette devolatisation equation, which gives the burn rate in free air as a function of the described process and material properties for paper briquettes. Limitations of the model are then discussed.

Chapter 7: Conclusions and Recommendations: Conclusions from each chapter are summarised and resulting recommendations made for future work.

Chapter 2

Literature Review

This chapter is divided into three sections. In the first part, a review is given of factors affecting the manufacture of briquettes. The purpose of this review was to identify the factors that need to be controlled to manufacture briquettes of a consistent and repeatable quality. The second section provides a review of the influence of different fuel properties on combustion behaviour. Briquetting changes the apparent density and size of the fuel, which essentially manipulates its combustion characteristics. The aim was to gain an understanding of the relationship between the properties of the manufactured briquette and how it burns. In the third section, a review is made of research concerning the numerical modelling of the combustion of biomass. It includes pyrolysis and volatile combustion, radiation and convective heat transfer. This provides an informative insight into the mechanisms involved in the combustion process, and gives appropriate approaches to modelling them.

2.1   Manufacture of Briquettes

2.1.1   Introduction

Much of the work in the literature on briquette manufacture, both theoretical and experimental, focuses on the manufacture by compression of residues with a low-moisture content ($< 25\%$, dry basis), at moderate to high-pressure (>5 MPa). However, the interest of this study is briquetting that can be done at low pressures in a rural community. Therefore, in order to understand the different parameters that need to be considered in the formation of briquettes, where it is thought helpful, literature on briquetting with high pressure processes is also

included within this review, and its relevance in relation to this work discussed. The aim was to identify the most important factors that needed to be controlled to produce repeatable briquettes of a consistent quality. In turn, this informed the development of a manufacturing methodology that was then used in the experimental work of this thesis (details of this are given in Chapter 3).

2.1.2   Definition of briquetting and its advantages

Biomass briquetting can be defined as the densification or compaction of biomass material by the application of pressure. Briquettes are distinguished from pellets by their size. Pellets typically have a length of 5 to 30mm, compared to briquettes which can range from 30mm to 200mm in diameter and be from 50mm to 400mm in length [42, 43]. Olorunnisola reviews the mechanical advantages of briquetting [43]: the bulk density of the material is increased, making transportation easier and cheaper; the energy content per unit volume of material is increased; a homogenous product is obtained from an often hetrogeneous mix of materials; a uniform quantity of energy per unit of combustion feedstock is maintained and a highly cohesive product is obtained from materials that might otherwise be difficult or expensive to process.

2.1.3   Methods of densification

There are two main types of compression process. One is a continuous or semi-continuous extrusion process which depends on friction forces from the side of the die acting to produce compression. The other is a discontinuous process, in which a single briquette at a time is produced in a closed mould [43]. The continuous process is generally associated with larger scale industrial production, and is normally involves compression at high-pressures. Whereas, the mould and press briquetting method is more commonly seen in smaller scale set ups, and might be either low or high pressure compression, depending on the situation. It is a mould and press that will be employed to form briquettes in this study.

2.1.4   Pre-processing of biomass residues

Before briquetting, biomass material often needs to be broken down in size by processing. Depending on the residue, in a rural setting this might involve chopping, crushing and hammering the material by hand or using hammer mills, hand cranked devices or a pestle and mortar [44]. This process can potentially

consume a large amount of energy, and therefore the most suitable method for the individual situation needs careful consideration. For some materials this step might be less energy intensive than for others [45]. For example, residues such as rice husks, peanut shells, maize-milling residues and waste papers require minimum chopping and pounding to break them down, compared to harder materials such as palm nut shells. These residues can be formed into briquettes alone, or mixed in blends. For example, they might be blended with other material that would otherwise be hard to break down (such as cashew nut shells), facilitating the amalgamation of the harder materials, and considerably reducing the processing labour required in chopping and crushing them.

2.1.5   Briquetting at different pressures

Many materials contain naturally occurring binders such as resin, wax or wood lignin. For example, where plant matter is concerned, it is the lignin constituent of the biomass material, a major component of most plant matter, which, under suitable compression conditions, acts as a binder and holds the briquette together. However, adequate pressure is required to break cell walls and allow amalgamation. This occurs at moderate pressures greater than around 5.0 MPa [43], but of course this depends on the specific properties of the material. In some processes, heat can be applied before or during compaction to activate the material's built-in binder and reduce the pressure required [46, 47]. Manufacture of briquettes by compaction at high pressures, requiring a hydraulic press for example, while applying heat is, however, an energy intensive process, and often unpractical for a rural setting. Moreover, equipment is expensive and more than likely unavailable, but even if it were it would be unaffordable for subsistence communities.

Basic hand presses that could be fabricated from limited equipment in rural areas might only be able to achieve low pressures less of than 1 MPa[1]. However, the compaction of partly dried biomass material (which has a moisture content of <25%) at such low pressures (less than 5 MPa), is unlikely to produce stable briquettes. This was demonstrated by Faborode et al. who, in attempting to compress straw with a moisture content of 8% at such pressures, found it was impossible to form briquettes that held together [48]. For briquetting to be feasible in rural locations, an appropriate method is needed that will bind the residue matter together at low at compression pressures. In this section, methods

---

[1]For example, a 1m lever press with a person exerting a force of 750 N on the end of the lever, would compress a pulp in a cylindrical briquette mould (with a diameter of 60 mm, placed 0.3 m from the flucrum), with a pressure of around 0.9 MPa.

and theory relating to the formation of briquettes in smaller scale processes are discussed.

2.1.6   Briquetting systems suitable for low pressures

Fibrous residues are common in rural subsistence farming communities. In order to overcome the need for their high pressure compression to form briquettes, natural decomposition processes can be used to break fibres down, and this is found to facilitate bonding [30]. This can be done by first chopping the residues (pre-processing), before leaving them to be further broken down by fermentation until the fibres separate (to achieve this the agro-residues are moistened, covered and left in a warm place to decompose). The material is removed when it begins to take on a sludgy texture and can then be pulped like papier mâché. The resulting mixture can then be pounded, for example in a mortar and pestle (see Figure 2.1), until it takes on a mushy consistency and stable balls can be formed by hand. The result is a mass of pulp that can be compressed in a mould to form briquettes under low pressures [30] without the addition of a binder being necessary. In the fermentation process the structure of the lignocellulosic material breaks down and this facilitates the interlocking of fibres during the densification process. This technique, although potentially labour intensive, allows the manufacture of briquettes from crop residues in a rural setting. One disadvantage, however, is that it produces wet briquettes that need to be dried for a considerable time in the sun before being burnt. This is compared to briquettes formed from residues with a low-moisture content, using a high-pressure process, which after the densification process can be burnt immediately.

The success of the method has been demonstrated by an American NGO called the Legacy Foundation, who have established various briquetting projects around the globe, often as small scale rural enterprises [30]. Figure 2.2 shows some images of low-tech presses that can be fabricated with limited equipment.

2.1.7   The use of additional binders

Some materials, however, are difficult to breakdown down by fermentation, or take a long time. Examples would be sawdust or harder materials like shells[2]. These materials need to be agglomerated with the addition of a binder. Examples of some combustible binders include natural resins, tar, animal manure, fish waste,

---

[2]shells that are difficult to briquette without a binder would include cashew nut shells, palm nut shells, for example.

Figure 2.1: In a rural setting materials could be broken down with a pestle and mortar such as shown here.

algae and starch. Some common non-combusible binders would be clay, mud and cement [45].

Generally, the greater the quantity of binder used in manufacture, the greater the resulting relaxed briquette density, durability and sheer strength of the briquettes [50]. The amount of binder selected should give the final product its required strength, so that it is able to withstand handling, transportation and storage [47], and for the safety of those manufacturing the briquettes it should be non-toxic. On the other hand, the effect of the binder and the amount present on a briquette's combustion, the emissions given off when it burns and the residue left after combustion, also need to be considered carefully. Theoretical details on how binders work, and further information on how to select one may be found in [47] and [51].

As an alternative to binders, stable briquettes can be formed by blending residues that would otherwise need a binder with residues or processing wastes that naturally bind well [44], for example blending decomposed banana skins with sawdust [52].

Densification After Carbonisation

Another method that is practiced is the carbonisation of the residues before their densification. In this case the residues are not pre-processed but are placed directly into a charcoal kiln before being ground down and briquetted. This process requires the use of a binder to hold the charcoal particles together after compaction.

(a) A press that uses a car jack
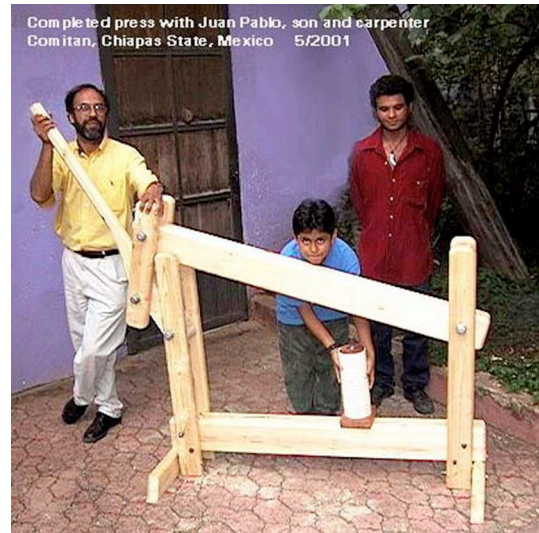
(b) A press designed by the Legacy Foundation

(c) A lever press

(d) A screw press

Figure 2.2: Some examples of simple low-tech briquette presses. Reproduced with permission of the Legacy Foundation [49].

It has been successfully employed in Nepal [53]. This will not be considered further in this study, because, as outlined in the introduction and social context (Chapter 1), this thesis is concerned with alternatives to woodfuel for the rural poor, who normally burn firewood rather than cooking on charcoal.

2.1.8   Factors governing the manufacture of briquettes

In order to be able to manufacture reproducible briquettes from a given material, it is important to understand the factors that have an influence on their final properties. There are some principal factors that govern how briquettes form: the design of the die, the method of load application (for example dynamic or static), the loading rate, the maximum pressure applied, the time for which that pressure is maintained (hold time) and the material characteristics, for example particle size and moisture content. In following sections, the literature is reviewed on the influence of these factors.

2.1.9   Compression characteristics

O'Dogherty [54] gives a review of the mechanical behaviour of compressing straw. Although focusing on straw, it covers important properties and relationships that are important in the design of briquetting equipment for any fibrous material. In this work, O'Dogherty presents empirical relationships for the compression characteristics of materials in closed dies: this includes the relationships between pressure and density while the briquette is in the die, and the relationship between pressure and the relaxed density when the briquette has been removed from the die. The latter is of interest to this work, and Chin et al. [50] have determined empirical constants for these equations for various biomass materials. O'Dogherty also reviews the specific energy required to form briquettes and eject them from the mould, and the variation with die geometry. Such considerations are important in the design of efficient and practical briquetting machines. A more theoretical analysis of the compaction process is given by Faborode et al. [48], who considers models of deformation during compression, and examines the effects of different process variables on the compressive behaviour of fibrous plant materials.

2.1.10   The effect of die pressure on relaxed dry density

Briquettes formed by compression in a die relax and expand over time once they have been removed. This is known as the relaxation of the briquette. It can be

used as a measure of a briquette stability and durability [28, 48]; the more stable the briquette the less post-die expansion. Chin et al. found that the relaxation behaviour of the briquette depended on the type of biomass residue [50]. However, they found that for most types of biomass the maximum rate of relaxation occured within 10 minutes of removal from the die, followed by a gradually decreasing relaxation for the next 2 hours. When expansion has ceased, the relaxed length can be measured and the relaxed density found. Chin et al. propose the following relationship between the relaxed density and die pressure:

$$\rho = a \ln P + b \qquad (2.1)$$

where ρ is the relaxed density, P is the compaction pressure and a and b are empirical constants. This form of relationship is supported by results given by Husain for briquettes of palm shell and fibre [29].

2.1.11   The effect of dwell time

The amount of relaxation that occurs on removal of the briquette from the die is also found to be a function of the hold time (dwell time) during the compression, that is, the duration for which the maximum pressure is applied at the peak of the compression sequence [48]. Chin et al. [50] reported that the relaxed briquette length reduces with increasing dwell time, until a limit in the reduction in briquette length is achieved. They conclude that, in general, a dwell time of 20-40 seconds will produce a briquette with the smallest percentage relaxation possible. For some materials, other studies have shown that the required time is less, for example O'Dogherty et al. found that for straw, the relaxation increased up to a dwell period of 10 s, with no appreciable increase observed for longer periods. What is clear is that choosing a dwell time beyond the minimum required for minimum relaxation does not have any additional adverse affect on the final relaxation characteristics. Choosing a hold time of greater than 40 seconds, therefore means, that there does not need to be any more rigourous control of this variable (timing, for example, is not necessary) to manufacture briquettes of repeatable density. It is also interesting to note that repeated application of the same (final) pressure on the compacted material is found to produce insignificant changes in the final relaxed density of the briquette [48].

Chin et al. [50] propose a relationship between the dwell time and the combustion rate ($\dot{m}$) of a briquette (valid up to the maximum dwell time for the most stable briquettes):

$$\dot{m} = e\tau^f \tag{2.2}$$

where e and f are empirical constants and τ is the dwell time in seconds.

2.1.12 Effect of moisture content

Moisture content plays an important role in the compaction of many biomass materials. For compression of materials in their raw collected state (normally under high pressure), there is found to be a practical range of moisture content values (moisture content prior to compression) where the formation of stable and compact products is feasible [55]. It has been demonstrated that if the moisture content is too high, there is a decrease in briquette density and stability (cited in [54]); O'Dogherty et al. showed that above a certain moisture content it is not possible to form a coherent briquette because of the high relaxation of the material on removal from the die (cited in [54]). The upper moisture limit for stable briquette formation is dependent upon the feedstock materials. For hay, for example, a moisture content of about 25% or less is required [56]. On the other hand, Bellinger et al. [57] showed that an increase in energy was required to form briquettes as the feedstock moisture content was reduced. Furthermore, an adequate moisture is believed necessary to act as a lubricant and reduce friction between particles [58]. Chin et al. suggest that there is an optimum moisture content for the formation of the most dense briquettes, and for briquettes formed between 5-7 MPa they suggest that a moisture-content of around 20% shows the least relaxation after compaction [50] (in an investigation on sawdust, rice husk, peanut shell, coconut fibre and palm fibre).

The compression process has been thought of in terms of two distinct stages [48]: an inertia stage and an elastic stage. In the inertia stage, air is squeezed out from between the voids, and in the elastic stage, the briquette and binding formation takes place. Experimental investigations [50, 55] show that for a given constant compression pressure, there is a relationship between the final relaxed density and the material moisture content. As the moisture content increases there is an exponential decrease in relaxed density:

$$\rho = ge^{(-\lambda m_w)} \tag{2.3}$$

Where g and λ are empirical constants, ρ is the relaxed density and m_w is the moisture content of the briquette. Chin et al. give empirical values for these

frequency and exponential factors for various biomass materials [50] under given conditions.

Cowin [59] described the moisture content of biomass material in terms of free and bound moisture. Free moisture is water in the cavities between the wood fibre cells held by capillary forces, whereas bound moisture is water within the cell membranes of the fibres, held by hydrogen bonding. The fibre saturation point is the limit at which the wood cells of the material become completely saturated, but there is no free-water between the cell cavities. Adding moisture beyond this point will increase the free moisture content of the wood. In wood science, the fibre saturation point is considered to mark significant changes in the physical and mechanical properties of the material [60]. In the wet low pressure briquetting method (described in Section 2.1.6), where materials are broken down by fermentation, the feedstock is often beyond the fibre saturation point before compression. The consequence of the amount of free-moisture on the empirical constants in Equation 2.1, is not clear from the literature. Moreover, the work in the literature has focused on briquettes formed under higher-pressures than might be achievable in rural setting with a hand-press. The effect of moisture content on the formation of briquettes using the low pressure wet technique described in Section 2.1.6 has not been detailed in the literature. This does, however, need to be established in order to understand to what extent the free-moisture needs to be controlled in the manufacture of repeatable briquettes with the described wet low pressure process.

2.1.13 Particle size distribution

It has been observed that the particle size of biomass feedstock (especially for non-fibrous type biomass) has a large influence on the stability of the final briquettes formed [43]. For certain biomass residues, such as hard shells, the act of breaking them down into smaller irregular shapes can help fibres and particles to pack more closely, therefore aiding agglomeration [47]. However, for some fibrous materials, this does not always result in stronger bonding. Faborode et al. examined the effects of mechanical pre-processing (chopping and grinding) on the formation of straw briquettes in closed dies, between pressures of 8 MPa to 50 MPa. Although greater difficulty is found in binding unchopped straw compared with chopped straw, and a longer hold time is required to achieve binding for the long material, Faboraode's results indicate that when binding does take place, it is preserved better in the long straw on ejection from the die [48]. Put another way, for high pressure compaction, briquettes formed from unchopped straw were

more stable, although more energy was required for their formation to overcome frictional forces. This suggests that the length of the fibres has an influence on briquette stability. The large ranging nature of different residues, however, necessitates that the effect of particle size distribution needs to be considered on a residue by residue basis.

2.1.14   The effect of compression speed

For high pressure dry compaction (rather than the compression of partly-fermented material) the speed of compression is critical in determining if irrecoverable elastic deformation occurs on the application of the load [61]. The compression speed affects the magnitude of the binding force [48]; a rapidly applied load, would give no time for permanent creep to take place. In comparison, in the compression of a highly saturated feedstock pulp, as encountered with the wet-briquetting process, the speed of compression has to be slow enough to give sufficient time for water to flow out of the mould.

2.1.15   Summary and closing remarks on briquette manufacture

This section has reviewed literature on the manufacture of biomass briquettes. For biomass materials such as straw, maize husks and sawdust, briquettes can be formed without a binder at high pressure. However, such pressures are not practically achievable in rural communities in developing countries. There is, however, a low pressure 'wet' briquetting technique which relies on the partial decomposition by fermentation of the biomass. It is low pressure briquetting which is of interest in this work, firstly because this is of most use to rural subsistence communities, secondly, the understanding of briquette combustion behaviour will help with stove optimisation; and thirdly, as far as the author is aware, little work has been done on the combustion of low pressure biomass briquettes of this nature.

The above review concludes that there are a number of factors that have to be controlled in briquette manufacture in order to form briquettes of a consistent repeatable quality: the method used for pre-processing should produce pulps with an approximately consistent fibre size distribution for each batch of briquettes; it is important to use a sufficient hold-time in compression in order to minimise the effect of this variable on the physical properties of the final briquette; the amount of charge loaded in the die for each briquette should be controlled; the importance

of material moisture content in forming briquettes under high-pressures has been highlighted. Unfortunately, the published work to date only considers briquettes formed at relatively low moisture contents of less than 25%. Saturated, partly-decomposed mixtures, as are encountered with the fermentation method, are not documented in the literature. A study in Chapter 3 is carried out to determine the effect of initial moisture content on briquette final density for the wet low pressure briquetting process, and thus understand the relative importance of its control in the manufacturing process.

This section has reviewed the literature to inform briquette manufacture. The next section reviews the literature that will help understand the processes at play when briquettes are burned, and how these processes can be modelled.

2.2　Introduction to Biomass Combustion

The current understanding of the combustion of different agricultural residues in a densified state, as a function of specific material properties, forms the objective of this section. There is, however, a lack of literature that refers specifically to the combustion of briquetted residues, and so the approach taken has been to review general combustion literature concerning wood, focusing, where possible on work that is relevant to domestic cookstoves, and inferring how this might relate to the burning of residues.

Many of the fundamental phenomena observed in biomass combustion, which are most relevant to cookstoves, have been extensively studied and mainly focus on understanding how wood burns. It includes modelling of both the solid and gas phases and heat transfer. The field of combustion is extensive and this section does not seek to provide a comprehensive review, but rather focuses on the areas that are most relevant. In Chapter 1 of this study it was established that this work would focus on briquettes that could be produced in a rural area of a developing country. It was concluded that for this to be done with limited equipment, a low pressure method would be required. The size of each briquette would need to be large enough to provide a suitable alternative to woodfuel, and be practically and economically manufacturable using a discontinuous hand-press method (producing pellet fuel with a hand-press, for example, compared to larger briquette fuel, would be much more time consuming per kg of densified residue). This review, thus focuses on those areas relevant to developing a tractable approach for understanding the combustion of large particles of densified biomass, in the form of briquettes (rather than pellets). In the context of combustion models, briquettes

are considered to be 'large-particles'[3]. In a rural context in the developing world, briquettes would typically be burned under natural convective airflow conditions. For the rural dweller, this might either be in a domestic cookstove, or on an open three stone fire. This is in contrast to providing a constant flow of air to the fuel by forced convection, which requires fans or bellows. For most rural dwellers these would either be unavailable, or only used for the ignition of the fuel briquettes. It is the literature most relevant to large biomass particles and natural convective flows that this review will draw upon. Another aspect that it was considered important to review, was the effect of briquette material properties on combustion. Biomass comes from many different sources, and in a subsistence farming community there may be a variety of different potential feedstock streams. Therefore, an understanding of the combustion behaviour of different residues, with knowledge of the relative influence of different material properties, is required.

What follows in this section is first an overview of biomass combustion, and then a focus on the effect of different material properties on the pyrolysis of solid biomass fuels. Models of the energetics of pyrolysis are considered, and finally, models of heat and mass transfer are reviewed. The chapter provides the foundation for the development of a physically realistic semi-empirical model that can account for the experimental results found from burning biomass briquettes of different sizes and geometries. Of particular interest is the effect of different factors on the briquettes' burn rate. Understanding how material properties affect the burn rate, and therefore power output, of briquetted biomass fuel is useful in the context of cooking, because different cooking processes require different combustion rates: for example, rice or a casserole type dish can be simmered on a low heat for a long time, whereas frying requires a more intense heat. The development and application of an analytical model that takes into account important briquette properties, such as density, moisture content, size and shape, would, provide a means to make predictions of a cookstove's power output in advance, and could also be used in the numerical optimisation of multi-fuel cookstoves.

---

[3]Large-particles can be defined as those for which during thermal decomposition, there are internal temperature gradients, which limit the rate of pyrolysis. This is in contrast to small particles, in which the temperature in the particle can be considered essentially uniform and the rate is controlled purely by the chemical kinetics.

2.3   Overview of Solid Fuel Combustion

The burning of biomass[4] is a complex process involving both gas phase and solid phase phenomena. It depends on a large range of different factors and processes, and there have been numerous attempts to develop simplified models to understand these processes, and understand the most important parameters affecting them. In general terms, models assume that during combustion the solid fuel undergoes three stages of mass loss: drying, devolatisation[5] and char combustion. Flaming combustion of the volatiles at the surface of the solid then drives further thermal decomposition. Dividing the decomposition into key stages is helpful because it identifies the key processes that are occuring during the combustion of a fuel. The relative significance of each of these processes in a particular fire, is dependent on the properties of the fuel and the environment in which it is burning. These factors are discussed later.

Briquettes are large particles, and when heated temperature gradients are set up in the solid which drive, and limit their thermal decomposition. Heat progates into the briquette, evaporating moisture and when the surface becomes sufficiently hot a process of thermal decomposition of the biomass takes place, known as pyrolysis or devolatisation. The pyrolysis front moves into the briquette, driven by the temperature gradient. The small volume of the solid which is undergoing pyrolysis at any one moment in time is known as the pyrolysis reaction zone. Figure 2.3 illustrates this. In this process, gaseous volatiles are released which flow out of the briquette and undergo secondary reactions as they progress, leaving a residual char, a carbon rich porous matrix. On leaving the solid matrix of the briquette, the volatiles are heated and mix with oxygen and ignite. This exothermic gas phase combustion reaction results in a flame, which feeds heat to the solid surface. As the surface of the briquette becomes hotter in response to the imposed flux of heat from the gas phase reaction, the pyrolysis wave penetrates deeper and deeper into the virgin solid, causing further devolatisation [63]. The char layer that is left behind undergoes heterogeneous combustion, reacting with oxygen, releasing heat. This is referred to in the literature as char combustion. During the devolatisation phase, the outflow of volatiles (known in the literature as blowing) from the fuel surface has been shown to inhibit oxygen from reaching the char

---

[4]Biomass includes any biomass residues and wood. Up to now, wood has been the predominant subject of large-particle biomass studies in the literature.

[5]*devolatisation* is used interchangeably with *pyrolysis* to mean 'the thermal degradation [of a solid] in the absence of an externally supplied oxidizing agent' [62]. This is compared to *Gasification*, which means 'thermal degradation in the presence of an externally supplied oxidizing agent' [62].
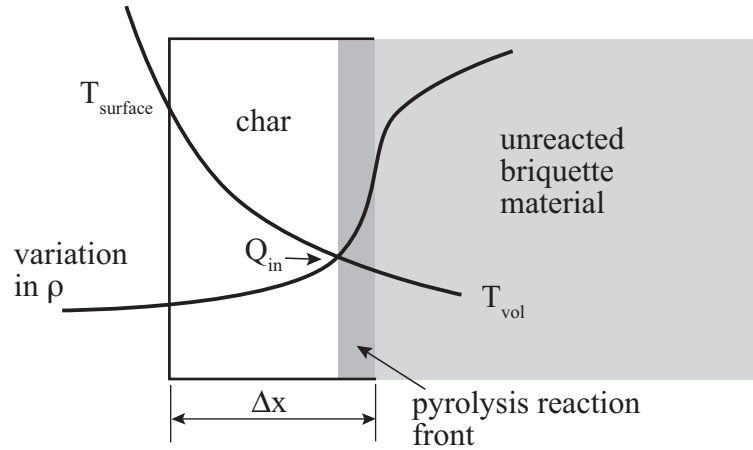
Figure 2.3: An illustration of the the variation in temperature and density in a pyrolysising 'large particle'.

.

surface. Often, the outward flow is sufficient to prevent significant char combustion until almost all of the fuel has been pyrolysised [64], allowing the devolatisation and char combustion processes to be modelled separately. However, there are cases, such as in a stoked fire, or with large logs, where all three processes, moisture evaporation, devolatisation, and char combustion, will occur simultaneously. The modelling of this type of fire must take each of these aspects into account. It is the extent to which each of these processes are modelled, and the simplifications and assumptions which are made by different authors, that has resulted in models of varying degrees of complexity. This is further discussed in Section 2.7, which considers the modelling of large solid biomass in more detail.

2.4 Considerations Concerning Important Intrinsic Biomass Material Properties

The rates of drying, devolatisation and char combustion are controlled by both fuel properties and the combustion environment. For example, in terms of the fuel chemical properties, coal has fewer volatiles and more fixed carbon, compared with biomass, and therefore char combustion, rather than pyrolysis, will be the more significant factor determining its combustion rate. Another example is a fuel with a high percentage moisture content. It will be harder to ignite and will burn more slowly than a dry fuel. The combustion environment also has a significant effect. For example, if a fire is lit in a well insulated and vented combustion chamber, in contrast to a fire lit in the open, less heat will be lost to the surroundings resulting in higher temperatures, faster burn rates and better

combustion efficiency. This section provides a review of how the fuel properties and the combusiton environment affect the rate of drying, devolatisation and char combustion in a solid. This provides the understanding required to predict the burn rate.

In considering how the material properties affect combustion, there are two main aspects to take into account. Firstly, an understanding is needed of how intrinsic material properties, such as the ash and volatile content, affect the thermochemical decomposition of the solid to pyrolysis gases. Secondly, it is necessary to understand the effects of process variables. These are factors such as the briquette density that can be varied during briquette manufacture.

Some standardised solid fuel analysis test methods, often used to characterise and compare the intrinsic material properties of biomass, include the proximate analysis, ultimate analysis, calorific value and rate of devolitisation. The proximate analysis gives an idea of the bulk components that make up a fuel, which relate closely to its combustion behaviour. The objective of the ultimate analysis is also to determine the major constituents of the biomass, in terms of its elemental chemical composition, rather than its bulk components. The calorific value is a measure of the fuel's energy content, and the rate of devolatisation describes how fast the fuel burns. These intrinsic combustion properties of different biomass materials vary; a good review is given by Jenkins et al. [65]. They are properties, however, which are defined for biomass in its original undensified state, and many only at ambient temperature [66]. They do not give a compete description of how the biomass will behave when densified to form briquettes. Even though briquettes might be made of the same material, the density, moisture content, size and shape can be made to vary significantly in the manufacturing process.

In the first part of the following section, the meaning of proximate and ultimate analysis results obtained for a biomass sample are discussed. In the second part, other important fuel properties that have an influence on the combustion of large biomass particles are reviewed. Of critical importance in this study, which is considering fuel that is going to be burned in cookstoves, is the effect of material and physical properties on the burn rate, the heat output, ease of ignition, harmful emissions, and any effects regarding the continuous efficient operation of burning biomass fuel in a domestic cookstove.

2.4.1   The Proximate Analysis

The proximate analysis is a standardised analysis procedure [42] that attempts to quantify some key physical characteristics of biomass, which affect its combustion characteristics. It does this by considering biomass to be made up of four main components: moisture content, volatile matter, ash and fixed carbon, and then determining the relative proportions of these by various procedures. In the following sections a brief description is given of what each of these components is, how each one is found, and their significance.

Moisture content

The moisture content is a measure of the amount of water in the fuel. In solid fuels, moisture can exist in two forms: as free water within the pores and interstices of the fuel, and as bound water which is part of the chemical structure of the material [67]. The moisture content can be found by taking a small pre-weighed sample and oven drying it at 105ºC[6] until consistency in the sample's mass is obtained[7]. The change in weight can then be used to determine the sample's percentage moisture content. In the literature, moisture content is presented either on a wet basis, also known as the moisture content as received, (this is the biomass' moisture content as a percentage of the total as received mass[8]), or on a dry basis, which is the moisture content as a percentage of the dry mass[9]. In this thesis the convention adopted is to present moisture content on a dry basis, unless otherwise stated.

Moisture content is a very important property and can greatly affect the burning characteristics of the biomass [69]. It affects both the internal temperature history within the solid, due to endothermic evaporation, and the total energy that is needed to bring the solid up to the pyrolysis temperature [70]. During combustion, moisture in the biomass will absorb heat by vaporisation and heating of the resulting vapor, significantly reducing the heating value of a given fuel. The consequence is that there is less heat to drive the pyrolysis reactions, resulting in lower combustion temperatures. This can result in incomplete combustion of the volatiles and the deposition of unburnt carbon (smoke) in the stove's chimney and on the bottom of cooking pans, making them difficult to clean. Significant build up can result in resistance to flow of the flue gases and reduced heat transfer to the

---

[6]The free water is the first to be driven off, as this is held only by capillary forces.

[7]This is defined as a change in mass not exceeding 0.2% of the total mass of the sample, heated at 105°C, over a period of 60 min [68].

[8]The wet basis moisture content can be written as: $m_{water}/(m_{water} + m_{solid})$

[9]The dry basis moisture content can be written as: m_{water}/m_{solid}

pans. A high moisture content can also cause difficulty with ignition. Moreover the moisture limit for self-supporting combustion, above which there is insufficient energy liberated to evaporate the moisture and heat the matter to the pyrolysis temperature, is 65% on a wet basis for most biomass fuels [65]. Practically speaking, trying to burn fuel with such a high moisture content will result in significant products of incomplete combustion, and an additional supplemental fuel would also be required (for example dry biomass or natural gas).

Biomass briquettes burning in a cookstove represent a similar system to what is referred to in the literature as a packed-bed of particles, and therefore it is likely to have analogous behaviour. The effect of moisture content level in the fuel for such packed-bed systems was investigated by Yang et al. [71], who identified that during combustion moisture evaporates via two mechanisms: convective drying by primary air, and radiation drying from the flame front [69]. Yang et al. found that the maximum rate of burning with a wet fuel can be several times lower than with a dry fuel, and that the combustion reaction zone decreases in size with increasing moisture content.

Volatile Matter and Fixed Carbon

The volatile matter represents the components of carbon, hydrogen and oxygen present in the biomass that when heated turn to vapour, usually a mixture of short and long chain hydrocarbons. It is determined by heating a dried ground sample of biomass in an oven at 900ºC for 7 minutes [72]. The amount of volatile matter in the biomass can then be calculated as percentage of the weight loss of the sample.

In almost all biomass, the amount of volatile matter is higher than in bituminous coal. Biomass generally has a volatile content of around 70-86% of the weight of the dry biomass [62], compared to coal, which contains only about 35% volatile matter. Consequently, the fractional heat contribution of the volatiles is more for biomass [73]. This makes biomass a more reactive fuel than coal [62], giving a much faster combustion rate during the devolatisation phase.

The volatile content has been shown to influence the thermal behaviour of the solid fuel [62], but this is also influenced by the structure and bonding within the fuel, and is therefore hard to quantify. Low-grade fuels, such as dung, tend to have a low volatile content resulting in smouldering combustion[10]. The consequences

---

[10]Smouldering is a heterogeneous flameless combustion process and occurs on the surface or within the porous fuel [74]. The combustion is incomplete and it results in significant amount of smoke and toxic gases being released.

of this for cooking on a woodstove are that the hot gases are less likely to impinge on the bottom of the pan and there will be less radiative heat transfer (because of the lack of flames), reducing the heat transfer efficiency [75].

After the volatiles and moisture have been released, ash and fixed carbon remain. The relative proportion of volatiles, moisture, fixed carbon and ash are often quoted for biomass fuels. The percentage of fixed carbon is normally determined by difference from the other quantities [73], and is given by:

$$\text{Fixed Carbon} = 100\% - (\%\text{ash} + \%\text{moisture} + \%\text{volititles}) \qquad (2.4)$$

Essentially, the fixed carbon of a fuel is the percentage of carbon available for char combustion. This is not equal to the total amount of carbon in the fuel (the ultimate carbon) because there is also a significant amount released as hydrocarbons in the volatiles. Fixed carbon gives an indication of the proportion of char that remains after the devolatisation phase.

Ash content

Ash is the non-combustible component of biomass and the higher the fuel's ash content, the lower its calorific value [62]. It is both formed from mineral matter bound in the carbon structure of the biomass during its combustion [66] (the inherent ash), and is present in the form of particles from dirt and clay introduced into the fuel during harvest, transport and processing (the entrained ash) [62]. The ash content is determined by heating a dry sample of biomass in an open crucible in a furnace at 900ºC. Depending on the type of biomass, the ash content can vary between 0.8% for groundnut shells [17], for example, to as high as 23% for rice husks [73] (for means of comparison pine wood has an ash content of around 1% [73]. Tables of data for a range of biomass residues are given by Demirbas [73].

Ash is known to cause problems in combustion systems, notably because of slagging and fouling, and its tendency to increase the rate of corrosion of metal in the system [62]. There have been various empirical indices which have been developed to try and quantify this undesirable behaviour by relating it to the composition of fuels. These have mainly been for fuels such as coal, and have proved of limited value for biomass. However, one simple index which has become popular is known as the alkali index. This expresses the quantity of alkali oxide in the fuel per unit of energy. Above a certain determined threshold, fouling is more probable. Straws and grasses, for example, have relatively high alkali indices, which is consistent with the high ash content of these fuels. Although

the alkali index does not fully describe the expected fouling behaviour, it is useful as a general guide [65]. Further details on the effect of biomass composition on ash formation are given in the review by Jenkins et al. [65]. If the alkali metals are removed from the biomass, it is known to increase the fusion temperature of the ash, the temperature at which it conglomerates together. Experiments have shown that this can be done by washing or soaking the biomass in water to leach the alkali metals, and this gives significant reductions in the fusion temperature of ash. In fact this simple technique has been shown to remove more than 80% of the alkali and most of the chlorine, which has the added advantage of reducing corrosion and acid gas emissions [76]. This is significant for the briquettes produced by the low pressure wet technique, described in Section 2.1.6, because, as part of the procedure, most biomass is soaked in water for a significant period of time, thereby leaching the alkali metals and producing briquettes which will burn with the aforementioned benefits. Nevertheless, the ash-fusion behaviour is important in determining the propensity for the formation of slag deposits, which can occur at temperatures around 1300ºC [66]. In practical cooking situations such temperatures would probably not be reached, and slagging of cookstove surfaces is unlikely to be experienced.

However, when fuels with a high ash content are burnt in cookstoves, the residual ash, if not mostly removed, will adversely affect the clean air flow in the cookstove. This must be taken into account in cookstove design, so that the stove performance is not significantly impaired due to inadequate air flow due to a build up of ash. On the other hand, a thin layer of ash helps in the distribution and preheating of incoming air, enhancing combustion efficiency. When biomass with a high ash content is burned regularly, the affect of the corrosive nature of ash on the cookstove durability would need to be considered [66], for example with rice husk briquettes.

Furthermore, ash can also have a significant influence on the heat transfer to the surface of the fuel, as well as affecting the diffusion of oxygen to the fuel surface during char combustion [77], and this is discussed later in Section 2.7.4.

2.4.2 The Ultimate Analysis

Ultimate Analysis involves the estimation of important chemical elements that make up the biomass, namely carbon, hydrogen, oxygen, nitrogen and sulphur. The basic method for doing an ultimate analysis is to burn a sample of biomass in a platinum crucible in a stream of air to produce carbon dioxide and water, the mass fractions of which are determined by gas-analysis procedures (for example

see [17]) and the percentage of C and H calculated [78]. If the ash and moisture contents are known, the amount of oxygen can be determined by the difference.

Analysis of biomass using this method reveals the principal constituent as carbon, which comprises between 30 to 60 % of the dry matter. After that, typically 30 to 40 % is oxygen. Hydrogen is the third main constituent making up between about 5-6%. Typically nitrogen and sulphur (and chlorine) normally make up less than 1% of dry biomass[11]. The composition of a wide range of selected biomass fuels is given by Jenkins et al. [65]. Compared with other fuels (such as coal or peat), biomass contains relatively high amounts of oxygen and hydrogen [62].

The resulting composition of biomass affects its combustion characteristics. The total overall mass decrease in the fuel during the volatile combustion phase of the combustion is increased as the hydrogen to carbon ratio of the fuel increases, and, although to a lesser extent, as the oxygen to carbon ratio increases [65]. In terms of energy available in the fuel, one significant collection of natural fuels shows a linear correlation of the heat of combustion at 400ºC with the carbon content of the analysis (cited in [79]). The high volatile content of biomass means it can lose over 90% of its mass in the develotisation stage of combustion, compared with coals which lose between 5 and 65% of their mass by this process.

2.4.3   Calorific Value

The calorific value (or heating value) is the standard measure of the energy content of a fuel. It is defined as the amount of heat evolved when a unit weight of fuel is completely burnt and the combustion products are cooled to $298K$ [80]. When the latent heat of condensation of water is included in the calorific value it is referred to as the gross calorific value (GCV) or the higher heating value. However, in stoves, any moisture that is contained in the fuel and which formed in the combustion process, is carried away as water vapour, and so its heat is not available. It is useful, therefore, to subtract the heat of condensation of this water from the gross calorific value. The result is known as the net heating (NCV) or lower heating value.

The heating value of a particular fuel relates to the amount of oxygen that is required for complete combustion. For every gram of oxygen burnt, 14,022 joules of energy are released. Consequently, fuels containing carbon with a higher degree of oxidation will have a lower heating value, because less oxygen is required for

---

[11]N.B. Nitrogen, Sulphur and Chlorine are significant in the formation of harmful emissions, and Sulphur and Chlorine have an effect on reactions forming ash.

their complete oxidation. In contrast, when fuels contain compounds such as hydocarbons, which have a lower degree of oxidation, this tends to raise the heating value of the biomass [65]. It is for this reason that biomass fuels, in which the carbon is present in a partly oxidised form, have a lower heating value than coal. There have been various attempts at correlating the heating value to the composition of the material, and it has been found that the higher heating value of biomass can indeed be calculated from elemental composition. For example the Vondracek formula originally developed for coal has been found to give a good approximation (see [81] for details).

The calorific value is limited by fuel moisture content, because, as discussed in Section 2.4.1, heat is used to vaporise the water, lowering the heat released. Furthermore, it is also limited by the ash concentration in a fuel; approximately every 1% addition of ash translates to a $0.2 \ MJkg^{-1}$ decrease in the heating value.

This section has given an overview of some standard analysis procedures for undensified biomass. Further details and references to the test standards are given by Jenkins et al. [66].

2.5 Considerations of Properties Specifically Relevant to Densified Biomass

When residues are formed into briquettes by compression, the bulk density of the material is modified, with the shape and size of the resulting block of compressed material determined by the mould used in the manufacture. There is potential for there to be, therefore, a large variation in these quantities between briquettes. The biomass properties described in Section 2.4 do not consider the effects of densification on biomass combustion behaviour. This section discusses the effect of density and briquette size, seeking to address this and gain a fuller understanding of the key factors influencing briquette combustion. Literature directly relating to biomass briquettes is limited, and therefore, where helpful other relevant combustion studies are reviewed and inferences made in relation to briquettes.

2.5.1 Material density

The material density of biomass can vary enormously, from around 100 kgm^{-3} for light dry straw, to over 2000 kgm^{-3} for highly compressed biomass fuels. It is a factor largely determined by the fuel manufacture, as was discussed in Section

2.1. The higher the density of the fuel, the greater the energy density. For a stoked fire, this therefore influences the ratio of energy input per unit volume into a cookstove's combustion chamber [62]. The fuel briquette's density will affect its bulk thermal properties: the thermal conductivity will be reduced as the density is decreased (increased fuel porosity), but the lower the density, the less heat is required for a specific volume of fuel to reach the ignition temperature. As a result the ignition time, and the rate of thermal decomposition will be affected. There is little data in the literature on the variation of the thermal properties of compressed biomass as a function of density, and how this relates to the rate of pyrolysis of large biomass particles. Although, Yang has carried out a study on biomass pellets in a packed bed and this does give a broad understanding of the behaviour to be expected: the general trend found is a decrease in burning rate for an increase in material density.

Yang also found [69] that the denser a material the thinner the pyrolysis reaction zone, which reduces the time that the reacting gases are *in this reaction zone*. This produces the interesting result of an increase in the concentrations of the gases CO, CH_4 and H_2 leaving the fuel surface for denser fuels. If valid for large biomass particles, it would be of interest in understanding the emissions performance of cookstoves in relation to the fuel. Furthermore, density might also affect the residence time of the gases within the *char matrix* of compressed biomass material; materials compressed to a higher density will tend to have a lower porosity, and the density of the final char, after devolatisation, might also have a lower porosity. This would increase the residence time of volatile gases in the porous char, leading to secondary reactions becoming more important [70]. This might also be a cause of a change in the emission characteristics with material density. In summary, there are therefore two key factors that changing the fuel density affects: the size of the pyrolysis reaction zone and the residence time of volatile gases in the porous char matrix.

In the combustion process of solid fuels the density is not constant; the density of wood is known to decrease continuously with the increasing degree of pyrolysis for a given volume. In general, the variation in local density is determined by the degree of advancement of the pyrolysis reactions and can therefore be calculated from kinetics data [82]. Figure 2.3 illustrates graphically how the density of the fuel might vary through a pyrolysising solid. Despite this variation, in Bamford's seminal study, the density was assumed constant throughout the combustion[83] and this produced satisfactory results in modelling the rate of pyrolysis. Kanury et al. [84] consider the pyrolysis process as the transformation of volatile filled pores in a carbon matrix changing into gas-filled voids, leading to an expression

for the density as a function of the degree of pyrolysis. They do not, however, apply this in a numerical model.

2.5.2 Briquette size and shape

In a similar experiment to the investigation of material density, with fixed primary air volume flow rates to the fuel, Yang et al. studied the effect of particle size, from 2 to 35 mm on burning rate in a fixed-bed [69]. Generally, it was found that larger particles have a lower burning rate. Another interesting observation was that larger particles emit lower CO levels at the top of the bed than smaller particles, with volumetric percentages ranging from 12 to 17%. It is interesting to note that Yang records that out of calorific value, particle size and material density, particle size has the strongest effect on burn rate, followed by material density with calorific value having the least effect. Altun et al. investigated the influence of coal briquette size and shape on the combustion kinetics [85] and reported size to be one of the most critical influencing factors. In the same work, it was reported that the effective activation energy for combustion had a tendency to increase as the briquettes were enlarged in size and volume, making the briquettes harder to ignite and to sustain burning. The geometry was found to be important too: it was observed that the activation energy tended to decrease as the length to diameter ratios approached unity when the size of briquettes was changed with and without the volume being kept constant. Likewise, when the briquette length to diameter ratio increased, and particularly to around 2, the activation energy was observed to increase significantly, making the combustion much more difficult. Although this thesis does not consider coal briquettes, Altun et al.'s study does give an indication of the significant influence of size and geometry on combustion behaviour, thereby suggesting the importance of its consideration in this investigation.

Biomass has a low thermal conductivity, and when compressed to form a large solid, this will lead to very steep temperature gradients as heat is transferred from the gas phase into the interior of the solid material during pyrolysis [70]. Therefore, with thick solids (say a log shaped briquette with a diameter approximately larger than 10cm) charring will occur on the surface a long time before the inner regions are dried, delaying the onset of pyrolysis within the briquette. It should also be noted that the larger the size of the solid the greater the likely residence time of the volatile gases within it, which is more likely to result in a greater extent of secondary pyrolysis reactions [70], and these might be exothermic. The consequence of this is that the simplest models of the kinetics, which assume a single one step global reaction, (discussed in Section 2.7.1) may not be found

adequate to describe the decomposition rate beyond a certain size of particle, when secondary reactions become more significant.

The Legacy Foundation, an American NGO, have produced manuals describing the low pressure briquetting technique. They suggest that the best shape to make a briquette is a cylinder with a central hole, commonly known as a holey briquette [33]. They suggest that the central hole acts as an insulated combustion chamber as well as a 'mini-chimney', giving a draught to drive the combustion and that its presence greatly improves the performance of the combustion compared to not having a hole [30]. However, there has been no rigourous study examining the effect of the central hole and its effect on the rate and efficiency of the combustion. This is an aspect which will be considered in this thesis.

2.5.3 Thermo-physical properties

In large biomass particles, the devolatisation rate is limited by the heat transfer rate, rather than the reaction kinetics. Therefore, a knowledge of the thermal properties of a solid are vital to understand factors affecting the burn rate. Heat can be transferred in a burning solid by several mechanisms: thermal conduction, convection of heat by the flow of volatile gases, and radiation within pores inside the solid. Heat transfer by thermal conduction is considered the most important of these three mechanisms. Its rate is controlled by the magnitude of the temperature gradient, as well as the materials thermal properties: its thermal conductivity, specific heat capacity and diffusivity.

In contrast to wood, which is anisotropic [84], briquettes are more isotropic in their nature because of the random distribution of the fibers in the feedstock used in the briquetting process. Their thermal properties will therefore also be more isotropic, allowing simplifications to be made in modelling their pyrolysis. This is discussed in Section 2.7.

Thermal conductivity (λ)

Ravi et al. found the thermal conductivity of an annular bed of compacted sawdust to be around $0.06 W m^{-1} K^{-1}$. Because of the nature of the material, compressed forms of other biomass residues are likely to have a conductivity of a similar order of magnitude. In order to show that thermal gradients within a briquette will be

important, the Biot number for a briquette can be calculated[12]. The result is Biot number greater than 1. The consequence of this is temperature gradients are set up within the pyrolysing solid [86] and heat transfer is, and must be modelled as, non-steady state.

In theoretical analyses, generally the thermal conductivity during pyrolysis is taken to vary in proportion to the temperature, moisture content, density and degree of conversion of the wood. Ragland et al. give an expression for the variation in conductivity of virgin wood which varies as a function of moisture content and temperature [66]. This can be used in developing a theoretical model of pyrolysis.

When pyrolysis has finished, a porous char remains. At room temperature this is reported to have a thermal conductivity of 0.052 $Wm^{-1}K^{-1}$ for maple, beech and birch [66]. Although this is in fact dependent on the char density, which in turn depends on the environmental conditions of the pyrolysis, such as the surface heating. Various authors note that experimental data detailing the variation of density, and hence thermal conductivity, with degree of pyrolysis, temperature and for different combustion conditions is not available and is needed [66, 82, 83].

Specific heat of dry biomass (c_p)

This is a measure of the average energy required to raise the temperature of a unit volume of the solid by one degree. As heat is transferred into the solid, this affects the rate at which material within reaches a sufficient temperature for pyrolysis to occur. For a particular solid, specific heat capacity varies with moisture content, temperature [66] and with the degree of thermal degradation, as pyrolysis progresses [84]. Ragland et al. give equations for the variation of heat capacity with moisture content [66]. However, measurements of the variation with respect to degree of thermal degradation is not discussed in detail in the literature, and therefore is an area that requires further work.

Thermal diffusivity (α)

From the above properties, the thermal diffusivity of the material can be deduced from the definition: $\alpha = \lambda/\rho c_p$. This is a measure of the ability of the compressed biomass to conduct thermal energy relative to its tendency to store thermal energy

---

[12]The Biot number can be found from: $Bi = hL/k$, where h is the heat transfer coefficient at the surface, L is a characteristic length and k the thermal conductivity of the material. A simple calculation can be made with approximations for L and h.

[87]. Therefore, the larger the value of α, the more rapidly the pyrolysis front will move into the compressed material.

2.6   Discussion

Biomass briquettes can be made from a myriad of different biomass materials; from woody matter, such as sawdust, herbaceous materials such as straws, grasses, through to agricultural residues like animal manure. There are various standard analysis procedures, which have been described, for the determination of different properties affecting the combustion behaviour of biomass. For instance, knowing the ash content will give an indication of whether the combustion system (for example a Rocket cookstove) is likely to clog up with a particular biomass fuel, allowing measures to alleviate the (potential) associated problems to be considered. The volatile content of the fuel gives an indication of its reactivity and whether a greater portion of the heat will be released with flaming combustion or by char combustion. Knowing the heat content will give an indication of the amount of energy available to be released from the fuel, and knowing the moisture content gives an indication of the amount by which the effective heating value is reduced. These properties alone are intrinsic to the biomass. However, they do not fully describe the combustion behaviour of a material in the form of a densified large particle.

This review has shown that there are other bulk material properties that are important in determining the combustion behaviour when biomass residues have been compressed. These are the density, size, shape and the bulk material thermal properties in the densified state. Density has been shown to be an important factor. As it increases, the rate of devolatisation has been demonstrated, in small particle experiments, to decrease. In terms of particles size and shape, for coal these have been shown also to be very significant in determining the rate, but this has not been fully investigated for large compressed biomass particles. Finally, the thermal properties of the compressed biomass change as a function of the density, moisture content, temperature and degree of degradation, but this has not been fully investigated in the literature. These are all important properties in determining how a briquette will burn. Briquettes have the flexibility that they can in fact be manufactured to different sizes and shapes, densities and dried to have different moisture contents (process dependent variables), which makes understanding the effect of these different properties, important in designing for a particular cookstove combustion system.

A method of comparing the burn rate of briquettes, and understanding the relative effect of both process and intristic material properties of large biomass particles (briquettes) in their densified state, is lacking in the literature. This, however, would be a helpful tool to allow meaningful quantitative comparisons to be made between briquettes with different densies, moisture contents, different sizes and shapes and made from different materials. These variables can, to a certain extent, be controlled in briquette manufacture. Changing these variables and assessing their affect on the burn rate will form part of the study of this thesis, and the methodology used for their investigation is described in Chapter 3.

It has also been identified that there is a lack of data in the literature on the thermal properties of biomass briquettes of different materials as a function of density, and there is no simple methodology that has been assessed for making these measurements for compressed biomass. From a scientific viewpoint, independent determination of these thermal parameters is vital for the verification and validation of combustion models. It has also been noted that there is a need for further work on the temperature dependency of thermal conductivity [66]. In Chapter 5 a methodology is suggested and preliminary results obtained in order to fill these gaps in the literature.

2.7 Modelling the Pyrolysis of Large Biomass Particles

In conventional modelling of the pyrolysis of large biomass particles, a model for heat transfer and mass transfer is coupled with a kinetic model that describes the chemical thermal decompostion reactions occurring during pyrolysis. It is the material properties discussed in the previous section that determine the characteristics of this thermal decomposition. This section is divided into two parts. In the first part, modelling the kinetics of the thermal break down of solid biomass is discussed. In the second part of this section, pyrolysis models for the decomposition of large solid particles, formed when biomass is compressed into briquettes, is reviewed and discussed. These are non-steady state models that couple the kinetic models, describing the thermal decomposition, with heat and mass transfer models.

2.7.1   Modelling pyrolysis

Pyrolysis begins when the components of the biomass, mainly cellulose, hemicellulose and lignin [65], become unstable with increasing temperature and begin to break down. This begins at about $250°C$ and leads to many chemical products being formed. It is a complex process, and the detailed reaction pathways of the reactions are not completely understood [65]. They depend on the aforementioned material properties as well as on environmental combustion conditions, such as the heating rate [88]. The general global set of pyrolysis reactions for cellulose are given by Jenkins et al. [65] and Zaror et al. [70].

Although detailed reaction pathways are not understood, the overall thermal decomposition process can be broadly classified into primary and secondary stages. The primary stage is thought to depend only on the temperature at the point at which the pyrolysis occurs [86]. The secondary reactions of the volatile gases occur within the solid as the gases flow out of the solid, and are dependent on other factors, such as the residence time of the gases within the solid; the larger the solid and the internal resistance of the char layer to gas flow, the greater the extent of secondary pyrolysis [70]. Therefore, the reactions very much depend on the porous structure of the char left after devolatisation. The details of all of the mechanisms involved and when they occur is not fully understood. However, Alfredo [89] concludes that although the physical structure of the material strongly influences the extent of secondary pyrolysis that occurs, this is not the rate limiting step, instead the rate is primarily dependent on the chemical characteristics of the sample and the rate of heat transfer to it. The secondary reactions are considered to be very exothermic [70], and thus heat generated from them will have a direct influence on the rate of both the primary and secondary decomposition stages. (See Section 6.5.3 for a further discussion on secondary reactions in relation to the briquette experiments carried out in this work).

Different models for the primary reactions have been introduced by authors. They range in complexity from a single overall reaction scheme to more complex sets of independent parallel reactions, and have been reviewed by Winter [90]. They do not, however, explicitly take into account secondary pyrolysis.

Modelling the kinetics and energetics of pyrolysis

In order to model pyrolysis, an understanding of the kinetics of the decomposition reactions is required. They are poorly understood, however, there are some schemes that have been successfully applied to describe the overall reaction [70].

The most common kinetic model for cellulose and wood pyrolysis assumes that the feedstock thermally decomposes via a single global reaction producing char and volatiles:

$$Fuel \xrightarrow[k_r]{} (1 - \Psi) \times Volatiles(V) + \Psi \times Char\ Residue(S) \qquad (2.5)$$
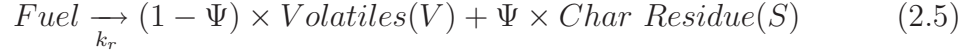
where Ψ and $(1 - \Psi)$ are the fractions of char and volatiles, k_r is the apparent rate constant. The rates of consumption and production are described by [77]:

$$\frac{dm}{dt} = k_r(1 - x)^n \qquad (2.6)$$

where x is the mass fraction (m/m_0), n is the reaction order and k_r can be expressed as:

$$k_r = k_0 exp(-\frac{E}{RT_s}) \qquad (2.7)$$

where E and k_0 are the apparent activation energy and pre-exponential factor, respectively and R is the ideal gas constant. Here, the kinetic parameters E, k_0 and n have no thermodynamic significance in these equations, but are obtained by fitting experimental data to the equation. Roberts et al. thermally decomposed specimens of wood under isothermal conditions showing that a first order reaction was an adequate approximation of the rate of the overall reaction [91]. In terms of its application in larger particle models, numerous authors have successfuly used it within wood combustion models, for example Bamford et al. [83], Tinney [92], Kanury et al. [84], Roberts [82] and Liliedahl et al. [93].

Some experimental values for E and k_0 for wood are given by Ragland et al. [66]. However, for large particles[13] there is not any real physical thermochemical meaning attached to these values, and they appear to be dependent on experimental conditions, the specific sample type, and its preparation [70]. Thus, although this method has been shown to give satisfactory predictions of the rate of devolatisation, it does not give any insight into the detailed chemistry involved. Furthermore, these simple kinetic models assume the final density of the specimen after devolatisation is known *a priori* (the char density). For known and constant environmental conditions, this assumption might be sufficient. However, the final char yield is dependent on the burn conditions and often the final weight is not known. Also, in this method, the composition of the volatiles is not distinguished.

---

[13]See Section 2.2 for a definition of 'large particles'.

Below, some more complex models that address some of these shortcomings, are briefly reviewed.

Other reaction models

Alfredo [89] suggests from experimental observation the existence of two overall reactions during wood pyrolysis that occur at different temperatures. This suggests a model where the wood is thought to be composed of two materials with distinctly different reactivities, which are thought to decompose independently of each other. Alfredo applied such a model to wood and cellulose pyrolysis under isothermal and non-isothermal conditions [89]. For wood, the model was able to predict the rate of volatile evolution during pyrolysis with some accuracy. However, this model, like the single reaction based model, is not capable of predicting the product yield. Therefore, these models are in fact of little practical use if the amount of final residue is not known in advance. One way of overcoming this problem would be to accumulate a large amount of experimental data for compressed biomass materials, for example, and find empirical correlations between the final char density and the various process conditions affecting it.

Franz et al. verified a model of wood pyrolysis where wood is assumed to decompose into gas, tar and char [94]. The applicability of the model to large particles burning independently or in a fixed bed has not been verified. Another reaction model, consisting of three independent steps to model the kinetics of decomposition, is described by Radmanesh et al. [95]. The model has been tested with various types of biomass, and the model is shown to predict the devolatisation behaviour successfully. It allows the effect of a different heating rate to be predicted, and enables a map of the key products during biomass decomposition to be made (the char, abundant gases H_2, CH_4, CO, CO_2 and liquids tar and water). This would be useful, for example, when modelling gasification, where the composition of the final pyrolysis gas products affect its heat content, or when the goal is to produce a high yield of pyrolysis bio-oil. It was also found to be very useful when trying to make predictions of biomass pyrolysis under different combustion heating conditions. Further details of these models and references to more complex schemes are given in Winter's review [90].

The complexity of the model needed very much depends on the application and the detail required. In the case of this study, experiments were conducted to compare the behaviour of different material properties under constant environmental combustion conditions. In terms of modelling the results, the objective was to predict and understand the parameters affecting the overall rate; a prediction

of the final char yield was not considered necessary. Therefore, for simplicity and because of its proven robustness in other studies, the simple one-step global reaction kinetic model described in this Section (2.7.1) was considered sufficient, and is applied in modelling the pyrolysis of biomass briquettes in Chapter 5.

2.7.2 Coupling kinetics with heat and mass transfer models

Pyrolysis models begin from the first premise that the primary transformations are thermally driven [86]. Conventionally, thermal models, which describe the time dependent temperature distribution, are coupled with kinetic models, as previously stated. This section overviews models of heat and mass transfer for large pyrolysising solids.

Briquettes, as discussed in Section 2.2, are defined in the literature as 'large particles', meaning the heat transfer into the solid is the factor limiting the rate of pyrolysis, rather than the chemical kinetics; the rate of devolatisation is in fact a function of local temperature [86]. This review presents an overview of the history of wood combustion models for such particles. It provides a background to understand the key processes and mechanisms involved in pyrolysis, and gives an idea of the complexity of trying to model the interactions that are involved. As stated earlier, the models discussed essentially vary in degree of complexity depending on the simplifying assumptions made by different authors. The review in the following section begins by looking at a model introduced by Bamford et al. [83].

Heat transfer models for pyrolysising solids

In a pioneering study Bamford et al. presented a simple general model of pyrolysis [83]. The model is based on the assumption that devolatisation is thermally driven, and the rate can be described by the simple unimolecular law described in Section 2.7.1 (Equation 2.6). It combines these kinetic equations for rate of decomposition, with those describing heat transfer into the solid by conduction, and includes an additional term taking into account the production of heat by exothermic reactions, which are assumed to occur when the pyrolysis gases are released. Equations were solved by a finite difference method. As pyrolysis gases are produced Bamford et al. assumed that they are able to leave the solid matrix immediately on formation, without any thermal interaction with the solid char.

The relative importance of internal and external heat transfer and the pyrolysis kinetics is described by Pyle and Zaror [86], and it allows simplifications to be made to Bamford's model [86] in different situations. For example if the rate of internal heat transfer is very fast compared with the pyrolysis rate, then the temperature in the solid could be considered to be constant.

Various authors have applied Bamford's model [89, 91, 92]. Kung [63] adapts the model to incorporate the convective-heat transfer due to the outward flowing volatiles including terms to account for an endothermic nature of pyrolysis. The gases are assumed to leave the solid without resistance or accumulation in the material pores. Perry et al. [84] gives a Peclet number[14] for heat transfer in the solid, as the ratio of the energy flux transferred by volatiles by convection to the heat transferred by conduction. For circumstances where the heat transfer by convection of the volatiles out of the solid is small compared with conductive heat transfer, this ratio will be small, and the assumption to neglect volatile flow is valid. However, for cellulose cylinders burning in air, their analysis suggests that neglecting the convective term could cause a misrepresentation of the heat flux into the specimen, and that this would become more pronounced as specimen size increases. Fan et al. [96] investigate the pyrolysis of a solid reactant to both a fluid and soild product, and introduce a term in the energy equation to take into account heat transport due to mass diffusion. Kansa et al. [97] introduced the idea of the momentum equation for the motion of volatile gases within the solid, accounting for non-zero pressure gradients and non-uniform convective gas velocities. The model takes into account the percolation of volatiles, and the resulting convective heat transport into both the cold and hot char regions as well as into the cooler unburnt material.

Maa et al. [98] were the first to apply the heat conduction equation with a heat convection term in a shrinking core formulation. In their model, pyrolysis is assumed to take place at the surface of an unreacted shrinking core of material, which is surrounded by reacted material; the char. With respect to pyrolysis, char is thought to be inert, and hence pyrolysis is thought to occur at the interface between two solid regions. The thickness of the pyrolysis front is assumed to be negligible giving a sharp interface between the unreacted material and the reacted char layer. This assumption is valid for high temperature gradients within the solid. In this study Maa et al. completed a sensitivity study of different parameters concluding that for large particles the four most significant variables on the rate of pyrolysis are the temperature at the reaction front, the activation

---

[14]A dimensionless number that relates the rate of advection of a flow to its rate of its thermal diffusion.

energy for pyrolysis, the kinetic constant, and the bulk density of the material. To account for simultaneous moisture content evaporation, devolatisation and ash production in the burning of large particles, Souza Costa et al. [74] apply the idea of a thin advancing front in their model for a one-dimensional semi-infinite log. They presented a steady state model in which the log is divided into four advancing regions: (1) the moist or unburnt fuel zone, (2) the dry fuel zone, (3) the char zone and (4) the ash zone. They then solve the energy equation for each zone, considering heat conduction, convection and radiation in the porous matrix of the log, with external radiation and convection around the log. The theoretical burning rates showed good agreement with experimental data for a smouldering log. Although the study is for smouldering, rather than flaming combustion, the method of modelling the pyrolysis process in defined zones is interesting, because it provides a systematic way to model the processes of moisture evaporation, char combustion and devolatisation of the material simultaneously for large particles. Roberts presents a simplified model with a front advancing at a constant speed into a virgin solid [82].

Di Blasi has developed a very comprehensive one-dimensional model taking into account the main processes occurring in a porous particle [99]: heat transfer by convection, conduction and radiation, the convective transport and accumulation of volatiles and gas pressure and velocity variations. De Blasi goes on to employ this model in a theoretical investigation of the effects of the variation of physical properties (density, thermal conductivity, specific heat capacity, permeability of the solid to gas flow) on the product yield and conversion time in pyrolysis of biomass. However, this model is not verified experimentally.

There is limited work modelling specifically large particles of densified biomass (briquettes). However, Ravi et al. do present a semi-empirical model for pyrolysis in a compacted bed of sawdust [100]. Simliar to Bamford et al.'s work, the model assumes a single first-order reaction scheme. The model assumes heat transfer purely by conduction and therefore ignores heat transfer by the volatiles of the bed. They suggest a simple model for calculating the thermal conductivity of the bed as a function of void space, thermal conductivity of the char, sawdust and bed moisture content. A sensitivity study in this work, reveals how important a knowledge of the rate of thermal heat transfer and the parameters affecting it are. They suggest that the reason for the discrepancy between their experimental data and the model prediction, is that the flow of volatiles in the char are in fact involved with heat transfer and secondary pyrolysis reactions. Further work is thus required to address the shortcomings of their study, and to more fully understand pyrolysis behaviour of compacted biomass.

Many of these models are essentially attempting to refine the assumptions made by Bamford et al. in their seminal model [83], taking into account other physical processes that were not considered. Often, however, they are computationally intense, and have limited experimental validation, especially of the individual mechanisms they attempt to model. Experimental validation that does exist focuses on the application of the model to just one given material (for example a particular species of wood) which has a constant density . Biomass briquettes provide a means to more rigorously validate (or invalidate) existing combustion models, in terms of their accuracy in predicting combustion behaviour as a function of different material properties. Specifically, properties that would be difficult to vary experimentally when wood is used can be much more easily varied when briquettes are used. For example, briquettes of the same material can be pressed to different densities, which will modify the thermal diffusivity of the compressed material. There is also a lot of flexibility in the shape and size of the briquettes which can be formed. Models have not been experimentally tested over such property variations of a single material.

It is concluded that an appropriate and simple combustion model needs to be developed or adapted for briquettes. It should then be experimentally verified for different densities, moisture contents, sizes and geometries of briquette.

2.7.3 Thermal parameters in modelling

In developing a model, it is important to choose sensible values for the thermal properties of the material pyrolysising and know their dependency on the degree of charring and temperature. This allows the physical validity of the model to be assessed. Moreover, from a scientific viewpoint, the model can only be verified through experiments in which the thermophysical parameters are measured or estimated independently of the model and not derived through the fitting of a model to experimental data [93].

Below, the specific heat, thermal conductivity and thermal diffusivity are considered.

Thermal conductivity

Thunman et al. suggest that effective thermal conductivity is one of the most important parameters for modeling thermal decomposition. Some analyses assume a thermal conductivity that varies in proportion to density. However, although this assumption simplifies computation, it neglects the effects of increasing

temperature and varying structure during pyrolysis [82] and receives no direct experimental support. Saastamoinen [101] presents a model for the variation of local thermal conductivity in the particle using an analogue to net electrical resistance, the effects of moisture are also included. Thunman et al. suggest another mathematical model for the variation of thermal conductivity of wood during conversion based on the pore structure in the wood [102]. Again, there is no significant experimental validation for these models.

Specific heat of dry biomass

Roberts [82] suggests for wood, that after pyrolysis, the specific heat would change very little. He argues that at $20°C$ wood has a specific heat of about 1.4 $Jg^{-1}K^{-1}$, which is shown to increase with temperature, but decreases with the degree of pyrolysis at a particular temperature. Complete pyrolysis leaves a char with approximately 90% carbon content. Since the specific heat of carbon at $500°C$ is 1.6 $Jg^{-1}K^{-1}$, the change of specific heat on heating wood from a temperature of 20 to $500°C$, and its consequent conversion to char, is likely to be minimal. As a first approximation, this property can therefore be assumed to be constant.

Thermal diffusivity

In their model of wood combustion, Bamford et al. simplify the problem and assume a constant thermal diffusivity as a function of the degree of charing, with satisfactory agreement with experiment [83]. Such an assumption might be valid for models that simply aim to predict the burn rate and heat output, as required in this work. However, models seeking to more fully understand the change in thermal properties and the effect of this on the decomposition process will need to be more complex. One simple model of the change of thermal diffusivity with the degree of degradation is suggested by MacLean (cited by Perry et al. [84]). It arrives at the following relation to calculate the change in thermal diffusivity as a function of the density during degradation, which Maclean claims to be accurate enough for all practical purposes:

$$\alpha = r - x\rho \tag{2.8}$$

where r and x are constants which depend only on the type of wood and the environmental heating conditions.

2.7.4   Char combustion

During the flaming combustion stage of a solid when devolatisation is occurring, the outflow of volatile gases has been shown to inhibit the diffusion of oxygen to the char surface, limiting char combustion (see Section 2.3). In a combustion model, during the devolatisation phase, it is, therefore, reasonable to ignore char combustion. However, in a stoked cookstove, where a number of particles are burning simultaneously, it cannot be ignored. Although it can be modelled separately from the pyrolysis, rather than as a coupled mechanism (because particles that are devolatising can be assumed not to be burning by char combustion). Here, a brief overview is given of char combustion.

A char matrix is left as pyrolysis occurs, and volatiles are released from the compressed biomass material [103]. The char burns by reaction with oxygen, giving the primary products of CO and CO_2, with the ratio of these two components determined by the temperature level [69]. Char combustion can therefore be, to a close approximation, described as follows:

$$C(s) + \Lambda O_2 \longrightarrow 2(1 - \Lambda)CO + (2\Lambda - 1)CO_2 \qquad (2.9)$$
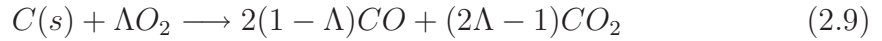
where Λ is a value between 0 and 1 and is a function of the gas phase temperature. Char combustion has been modelled using a shrinking core approach, where the reaction is assumed to occur at the outer skin of the particle and move into the unreacted solid. As this occurs, an inert solid is left behind, known as ash. In this model a thin gas film is imagined surrounding the particle, the gaseous reactants diffuse through this film, and then through the blanket of ash, to reach the unreacted core. After the reaction takes place, the products diffuse back through the ash layer to the exterior of the solid and then through the gas film into the main body of the fluid [104]. This model assumes the reaction to take place on a sharp interface between the ash and the unreacted solid, whereas the reaction may well occur along a diffuse front. The combustion rate is assumed to be controlled entirely by oxygen diffusion through the gas boundary and ash layer; the model does not take into account temperature gradients set up within the particles and between the particles and the bulk fluid.

Biomass briquettes can be made from a large range of different residues, which will have different percentage ash contents, and where the ash will have very different elemental compositions (see [65]). In a study on 'biocoalbriquettes' [77] (briquettes manufactured from a mixture of coal and biomass under high pressure compaction)

Kim et al. reported a close experimental correlation between the effective diffusion coefficient of oxygen in the ash layer and the porosity in the ash layer such that:

$$log(D_a) = 1.757\epsilon_{ash} - 5.5546 \qquad (2.10)$$

where D_a is the effective diffusion coefficient of oxygen through the ash layer, and ϵ_{ash} is the porosity in the ash layer defined by:

$$\epsilon_{ash} = 1 - Ash_b \frac{\rho_b}{\rho_{ash}} \qquad (2.11)$$

where Ash_b is the ash fraction in the biocoalbriquette, ρ_b is the density of the biocoalbriquette and ρ_{ash} is the density of the biocoalbriquette ash (for further details of the calculations see [77]). Ash content thus is likely to influence the char combustion rate.

It was found that as the compression pressure increased, the porosity of the char layer was found to decrease until a certain point was reached after which it remained nearly constant. It is also suggested that the higher the volatile content, the more pore void space will be created after devolatisation, meaning a higher porosity [77]. For biomass briquettes, where the compressive pressure can be controlled and the volatile content varies between residues, considering these factors is important when trying to understand and model char combustion.

2.8   Summary and Discussion

A review of the manufacture of briquettes has been presented that identifies the factors that need to be considered in producing repeatable and consistent briquettes. These details inform the methodology presented in Chapter 3, designed to provide briquettes with consistent controlled properties for use in this study. Much of the work into briquette manufacture has focused on producing briquettes at high pressures (greater than 5 MPa). In rural areas of developing countries, simple hand-presses cannot achieve sufficient pressure for amalgamation of most biomass residues in their unprocessed state. A wet-briquetting technique was identified in which the natural fermentation of the fibres is used to break them down and form a pulp before briquetting them. This has been shown to work particularly well for more fibrous residues. However, there is a hole in the literature regarding the influence of briquette feedstock moisture content on final briquette dry density. This needs to be understood in order to know the extent to which

it needs to be controlled in the manufacture of controlled repeatable briquettes. This is addressed in Chapter 3.

Different parameters used to classify the combustion properties of loose biomass were highlighted. Large particles of compressed biomass were then considered. It was found that most of the literature to date has focused on the combustion modelling of wood, and there is a gap in the literature regarding studies on biomass briquettes with varying bulk properties such as density, size and geometry. In order to address this, a systematic method is required to be able to quantitatively and systematically compare the combustion behaviour of briquettes with different physical properties. In Chapter 3 an experimental methodology is presented to achieve this goal. Chapter 4 then aims to link the physical characteristics of the briquettes; the briquette density, moisture content, briquette size and shape, to some of the burning characteristics; the burn rate, and therefore power output, total burn time, in a more general way. Experimental work is conducted in order to investigate the effects of these different parameters, establishing the degree of importance of different factors.

There are other parameters that are likely to vary between briquettes of different materials and densities, but these are more difficult to investigate experimentally. In particular, the literature has revealed that there has been little systematic work on the effect of changing material thermal properties on the burn rate for biomass briquettes. An analytical model would provide a means by which material parameters can be varied and behaviour investigated in much simpler ways. A simple, appropriate and tractable method was required, which would allow the prediction of the experimental data in Chapter 4, giving a physical explanation for the behaviour of the observed experimental results, and providing a means to investigate factors that are very difficult to control experimentally. In order to identify the simplest approach, Bamford's model was chosen instead of the more complex options. This could be, if necessary upgraded to include additional factors (and the effect of including each factor identified, and its importance assessed). Moreover, the potential of briquettes to test the robustness of a simple model over varying material properties could be exploited.

A semi-empirical model is presented in Chapter 4 based on Bamford's approach. It uses a global first order one-step kinetic reaction, as described, which has been found to be an acceptable approximation by many authors modelling wood combustion. However, in order to use this model to investigate the relative effects of the thermal parameters (thermal conductivity, heat capacity, thermal diffiusivity), realistic values were required. It was found, however, that there is a

lack of thermal parameter data in the literature for compressed biomass residues at different densities, moisture contents and temperatures. This is addressed in Chapter 5 by the adaptation of a heat-probe method from the soil literature, which is able to measure the thermal conductivity and heat capacity of a sample simultaneously. Some preliminary data was obtained. The method provides a helpful tool for briquettes, by which further data can be found for use in future studies.

In the chapter which follows, an experimental methodology is developed to compare the burn rate, combustion temperature (and in the future potentially to compare emissions characteristics) of different biomass materials in a densified state. It allows the effect of different properties to be systematically investigated and their relative importance determined. In particular, the method is used in Chapter 4 to investigate the effect of briquette density, and geometry on the rate of pyrolysis.

Chapter 3

Methodology

In this study, an approach was taken in which experimental work was conducted before modelling in order to establish the effect and relative importance of different factors on the rate of combustion. A model was then developed based on Bamford's approach [83] to analyse the experimental data and provide a physical explanation for the behaviour of the observed experimental results (Chapter 5). The model also provides a means to investigate factors that are very difficult to control experimentally, such as the influence of changes in material thermal properties (conductivity, heat capacity and diffusivity). This chapter focuses on the practical experimental approach to realise the above, while the analytical model is introduced in Chapter 6.

The manufacture of briquettes in rural locations is the central interest of this study. It is possible to form briquettes from waste crop residues, in rural locations of developing countries with limited equipment, using a wet process with a hand operated press [44], as discussed in Chapter 2, Section 2.1.6. In this study, the aim was to investigate the combustion behaviour of briquettes formed by this low-pressure method, which is much more accessible to poorer communities than high pressure processes (see Chapter 2). To do this in a rigorous way, it is important to be able to form briquettes of a reproducible nature, and burn them in a controlled way. A methodology was, therefore, required to produce briquettes with a similar process to hand made briquettes (in terms of pressure and method of pulping the feedstock residue), but more consistently, in order to enable parametric studies to be carried out and trends in combustion behaviour observed. The first part of this chapter explains how the briquettes were manufactured. It considers how feedstock material was prepared to produce a consistent pulp, and how the briquettes were formed in moulds, under compressive pressures achievable with simple hand presses. In order to know to what extent the wet feedstock moisture

content had to be controlled in pulp preparation, a short study was completed on the influence of the moisture content of the pulped residue on final briquette dry density.

In the second part of this chapter, the experimental technique used to systematically evaluate the combustion characteristics of briquettes is presented. The method provides a means to systematically carry out parametric investigations on the combustion characteristics of densified biomass (see Chapter 4). Results obtained from these tests are used in Chapter 5 to develop a simple numerical semi-empirical model of the rate of release of volatiles from the fuel surface as a function of fuel properties and the surface heat flux.

3.1 Briquette Preparation

3.1.1 Residue selection

This study requires a ready supply of consistent material from which to manufacture and test briquettes. Although not a crop residue, newspaper was chosen as the feedstock material for this study: paper is a cellulose material made from wood, and therefore considered to be biomass [65]. It is readily available in the UK, and is easy to break down and bond. Furthermore, because of its fibrous nature it was thought likely to behave in a similar way in the densification process to other fibrous organic residue matter, such as maize husks after they have been partly decomposed; it is this type of crop residue material that is more likely to be readily available for briquetting in rural locations[1] (see Chapter 1). A large number of out-of-date newspapers from the same printing batch were sought, this would minimise variations in the results that might have been caused by inhomogeneity of material between batches.

3.1.2 Residue pulping

In order to form briquettes from an agricultural residue, the structure of the material needs to broken down and pulped to give a random distribution of unconnected fibres, before it can be reformed into briquettes. Residues need

---

[1]N.B. In Chapter 4, the combustion behaviour of newspaper briquettes is compared to that of sawdust briquettes (manufactured in the same way as described here, but using a starch binder), and industrially produced rapeseed oil briquettes. It is observed that the combustion behaviour of the different fuels follow similar trends, suggesting that the results from one fibrous material are probably representative of a broad range of other fibrous materials.

to be chopped, partly decomposed, soaked and pulped in order to form a charge of wet material for the mould. In a rural situation this might involve firstly hand pounding using a large mortar and pestle, or using manually driven threshing/chopping technologies, followed by partial decomposition of the material, which might take between two and six weeks depending on the local climatic conditions. These can then be mixed with water and pulped (see [33] for more details on this process). Newspaper is quicker to break down than many agricultural residues, and after only around 5 days soaking it is ready to pulp.

In this work a large batch of newspaper was obtained from a single source. It was shredded with an electric paper shredder and then soaked for at least 5 days. The excess water was then drained off and the remaining matter was pulped in an industrial food mixer (M20-A mixer 0.75kW) for about 10 minutes until all the paper had broken down and the mixture had reached a uniform consistency. During this pulping process, a quantity of water equivalent to the mass of drained pulp was added; it was found from experience that this produced a pulp that was easy to handle for loading into briquette moulds.

Moulds and loading the charge

Moulds and plungers were manufactured to form the briquettes: cylindrical moulds (of different dimensions) with a central solid cylinder passing along the central axis, to form briquettes with a central hole (holey briquettes); and large rectangular shaped mould (150x150mm) to form a large briquette, that could be cut into smaller slabs. In order to control the mass of charge used for each briquette, the pulp was weighed, before being loaded by hand.

3.1.3   Residue compression

The briquettes were formed by compression of the pulp in the mould with an Instron compression test machine (see Figure 3.1). A range of pressures between 0.1 and 2 MPa was used to form briquettes with densities between 200 and 500 kgm^{-3}. For a briquette with a diameter of 60mm, the lowest of these pressures could be achieved by hand pressure alone and the highest would be attainable using a double action press (see the Legacy Foundation press in Figure 2.2b). The compression speed was initially set to 10 mm/min, while measuring the resultant compressive force (and therefore pressure). The piston was lowered, compressing the pulp, until the desired pressure was reached. It was observed that if the compression piston was held stationary at this point, the resultant force on the

Figure 3.1: The Instron compression machine used for forming the briquettes. A cylindrical mould used to form briquettes with a central hole can be observed. Notice the small holes riddled around the mould to allow the expulsion of water from the pulp during compression.

piston (equal to the force applied by the piston and therefore proportional to the pressure) would reduce as water flowed out of the pulp. In order to keep a constant pressure during this water expulsion and relaxation phase, the speed of the compression piston was continually reduced, according to the rate of relaxation, keeping the resultant force on the piston constant. This was done until the compression speed reached zero; this occurs when the water is no longer being expelled, and the relaxation of the material has stabilised. The pressure was held for 20 seconds. With this method, it was found briquettes could be formed with a density reproducible within $\pm 12 kgm^{-3}$ (this figure was arrived at for briquettes produced with measured final dry densities ranging from 250 to 350 kgm^{-3}). The associated uncertainty is due to a combination of factors, such as variations in the amount of charge in the mould, the control of the compression velocity by the operator, and includes the uncertainty associated with the measurement method used for the determination of the dry density of the final briquette (see Section 3.1.5).

3.1.4   Drying briquettes

After the briquettes have been ejected from the mould, they need to be dried. If left in the open air, the moisture content of the briquette will fluctuate depending on the climatic conditions of the drying environment; as the temperature and humidity change, the rate of change of moisture in the briquette will be affected. Thus, it is a difficult variable to control, especially between different batches of briquettes. If meaningful comparisons are going to be made of the effect of process variables, then this parameter needs to be carefully controlled. In order to do this, the briquettes were dried in a temperature controlled environment, by placing them in a thermostatically controlled oven at 373 K (105° C). The onset of pyrolysis starts at approximately 550K [88], and therefore does not occur at this drying temperature. The briquettes were oven dried to reach 0% moisture content (for further details of the British Standard detailing the procedure see [68]). The majority of the combustion experiments undertaken in this study were conducted with oven dried samples. On removal from the oven the briquettes were placed in a sealed container with silica gel (a desiccant, which when placed in a well sealed space will minimise the humidity) and were allowed to cool to room temperature. Figure 3.2 shows a slab briquette and cylindrical briquette with a central hole after they have been removed from the oven.
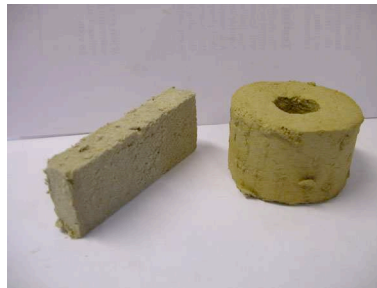
Figure 3.2: An example of the two geometries of briquette investigated.

3.1.5   Determining briquette density

All irregular parts of the briquette were removed by cutting and sanding, and they were again placed in the oven to drive off any moisture that had been absorbed during this process.

A stereometric method [105] was used to determine briquette density. This was chosen over displacement methods in order to ensure the briquettes, which would later be burnt, remained dry and were not structurally affected by the

measurement. In this stereometric method the briquettes were weighed using a mass balance, which had a precision of $\pm$ 0.01g. The dimensions of each briquette (see Figure 3.3) were measured using callipers as follows: for slabs, the height and width of the briquette were measured at three approximately equally spaced positions along each side, and the mean calculated. The thickness was measured at each of the four corners of a slab and the mean taken. For cylindrical briquettes with central holes, the height was measured in four positions (90° to each other around the briquette), the external diameter of the briquette was measured in three positions (at the top, middle and bottom). The diameter of the internal hole was measured twice at both ends of the briquette (with the two measurements at perpendicular orientations). The volume of the nearest geometrical shape was then calculated and hence the density determined[2]. Briquettes were then put back in the oven for a short time to drive off any atmospheric moisture that may have been absorbed, and then transported in a sealed silica gel filled container to the combustion rig to be burnt immediately.
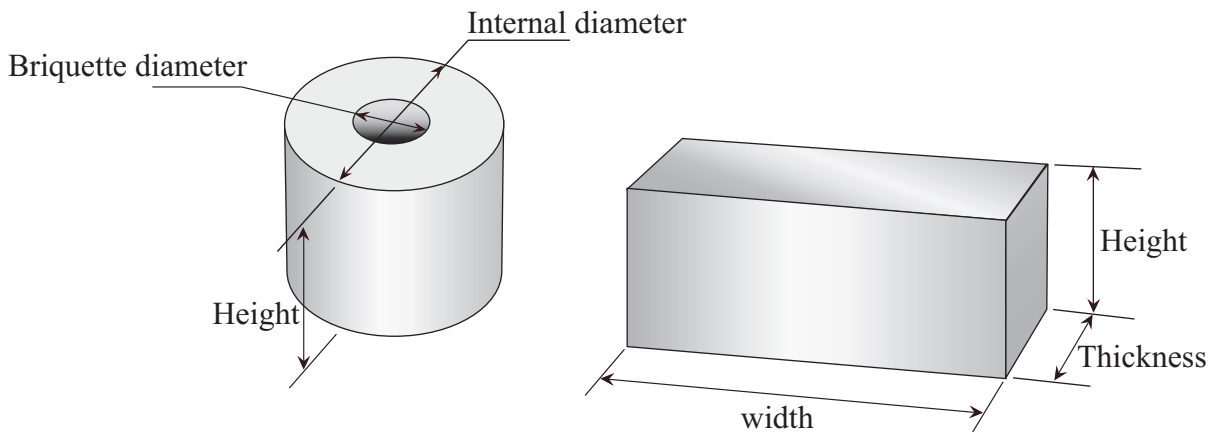
Figure 3.3: The dimensions measured for a slab briquette and a cylindrical briquette with a central hole.

3.1.6   The re-addition of moisture to briquettes

In Chapter 4 an experiment was carried out investigating the effect of briquette moisture content on the normalised burn rate. In order to control the moisture content, briquettes were first oven dried, as described in Section 3.1.4, and water was then re-added to the briquettes in a controlled way. The dry mass of the briquette and its mass after the addition of water can be found by weighing, and

---

[2]For example, for a slab shaped briquette the equation for a cuboid was used to approximate its volume.

thus the moisture content of the briquette on a dry basis[3] is easy to determine. The procedure adopted was as follows: the briquettes were weighed on a mass balance and the dry mass recorded; different quantities of water were then measured out with a pippette and left on the surface of the briquette to be absorbed; the briquettes were then sealed in small air-tight bags and left for 10 days for the moisture to diffuse throughout the material; each briquette was then weighed again, and the resulting moisture content (dry basis) was recorded before they were burnt in free air as described in Section 3.3.

3.1.7 Summary of range of briquette dimensions tested in this study

Table 3.1 gives a summary of the range of dimensions of slab shaped briquettes made from different materials tested in this study, while Table 3.2 gives the range of dimensions for newspaper cylindrical briquettes with a central hole. Maximum (max) and minimum (min) values of the briquettes are given for each dimension, indicating the range tested. A more detailed breakdown of each of the briquettes used in the investigation is given in Appendix A.

	Newspaper	Rapeseed oil residue[*]	Sawdust	Pinewood
Height_{max} $[mm]$	70.93	54.1	53.98	64.16
Height_{min} $[mm]$	32	35.54	33.28	33.42
Thickness_{max} $[mm]$	26.65	6.45	16.98	7.87
Thickness_{min} $[mm]$	10.3	2.03	10.13	2.28
Width_{max} $[mm]$	90	104.99	92.36	113.89
Width_{min} $[mm]$	76.32	69.72	89.46	109.61
Density_{max} $[kgm^{-3}]$	407.6	1082.1	286.8	522.9
Density_{min} $[kgm^{-3}]$	184.5	971.8	253.7	435.8
A/V_{max} $[mm^{-1}]$	0.278	1.041	0.256	0.927
A/V_{min} $[mm^{-1}]$	0.131	0.373	0.178	0.303

Table 3.1: A summary of the range of slab shaped briquettes used in the study.

[*] The briquettes made from rapeseed oil residue were commercially purchased, see Section 4.4 in Chapter 4 for details of how these were used.

---

[3]Moisture content on a dry basis is defined as the percentage moisture of a sample calculated relative to the dry weight of the sample.

	Newspaper
Height$_{max}$ [mm]	61.28
Height$_{min}$ [mm]	13.26
Thickness$_{max}$ [mm]	80.03
Thickness$_{min}$ [mm]	42.21
Width$_{max}$ [mm]	44.29
Width$_{min}$ [mm]	20.93
Density$_{max}$ [kgm^{-3}]	508.4
Density$_{min}$ [kgm^{-3}]	211.5
A/V$_{max}$ [mm^{-1}]	0.267
A/V$_{min}$ [mm^{-1}]	0.107

Table 3.2: A summary of the range of cylindrical newspaper briquettes with a central hole used in the study.

3.2 Experimental Study of the Effect of Pulp Moisture Content on Briquette Final Density for the Wet-Briquetting Process

In the low-pressure wet briquette manufacturing process, the moisture content of the pulp can vary significantly, depending on how much water is added during the processing by the producer. What is not clear from the literature, as highlighted in Chapter 2, is the effect of pulp-moisture content on final briquette dry density. The relative magnitude of the influence will determine the extent to which the charge moisture content must be controlled in the briquette manufacturing process; the objective is to produce briquettes of a reproducible density in order to allow the systematic investigation of various process variables. In this section, a simple experiment is carried out in order to address this gap in the literature and inform the methodology.

3.2.1 Methodology

Material preparation

Newspaper was shredded in an office paper shredder and left to soak in a bucket for a week, as described in Section 3.1.2. The paper was then removed from the bucket and the excess water allowed to drain off. The mass of paper was then divided into three containers. To the first container a mass of water equal to half the pulp mass was added, to the second container a mass of water equal to the

mass of the wet pulp, and to the third, a mass of water twice the mass of the pulp was added. Each of these three mixtures was then blended in an industrial food mixer. Samples of pulp from each of the three buckets were taken, and the moisture contents determined by the oven dry method (see Section 3.1.4); in this way, the different moisture content of the three charges to be loaded in the moulds was determined.

Material compression

The pulp was loaded into a cylindrical mould with an external diameter of $63.4mm$ and a central hole diameter of $22.4\ mm$ (the height of the briquette can be varied by changing the charge mass in the mould). The briquettes were formed by compression at $0.76MPa$[4], and were oven dried at 105^oC (see Section 3.1.4). The relaxed density of each briquette was measured as described in Section 3.1.5. The results are recorded in Table 3.3.

3.2.2   Results

Table 3.3 gives a summary of the results. The moisture value given for each sample is the average moisture content obtained from repeats of the oven dry method on each of the different pulps. The consequence of these results on the methodology is described in the next section.

3.2.3   Discussion and conclusions

A student t-test was carried out on the three independent data samples above, with different pulp moisture contents. The results of this suggest that there is not a statistically significant difference between the three means. Consequently, this suggests there is no statistical correlation observed between the final dry density and the initial moisture content of the pulp across the three pressures tested. It can therefore be concluded that for newspaper, the amount of moisture in the pulp does not have a significant effect on the density of the final briquette in

---

[4]A compressive pressure was chosen here to be representative of what might be achievable in a rural location, with a woman forming briquettes with a simple leaver press. $0.76MPa$ corresponds to a woman with a weight $650\ N$ pushing with a force equivalent to a third of her weight on a $1m$ length lever with the briquette sample placed $0.3\ m$ from pivot point, using a mould with the same dimensions as above. The force was estimated based on women, because it was ascertained from the literature that in many developing countries women are the primary collectors of fuel wood and have responsibility for cooking in the home [106], and would therefore be more likely to be the ones making the briquettes.

| Mean | Briquette Dimensions [mm] | | | Mould | Relaxed density $[kgm^{-3}]$ |
moisture [%]	Height	ED	ID	charge* [g]	(dry briquettes)
650	29.48	61.86	22.15	200.0	344.81
650	36.56	61.53	21.98	250.0	360.73
650	43.62	61.51	21.93	300.0	356.04
815	30.97	61.46	21.99	266.6	348.55
815	35.44	61.52	22.21	300.0	353.37
815	43.60	61.43	22.14	400.0	339.80
1300	22.38	61.78	22.07	300.0	350.50
1300	26.21	61.61	22.05	350.0	337.58
1300	27.59	61.70	22.22	400.0	354.09

Table 3.3: Experimental results of the effect of pulp moisture content on final relaxed density. *The mass of wet pulp in loaded into the mould

the range tested. Furthermore, the mass of charge loaded in the mould did not have a statistically significant effect on the final density of the briquettes. These results are important because they suggest that for newspaper pulp, the moisture content does not have to be carefully monitored in the production process, and therefore, can be chosen to have the best handling characteristics for loading it into the mould. Pulp with a very high moisture content is sloppy and difficult to handle, and for a manual process where the operator is loading the pulp into the mould by hand, it might not be the most suitable consistency. However, for an automated process a very wet pulp that will flow easily into a mould could be very beneficial. Moreover, the higher the moisture content of the pulp before pressing, the greater the proportion of the mould volume taken up by water. Therefore, when using pulp with a lower moisture content, higher mass, or taller briquettes can be manufactured using a smaller mould. However, if the moisture content is too low, the mixture will be crumbly and difficult to load into the moulds. It was found that adding approximately a mass of water equal to the drained mass of pulp produced a mixture that bonded well, and was easy to handle.

The above results concerning the amount of pulp loaded in the mould is useful, because it means that within reasonable practical limits of $\pm$ several hundred grams, the charge mass that a user loads in the die will not lead to a briquette of a significantly different density being formed. This result is very important for the production of briquettes in the field where, in a rural situation, it would be practically very difficult to control the moisture content of the pulp, and the exact amount loaded in the press. It is important to note that these results do not conclude that there is no effect on the final dry density caused by differences in the moisture content of the pulp, but that the effect is small in the range

tested compared with the influence of other factors affecting the uncertainty. The uncertainties in the final briquette dry density are difficult to quantify on an individual basis without more detailed study. Factors that contribute to the uncertainty include: lack of very sensitive control of the piston during compaction (leading to small variations in the compression force), non-consistent changes in the rate of compaction between briquettes, different frictional forces for different size and designs of mounds and plungers, and lack of sensitive control in ejecting the briquettes from the moulds.

These results for the wet-briquetting process suggest very different behaviour compared to briquettes formed with unsaturated biomass materials at high pressures. In high-pressure, low-moisture content compaction, the final briquette density is strongly dependent on the initial moisture content, as discussed in Chapter 2. In the wet process, during compression, water is squeezed out from between the fibres of the saturated pulp. Further increasing the moisture content, in the case of newspaper pulp, appears to simply increase the rate of expulsion of the water for a given compression pressure, not significantly affecting the final density of the compaction.

The properties of other residue feeds may be significantly different. The magnitude of the effect of adding additional moisture to the pulp during compression is likely to be dependent on the porosity and structure of the pulp material during the compression phase. For this conclusion to be valid for other biomass materials, further tests are required. For other fibrous residues of a similar nature to paper, it would seem reasonable to assume that the conclusions of this simple study are valid; that is to say that the initial moisture content of the charge doesn't affect the final dry density of briquettes formed using the wet-process.

3.3   Combustion Testing

Once the briquettes had been formed, oven dried and the densities determined, they were taken to the combustion rig to be burnt. The following section gives a description of the experimental set-up and procedure employed.

In the test used to determine the effect of process variables, the briquettes were burnt in free air. In each test a single briquette was placed in the centre of a steel wire mesh grid resting on two supporting refractory bricks, allowing the free flow of air under and around the briquette. As shown in Figure 3.4, these bricks were positioned on top of a mass balance (Metler Tornado) interfaced with a PC to record instantaneous measurements of the mass every 10 seconds throughout

the combustion process. Smoke was extracted using an extraction hood method [107]. The extraction rate was set so that it was sufficient to capture all smoke, but had no visible effect on a match flame held in the position normally occupied by the briquette. Ballard- Tremeer et al. [36, 107] have statistically shown, to a 95% confidence level, that such extraction rates have no effect on the burn rate.
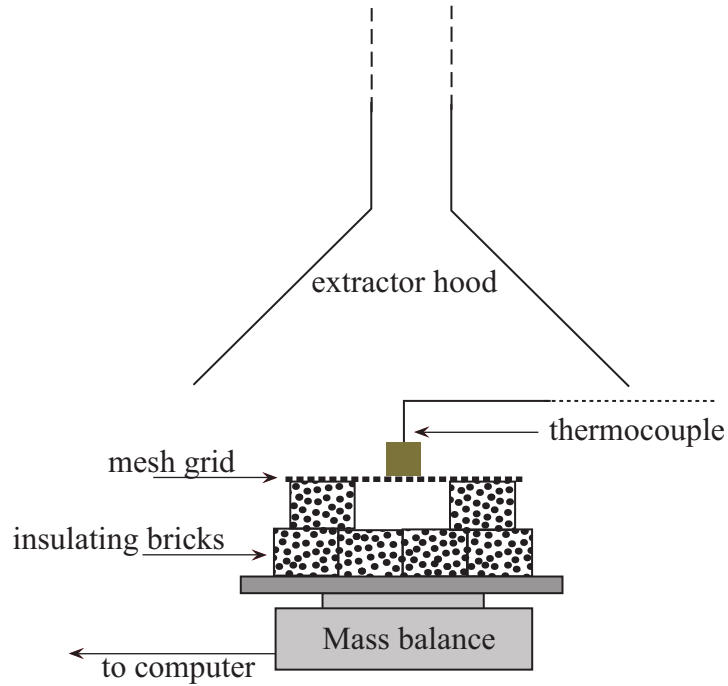
Figure 3.4: A diagram of the experimental set up

Each briquette was ignited by placing a small amount of firelighter on a platform $4cm$ directly beneath the mesh, but unconnected to the mass balance. Enough firelighter was used to ensure the whole of the bottom surface of the briquette was ignited simultaneously, avoiding flame spread in the transverse directions. After igniting the firelighter, it was left beneath the briquette until all parts were flaming. Mass loss was recorded until the mass of the briquette was 5% of its initial mass. Mass loss readings were normalised by the initial briquette mass, and a graph of normalised mass was plotted against time. Over repeated experiments with variations in the amount of firelighter used as an initiator, it was observed that the quantity used does not significantly affect the resulting normalised burn rate (NBR)[5].

Figure 3.5 shows a sample curve of a mass/initial mass versus time. There are three phases of the burn marked: Phase (1) is the ignition phase. Phase (2) is the

---

[5]The normalised burn rate (NBR) is the gradient of the steady-state flaming combustion phase of the normalised burn curve for the briquette (see Phase (2) in Figure 3.5).

steady state flaming combustion phase; volatiles are being released from the solid, mixing with oxygen and burning in the gas phase. Phase (3) is when the flame dies and the briquette decomposes further solely by a char combustion mechanism. The gradient of Phase (2) is the normalised steady-state combustion rate, referred to here as the normalised burn rate (NBR). A series of photos is given in Figure 3.6 showing the different stages of combustion for a cylindrical briquette.

For each briquette burnt, a graph of mass decrease as a function of time was plotted and the NBR was calculated by doing a least squares fit between 0.9 and 0.3 of the normalised mass. The normalised burn rate is used, because it allows the relative burn rate of briquettes of different initial masses and geometries to be compared.
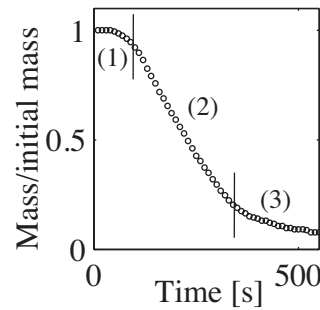
Figure 3.5: A typical normalised mass decrease curve for a burning slab
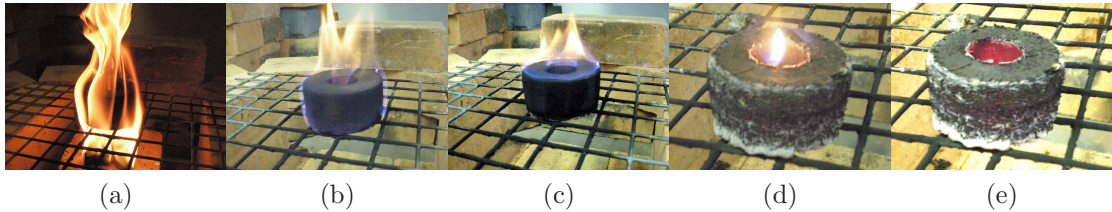
Figure 3.6: Different stages of combustion of a cylindrical briquette with a central hole. Stage (a) is the ignition phase, a firelighter can be observed burning under the briquette, stages (b)-(c) are phases in the flaming combustion, stage (d) is at the end of flaming combustion, and finally in stage (e) there is no flame and the briquette decomposes purely by char combustion.

3.4   Concluding Remarks

This chapter has presented the methodology that is used in Chapter 4 to explore the combustion of briquettes in free air. It has included a description of the

preparation of the briquettes from pulp, and a simple method of burning a single briquette on a mesh grid, which provides a convenient way to compare the combustion properties of different materials. In the next chapter, briquettes are manufactured from newspaper waste using the wet-process described here, and the combustion test is employed to investigate the effect of process variable properties on briquette burn rate (namely density, moisture content, geometry and size). More specific methodological details are given where necessary in the descriptions of each particular experiment.

Chapter 4

Experimental Study on the Burn Rate of Briquettes

In the previous chapter, an experimental technique was presented for studying the burn rate of briquettes in free air. In this chapter, this technique is used to explore the effect on the burn rate of variables that can be controlled during briquette manufacture (process variables). In particular, parameters that can be controlled in the manufacture of briquettes from any given biomass material are studied, namely the density, moisture content, shape and geometry and size of the briquette. In the first part of this chapter, the effect of briquette density on the burn rate is investigated for newspaper briquettes and a correlation is found. In the next part, the effect of briquette moisture content on the burn rate was investigated, and an experimental correlation also identified. In the final section, the effect of geometry on the rate of burn is studied by considering cylindrical briquettes burning in free air, and an analysis completed to explain the results.

4.1 The Effect of Briquette Process Variables on the Normalised Burn Rate of a Briquette in Free Air

4.1.1 The effect of density and size

From the literature it is clear that a material's density has a measurable effect on its burn rate, and therefore, the power output of a burning briquette (see Chapter 2). Indeed, it has been shown that for a variety of materials, such as sawdust, rice

husks, peanut shells, coconut fibres and palm fibres [50], that the compaction pressure affects the final briquette density. The briquette manufacturer has significant control over this variable in the production process, and can control it by varying the compression pressures used. For a given material, in order to design a briquette with a given power output, a knowledge of the relationship between density, size, geometry and burn rate is necessary. In turn, this informs the specifications of the briquette press required. In this section, the work on briquettes undertaken by Chin et al. [50] is validated and developed, and an empirical correlation of the effect of density on normalised burn rate is determined for newspaper briquettes.

As discussed in the literature review, O'Dogherty [54] proposed the following relationship between density and compaction pressure:

$$\rho = a \ln P + b \qquad (4.1)$$

where P is the compaction pressure and ρ is the final relaxed density. Chin et al. have determined the empirical constants a and b for a selection of biomass materials [50].

In the same study, it was found that the burn rate of the briquetted residues tested obeyed an empirical rate law of the form:

$$\dot{m} = \zeta P^{\mu} \qquad (4.2)$$

where ζ and μ are empirical constants, which are given by Chin et al. for different biomass materials. The burn rate can, therefore, be written as a function of density:

$$\dot{m} = F e^{(-\beta \rho)} \qquad (4.3)$$

where F can be written as $\zeta e^{(-b\mu/a)}$ and β is $-\mu/a$. These constants can be calculated from the data provided in Chin et al.'s paper for a range of different biomass materials. Equation 4.3 thus can be used to describe the variation in burn rate as a function of briquette density for these materials. The values of the above constants found from this simple calculation are given in Table 4.1.

In Chapter 3, it was decided that newspaper would be used as the primary material in the investigations into process variables in this study. In order to validate Equation 4.1 for newspaper, briquettes were manufactured under a range of compaction pressures using a cylindrical shaped mould with a central hole (an

aluminium mould was used with an external diameter of $63mm$ and an internal diameter of $21mm$). They were then oven dried, and their dry density determined (see Chapter 3 for details). Figure 4.1 shows a typical curve of how the dry density varies with compressive pressure for forming newspaper briquettes. The density is found to vary as a linear function of the natural logarithm of the compression pressure; this is the same trend observed in the compression of other biomass materials (as described by Equation 4.1). This gives some confidence that newspaper is representative of other biomass residues.

Material	a	b	ζ	μ	F	β
Sawdust	78.3	185.6	2.007	-0.357	4.678	0.0046
Rice husk	20.5	344.1	1.2700	-0.315	251.2	0.0154
Peanut shell	36.5	415.4	1.045	-0.267	21.82	0.0073
Coconut shell	60.6	54.10	1.095	-0.270	1.393	0.0045
Palm fibre	67.1	1.300	0.9910	-0.291	0.9966	0.0043

Table 4.1: Calculation of the constants F and β from Chin et al.'s data [50], which was found for a compaction pressure range of between 5 and 7 MPa.

Chin et al.'s study, however, was limited to briquettes made in a die with a diameter of $30mm$ loaded with $4g$ of material; these briquettes are much smaller and of a significantly lower mass than those being considered in this work. Moreover, the lower end of the range of pressures under which the constants in Table 4.1 were determined (5-7 MPa), is at the limit of what can be achieved with a simple hand-press. Furthermore, Chin et al. do not explicitly discuss the effect of briquette density on burn rate. The constant F in Equation 4.3 is specific to the experimental conditions and briquette dimensions used by Chin et al., and it is not clear if the constant β has a dependency on factors other than the density. Validation of the correlation described by Equation 4.3, is therefore, necessary with briquettes of larger sizes, lower densities and different shapes, in order to confirm that the constants in the empirical expression are not in fact simply a function of experimental conditions and dependent on inter-connected variables (put another way, it is necessary to access the co-variance). A more detailed exploration of Equation 4.3 was therefore carried out, accessing in a more rigourous way the effect of β and F on briquette density, size, geometry, and this is presented in the sections that follow.
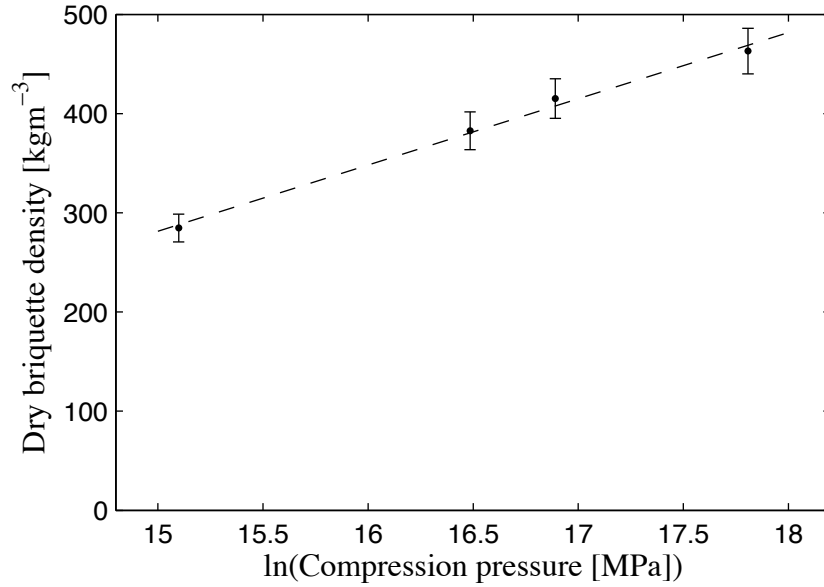
Figure 4.1: A typical graph of the variation of briquette density with compression pressure. Notice the natural log of the compression pressure has been plotted on the x-axis. This graph is for a cylindrical briquettes with a central hole, the mould has an external diameter of $63mm$ and an internal hole diameter of $21mm$.

4.1.2   Methodology overview: the effect of density

Slab shaped briquettes were manufactured with three different densities and four different dimensions from pulped newspaper, as described in Chapter 3. Cylindrical shaped briquettes with central holes at different densities were also prepared by the same method (details of all of the briquettes manufactured are given in Tables A.2 and A.5 in Appendix A).

The range of densities considered is within the range that a producer could form with a simple hand press (typically with a simple leaver hand press forces of between 1-20kN can be comfortably be achieved depending on the briquette press design).

The briquettes were ignited and burnt in free air on an open mesh grid, as described in Chapter 3. For each briquette, the mass-decrease as a function of time was measured, and the normalised quasi-steady state burn rate was calculated. Details of the numerical results are given in Table A.2 in the Appendix, in following sections the results are presented in a graphical format.

4.1.3   Results

It was found that the results for briquettes of different dimensions, could be correlated onto a single graph by plotting the briquettes' surface-area to volume ratio (A/V ratio) versus their measured normalised burn rate (NBR). This is a very helpful observation because it allows briquettes of a large range of different sizes, shapes, densities and materials, all to be plotted on the same graph, and the relative normalised burn rate to be compared. Figure 4.2 shows how the NBR of slab briquettes varies as a function of the A/V ratio for three different densities. The curves show that the normalised burn rate varies as a linear function of the A/V ratio (in practical terms, slabs with a high area to volume ratio will be those that are either thin or short). The briquette dimensions clearly have a significant influence on the normalised burn rate of the briquettes, demonstrating that the constant F in Equation 4.3 is more than simply a function of material properties alone.
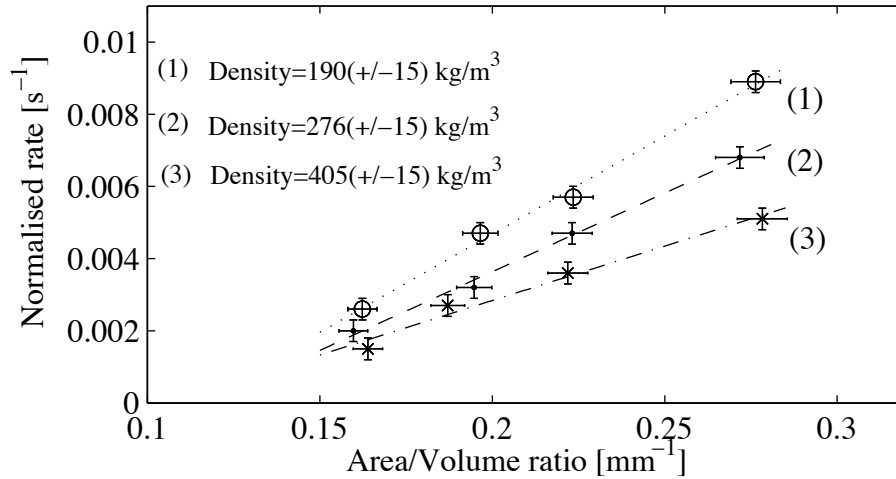
Figure 4.2: The effect on the burn rate of the area-to-volume ratio for three different density slab shaped briquettes. The raw data for these points is given in Table A.2 in the Appendix.

In order to understand the effect of A/V ratio on briquette design, it is helpful to take an empirical example. A slab shaped briquette of density 276 kgm^{-3}, with a height of 50 mm, a thickness of 80 mm and a width of 25 mm would have an A/V ratio of 0.145 mm^{-1}. Its dry mass would therefore be 27.6 g. If the rate is assumed to vary according to line 2 in Figure 4.2, it will have a normalised burn rate of 0.00170 s^{-1} giving a steady state burn rate for a single briquette of 0.046 gs^{-1}. Changing the thickness of this briquette to 20 mm would increase the A/V ratio to 0.165 mm^{-1}, resulting in a increase in burn rate to 0.054gs^{-1}, about 20%. This clearly demonstrates the importance, in designing briquettes, of considering

their A/V ratio. It is also important to note from Figure 4.2 that the lower the briquette density, the steeper the curve, meaning that the effect of size and shape on the burn rate of a briquette is more significant the lower the density.

It was observed while carrying out the experiments, that as the A/V ratio is decreased, there comes a point when combustion cannot be sustained in free air, beyond this point there is not sufficient heat transferred into the solid to sustain the pyrolysis reaction without an external source of heat[1]. In practice, briquettes are not burnt alone in free air, but rather in larger fires or in stoves with multiple briquettes. In this case the critical point beyond which combustion is not sustained will shift towards smaller values of the A/V ratio; heat is transferred between particles and the stove body so that the rate of heat loss per second to the surroundings per unit surface area of the briquettes is reduced and more heat is transferred into the solid.

4.1.4   Identifying the effect of density

The equations for the curves fitted to the data in Figure 4.2 can be used to find the normalised burn rate at given densities over a range of A/V ratios. Figure 4.3 gives the results, showing how normalised burn rate varies as a function of briquette density. The six curves are for different A/V ratios: the bottom curve gives results for briquettes with an A/V of 0.20 ± 0.005 mm^{-1}, and the top curve for briquettes with an A/V ratio of 0.35 ± 0.009 mm^{-1}. A least squares fit shows that an exponential function gives a satisfactory fit, and the group of curves can be written according to the equation:

$$NBR = \Xi e^{-\beta\rho} \tag{4.4}$$

where ρ is the briquette density in kgm^{-3}, Ξ (known as the exponential frequency factor[2]) is a function of a briquette's A/V ratio. β is a constant that was determined for newpaper by a least squares fit of Equation 4.4 of the points in Figure 4.3 for each A/V ratio. Table 4.2 gives the values for Ξ and β for a least squares fit of each of the six curves in Figure 4.3. This gives a mean value for the constant β of 0.0023 ± 0.0002 for the newspaper slab briquettes burnt in these experiments, over the above range of A/V ratios.

---

[1]The critical point of self-sustaining combustion as a function of the area-to-volume ratio for briquettes burning in free air can be investigated using the model presented in Chapter 5, but this has not been completed in this study.

[2]in the exponential relationship $\dot{y} = Be^{-mx}$, B is known as the frequency factor and m as the exponential exponent.
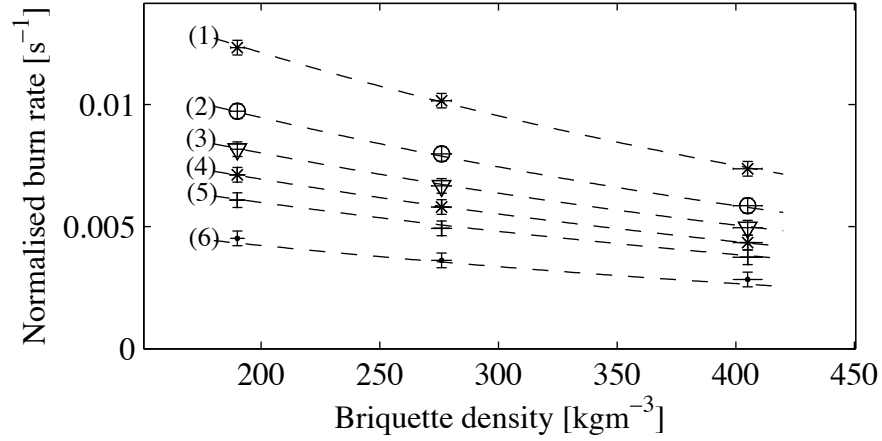
Figure 4.3: The variation in normalised burn rate of a briquette with briquette density for different area/volume ratios of the briquette. For curve (1) A/V= 0.35 $\pm$ 0.009 mm^{-1}1, (2) A/V=0.30 $\pm$ 0.008 mm^{-1}, (3) A/V=0.27 $\pm$ 0.007 mm^{-1}1, (4) A/V=0.25 $\pm$ 0.007 mm^{-1}, (5) A/V=0.23 $\pm$ 0.006 mm^{-1}, (6) A/V=0.2 $\pm$ 0.005 mm^{-1}.The dashed curves show that for each data set the points follow an exponential relationship of the form given in Equation 4.4.

A/V ratio [mm^{-1}]	Ξ [s^{-1}]	β
0.35	0.0196	0.0024
0.3	0.0153	0.0024
0.27	0.0127	0.0023
0.25	0.0110	0.0023
0.23	0.0093	0.0022
0.20	0.0067	0.0021

Table 4.2: This table gives the values of the constants Ξ and β for Equation 4.4 for different briquette A/V ratios. The frequency factors, Ξ, are plotted as a function of A/V in Figure 4.4.

Figure 4.5 gives a limited set of measurements performed on cylindrical briquettes with a central hole showing how normalised burn rate varies as a function of density. A least squares fit to this curve gives a exponential constant (β) of 0.0022 with an uncertainty of approximately ±0.0002, equivalent to the uncertainty associated with the slab experiments. The briquettes used in this experiment had an external diameter of 62.8 $\pm1mm$ and central hole diameter of 21.6 $\pm1mm^3$. The height, however, in these initial tests was not controlled and varied between 40 mm for the higher density briquettes (around 500 kg/m^3) and 60 mm for the two lowest density ones (around 200 kg/m^3). This difference in height between samples leads

---

[3]The briquettes expand slightly after extraction from the mould, which is why the dimensions are slightly greater than the mould dimensions.
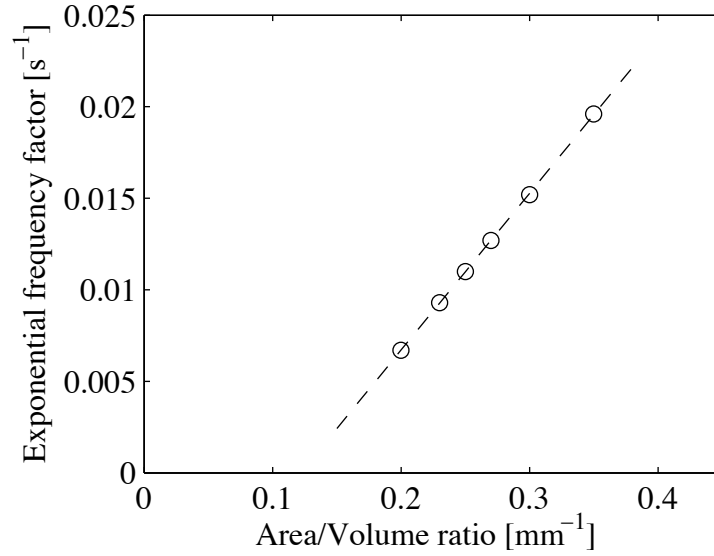
Figure 4.4: A graph showing the relationship between the exponential frequency factors Ξ and the briquette A/V ratio.

to a significant variation in the A/V ratio of the briquettes from 0.136 to 0.152 mm^{-1}. For slabs, according to Equation 4.5, this would be expected to result in a variation in burn rate of around 50%. However, for cylindrical briquettes with a central hole, more detailed work in Section 4.2 shows that, because of the role of the central hole, when the A/V ratio is modified by changing the height alone, for certain A/V ratios the normalised burn rate will be less affected; in this case, for the different height briquettes, about a 20 % difference between the two normalised burn rate should be expected. Therefore, the trends suggested by this curve, despite the different A/V ratios of the samples, are worth taking note of. Indeed, cylindrical briquettes appear to exhibit a very similar exponential behaviour to slabs, and the average value for β was also found to be 0.0023. This suggests that the constant β is not significantly affected by changes in briquette geometry. Its independence of briquette size and geometry would suggest that it is probably a material dependent constant.

Values of β can be inferred from the results of Chin et al. for some other biomass residues [50]. Although Chin et al. do not consider newspaper briquettes, the value of β found in the present study is of the same order of magnitude as values for other biomass materials, which can have been calculated from simple manipulation of their data (see Table 4.1). Chin et al. infers that these values should be considered material constants, although give no clarification as so why this should be the case. The experimental results from this study, discussed above, provide some support to suggests that this implicit assumption is indeed valid.
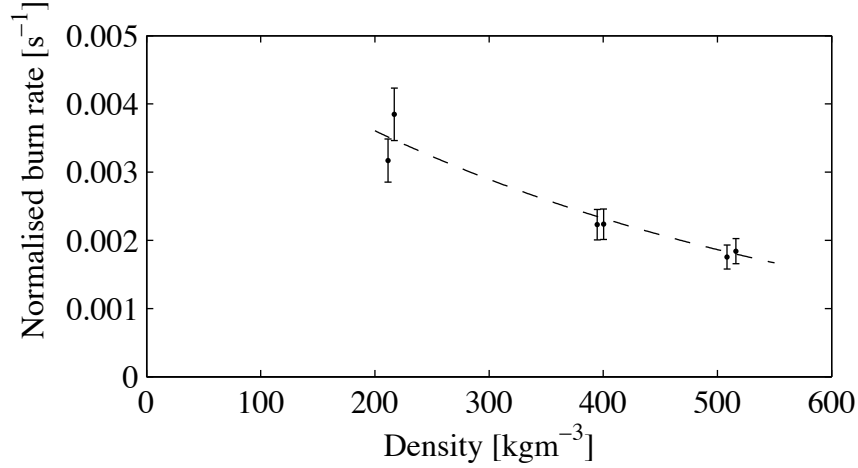
Figure 4.5: The effect of density on the burn rate: preliminary data for cylindrical briquettes with a central hole. The error bars indicate the minimum expected uncertainty.

Figure 4.4 is a plot of Ξ as a function of A/V ratio, indicating there is a linear relationship between these quantities. Consequently, for a slab shaped briquette burning in free air with a given A/V ratio, Ξ can be calculated. Therefore, if β, is considered a known material dependent constant, the normalised burn rate for a slab shaped newspaper briquette in free air can be determined according to the equation:

$$\Xi = \frac{\sigma A}{V} - \omega \rightarrow NBR = (0.074\frac{A}{V} - 0.0076)e^{-\beta\rho} \qquad (4.5)$$

(for newspaper briquettes the constants σ and ω were determined using a least squares fit).

Differentiating Equation 4.5 with respect to the A/V ratio or the density gives an indication of the sensitivity of the normalised burn rate with respect to each of these factors. Table 4.3 gives an example based on a notional briquette, which again illustrates how significant a factor the A/V ratio is in determining the normalised burn rate for briquettes burning in free air.

	Initial values	5% change	Initial NBR	changed NBR	% change in rate
A/V	0.155	0.162	0.000844	0.00107	27.0
Density	400	420	0.000844	0.000806	4.5

Table 4.3: The relative change in the normalised burn rate (NBR) for a briquette burning in free air, caused by changes in the briquette density and its A/V ratio.

The resulting change in the normalised burn rate with A/V and density given in Table 4.3 shows that the A/V ratio of the briquette has a much more significant effect on its normalised burn rate compared to density. Therefore, the size of a briquette has a very significant influence on its burn rate, and this is a factor that must be taken into account, and can be taken advantage of in briquette design for a particular cooking situation.

Newspaper slab results

In order to further validate the correlations above more generally, further combustion tests were carried out for newspaper slabs varying their density, and A/V ratio (by changing in different combinations the height, thickness and width of the briquettes). Table A.2 in Appendix A gives details of each of the tests completed. The results, over the range of briquette densities investigated, were then all correlated on a single figure by dividing the normalised burn rate of each result by the density factor: $exp(-0.0023 * \rho)$, identified in Section 4.1.4. Figure 4.6 shows the result. The 95% confidence intervals are plotted to give an indication of the associated uncertainty. This result is important firstly because it further suggests that the exponential exponent factor, β, in Equation 4.5, is not significantly coupled to geometrical factors of the briquette; it is possible to collapse all of the data for the whole spectrum of slabs of different density and dimensions onto one curve. Secondly, it shows that the A/V ratio of briquettes is a useful quantity for correlating the variation in the normalised burn rate for changes in briquette dimensions; the data points on this graph result from changes in different combinations of briquette dimensions, not only changes in briquette thickness. The consequence of this is that for a given density, the percentage change in the NBR for a briquette, as a function of changes in its physical dimensions, can be estimated.

The trend of increasing normalised burn rate with increasing briquette A/V ratio can be qualitatively understood: the greater the A/V ratio, the larger the surface area of the briquette bounding its volume. Therefore, for a given uniform heat flux on the surface, the greater the total heat flux per second transferred into into the solid per unit volume, resulting in a greater normalised burn rate. Indeed, this appears to explain the trend observed in Figure 4.6.
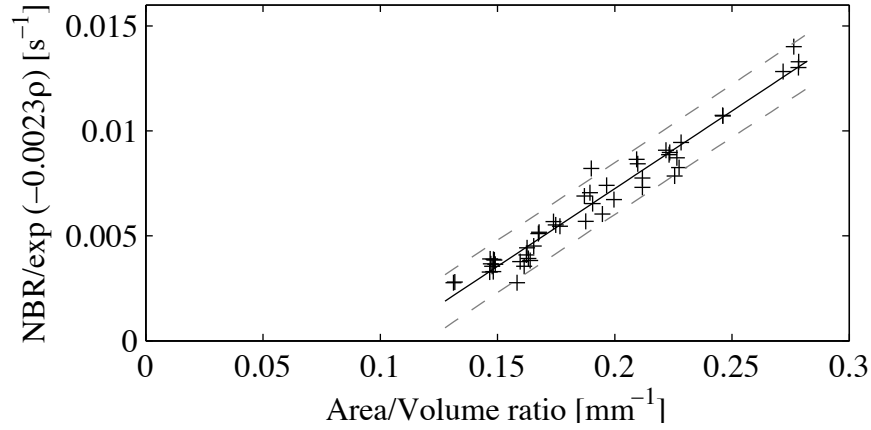
Figure 4.6: Data for all the newspaper slabs. The NBR has been divided by the density factor, exp(-0.0023ρ), in order to collapse the data onto a single curve.

4.1.5 Identification and discussion of some of the key factors affecting uncertainty in the NBR

There are some imprecisions associated with the preparation of the briquettes, which lead to uncertainties in the A/V ratio and density in these experiments. There are other uncertainties relating to the homogeneity of material properties, and others relating to the combustion environment, which are difficult to quantify. Each of these will have an affect on the measured normalised burn rate, thus leading to a relative uncertainty in its measurement. This section seeks to identify the key factors affecting this uncertainty in order to allow a correct interpretation of the trends in results presented in this chapter.

Measurement uncertainties

There is an uncertainty associated with cutting briquette slabs. This intrinsically affects the determination of a slab's volume, and therefore the determination of its density when using the stereometric method described in Chapter 3. It therefore, also results in uncertainties in the A/V ratio. The normalised burn rate in free air has been shown to be related to both the density and A/V ratio by Equation 4.5, and thus uncertainties in these quantities result in uncertainties in the predicted normalised slab burn rate.

The magnitude of these uncertainties can be estimated as follows: in the stereometric method used to determine the briquette density (see Chapter 3), the

volume was determined by calculating the volume of the nearest geometrical shape, in this case a cuboid. The samples were measured using callipers with a precision of $0.1mm$: the height of the slab was measured in three places, one at each side of the slab and another in its centre; the width was also measured in three locations, at the top, bottom and in the centre; the thickness was measured in each corner of the slab, allowing an assessment of the uniformity of the slab thickness cut. The mean of each of set of readings was taken. In order to estimate the uncertainty associated with the inhomogeneity of the slabs, the standard deviation of these measurements was found. This was taken as an estimate of the standard error, because the spread represents the physical deviation due to the inhomogenity, which dominates the error, rather than an instrument related uncertainty, which is comparatively small (the instrument uncertainty is a result of the measurement accuracy of the callipers, $\pm 0.01mm$, and the mass balance used, $\pm\ 0.01g$).

The relative uncertainty in the A/V ratio can be estimated using the standard method of propagation of errors as given below:

$$
\begin{aligned}
\frac{\delta(A/V)}{(A/V)} &\approx \frac{\delta A}{A} + \frac{\delta V}{V} \\
\frac{\delta A/V}{(A/V)} &\approx \frac{2[(W+H)\delta L + (W+L)\delta H + (L+H)\delta W)]}{\overline{A}} \\
&\quad + \frac{(H\times W)\delta L + (H\times L)\delta W + (W\times H)\delta W}{\overline{V}}
\end{aligned}
$$

This expression was applied to the measurements taken for every briquette manufactured, in order to estimate the uncertainty associated with its A/V ratio. Finally, an estimate of the value of the expected uncertainty in the A/V ratio for a given measurement was calculated as the mean percentage deviation in the A/V ratio over all the briquette measurements. This estimate gives a $\pm 7\%$ uncertainty in the A/V ratio for a briquette made with the method described in Chapter 3.

In a similar manner, the relative uncertainty associated with the sample density can be estimated as follows:

$$
\delta\rho = |\frac{\partial\rho}{\partial M}|\delta M + |\frac{\partial\rho}{\partial V}|\delta V \therefore \delta\rho = |\frac{1}{V}|\delta M + |-\frac{M}{V^2}|\delta V \tag{4.6}
$$

The uncertainty in the mass measurement is small compared with that of the A/V ratio: the samples were weighed to a precision of $\pm\ 0.01g$, and for a typical briquette with a mass of $50g$, this corresponds to a relative uncertainty in the

mass of $\pm$ 0.02%, which is found to be negligible compared with the uncertainty in the A/V ratio.

The normalised burn rate is a linear function of the A/V ratio, in the range investigated in this study, and thus a minimum uncertainty of $\pm7\%$ can be expected in the normalised burn rate. This was used on graph error bars to give an estimate of the minimum error.

4.2   Briquettes with a Central Hole

One of the initial objectives of this thesis was to investigate whether the geometry of a briquette has a noticeable effect on the normalised burn rate in free air. A briquette geometry that is become common in the field of briquetting is the cylindrical briquette with a central hole. On the surface of a slab briquette, no one part of the briquette surface has a view of another part of the briquette surface. The cylindrical briquette with a central hole is different in this respect, where points on the surface within the central hole are in line of sight of other points within this internal surface. This allows heat to be transferred by radiation between these points. In this section a study is presented assessing the influence of this geometrical consideration on the normalised burn rate.

4.2.1   Methodology and results

Cylindrical briquettes with a central hole (holey briquettes) were manufactured from pulped newspaper, as per the description given in Chapter 2; the details of their dimensions and densities are given in Table A.5 in Appendix A. Five independent series of holey briquette tests were carried out. In the first two tests the external and internal diameter of the briquettes were kept constant, and the height was varied. Figure 4.7 shows the results from these tests. The NBR has been further normalised by the density factor, $exp(-0.0023)$, in order to remove fluctuations in the results due to variations in the briquette densities, allowing trends to be more easily observed. For comparison, the curve from a least squares fit of the slab results, has also been plotted on the same graph (further details of these results can be found in Section 4.1.4). Varying the briquette height changes the A/V ratio; taller briquettes have smaller A/V ratios'. It can be observed from Figure 4.7 that as the briquette A/V ratio decreases (increase in briquette height), there is a significant deviation from the normalised slab briquette burn rate. However, when the A/V ratio is large (when the height of the holey briquette

is small) the NBR tends to the same curve as for slab briquettes. In other words for low A/V ratios, cylindrical briquettes with central holes tend to have a faster burn rate than slabs of the same A/V ratio.
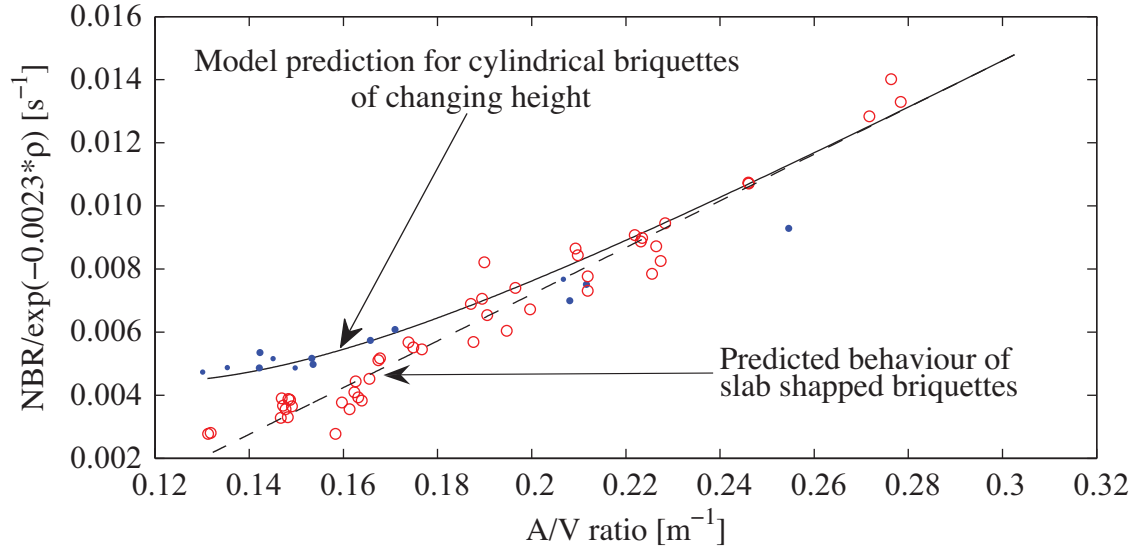
Figure 4.7: The variation in NBR/exp(-0.0023*density) with A/V ratio for cylindrical briquettes with a central hole (●) and for slab briquettes (○).

Overview of the analysis

An initial hypothesis was made that the reason tall holey briquettes have a higher normalised burn rate than slabs with the same A/V ratio is primarily due to the exchange of heat that occurs between surfaces within the briquette central hole; the taller the briquette the lower the proportion of heat lost by radiation to the surroundings. Another explanation that has been suggested to explain the difference in NBR, is a chimney effect, where the presence of the central hole draws more oxygen by natural convection [30] causing a hotter burn and a faster rate. Indeed, it is likely that there will be a small draft effect, but it will be assumed in this initial hypothesis that its influence on the rate is small, compared to the increase in heat exchange occurring within the central hole. The central hole effectively provides an insulated combustion zone. Less heat transfer by radiation to the surroundings from this surface produces higher temperatures within the hole compared with the outer briquette surface, which is exposed to the ambient radiant field. The steeper temperature gradients result in an increased rate of heat transfer into the solid at this surface, and consequentially the soild biomass is heated to the pyrolysis temperature at a faster rate. The result is a faster rate

of devolatisation for the surface within the central hole, compared with the part of the briquette surface directly exposed to the atmosphere.

In order to assess this hypothesis, a simple semi-empirical model was derived, which assumed the increase in rate was due to heat exchange within the inner surfaces of the hole. This was calculated by considering the atmospheric view-factor the of the surface within central hole. For a point on the briquette's surface, the atmospheric view-factor is defined as the proportion of radiation radiated to the atmosphere. In a similar way, the proportion of radiation that is emitted and reabsorbed within the surface of the central hole can be described using an internal view-factor. It can be calculated by considering how much each unit area of the surface in the hole sees the other parts of the internal surface. An element towards the top of the briquette will see a greater portion of atmosphere than an element located in the centre of the hole, and thus the element in the centre will have a greater internal view-factor (and thus a smaller atmospheric view factor). As the height increases, the area of the surface elements towards the top of the central hole, which have a high atmospheric factor, make up a smaller proportion of the total central hole internal surface area. Therefore, the greater the height, the lower the proportion of heat radiated to the atmosphere, and thus the faster the pyrolysis rate. A tall cylindrical briquette with a central hole and a low A/V ratio, will thus be maintained at a higher normalised burn rate compared to a slab with the same A/V ratio.

If the briquette height were to tend to infinity, the view factor would tend to one, and the the rate would be limited by the availability of oxygen supplied by the draft through the central hole, something which is assumed to be abundantly available in the view-factor treatment considered here. For very tall briquettes, it is therefore likely that limiting effects associated with the chimney draught will become more important. In the following section, a more detailed numerical analysis is completed based on the view-factor hypothesis, and the results are compared with experiment.

Details of analysis

The surface of the briquette can be thought to be made up of two parts: the outside surface that only sees the ambient radiant field (the atmosphere), and the surface with a view-factor within the central hole. The surface area of the outside of the briquette which 'sees' only the ambient radiant field was calculated, not including the central hole region; this area has view-factor with the atmosphere of 1. It is assumed that Equation 4.5 is able to predict the quai-steady state burn

rate of this part of the briquette surface. On the other hand, within the central hole region, it is assumed that the burn rate is the sum of the burn rate for a slab in an ambient radiant field, plus an amount, δR, to account for the radiation exchange between the internal surfaces within the central hole. In this analysis, an attempt is made to calculate δR.

In order to calculate δR, the changing heat flux at the surface was considered:

$$Q_{rad}^{f-s} + Q_{convec}^{f-s} = Q_{rad}^{s-a} + Q_{in} \tag{4.7}$$

The radiative and convective flux to the surface can be written as follows:

$$Q_{rad}^{f-s} + Q_{convec}^{f-s} = A(\sigma(\epsilon_f T_f^4 - \epsilon_s T_s^4) + h(T_f - T_s)) \tag{4.8}$$

If the view factor of a small cylindrical surface, δA_j, inside the internal hole of the briquette is considered, the heat loss to the atmosphere from an element j can be found as follows (see Figure 4.8 for a diagram of a briquette central hole; a cylindrical surface element, δA_j has been shaded).
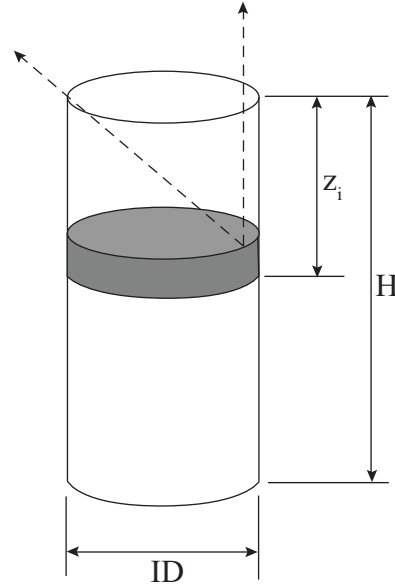
Figure 4.8: A diagram of the central hole through a briquette. In the analysis, the view-factor with the atmosphere of bands of thickness δz, as shown, are calculated. A summation is made over the whole surface within the central hole.

From the definition of radiation intensity, the rate at which radiation leaves surface element j, and is transmitted to the atmosphere may be expressed as:

$$dq = I_j cos\theta d\omega dA_j \tag{4.9}$$

where I_j is the intensity of radiation leaving surface j, and $d\omega$ is the solid angle subtended by dA_j with the atmosphere.

The solid angle of the surface j with the atmosphere can be written as:

$$d\omega = sin\theta d\theta d\phi \qquad (4.10)$$

and therefore, the total heat radiated from surface j to the atmosphere per unit area, assuming that the radiation is diffuse (independent of direction), can be expressed as:

$$\frac{dQ}{dA} = I \int_0^{2\pi} \int_0^{\theta} cos\theta sin\theta d\theta d\phi \qquad (4.11)$$

therefore:

$$\frac{dQ}{dA} = 2\pi I \int_0^{\theta} cos\theta sin\theta d\theta \qquad (4.12)$$

where

$$\frac{dsin^2\theta}{d\theta} = 2sin\theta cos\theta \qquad (4.13)$$

and I is the intensity of the emitted radiation.

Therefore:

$$\frac{dQ}{dA} = \frac{2\pi I sin^2(\theta)}{2} = \pi I sin^2(\theta) \qquad (4.14)$$

where

$$\theta = atan(\frac{ID}{H}) \qquad (4.15)$$

and the total intensity, I of a black body can be written as [87]:

$$I = \frac{\sigma T^4}{\pi} \qquad (4.16)$$

Therefore Equation 4.14 becomes:

$$\frac{dQ}{dA} = \epsilon_s \alpha \sigma (T_s^4 - T_a^4) sin^2(atan(\frac{ID}{H})) \qquad (4.17)$$

where ϵ_s is the effective emissivity of the surface and α accounts for the absorption of emitted heat by the gas phase. If ϵ_g is the emissivity of the gas, and it is assumed that the absorptivity of the gas can be written as $(1 - \epsilon_g)$ [108] then the total heat

transferred to the atmosphere from the area j can be written as:

$$\frac{dQ}{dA_j} = \epsilon_s(1 - \epsilon_g)\sigma(T_s^4 - T_a^4)sin(atan\frac{ID}{z_i})^2 \tag{4.18}$$

$$\Rightarrow dQ_{loss} = (\pi ID\delta z)\epsilon_s(1 - \epsilon_g)\sigma(T_s^4 - T_a^4)sin(atan\frac{ID}{z_i})^2 \tag{4.19}$$

It is the temperature at the surface of the outer char layer that determines the rate of heat transfer into the densified biomass (see Figure 4.9). An approximate heat flow Q_{in} was estimated by assuming a latent enthalphy of devolatisation for biomass, H_{solid} of 1.3 $MJkg^{-1}$ [109] and assuming:

$$\frac{dM}{dt} = \frac{Q_{in}}{H_{solid}} \tag{4.20}$$

taking a typical experimental burn rate from experimental data. Equations 4.7, 4.8 and 4.19 were then solved to determine the temperature of the surface. This was compared with the surface temperature calculated when Q_{in} was assumed to be negligible. The consequence of ignoring this term is about a 0.0006% difference in temperature, which is negligible. This implies that the surface temperature is primarily determined by the energy balance of factors external to the briquette, namely by the view-factor of the wall with the atmosphere. Consequently Q_{in}, which is difficult to determine, can be neglected in a first approximation when estimating the surface temperature of the briquette walls within the internal hole.
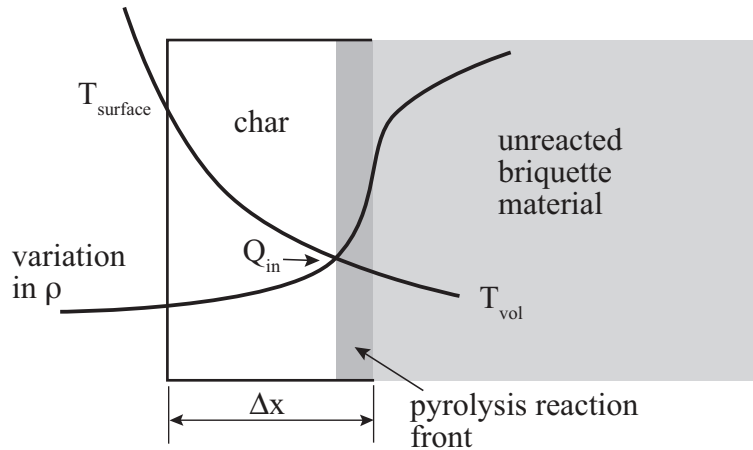
Figure 4.9: Heat is transferred through the solid char layer to the virgin material, a surface heat flux results in higher surface temperatures, a steeper internal temperature gradient and therefore a faster rate.

The change in pyrolysis rate for at element j within the central hole was assumed to be proportional to the relative change in heat flux at its surface. In order to simplify the problem further, each of area element within the central hole is treated as a one-dimensional case where the pyrolysis front is assumed to travel perpendicular to the solid surface (see Chapter 2 for a more detailed description of advancing pyrolysis fronts). With these assumptions, the total change in pyrolysis rate for an element in the central hole can be found from:

$$\delta Rate_i \propto \alpha (1 - \frac{Q_{loss}(z)}{Q_{lossVF=1}}) \tag{4.21}$$

where α is a constant of proportionality. Therefore:

$$\delta Rate_{total} = \alpha \int (1 - \frac{Q_{loss}(z)}{Q_{lossVF=1}}) dz \tag{4.22}$$

It can be seen from Equation 4.21, that in moving towards the top of the hole, the view-factor with the atmosphere will tend to 1, and therefore the heat loss will tend to the heat loss from a surface in direct contact with the atmosphere, where there is no re-radiation, $Q_{lossVF=1}$. At the limit:

$$\frac{Q_{loss}(z = 0)}{Q_{lossVF=1}}) \longrightarrow 1 \therefore \delta Rate \longrightarrow 0 \tag{4.23}$$

Likewise, in a very tall briquette, in the central region of the central hole, almost no heat will be radiated to the atmosphere: $Q_{loss}(z) \longrightarrow 0$ and thus: $\delta Rate \longrightarrow \alpha$.

The total burn rate for the central holed briquette is in this way found and then normalised with respect to its initial mass to give the normalised burn rate.

This analysis suggests that cylindrical briquettes without a central hole, or solid briquettes of any geometry should burn at the rate predicted for slabs, provided they have no internal angles that would cause one part of the surface to transfer heat by radiation directly to another part. For example, a triangle shaped briquette should burn like a slab, whereas a star shaped briquette should have a faster normalised burn rate than a slab because of additional radiation heat transfer between each point of the star. Further experimental work is required to validate this theory for other such geometric forms of briquette.

Validation of the model: further experimental results for cylindrical briquettes burning in free air

Further experiments were carried out in which the A/V ratio was varied by changing all the dimensions of the holey briquettes: heights, external and internal hole diameters. Details are given in Table A.5 in Appendix A. They were burnt in free air on a mesh grid, as described in Chapter 3. The constant of proportionality, α, described above, was found by least squares regression of Equation 4.22 to the experimental data to give a value of 3.514×10^{-6}. The resulting predictions of the model are compared with independent experiments in Figures 4.10a to 4.10d: Figure 4.10a shows results where primarily the height was varied, Figure 4.10b shows data for when both the external diameter and height are varied and the internal diameter is kept constant, Figure 4.10c is where the thickness of the briquette wall is kept constant and the diameter of the internal hole was varied and finally Figure 4.10d gives results for briquettes where both the height and density of the circular briquette were varied. The error bars on the measured data represent the 95% confidence intervals previously calculated for the slab data. It is clear that in this instance all of the measured data lies within this confidence interval, an upper bound of the expected uncertainty. This suggests that the above model is helpful in predicting the burn rate of holey briquettes burning in free air (in systems where convection is forced this relationship would need to be re-examined).

4.3 The Effect of Moisture Content on the Normalised Burn Rate of Briquettes Burning in Free air

The review of Chapter 2 reveals that the moisture content of solid biomass has an effect on its burn rate. In order to understand the degree to which each factor needs to be controlled in briquette manufacture, it would be useful to know the relative importance of moisture on the normalised burn rate compared with density and A/V ratio. The normalised burn rate is directly related to the power output of a briquette; this study was designed to allow the equivalent decrease in power as a function of percentage moisture in a sample to be estimated.

(a) Data from experiment 1 and 2

(b) Data from experiment 3

(c) Data from experiment 4

(d) Data from experiment 5
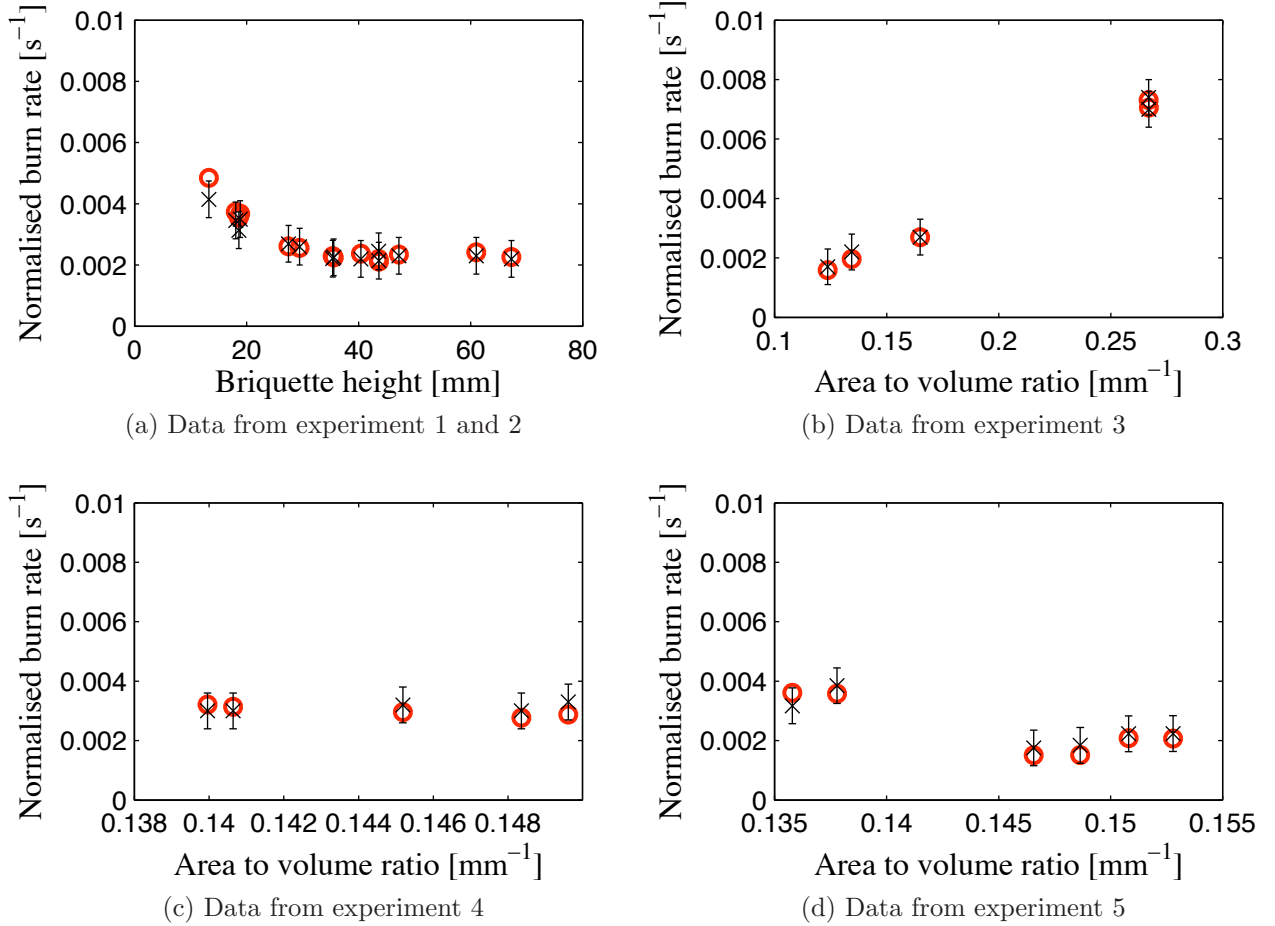
Figure 4.10: Results from 5 independent tests on briquettes with central holes. The details of the briquette dimensions and densities are given in Table A.5 in Appendix A. Each data point represents a single briquette combustion test, and has been plotted with the prediction from the view-factor model, see Section 4.2.1; the '×'s' are the data points, and the '∘'s' are the model predictions. It should be noted that in experiments 3, 4 and 5 different combinations of the briquette parameters were varied at the same time, therefore the reader should not attempt to observe trends in graphs (b), (c) and (d), where each experimental point can only be compared to its model prediction.

4.3.1   Overview of the methodology

In the investigation of the effect of different factors on the normalised burn rate of briquettes, it is necessary to have a method that allows relative comparison between different samples. Often it is helpful to see the overall global effect of a variable, while identifying interdependent behaviour between variables. One way of approaching this is to carry out a factorial experiment with respect to quantities that *are* understood, while changing one variable whose effect is as yet unknown, and then normalising with respect to the known behaviour. Although a full factorial experiment was not carried out here, the principles of this method are used in order to investigate the effect of moisture content on the normalised burn rate: the samples were normalised with respect to the free air burn rate, while the moisture content was varied. This allowed the results from briquettes of different sizes, densities and geometries to be correlated onto one curve, so that any statistically significant variations observed are a result of changing the other variable in the system, in this case the moisture content.

A controlled experiment was carried out where briquettes of different moisture contents were prepared and burnt on a mesh grid in free air, as described in Chapter 3. An outline of the method is given below, but further details of the method of sample preparation can be found in Chapter 3.

Cylindrical briquettes with a central hole and slab briquettes were prepared. After they had been oven dried and their dry density determined, different quantities of water were added to each of the briquettes. Briquettes were prepared with moisture contents ranging from 0 to 15 %. This is close to the typical range of moisture contents that would be expected for dried woodfuel, which normally has a moisture content of between 2 and 20% [66]. After the moisture had been left to diffuse throughout the material, each briquette was then burnt on a mesh grid in free air and the normalised burn rate recorded.

4.3.2   Results

The measured normalised burn rate for each sample was then further normalised by its equivalent predicted dry burn rate, and plotted against moisture content (dry basis), as shown in Figure 4.11. The dry burn rate prediction was calculated from Equation 4.5 for slabs, and from theory presented in Section 4.2 for holey briquettes. This method allows the comparison of the relative effect of moisture on the burn rate using a range of different size and geometry samples.

As the moisture content increases the NBR shows a clear tendency to decrease, as expected (see Chapter 2). If the trend shown in Figure 4.11 is assumed to be a linear function of the percentage moisture content ($\%M$), then a least squares regression on the data in the range tested, gives the following helpful approximation:

$$\frac{NBR_{wet}}{NBR_{dry}} = -C[\%M] + 1 \tag{4.24}$$

For the data points found in this experiment for newspaper briquettes, the constant C was found to take a value of 0.038 ± 0.01. The 50% confidence intervals for the data have been plotted, and give an indication of the expected uncertainty in the NBR from using this expression.
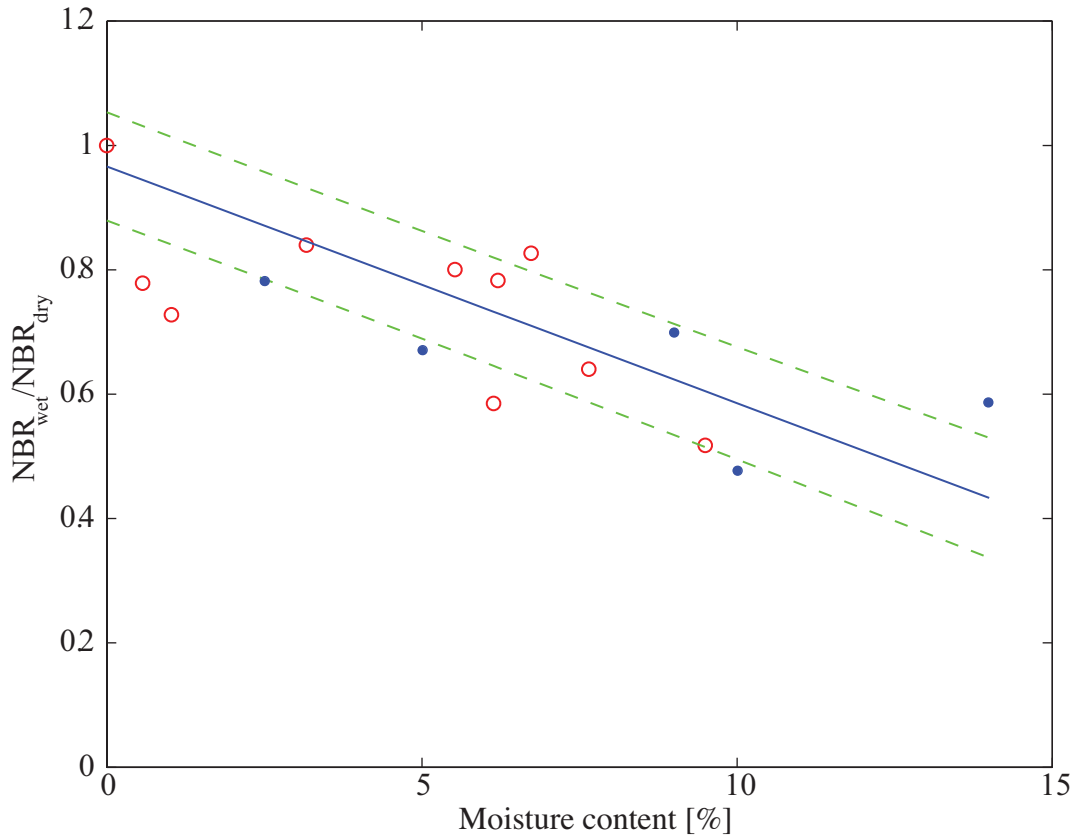
Figure 4.11: The effect of moisture content on the normalised burn rate of briquettes. 50% confidence intervals are plotted for the data. The dots (•) are results for slabs and circles (○) are results for holey briquettes.

4.3.3   Discussion and conclusions

The results shown in Figure 4.11 suggest that there is a statistically significant decrease in the normalised burn rate as the moisture content of the sample is increased, and in the range tested, a linear trend provides an adequate approximation within the limits of uncertainty. Equation 4.24 provides a means of determining the approximate decrease in rate as a function of the moisture content (dry basis). However, this is only an approximate trend for newspaper briquettes burning in free air, and would need to be further validated for different residues, greater moisture contents, and different combustion environments. The large degree of uncertainty in these readings may be due to inhomogenities in the moisture distribution in the sample, this being a consequence of the rather crude method used to add moisture.

4.4   Biomass Slabs of Different Materials

Thus far, the briquettes tested have been made from newspaper. In this section an investigation is made into some of the consequences of changing the feedstock. In particular, the objective was to identify whether the constants in Equation 4.5 are material dependent. Indeed, briquettes can be made from a vast number of materials, and it is beyond the scope of this work to complete a comprehensive analysis of the behaviour of large numbers of residues. Rather, three materials (solid pinewood, rapeseed oil residue and sawdust) were selected in order to quantify the type of variation in behaviour that might be expected. Pinewood was chosen in order to make a comparison of newpaper briquettes with the behaviour of wood, which is the current most common biomass residue burnt in developing countries. Commercial rapeseed oil residue briquettes were investigated as a second material, for two reasons. Firstly, because they have a much higher density than the low-density newspaper briquettes that were studied in the previous section, and secondly because they are made from very different materials to newspaper: in particular rapeseed oil residue briquettes have a significant oil content and a greater calorific value of between 22-24 MJ/kg [78], compared with newspaper, which has a value of between 18-19 MJ/kg. Finally, sawdust was chosen as this is a woody biomass residue, and is commonly available, for example in Ghana there are large quantities of sawdust available. Although not a very different material to pine, it is in a significantly different form and is very different from the rapeseed oil residue.

4.4.1   Slab results for other materials

The rapeseed oil residue briquettes used are a commercially available product known on the market in the UK as 'Green Dragon Briquettes[4]'. Pinewood was purchased from a local hardware store and the sawdust briquettes were made using a similar methodology to the newspaper briquettes, as described in Chapter 3, except a starch binder was mixed with the sawdust after soaking to aid binding at low compacting pressures. The briquettes and pinewood were cut up into slabs using a band-saw, in a similar way to the newspaper briquettes. Table A.1 in the Appendix gives details of the slab dimensions and the resulting normalised burn rate measured for this experiment. Table A.4 gives details of the prepared pinewood slabs, and Table A.3 gives the details for the sawdust briquettes. Samples were burnt on a mesh grid as described in Chapter 3.

Figure 4.12 shows results of the normalised burn rate of pinewood slabs and rapeseed oil residue briquettes as a function of their A/V ratio. The rape seed oil briquettes have a much higher density than pine slabs (1080 kgm^{-3} compared with 465 kgm^{-3}, respectively[5]). It is not possible to vary the density of either the soild wood, or the commercial rapeseed oil residue briquettes, and therefore, the coefficient β, describing how the normalised burn rate of these materials varies as a function of density, is not known. To find β for rapeseed oil residue briquettes, the raw material would have to be obtained, and further experimentation similar to the tests done on newspaper briquettes (described in Section 4.1) would have to be carried out.

It has been established that density has a significant affect on the normalised burn rate. Therefore, because of the significant difference between the pinewood and rapeseed oil residue briquette densities, it is not possible to make a meaningful comparison between curves in Figure 4.12. However, it is possible to compare the results with that of newspaper, whose behaviour in relation to changes in the NBR with density is now known. Figures 4.13 and 4.14 compare the behaviour of rapeseed oil waste and pine slab briquettes with newspaper briquettes at their respective densities, the normalised burn rate of the newspaper briquettes being calculated using Equation 4.5.

---

[4]They are available from http://www.greendragonfuel.co.uk (last accessed July 2010).

[5]with approximate uncertainty of $\pm 10\%$; uncertainty is discussed in more detail in Section 4.1.5.
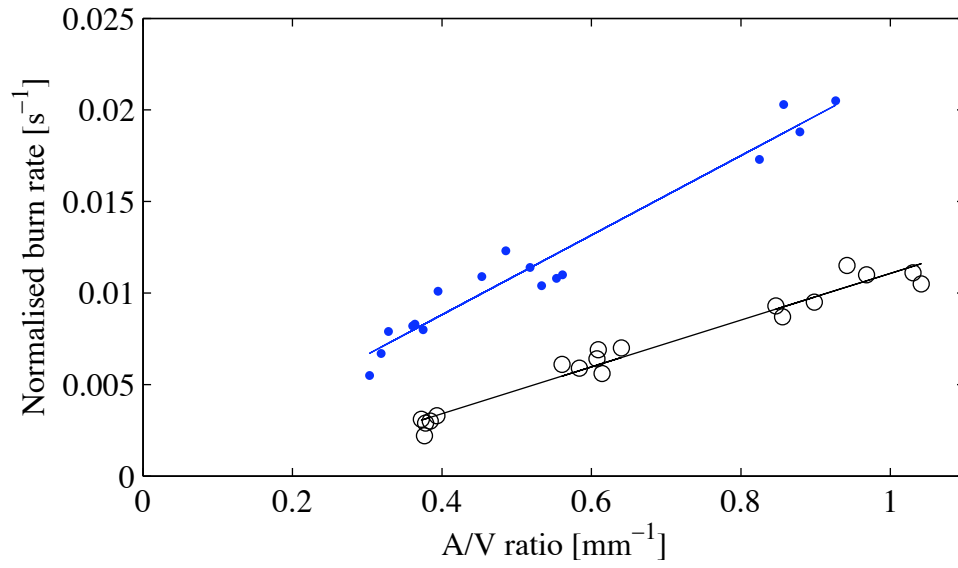
Figure 4.12:　The normalised burn rate of rapeseed oil residue briquettes (○) compared to pine slabs (●) as a function of their area-to-volume ratio.
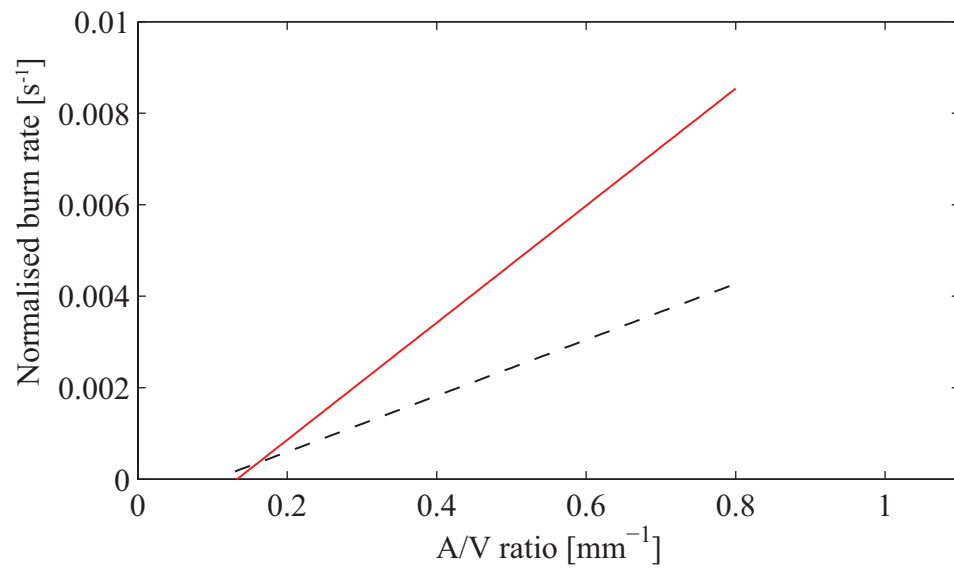
Figure 4.13: A comparison between newspaper briquettes (- - -) and green dragon briquettes (—) at the density of green dragon briquettes, $1080 \ kgm^{-3}$.
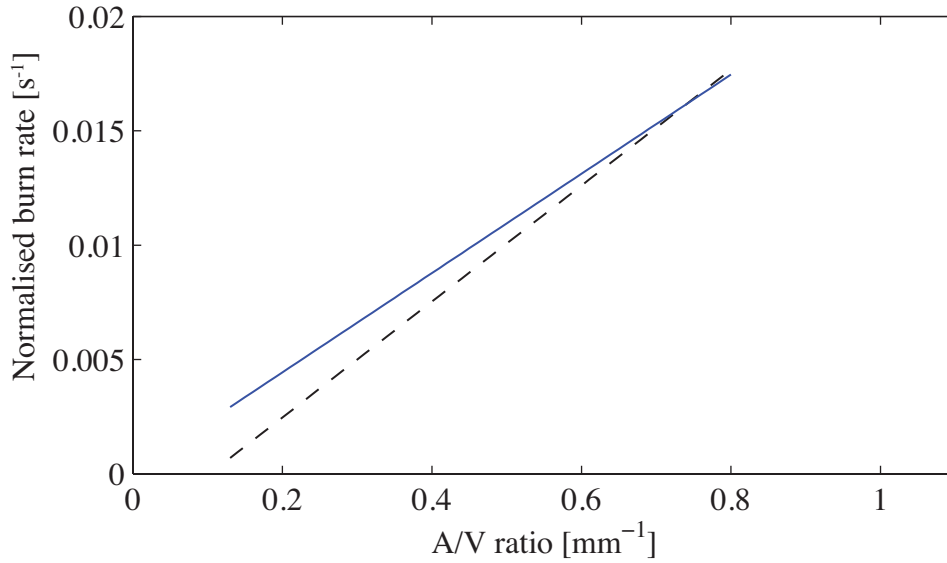
Figure 4.14: A comparison between newspaper briquettes (- - -) and pine slabs at the average measured density of the pine slabs (—), 465 kgm^{-3}. The dashed line for newspaper briquettes is a predicted line with an assumed density of 1080 kgm^{-3}; this line was calculated using Equation 4.5.

Figure 4.13 shows that the rate of change of the NBR with A/V ratio is greater for rapeseed oil residue briquettes than for newspaper. On the other hand, Figure 4.14 shows that the gradient of pinewood slabs is close to, but less than that of newspaper. Finally, Figure 4.15 gives a direct comparison between results for sawdust slabs and newspaper briquettes at a density of 272 kgm^{-3}. For the sawdust used in this test, the two results can be seen to follow the same curve. (N.B. In this case, results for newspaper briquettes were available at the same density as for the sawdust briquettes; these briquettes were made by compression in a similar way to newspaper briquettes, as described in Chapter 3, rather than purchased commercially).

The significantly different gradient for the rapeseed oil residue briquettes compared to newspaper suggest that the constants in Equation 4.5 are material dependent and cannot be assumed global values for all materials. This implies that the normalised burn rate is a material dependent, as well as size dependent quantity. It therefore suggests that newspaper, pinewood and sawdust have similar physical and material dependencies, whereas rapeseed oil residue briquettes are significantly different. Various factors might contribute to this difference, for example differences between the calorific values of the residues, the resistance to flow of the volatile products from pyrolysis and the thermal properties of the material that control the heat transfer into the solid. For example, if the constant,

σ, in Equation 4.5 is assumed to be a linear function of the calorific value, then the greater the calorific value, the steeper the gradient. Physically, this type of dependency is logical because the higher calorific value, the greater the quantity of energy available per unit mass of biomass material. A greater quantity of energy released per gram of volatiles burnt would most likely result in an increase in the energy transferred to the briquette surface per unit area (see Section 4.4.2 below for considerations on predicting the NBR as a function of calorific value in more detail). In terms of the flow resistance to pyrolysis products, a briquette made from a material where char properties inhibit the flow of volatiles, will have a shallower gradient compared to a material where volatiles can escape more easily. Considering the thermal properties of the materials, if for example the thermal conductivity of a sample was higher, then an increase in the A/V of a sample would lead to a greater proportion of energy transferred into the sample per unit surface area, resulting in a steeper gradient of the NBR curve. The relative effect of some of these factors is considered later in the numerical modelling in Chapter 6.
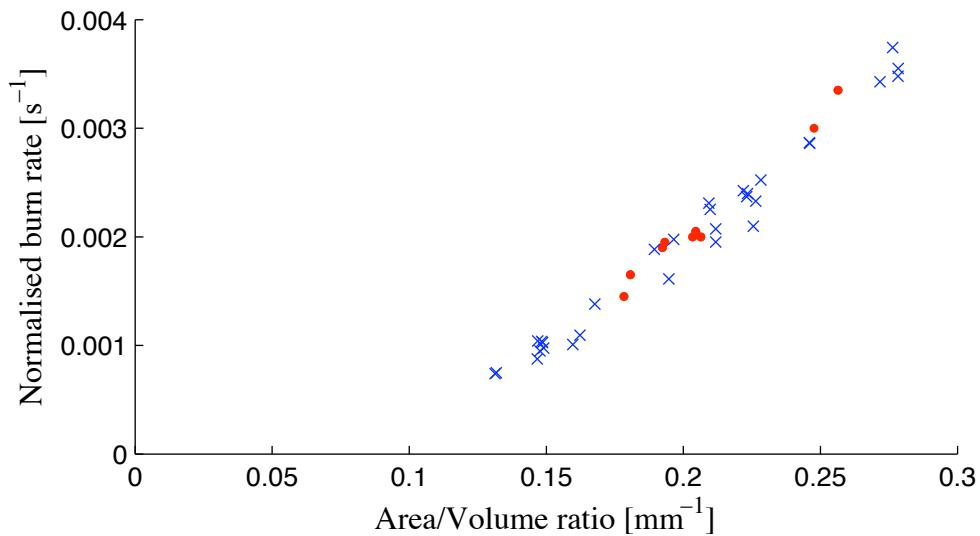
Figure 4.15: The burn rate of sawdust ($\bullet$) and newspaper ($\times$) at a density of 272 kgm^{-3}.

The constant ω in Equation 4.5 controls the intercept[6]. The results from this experiment, for combustion in free air, show that it takes a different value for each of the different materials tested, and therefore it is probably a function of

---

[6]It should be noted that this is a theoretical intercept to define the equation for prediction purposes, in practice the curve will not be defined below a certain A/V ratio, below which the heat release rate will be insufficient to sustain the pyrolysis reaction.

material properties. It is also probably a function of the combustion environment, for example it is likely that it is a function of the radiant field in which a briquette is placed and the advective flow of gas around the fuel. Further work is therefore required, to identify the factors that these quantities depend on, and how they interrelate.

It is also interesting to note that in both Figure 4.13 and 4.14 there is a particular A/V ratio where the newspaper briquettes and the respective material plotted have the same normalised burn rate. For green dragon briquettes, above this point the pyrolysis is faster than newspaper briquettes for the same A/V ratio, but below it newspaper briquettes will pyrolyse at a faster rate. The practical consequence is that large green-dragon briquette will have a lower normalised burn rate than an equivalent newspaper briquette of the same dimensions and density. These curves are for briquettes burning in free air, and the positions of the curves are likely to shift for briquettes in different combustion environments. For example, a particular size rapeseed oil residue briquette burning in a cookstove, where there is less heat loss to the surroundings, will have a much higher NBR for a given A/V ratio. If it is assumed that the form of this curve will follow a linear trend, as for briquettes in free air (although the point of equal rate may shift), then the consequence is that different materials would have to be made into different sized briquettes, in order to achieve the same power output in the same cookstove.

When performing this experiment it became clear for slabs, that below a certain A/V ratio samples tend to smoulder[7]. For the rapeseed oil residue briquettes this occurs for A/V ratios not much less than those investigated here; further tests would be required to identify this limit more precisely. This indicates that the A/V ratio effectively limits the ability of a materiel to undergo self-sustaining combustion in free air when subject to an ambient radiant field. Consequently, the behaviour close to the origin, below this critical A/V ratio, is impossible to investigate in free air. Moreover, for free air such results would be meaningless anyway, because samples simply smoulder. What is clear from observation is that the critical A/V ratio below which flaming combustion does not occur for a given material, is a function of the density, moisture content and combustion environment. In the quest for a more general understanding of the limits of

---

[7]Smouldering is the non-flaming combustion of a virgin material, it includes the drying of the material, its pyrolysis, and char oxidation. The char combustion is heterogeneous and occurs either in the interior or on the surface of the fuel, and the heat from the reaction is transferred into the solid and drives the future pyrolysis. Fernando et al. present a model of a smoldering log, in which further details are described [74], but this is not considered any further in this study.

self-sustaining combustion, it would be helpful to be able to define the critical limit in an empirical expression as a function of these factors.

4.4.2 A suggested method of developing the NBR equation to include calorific value

In order to predict the effective change in NBR that is caused by a difference in calorific value between two briquettes, it is assumed that the difference in the NBR will be equivalent to the change in rate that would be caused by adding moisture to the higher calorific value fuel in order to reduce its effective calorific value to the same as the other fuel.

According to the results of Section 4.3, where the effect of moisture on the NBR was investigated, the change in NBR due to moisture can be found according to the equation:

$$\frac{NBR_{wet}}{NBR_{dry}} = -0.0038[\%M] + 1 \tag{4.25}$$

where $\%M$ is the percentage moisture content on a dry basis. Moisture content is considered to reduce the effective heat content of a biomass fuel (also see Section 2.4.1 and 2.4.3), such that the effective reduction in the gross calorific value[8] due to moisture (known as the NCV) is given by (taken from [62]):

$$NCV = GCV\left(1 - \frac{w}{100}\right) - 2.444.\frac{w}{100} - 2.444.\frac{\nu}{100}.8.936\left(1 - \frac{w}{100}\right) [MJkg^-1, w.b.] \tag{4.26}$$

where 2.444=enthalpy difference between gaseous and liquid water at 298 K, 8.936=M_{H_2O}/M_H; i.e. the molecular mass ratio between H_2O and H_2, NCV is the net calorific value of the biomass fuel in $MJkg^{-1}$ (w.b.), GCV is the gross calorific value of a fuel on a wet in $MJkg^{-1}$ (d.b.), w is the moisture content of the fuel on a wet basis[9]. ν is the percentage concentration of hydrogen in the fuel by weight (d.b.), which it is suggested takes a value of around 6% for woody biomass fuels (which is what newspaper would be considered to be), and 5.5% for herbaceous biomass fuels.

---

[8]see Section 2.4.3 for a definition

[9]It is simple to find the wet basis moisture content from the dry basis (as has been used in this thesis) using the expression: $wb = (100 \times \%d.b.)/(\%d.b. + 100)$.

For a fuel with no added moisture, the NCV can be written, from Equation 4.26, as:

$$NCV_{dry} = GCV - 2.444.\frac{\nu}{100}.8.936 \tag{4.27}$$

for a given fuel the NCV can, therefore, be written using (4.26) and (4.27) as:

$$NCV = (NCV_{dry}+2.444.\frac{\nu}{100}.8.936)\left(1-\frac{w}{100}\right)-2.444.\frac{w}{100}-2.444.\frac{\nu}{100}.8.936\left(1-\frac{w}{100}\right) \tag{4.28}$$

This can be rearranged to find the effective difference in moisture content between a dry and a wet fuel, as a function of its dry NCV and wet NCV:

$$\frac{w}{100} = \frac{(NCV + 2.444 - (NCV_{dry} + C_1))}{(C_1 - 2.444 - (NCV_{dry} + C_1))} \tag{4.29}$$

where $C_1 = 2.444.\frac{\nu}{100}.8.936$

It is assumed that an equivalent moisture could be added to the rapeseed oil residue briquettes to reduce their effective calorific value to the same as newspaper briquettes. When this is found, the effective difference in NBR between the residues (caused by a difference in calorific value) can be found according to Equation 4.25. The relative increase in rate due to the modification of the calorific value of a fuel compared to newspaper can thus be found.

This method was used to estimate the expected relative increase in the NBR of the rapeseed oil residue briquettes compared to newspaper briquettes resulting from the difference in calorific value: as stated earlier, the calorific value for newspaper and rapeseed oil residue briquettes are 18-19 and 22-24 $MJkg^{-1}$, respectively. The effective moisture content was found using Equation 4.29 as follows:

$$\frac{ef_w}{100} = \frac{(Cal_{RSO} + 2.444 - (Cal_{NP} + C_1))}{(C_1 - 2.444 - (Cal_{NP} + C_1))} \tag{4.30}$$

where $ef_w/100$ is the effective (negative in this case) moisture content (wet basis), Cal_{RSO} is the calorific value of rapeseed oil residue briquettes and Cal_{NP} is the calorific value of newspaper briquettes, a value of 6% was used for h, as suggested above. $ef_w/100$ needs to be converted to a dry basis moisture content (as this is what is required for Equation 4.25). The effective dry basis moisture content can be shown to take a minimum value of 14.9% (for calorific values for rapeseed oil residue and newspaper of 22 and 19 $MJkg^{-1}$, respectively) and a maximum

value of 31% (for calorific values for rapeseed oil residue and newspaper of 24 and 18 $MJkg^{-1}$, respectively). Figure 4.16 shows the best fit of the rapeseed oil residue briquette results, and the prediction for newspaper briquettes of the same density (1083 kgm^{-1}), calculated using Equation 4.5. The dashed lines (- - -) show the maximum and minimum relative increase in gradient possible, resulting from the difference in calorific value predicted using this method. The shift in NBR suggested here appears to be of the right order of magnitude. There are various other factors that will have an influence on the gradient of this line that have not been taken into account in this calculation, such as the difference in material thermal properties, as discussed. Nevertheless, the method suggested here appears to provide a means by which the difference in NBR between two materials, caused by a difference in their different calorific values, can be approximated: in summary as a rough approximation, the difference in the NBR of a biomass briquette of material x compared to a newspaper briquette, can be written as:

$$\frac{NBR_x}{NBR_{NP-free-air}} = 1 - 0.038 * [\%ef_w] \tag{4.31}$$

where NBR_x is the normalised burn rate of briquette made from another residue x. $\%ef_w$ can be found from:

$$\frac{ef_w}{100} = \frac{(NCV_x + 2.444 - (Cal_{NP} + C_1))}{(C_1 - 2.444 - (Cal_{NP} + C_1))} \tag{4.32}$$

where C_1 is defined above and NCV_x is the Net Calorific Value for material x.

Further investigations with briquettes made from materials that have significantly different calorific values should be completed to further validate this method. A study should also be carried out to assess whether the deviation from the predicted and measured curves in this study can be accounted for by differences in other material properties (Chapter 5 addresses this to some degree by using numerical modelling to consider the effect of thermal material properties on the NBR).

4.4.3　Some notes on uncertainties

Figure 4.17 shows results for both pine slabs and rapeseed oil residue briquette slabs with lines plotted showing the expected uncertainties in the measurements: the solid lines are ±7%, the minimum expected uncertainty associated with the inhomogeneity in the shape of the sample (this was estimated for newspaper briquettes in Section 4.1.5 and is assumed to be the same in this case because the slabs were prepared by using the same cutting methodology). Approximately

60% of the points lie within this band of lines, indicating that that measurement error can account for a significant proportion of the scatter, but yet there are other sources of uncertainty unaccounted for here. Furthermore, if the relative uncertainty in the A/V ratio is considered a constant (7%), then as the slabs become thicker, the absolute uncertainty for a particular sample decreases. However, it is clear from observation of slab results data, that as the A/V ratio approaches zero, the uncertainty in the normalised burn rate does not become negligible; significant scatter is observed for slabs with a low A/V ratio.

Measurement uncertainty is clearly not the only source of error. In attempt to quantify the unaccounted for uncertainty, an additional absolute uncertainty was included. Figure 4.17 shows dashed lines corresponding to additional absolute uncertainty of $\pm 0.0006 \ s^{-1}$: 95% of the data lie within these confidence intervals.

This additional uncertainty could be due to a number of causes:

- inconsistencies in the material, both in terms of composition, and the homogeneity of the compressed samples, which might influence the heat transfer and diffusion of volatiles though the pore structure of the solid;

- effects of changing external environmental conditions (particularly humidity, temperature of the surroundings and fluctuations in air velocity around the
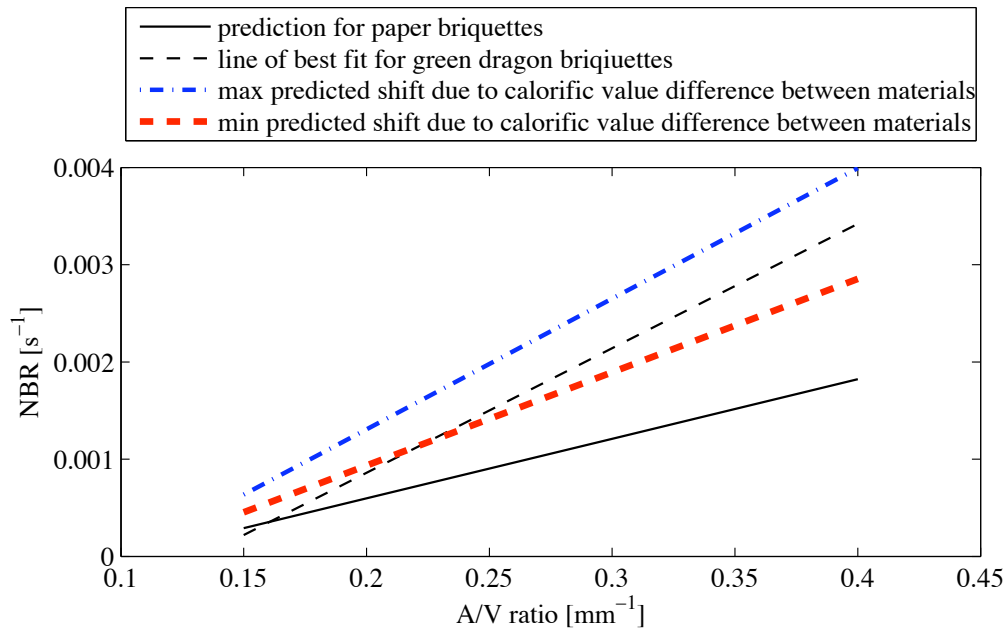
Figure 4.16: The relative affect of a difference in calorific value between materials on the NBR.

burning slab) during combustion. This is particularly pertinent because experiments were not all carried out on the same day;

- limitations in the experimental technique, such as in terms of ignition (variations in the time the firelighter was left in, and non-uniform ignition across the sample).
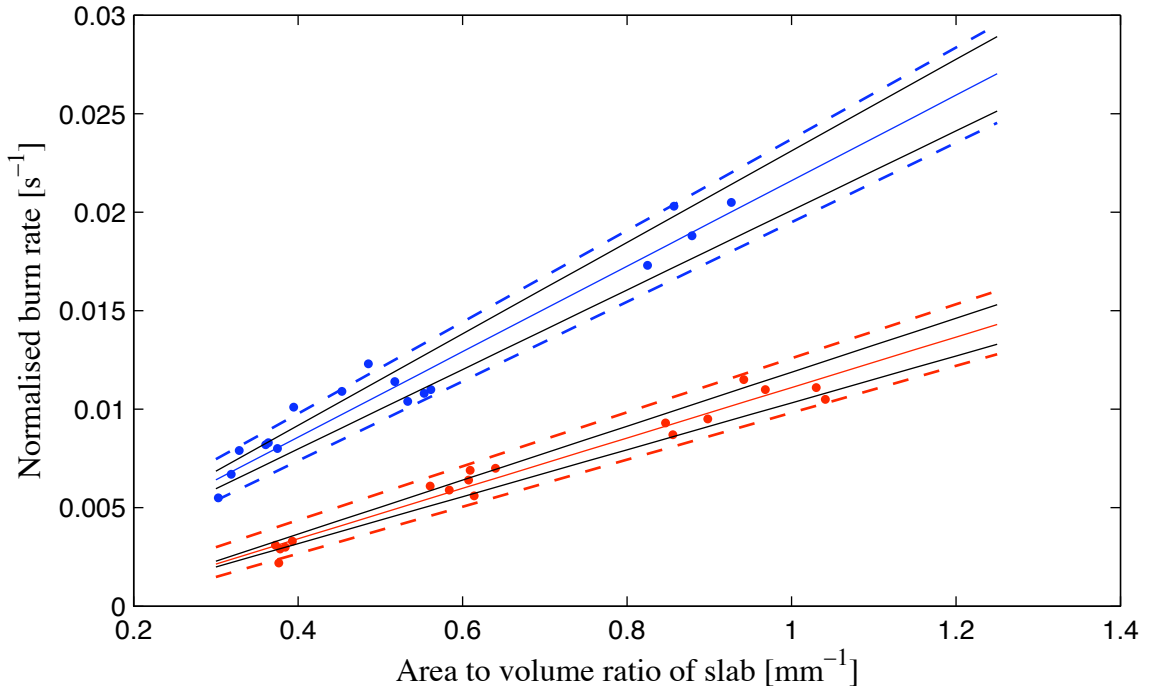
Figure 4.17: The variation of the normalised burn rate as a function of A/V ratio for pine slabs (top curve) and rapeseed oil residue briquettes (bottom curve).

4.4.4 Conclusions

In this section, an investigation was carried out into the NBR behaviour of pinewood, rapeseed oil and sawdust briquettes as a function of briquette A/V ratio. Slab-shaped briquettes of each of these materials were made and burnt. Each was found to be a linear function of the A/V ratio, in the range tested. However, it was found that rapeseed oil residue, which has a significantly different nature from newspaper, had a much steeper gradient on a plot of its NBR against A/V ratio. Whereas sawdust, which although different in structure is similar in its chemical make up to newspaper, had a very similar gradient on a plot of its NBR versus A/V ratio to newspaper, as did pinewood.

It was found that the difference in gradient could be accounted for as being due to differences in the combustion properties of the biomass residues (such as moisture content and calorific value) and briquette specific properties (such as density and A/V ratio): the effect of density and A/V ratio had already been explored in Section 4.1 and moisture has been looked at in Section 4.3. Here, an attempt was made to quantify the difference in rate caused by the difference in calorific value between two materials, and an expression was derived. The method appears to provide an acceptable fit with the measured results for approximation purposes. This suggests, that the calorific value is a very significant variable in determining NBR of compressed biomass. Further experimental validation of this technique is required for its verification, and an investigation into the relative effects of other combustion properties also needs to be carried out (for instance: volatile matter content, ash content, elemental composition of the residue).

4.5   Chapter Conclusions

In this chapter, the effect of process variables on the normalised burn rate of briquettes in free air has been investigated. An expression was found for the influence of density on the NBR of newspaper briquettes. Experimental tests were then carried out to confirm that the constants in this equation were not a function of briquette size or geometry. In terms of briquette size, it was found that it was possible to correlate the changes of NBR with size, by plotting NBR against briquette area-to-volume ratio (A/V ratio). For briquettes with no internal angles (for example slab shaped briquettes) this curve was a linear relationship, with decreasing NBR as the A/V ratio was reduced. These initial studies showed that the gradient of this line varied as a function of density and moisture content.

The effect of geometry was investigated by comparing the NBR of a holey briquette to slab shaped briquettes. It was found that the presence of the central hole resulted in a higher normalised burn rate than for slab shaped briquettes of the same A/V ratio, and this difference was found to become more pronounced as the view-factor of the internal surface of the central hole with the atmosphere was reduced (the taller the holey briquette, the more pronounced the effect). An expression was found, which was able to predict the normalised burn rate as a function of view-factor. This suggests, that this is a primary mechanism controlling the NBR. However, it is also indeed possible that a chimney draught effect is coupled with this, and further work must be completed in order to

fully assess the air flow behaviour within the central hole of the briquette during combustion.

The NBR behaviour of some different biomass residues was investigated. They were found to follow a very similar linear behaviour to newspaper briquettes. An expression for the change in NBR due to a difference in Net Calorific Value between two materials was suggested, and successfully used to predict the NBR as a function of A/V ratio for rapeseed oil residue briquettes compared to newspaper briquettes. This infers that calorific value is a very important variable in determining the gradient of the A/V versus NBR curve. Further investigations in Chapter 6, attempt to link the gradient of the A/V versus NBR curve, to the thermal properties of the biomass materials.

In the Chapter 5, which follows, a simple numerical model is suggested to better understand and model the underlying processes that are occurring during combustion in these regularly shaped briquettes. This is applied in Chapter 6, where the empirical expression for the NBR of a briquette as a function of briquette properties, is further developed to include material thermal properties.

Chapter 5

Numerical Model of Pyrolysis

The aim of this chapter is the development of a simple numerical model of pyrolysis that is able to predict the steady-state normalised burn rate of briquette slabs with different area to volume ratios, as well as enabling the investigation of other factors that are hard to explore experimentally. The objectives of the biomass combustion model are:

- the prediction of the quasi-steady-state normalised burn rate of briquettes of different sizes and geometries;

- to allow the mechanism of the devolatisation of the briquettes to be understood;

- to enable the investigation of the effect of changes in material thermal properties that are difficult to vary independently in experimental work, namely the thermal conductivity and heat capacity;

- to provide a connection between gas phase temperature and briquette burn rate to enable investigation into the effect of fuel properties on efficiency and emissions in stoves;

- to enable the development of semi-empirical expressions for the normalised burn-rate of briquettes that can be used in the field to estimate the expected briquette combustion rate.

In the first part of this chapter details of the model are presented and parameters that need to be determined highlighted. The part which follows describes a methodology for measuring some of these parameters experimentally, independently of the model. Chapter 6 then looks at optimisation and application of the model.

5.1 Development of a Devolatisation Model: Model Assumptions

The devolatisation of a briquette is a problem in non-steady state heat flow. The literature review revealed the current understanding of the process (see Section 2.3 and 2.7). Heat is transferred to the surface from the gas phase and into the solid. When the temperature in a particular region is sufficiently high, thermal decomposition of the biomass material into volatile gases occurs, which then pass through the char layer and out into the gas phase. In Section 2.7.1 a one-step global kinetics reaction model was reviewed that models the rate of thermal decomposition of the soild biomass as a function of its temperature. This approach will be used in this study. The modelling problem is thus two-fold: firstly, the time varying temperature profile within the briquette needs to be calculated; secondly, the resulting rate of decomposition that this causes needs to be predicted.

In order to address this problem, various authors have taken approaches with different degrees of complexity, which are reviewed in Section 2.7.2. One of the simplest models is presented by Bamford et al. [83]. In his pioneering study, he suggests a simple one-dimensional conduction model, which is shown to give good agreement with experimental results, predicting the change in temperature at the centre of a pyrolysing vertical sheet of wood [83]. The ideas from this approach have been applied in this study to investigate the effect of geometry on the normalised burn-rate. A novel approach is taken, in which the one-dimensional model prediction of the burn rate for a slab, per unit area, for a given thickness, is used to find the corresponding normalised burn rate of a slab, with a given area-to-volume ratio. The area-to-volume ratio has the units of m^{-1} and is therefore, dimensionally speaking, a one dimensional parameter, but yet it has a three dimensional meaning. In this way, the approach uses a one-dimensional model to approximate the prediction of a three-dimensional problem. The agreement of the experimental results suggest this methodology is appropriate.

5.1.1 Heat transfer into a solid briquette

The equation governing conductive heat transfer into a solid briquette can be written as [86]:

$$\frac{\partial (c_p \rho T)}{\partial t} = \lambda \left(\frac{\partial^2 T}{\partial r^2} + \frac{(\varsigma - 1)}{r} \frac{\partial T}{\partial r} \right) \tag{5.1}$$

where c_p, ρ and λ are the specific heat capacity, density and thermal conductivity of the solid, respectively. T is the local temperature, r is the position and ς is the geometrical factor, which is 1 for slabs, 2 for a rod and 3 for a sphere. In this instance, for one-dimensional slabs, ς is therefore taken as 1.

5.1.2   Decomposition kinetics

The decomposition of biomass is complex, there are many intermediate products, and final products formed [65] and neither the mechanisms nor the kinetics and energetics of the pyrolysis reactions are clearly understood [83, 86]. Different pyrolysis models from the literature have been reviewed in Chapter 2. In this model the one-step pseudo first order global pyrolysis reaction scheme has been chosen, as suggested by Bamford et al. [83] because of its simplicity and good agreement with experimental data [83, 86, 93, 100]. The rate of devolatisation is determined by a first order Arrhenius expression [83, 86]:

$$\frac{\partial \rho}{\partial t} = -k_r(\rho - \rho_{final}) \tag{5.2}$$

where ρ_{final} is the final density of the devolatised biomass, that is of the final char product and k_r is the reaction rate of the first order reaction. k_r is determined by:

$$k_r = k_0 e^{(-\frac{E}{RT})} \tag{5.3}$$

where E and k_0 are the apparent activation energy and pre-exponential factor respectively. These are assumed to be constant values throughout the decomposition. In this form, the final char yield cannot be predicted from the model. However, because we are concerned primarily with predicting the quasi-steady-state burn rate of the combustion, (during which cooking would be done), predicting the char yield is not of primary importance in this study. On the other hand, the sensitivity of the final char density chosen, ρ_{final}, on the predicted rate of decomposition, is important to assess and is considered in a later section.

5.1.3   Boundary conditions

Heat is assumed to be transferred to the surface of the briquette from the surrounding gas by a combination of convection and radiation. At the briquette surface:

$$\lambda \frac{\partial T}{\partial x} = h_c(T_g - T_s) + \sigma \epsilon_f(T_g^4 - T_s^4) - \sigma(1 - \epsilon_f)(T_s^4 - T_{at}^4) = H(T_s) \qquad (5.4)$$

where the temperature of the gas, T_g, is assumed constant and to take a value of $750K$, the average flame temperature for a burning newspaper briquette measured for slab experiments. The surface of the briquette is assumed to radiate as a black body. The final term in this expression accounts for heat loss from the slab surface, radiating through the flame, to the atmosphere [108]. This term is often not included because for many applications, the solid is assumed to be in a furnace where the temperature of the furnace walls is assumed to be the same as the gas phase temperature [86].

At the centre of the one-dimensional briquette, it is assumed that there is no heat loss, and symmetry is assumed with respect to the central axis. The boundary condition can be written for all time as:

$$\lambda \frac{\partial T}{\partial x}\bigg|_{x=0} = 0 \qquad (5.5)$$

5.1.4   Implementation of the one-dimensional model

The equations were solved using a finite difference approach, using an explicit method [110]. The slab was divided into N slices of thickness δd. The discretised equations for heat transfer within the slab are written as:

$$T_i^{n+1} = \frac{\alpha \delta t}{\delta r^2}(T_{i+1}^n + T_{i-1}^n) + (1 - \frac{2\alpha \delta t}{\delta r^2})T_i^n \qquad (5.6)$$

The equation for the surface boundary ($i = 0$), however, needs to be treated differently. It is assumed that i may be extended one step beyond the surface [83] to the point $i = -1$ so that (5.6) maybe written as:

$$T_0^{n+1} = \frac{\alpha \delta t}{\delta x^2}(T_{+1}^n + T_{-1}^n) + (1 - \frac{2\alpha \delta t}{\delta r^2})T_0^n \qquad (5.7)$$

where α is the thermal diffusivity of the solid briquette and is defined as:

$$\alpha = \frac{\lambda}{\rho c_p} \qquad (5.8)$$

Similarly, the boundary condition at the surface can be written as:

$$\lambda\frac{T_{+1} - T_{-1}}{2\delta d} = -[h_c(T_g - T_s) + \sigma\epsilon_f(T_g^4 - T_s^4) - \sigma(1 - \epsilon_f)(T_s^4 - T_{at}^4)] = H(T_s) \quad (5.9)$$

By the elimination of T_{-1} from Equation (5.7) and (5.9), the surface boundary condition can be written as:

$$T_0^{n+1} = (\frac{2\alpha\delta t}{\delta x^2})T_{+1} + (1 - \frac{2\alpha\delta t}{(\delta x)^2})T_0^n + H(T_s) \quad (5.10)$$

The central boundary condition, as defined in (5.4), can be written simply as:

$$\frac{T_{N-1} - T_N}{2\delta x} = 0 \quad (5.11)$$

and therefore at the central axis of the briquette:

$$T_{N-1} = T_N \quad (5.12)$$

Each of these equations is linked to the Arrhenius equation describing devolatisation, which can be written in terms of the mass of material in each slice δx as:

$$\frac{\partial m_i}{\partial t} = -k_i(m - m_{final}) \quad (5.13)$$

where

$$k_i = k_0 e^{(-E/RT_i)} \quad (5.14)$$

This can be discretised to take the form:

$$m^{n+1} = (1 - k_i\delta t)m^n + (\delta t k_i)m_{final} \quad (5.15)$$

5.1.5   Concluding remarks

A simple one-dimensional conduction based devolatisation model has been presented. In order to apply this model, sensible values for the surface heat transfer parameters h and ϵ_f, and for the material thermal properties k, cp and α need to be determined. There are many physical effects, such as the heat transfer in the outflow of volatile gases and the change in thermal properties as a function of temperature and degree of degradation, which have not been taken into account

in this model. Such limitations, and the extent to which it is valid to neglect them, are discussed in Chapter 6.

5.2 Determination of Model Constants

In order to evaluate solutions to the modelling equations given in Section 5.1, it is necessary to assign values to all of the constants: the thermal properties of the briquette, namely its heat capacity, c_p, thermal conductivity, λ, thermal diffusivity, α; and the heat transfer coefficients h and ϵ_f. However, there is limited data in the literature on the thermal properties of compressed biomass, and heat transfer coefficients are not available for either biomass briquettes or wood-slabs. In the first part of this chapter a novel heat-probe method is suggested as a simple, quick and low cost method to give estimates of the thermal properties of compressed biomass. The technique is then applied to dry newspaper briquettes. In the second part of the chapter, a method for the determination of the heat transfer coefficients is proposed and applied to slab briquettes. The associated uncertainties of each of the determined parameters are estimated. The methods described in this chapter provide useful tools for the determination of important modelling parameters for theoretical modelling investigations; the values found for newspaper briquettes are used in Chapter 6 to evaluate the devolatisation model given in Section 5.1.

5.2.1 Introduction: the need for a method for the determination of the thermal properties of biomass briquettes

In order to validate the numerical model, an independent method is required to determine the thermal properties of the particular briquette under study (namely the thermal conductivity, diffusivity and heat capacity). This is preferable to deriving these parameters through fitting of a model to NBR data. These thermal properties depend on many factors, such as on the material from which the briquettes are made, the density to which they are compressed and the moisture content. For the initial values of these thermal properties, wood combustion models often take general values from the literature rather than taking measurements of their specific sample (for example [64, 86]). This may be sufficient for wood combustion models when a particular species of wood is used and its moisture content known. On the hand, for biomass briquettes, due to their varied nature in terms of constituent materials, the conditions under which they are

formed and their moisture content, standard literature values are not available; there are likely to be significant differences between the thermal properties, not only for briquettes of different materials, but also for briquettes of the same material formed at different densities and moisture contents. Ravi et al. in their development of a pyrolysis model for a sawdust stove attempted to determine the thermal conductivity of sawdust by a direct measurement [100]. The method uses a cylindrical electric heater sited inside a cylindrical packed bed of sawdust, with thermocouples distributed within the sawdust bed measuring temperature profiles as a function of time. One-dimensional heat transfer theory is then used to calculate the thermal conductivity. This method is expensive and time-consuming and the technique only yields a value for one thermal property. Furthermore, for repeated measurements it would be difficult to control the packing density.

There is, therefore, need for a simple method for the determination of the thermal properties of a particular biomass briquette, which can then be used in numerical models. In this section, a method is presented that is both quick and simple. Its validity is assessed by using the technique to determine the thermal properties of newspaper briquettes at different densities. The method is versatile and could potentially be used in determining the thermal properties of the final char after the volatiles have been released from the briquette under particular experimental combustion conditions.

5.2.2   Review of a dual-probe heat-pulse technique

In soil research, a dual probe heat-pulse method has been suggested for the determination of the thermal properties of the soil. In this method a heat pulse is generated by one probe, the response measured by the other, and a numerical analysis of the response behaviour completed, which allows the thermal properties of to be found.

Campbell et al. developed an instrument to make a temperature measurement at some distance from a short duration pulsed heat source [111]. In their theoretical approach to analyse the results, they employed instantaneous heat line theory but did not take into account the duration of the heat pulse. This limited the technique to the determination of one thermal property, the volumetric heat capacity [112]. Bristow presented a theory for the radial conduction from a short duration heat pulse and compared this with instantaneous heat-pulse theory [112]. In this study, it was shown that the short duration heat-pulse theory could be used to extract the conductivity, thermal diffusivity and volumetric heat capacity from a single pulse measurement made with Campbell's probe. Bristow went on to present

preliminary results demonstrating the application of the dual-probe instrument for measuring soil properties. In later work, Bristow studied soils of different moisture contents and compared the results with independent estimates made by using standard procedures described in the literature [113]. His study concluded that small dual probes can provide reliable thermal properties of soils as a function of moisture content. Fontana et al. evaluated the performance of the dual probe for the measurement of the thermal parameters of some selected food products giving results within 7% of other data published in the literature [114].

These probes have up to now been predominately used for determining the thermal conductivity of soils, in which the probes can be pushed into by hand. They have not been used, however, for the determination of the thermal properties of briquettes of compressed biomass. Their use in biomass briquettes presents some problems, because once dried, the density and structure of briquettes prevents the insertion of the probes into the material without risk of damage. One solution to this is to drill some carefully sized holes for the insertion of the probe needles. The objective of this study is to evaluate the performance of using the dual probe for the measurement of volumetric heat capacity, thermal conductivity and thermal diffusivity for biomass briquettes when this method of drilling holes in the briquette is used. The thermal data are then used in the evaluation of the analytical model of pyrolysis.

5.2.3 Theory

The dual-probe sensor consists of two parallel stainless steel needles separated by a distance r. One of the needles contains a line source heater and the other a temperature sensing k-type thermocouple. With the probe inserted in a given material, a short pulse of known power and duration is applied to the heating needle and the response of the thermocouple as a function of time is monitored. The volumetric heat capacity, diiffusivity and conductivity can then be simultaneously determined from the temperature response [113, 115].

The determination of the thermal parameters is based on the solution of the radial heat conduction equation for an infinite line heat source. For a heat pulse of duration t_0 seconds, the rise in temperature as a function of time of the probe a distance r from the heat source is given by [113]:

$$\delta T(r, t) = \frac{q}{4\pi(\rho c)\alpha}[Ei(\frac{-r^2}{4\alpha(t - t_0)}) - Ei(\frac{-r^2}{4\alpha t})] \text{ for } t > t_0 \qquad (5.16)$$

where δT is the change in temperature $[K]$, t is time $[s]$, r is the radial distance between the line source and the heater needle $[m]$, q is the energy input per unit length of the heater per unit time $[Wm^{-1}]$, ρc and α are the volumetric heat capacity $[Jm^{-3}K^{-1}]$ and the thermal diffusivity $[m^2s^{-1}]$, respectively, of the material in which the probe is placed, and $-Ei(-x)$ is the exponential integral. The thermal properties can be determined by making use of the fact that the temperature response displays a maximum at a distance r from the heating probe at a particular time, and then taking the derivative of Equation 5.16 and setting the result to zero [112]. This yields expressions for the thermal diffusivity. Equation 5.16 can be rearranged to yield an expression for ρc which can be determined at the peak. The thermal conductivity (λ) can then easily be determined from the definition $\lambda = \alpha/\rho c$. An alternative method for determining the thermal properties, is to perform a non-linear fit of Equation 5.16 to the experimentally determined δT. This can be done, for example, using the Marquardt algorithm described by in a paper by Bristow et al. (cited in [113]).

5.2.4   Methodology

The dual heat probes used to make measurements consisted of two needles made from stainless steel tubing with external diameter $0.9mm$ and length $30mm$. The heat sensor was a chromel/constantan thermocouple and the heater needle contained a Evanohm heater. Details of probe construction are given by Campell et al. [111] and Bristow et al. [116]. The spacing between the probes in these tests was around $6mm$. For use in soft substances, such as fruit, this value can be calculated more precisely during the calibration procedure described in Section 5.2.5, however, with compressed biomass briquettes it is not possible to push the probes into the material without pre-drilled holes. Interference fit holes were drilled in the briquettes with a Bridgeport Series I milling machine to a precision of $\pm 0.5mm$. The probes were then inserted into the material so that their full length was covered. A heat pulse was produced by applying a voltage from a direct current power supply to the heater needle for 4 seconds, and the response at the other needle was then measured as function of time. A Campbell scientific datalogger was used to control the duration of the heat pulse, measure the voltage across the heater, and monitor the temperature response.

Briquettes of 4 different densities were prepared, and in each briquette three sets of holes were drilled in different locations. The briquettes were oven dried to achieve a close to 0% moisture content, then removed from the oven and wrapped in cling film to minimise water absorption while allowing them to cool to room

temperature. The probes were inserted into the pre-drilled holes and the system was left to reach thermal equilibrium, until the probe with the heat sensor in recorded a steady temperature. A heat pulse was then applied and the response measured. The probes were then removed, reinserted, and the system left to attain thermal equilibrium again, before another heat pulse was applied. This procedure was then repeated a third time for each set of holes. Figure 5.1 shows a typical heat-probe response for a newspaper briquette. The graph shows three repeat readings, which overlay each other, demonstrating the repeatability of the measurement. The thermal parameters can then be determined by performing a non-linear fit of Equation 5.16 to the temperature response.
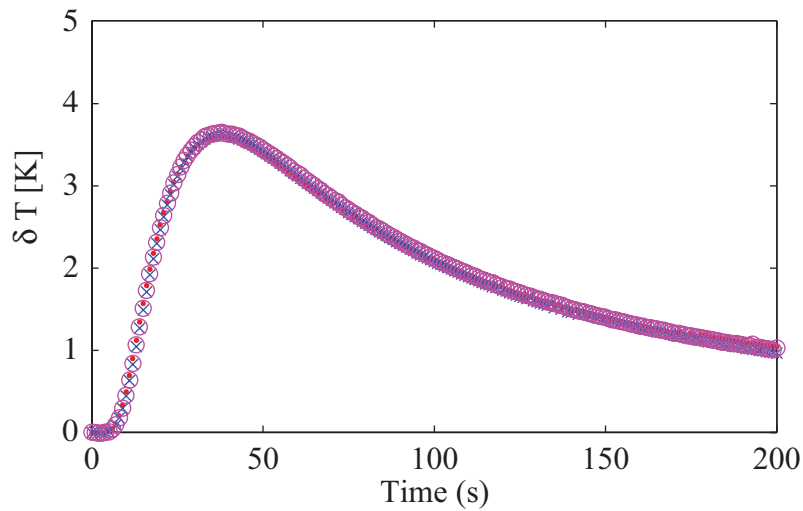
Figure 5.1: Typical results from the heat-probe method for newspaper briquettes. There are three repetitions for the same hole set plotted on this graph.

5.2.5   Calibration and estimation of uncertainties

Purpose and method of calibration

In order to assess the operation of the probes, the reliability of the fitting procedure, and the random uncertainty associated with this technique, the heat-probe technique was applied to a material with known thermal properties, water. A heat pulse was generated, the response measured, but rather than determining the thermal properties, a value for the probe separation using the known thermal properties of water was found using a numerical least squares curve fit. This

value of r could be cross-checked with a value obtained by physically measuring the distance between the probes. Then, to confirm the reliability of the procedure, and estimate the statistical uncertainty associated with the fitting technique when the value for r is known, a reverse-fit was done to find the values of the thermal properties of water. These were then compared with the literature values.

Calibration procedure

Water was immobilised with agar to stop convective currents developing during the heat pulse. It was assumed that the agar did not significantly alter the heat capacity of the water [117]. Campbell et al. made the calibration using only 0.2% agar, but it was found by Ochsner et al. that at such a concentration, the value of r found was not stable as the heat input varied [117]. However, they found that using 0.6% agar, gave values of r independent of pulse heat input.

The heat probe was inserted in the agar and everything was placed in a climate controlled chamber to maintain a constant temperature throughout each calibration test; this maintained a steady temperature of $22.2 \pm 0.2K$ for each of the repeat tests. The temperature of the probes and agar solution were given time to reach thermal equilibrium. A heat pulse, of power q was then introduced for 4 seconds, and the temperature response, δT, recorded as a function of time, as described in Section 5.2.4. The constants in Equation 5.16 were set to those of water (the data are given in Table 5.1, the values are interpolated from literature data [118] to give the thermal properties at the temperature at which the experiment was carried out). r was then found by way of a non-linear fit of Equation 5.16 to the first 90 seconds of the heat response curve using the method of Marquardt. Figure 5.2 shows a fit using three different values for the pulse duration, demonstrating the importance of correctly knowing this parameter. The agar solution was left to re-attain thermal equilibrium. This measurement was repeated 7 times. A least squared fit of Equation 5.16 to the measured data gave a value of r of $0.0058m$ with a 95% confidence interval of ± 0.0001. This was used below to estimate the statistical random error associated with this method.

Estimation of the errors associated with the dual heat-probe technique

Campbell et al. [111] and Klioyenberg et al. [119] have shown that heat capacity determined using the dual-probe method is sensitive to probe-spacing. First order error analysis suggests that a 2% error in the spacing will result in a 4% error in both the heat capacity [119] and the thermal diffusivity. Interestingly,
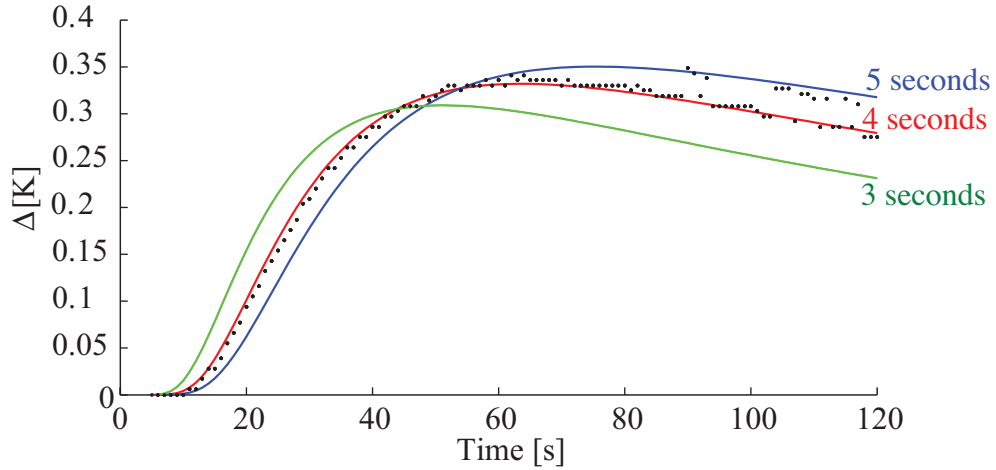
Figure 5.2: Numerical fitting Equation 5.16 to find the distance between the probes. The fit is done with three different values for t_0, showing that a heater duration period of 4 seconds clearly gives the best fit to the experimental data.

however, it has been shown that these errors are opposite in sign and cancel on determination of thermal conductivity [115]. The consequence of this is that the thermal conductivity measured by the dual-probe method is not sensitive to probe spacing.

Another potential error results from using the equation for an infinite line source with finite length probes. Kluitenberg et al. show that, for a fixed probe length, errors will increase as probe spacing increases [120]. For a probe length of about $30mm$, as used in this study, they showed that the errors will only start to become significant after about $7.5mm$, or in other words the assumption of the heater as an infinite line source is valid in the region used in this study where the distance between the probes is about $6mm$. One point that is important to consider is that as the probe spacing becomes smaller, the effective size of the sample is reduced and there may become a point where the sample volume might not adequately represent the material that is being tested [115]. In the literature a probe spacing of around $6mm$ is typical (for example [112, 117]).

Measurement errors of the other inputs must also be considered. One source is errors in q, the power of the heater, of which the total uncertainty is a combination of the uncertainty in resistance of the heater, the reference resistance and in the measured voltage across the heating probe. It is also likely that there will be errors associated with uncertainties in the timing of the probe heating period.

In order to assess the combined statistical random error associated with the system used in this study, a non-linear fit of Equation 5.16 using the Marquardt

algorithm, was completed for the same agar data used in the calibration (see the Subsection 'Calibration procedure' in this Section). The mean value for r of $0.0058m$, previously determined for each sensor, was taken as the probe spacing. By this method, values for volumetric heat capacity and thermal conductivity for each of the calibration tests were determined. The results are given in Table 5.1 alongside literature values [118]. The literature values were within the error bounds of the outcome obtained from the fit; the thermal conductivity and heat capacity were found to have a statistical uncertainty of about $\pm 7\%$ of the mean value (95% confidence interval, assuming a normal distribution about the mean). These repeat readings on a substance of known thermal properties, have thus given an indication of the statistical uncertainty that should be expected using this technique for determining unknown thermal parameters (when the distance between the probes, r, is known). Moreover, it verifies that the numerical fitting, using the Marquardt fitting algorithm, is able to identify the correct values.

Variable	Literature	Experimental	95% confidence interval	% Uncertainty
$\lambda [Wm^{-3}K^{-1}]$	0.602	0.594	± 0.04	7%
$\alpha [m^2 s^{-1}]$	1.44×10^{-7}	1.41×10^{-7}	$\pm 3.00 \times 10^{-9}$	5%
$C_p [kJkg^{-1}K^{-1}]$	4.17	4.22	± 0.3	7%

Table 5.1: A table of the thermal thermal parameters for water from the literature [118] and those obtained from the heat-probe method with this study.

Figure 5.1 shows a typical set of repeated results for the same briquette hole set, where the heat probe was removed and reinserted for each test. Figure 5.3 shows results for the two different sets of holes on the same briquette. The heat-pulse response for each hole set is for itself repeatable, however, there is clearly a difference in the response between the holes for the same briquette. There are two main possible causes for this disparity. Firstly, the briquette may be inhomogeneous, with significant variations in density between the different sets of holes. Secondly, uncertainty in the distance between the probes will lead to significantly different responses to the heat pulse, and thus also the thermal parameters calculated from the model fit (see Section 5.2.5). By writing an analytical expression for ρc_p, it is possible to understand the dependance of the heat capacity on the probe spacing. Rearranging Equation 5.16 gives:

$$(\rho c_p) = \frac{q}{4\pi\alpha\delta T}[Ei(\frac{-r^2}{4\alpha(t-t_0)}) - Ei(\frac{-r^2}{4\alpha t})] \tag{5.17}$$
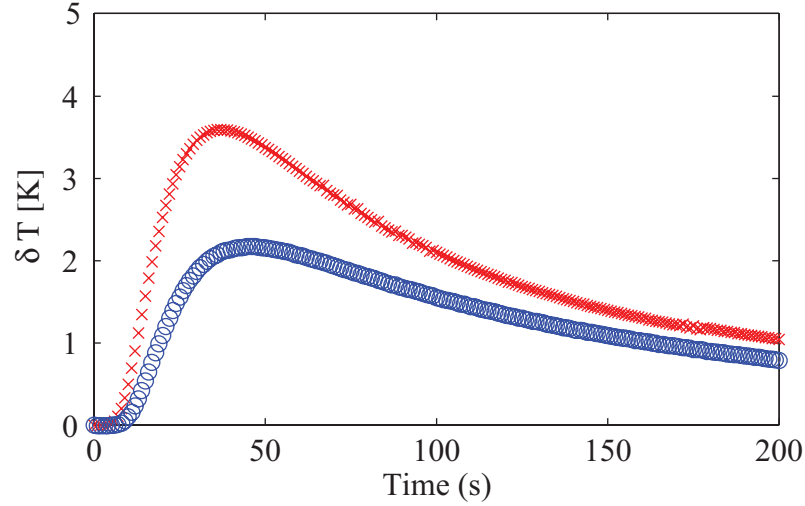
Figure 5.3: The heat-probe response for two different hole sets on the same briquette.

The value of the heat capacity is dependent on the height of the maximum peak and its position. It is clear from Equation 5.17 that uncertainty in the value of r will result in a shift in both the position and the peak height of the measured heat-pulse response. The magnitude of the shift can be estimated by the equation derived by Campbell for an instantaneous infinite heat source [111]:

$$\rho c_p = \frac{q}{e\pi r^2 T_m} \tag{5.18}$$

where T_m is the peak temperature of the response. Under the conditions of the heat-pulse tests in this study, this would result in a relative error of around 0.1% compared with using Equation 5.17 for a heat pulse of duration t_0 [119]. By applying Equation 5.18, it was found that an uncertainty in r of $\pm$ 0.5mm (8%) could result in an observed shift in response peak height, δT, of up to 1.5K. This shift corresponds to a 16% uncertainty in the heat capacity [119]. Inhomogeneity in the density in the briquette would also lead to an increase in this uncertainty. However, this was minimised by cutting the briquette samples into small squares, after the measurements had been made, and determining the local density in the area of each hole set; the density was determined using a sterometric method described in Section 3.1.5. The results shown in Figures 5.4 and 5.5 are plotted as a function of the measured local density.
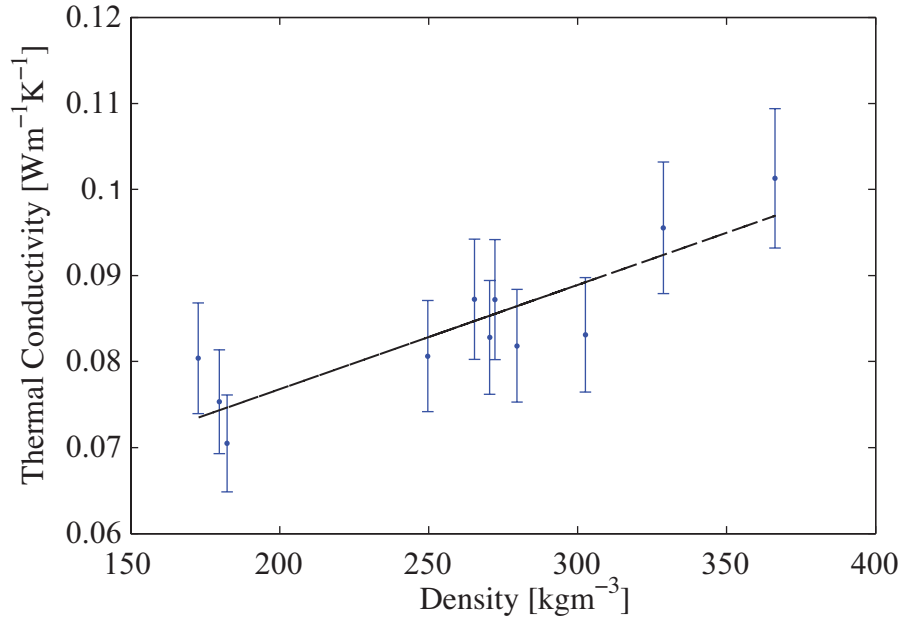
Figure 5.4: The variation in thermal conductivity as a function of density for compressed dry newspaper found using the heat-probe method.

5.2.6   Results and discussion

Figure 5.4 shows a graph of how the thermal conductivity varies as a function of material bulk density. There is a trend of increasing thermal conductivity as bulk density increases. In the range of densities tested (between about 175-375 kgm^{-3}, typical of briquettes formed by the wet method), the trend appears to be linear and a least squares fit of this data gives the following equation for the thermal conductivity of dry compressed newspaper as a function of density:

$$\lambda = 0.000121\rho + 0.0526 \tag{5.19}$$

This trend of increasing thermal conductivity as a function of bulk density is similarly observed for soils [121], and can be explained by the improved inter-particle contact as the porosity is decreased. The magnitude of the thermal conductivity obtained for dry compressed newspaper is of the same order of magnitude as that obtained by Ravi et al. for compacted sawdust [100] indicating that the value is reasonable.

Figure 5.5 shows the heat capacity measured over the range of densities tested, giving a mean value of 1612 JK^{-1}. It is assumed that the specific heat capacity of the briquette system is constant across the density range tested. This behaviour can be explained because the contribution to heat capacity of the air volume within
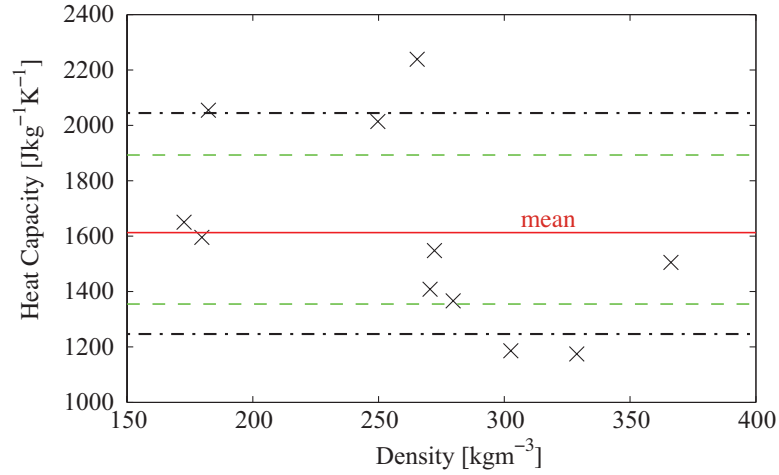
Figure 5.5: Heat capacity plotted as a function of density. One dashed line (- - - -) shows a prediction of the uncertainty associated with the imprecision in drilling the holes for the probe, and the other dashed line (- · - ·) takes into account the additional statistical uncertainty expected in the measurements.

the solid, (which makes up the porosity of the solid), can be shown to have an insignificant effect on the heat capacity across the range of bulk densities tested:

$$c_{total} = \frac{m_{air} \times c_{air} + m_{solid} \times c_{solid}}{(m_{air} + m_{solid})} \qquad (5.20)$$

where $m_{solid} >> m_{air}$

where c_{total} is the total specific heat capacity due to the solid and the air contained in the pores, c_{air} is the specific heat capacity of the air, c_{solid} is the heat capacity of the biomass solid, m_{air} is the total mass of air in the solid and m_{solid} is the total mass of the solid biomass material. In the range of bulk densities tested air contributes little to the total mass of a sample ($m_{solid} >> m_{air}$), and therefore, the heat capacity of the air can be neglected in the calculation.

Dashed lines on Figure 5.5 indicate the scatter in the results expected as a result of the uncertainty in the probe spacing, r. A second set of lines has been added that also include additional statistical uncertainty associated with the method, estimated from taking repeated measurements on immobilised water, described in Section 5.2.5. The results that are not within this uncertainty band can probably be explained by larger uncertainties in r than expected, most likely resulting from the drilling. Kiiskinen et al. studied the specific heat capacity of paper between a temperature range of 45-125 $°C$ and found it to vary between 1200 to 2300 $Jkg^{-1}K^{-1}$, depending on the composition and temperature of the paper.
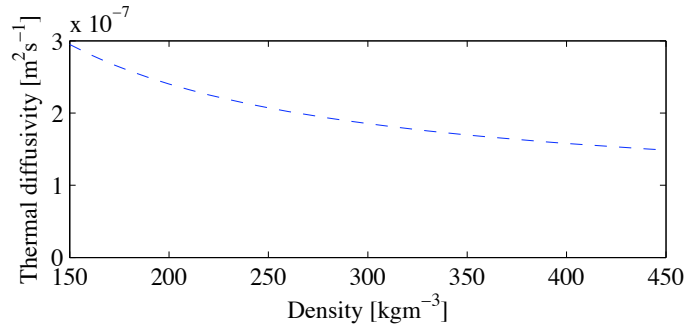
Figure 5.6: The resulting graph of how thermal diffusivity varies as a function of density if heat capacity is assumed constant and the curve for the change in thermal conductivity as a function of density is used.

Although the briquette temperature in this study was outside this range, it does indicate that the mean value found in this investigation is reasonable.

Figure 5.6 shows how the thermal diffusivity of a compressed newspaper briquette is expected to vary as a function of density if a constant value of $1612\ JK^{-1}$ is assumed for the heat capacity. It shows that as the density of a briquette sample increases, the thermal diffusivity decreases. This behaviour cannot be judged from the change in thermal conductivity alone, as storage effects influence the heat propagation: thermal diffusivity is a function of heat capacity, thermal conductivity and density, $(\alpha = \lambda/\rho c_p)$, and in this case total heat capacity, (ρc_p), is growing at a faster rate than conductivity. Increasing the density results in there being more material per unit volume, which requires more heat per unit volume to raise the temperature by the same amount. The large heat capacity of the soild means that this effectively outweighs the effect of increasing thermal conductivity. The result is a decreasing thermal diffusivity with increasing density. The consequence of this is that increasing the density makes it more difficult for heat to diffuse into the material, meaning that in pyrolysis, the temperature front will advance more slowly. This will mean a slower rate of advance of the pyrolysis front, and a slower overall normalised burn rate. This agrees with the experimental result of a decreasing normalised burn rate with increasing briquette density.

5.2.7   Concluding remarks on the heat-probe method and comments on further work required

A method has been developed and assessed for the determination of the thermal properties of biomass briquettes. The method has been applied to compressed newspaper, giving values which seem reasonable according to the literature.

However, the large uncertainties in the thermal probe spacing leads to significant uncertainties in the heat capacity and thermal diffusivity. The sensitivity of measured heat capacity on probe spacing means that the accuracy of this method is significantly limited by the precision with which the holes in the briquette can be drilled and measured. In its current state, it has been been shown only to be useful in giving approximate values for the thermal properties.

There are various means by which the accuracy of the method can be improved. One possibility is to reduce the relative error associated with the distance between the probes by simply increasing the probe spacing. This would also give a much more representative sample of the briquette volume. However, the probe length would also need to be increased, so that the assumption in the analysis of an infinite probe length remained valid. Another option would be to find methods of improving the drilling accuracy, such as making a drilling template, or using a computer-controlled drilling machine. It is also worth investigating designing a stiffer, sharp-ended probe that could be pushed into samples, especially for use in partially pyrolysised briquettes (char). This might be done for example, by decreasing the probe length or manufacturing a thicker probe. However, the effect on the assumptions in the model of an infinitely long and an infinitely thin heat source, need to be considered [119]. Such design modifications would therefore only be valid if the reduction in uncertainty from the increased precision in probe separation were to offset the increase in error from effects of finite probe length and the use of a more cylindrically thick heat source.

Data from work on soils clearly shows that as the moisture content increases, both the thermal conductivity and the heat capacity of the solid will increase [113]. Further work is required to determine the effect of moisture content on the behaviour of the thermal properties of biomass briquettes.

The heat-probe method investigated here provides a low-cost and practical means to determine the thermal properties of biomass briquettes. It could be further developed to collect data at different temperatures (for example by doing the tests with briquettes in an isothermal oven), and at different degrees of thermal degradation (by quenching the pyrolysis and measuring the thermal properties of the partly charred sample). Much further work is required for this to be possible. As it stands, the technique is able to give approximate values for the thermal properties of biomass briquettes (namely the thermal conductivity, heat capacity and thermal diffusivity) to be used in numerical models of their combustion. Indeed, the values obtained here will be used in the application of the numerical pyrolysis model presented in Section 5.1.

5.2.8   Determination of the coefficients of heat transfer to the surface of a briquette

There is very little work in the literature on the heat transfer of a flame to a burning vertical surface under natural convection, such as for the slabs in this study. Bamford et al. [83] suggest that heat transfer from a burning flame can be represented by a convective and a radiative heat transfer term with constant values for the flame emissivity and convective heat transfer coefficient. This assumption was applied in this study, and the total heat transfer coefficient at the surface of the briquette was considered to be made up of the following terms:

1. A convective heat transfer term of the form $h(T_f - T_s)$;

2. Radiation from the flame of the form $\sigma \epsilon_f T_f^4$ [83];

3. Radiation from the surface of the wood to the flame, where the surface of the char is assumed to behave as a black body as a first approximation;

4. Radiation loss from the surface to the surrounding atmosphere, through the flame, which is assumed to have an absorptivity of $(1 - \epsilon_f)$ [108].

This results in the following expression, which was assumed to account for the heat transfer at the surface of a briquette:

$$\frac{dQ}{dt}\bigg|_{surf} = A_s[h(T_f - T_s) + \sigma \epsilon_f (T_f^4 - T_s^4) - \sigma(1 - \epsilon_f)(T_s^4 - T_{at}^4)] \qquad (5.21)$$

5.2.9   Estimation of the heat transfer coefficients by experiment

In order to determine estimates for the coefficients of heat transfer at the surface, a simple method was used in which an aluminium slab was heated up by a flame, and a numerical fit made to the recorded temperature profile to determine the heat transfer coefficients.

The slab had dimensions $80 \times 88 \times 12.5mm$, a mass of 273.3g and was coated in soot from a flame. Aluminum was chosen, because a slab of these dimensions has a Biot number significantly less than 0.1[1]. This implies that the heat conduction inside

---

[1]The Biot number can be found from: $Bi = hL/\lambda$, where the thermal conductivity of Aluminium at 600 K is 218 $Wm^{-1}K^{-1}$ [122]. Even with an over estimate of h of 200, then $Bi \approx 200 \times 0.0125/218 = 0.0011$.

the slab is much faster than the heat conduction to the surface. Temperature gradients can be considered negligible and a lumped capacitance model can be applied to model temperature change as a function of time. A similar assumption was made and experimentally validated by Burham-Slipper in using an aluminium plate to assess the heat transfer in lieu of a pot in the optimisation of stoves [41]. It is therefore, sufficient to use a single thermocouple to measure slab temperature, and an $3mm$ K-type thermocouple was embedded at its centre.

The aluminium slab was placed on a mesh grid, shown in Figure 5.7a. A line of firelighters were then ignited below it to create a flame over the surface of the slab, as shown in Figure 5.7b. The temperature of slab was recorded every 2 seconds. As can be clearly seen in the figure the flames completely wrap the surface of the slab. The temperature of the flame was continually monitored using a $3mm$ K-type thermocouple.

(a) The experimental set-up of the slab experiment: An aluminium slab was placed on a mesh grid with a thermocouple to monitor its temperature.   N.B. the slab is black because it is covered in soot.
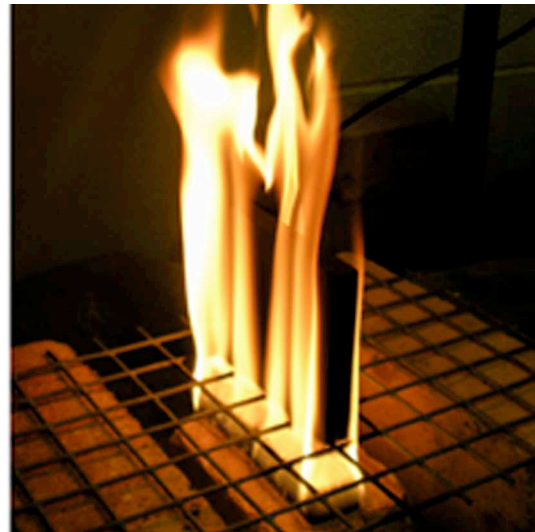
(b) Firelighters were lit beneath the slab in a row such that the flames enveloped it.

Figure 5.7: The heat slab experiment

The above experiment was repeated 7 times. Figure 5.8 shows 5 of those experimental repeats (for clarity[2]). The temperature of the slab can be seen to increase until an equilibrium temperature is reached where the heat supplied by the flame to the slab is balanced by the heat lost to the surroundings through the flame. At this point:

---

[2]The results omitted were not significantly different from the ones plotted.
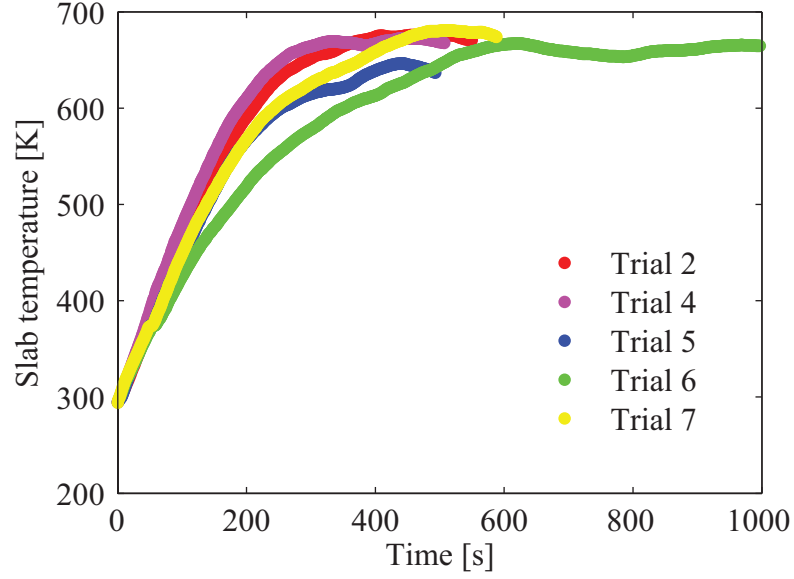
Figure 5.8: The temperature of the slab as a function of time for a sample of 5 repetitions. The labels correspond to the experiment numbers given in Table 5.2.

$$\left. \frac{dQ}{dt} \right|_{surf} \Rightarrow 0 \tag{5.22}$$

Using Equation 5.21, the value of ϵ_f in terms of h can be defined as:

$$\epsilon_f = \frac{2T_{uni}^4 + T_{at}^4 - h(T_f - T_{uni})}{T_f^4 + T_{uni}^4 - T_{at}^4} \tag{5.23}$$

where T_{uni} is the uniform temperature to which the aluminium plate tends. h can then be found by a numerical least squares fit of Equation 5.21 to the plate temperature data, where the value of ϵ_f is restricted by Equation 5.23. This was implemented in Matlab. The temperatures used in this calculation were as follows: the temperature of the surrounding atmosphere was taken to be 293K, room temperature; the flame temperature was taken as the mean averaged over repeat experiments, which was 750 K with a standard deviation of 50 (N.B. A compensation was not made for radiation in this measurement, and further refinements of this method should consider taking this into account); T_{uni} was taken as the mean uniform peak temperature of the slab measured over all the experimental repeats, which was 657 K with a standard deviation of 19.

The above analysis was completed for each of the experimental repeats and Table 5.2 shows the the results. If the standard deviation is taken as an estimate of the uncertainty, h has a mean value of 102 ± 26 and ϵ_f has a mean of 0.54 ± 0.07.

As an example, Figure 5.9 shows a fit of the above equations to the experimental curve 'trial 2' (see Table 5.2). The dotted lines show the best fit achieved when the values for the flame temperature, T_f, and the uniform slab temperature, T_{uni}, were defined as the mean values of 750 K and 657 K respectively (central dotted line). The other dotted lines (above and below the mean fit) indicate the limits of uncertainty in the fit, due to the uncertainty in the flame and slab temperature (750±50 K and 657±19 K, respectively).

Exp no.	ϵ_f	h
1	0.48	126
2	0.6	80
3	0.51	116
4	0.46	134
5	0.57	93
6	0.65	61
7	0.54	105
mean	**0.54**	**102.14**
s.d.	**0.06**	**26**

Table 5.2: Values obtained by a numerical least squares fit for the convective heat transfer coefficient, h, and the flame emissivity, ϵ_f, obtained for firelighters during the ignition phase for each of the 7 trials.

5.2.10 Discussion of the method

There are several limitations to this method. Firstly, it ignores the effects of the outflow of the volatiles as they leave the surface, which are likely to modify the convective heat transfer coefficient at the surface. This effect is further discussed in Section 5.2.11 below. Secondly, in the above methodology the heat transfer coefficients found were for firelighters. This is not a biomass briquette flame, however the coefficients for ϵ_f and h derived here are likely to be representative values of heat transfer to a solid enveloped by a flame, and they were used as constants in devolatisation model (described in Section 5.1). The validity of this assumption is assessed in Section 6.4 , where a sensitivity analysis on the effect of the heat transfer coefficients on the predicted normalised burn rate is completed. Finally, it should be noted that the value for the emissivity found for ignition is specific to this experimental set-up; the value for ϵ_f by its nature will be a function of the thickness of the flame[3] [123], which is related to the amount of firelighter

---

[3]$\epsilon_f = 1 - e^{-\kappa L}$ where κ is a property of the flame and L is the characteristic flame thickness [123].
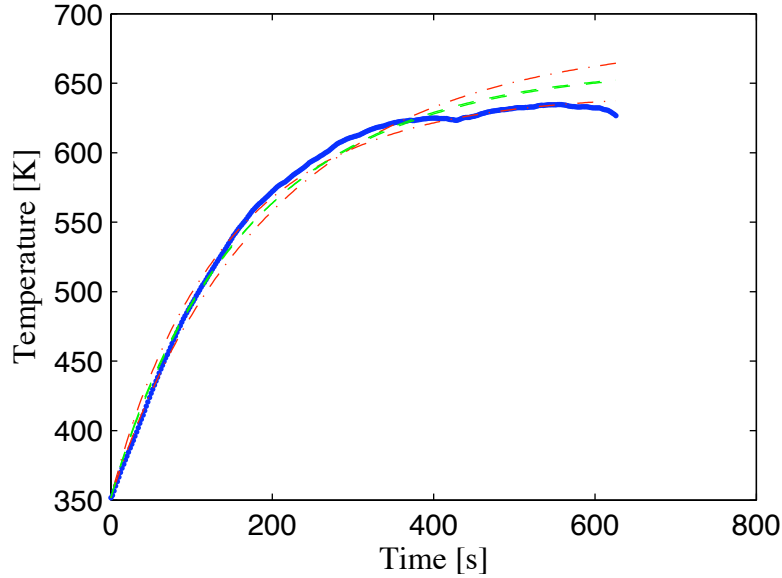
Figure 5.9: Data for 'trial 2' (see Table 5.2), is given as an example. The dotted lines show the best fit of Equation 5.21 to the data with the restriction of Equation 5.23. The outer dotted lines indicate the variation in the best fit at the limits of uncertainty associated with the flame and the final uniform slab temperature (see Section 5.2.9). The experimental curve can be observed to lie on the edge of the uncertainty bounds; 95% of the values of ϵ_f and h calculated from fitting these curves to data fall within the standard deviation uncertainty estimates given in Section 5.2.9.

used for the ignition of a slab briquette . Therefore it was important to control of the quantity of firelighter used in order to give a reproducible value of ϵ_f. The estimated uncertainty in the value of ϵ_f found by numerical fitting demonstrates the degree to which this has been achieved in the above experiment.

5.2.11 A discussion of the modification of the heat transfer coefficient, h, with blowing at the surface

In the above estimation of the heat transfer coefficients, the effect of transpiration of volatiles from the surface (known as blowing in the literature) during the devolatisation phase has been ignored. In the literature review, the inhibition of oxygen diffusion to the char surface by this effect was discussed (see Section 2.3), with the consequence being that the volatile and char combustion phases can be considered independently. However, it is also likely that the transpiration of volatile gases through the char layer will inhibit the interaction of the surface with the free-stream flow, and therefore reduce the convective heat transfer coefficient

[64]. In this section, the magnitude of the effect of volatile blowing on the convective heat transfer coefficient is estimated, by considering the modification of the Nusselt number by the outflow of gases.

The Nusselt number is defined as:

$$\overline{Nu} = \frac{hL_c}{\lambda} \qquad (5.24)$$

The modification of the Nusselt number with blowing can be found using the correlation [64, 124]:

$$\frac{\overline{Nu_m}}{\overline{Nu}} = \frac{\Upsilon}{e^{\Upsilon} - 1} \qquad (5.25)$$

where the blowing coefficient is defined by:

$$\Upsilon = \frac{M_v/M_\infty}{cf/2} \qquad (5.26)$$

where M_v is the mass flux of volatile gases, M_∞ is the free-stream mass flux and cf is the friction coefficient given by:

$$cf = \frac{\tau_0}{1/2\rho u_\infty^2} \qquad (5.27)$$

The boundary shear stress was found with [64]:

$$\tau_0 = 0.365 \frac{\rho_\infty u_\infty^2}{Re^{1/2}} \qquad (5.28)$$

which was used for the determination of τ_0 in small burning wood cribs by Burnham-Slipper [64].

The outward mass flux of volatiles can be estimated by considering the normalised burn rate of a solid. For example, a low density slab briquette with a density of 400 kgm^{-3} with dimensions $34 \times 14 \times 90mm$ will have a normalised burn rate of $0.0034s^{-1}$ (equivalent to $6.15gm^{-2}s^{-1}$). The magnitude of the free-stream convective flow mass flux can be estimated by assuming a characteristic flow velocity of between 1 to 3 m/s [125], and that the fluid can be considered to be air with a temperature approximately equal to the gas phase temperature of 750 K, having a density of 0.4663 kgm^{-3}. A flow velocity of 2 ms^{-1} gives a free-stream mass-flux equivalent to 930 $gm^{-2}s^{-1}$. Burnham-Slipper estimates the Reynolds

number for a burning wood-crib as 50<Re<500 [64]. A Reynolds number of 500 is used in this approximation. This gives:

$$\overline{Nu_m} = 0.81\overline{Nu} \tag{5.29}$$

and thus the effective heat transfer coefficient, h, is 20% lower due to the effect of blowing. This gives an indication of the magnitude of the effect of blowing on the heat transfer coefficient. The effect is in fact less than the uncertainty in h, which was estimated to be be around 26%. It is interesting to view this in relation to a sensitivity study looking at the effect of changes in h on the NBR of the briquette, and this is considered Section 6.4.1. There it is concluded that it is sufficient to ignore the effect of blowing in a first approximation, because the change in predicted normalised burn associated with the modification in h is less than the experimental uncertainty associated with measuring the normalised burn rate of a burning slab.

5.2.12   Concluding remarks on the determination of the heat transfer coefficients

A simple methodology has been suggested whereby the heat transfer coefficients, h and ϵ_f, were estimated for heat transfer to the surface of a slab enveloped with a flame. Firelighters were used to create a flame around an aluminium slab, and the temperature of the slab recorded as a function of time. The heat transfer coefficients were determined by numerically fitting to the temperature data, a differential equation describing the convective and radiative heat transfer. It was assumed as a first approximation, that the values determined for these coefficients were sufficient to estimate the heat transfer to the surface of a newspaper briquette. The values for h and ϵ_f determined using this method, were then used in the analytical model (described in Section 5.1) and applied in Chapter 6.

5.3   Chapter Summary and Closing Remarks

A one-dimensional pyrolysis model has been presented. Determination of appropriate values for the thermal parameters is important for the evaluation and assessment of the model's validity in comparison with experimental combustion data. In this chapter two simple methodologies are presented in order to determine some key thermal parameters for compressed newspaper briquettes:

- a heat-probe method was demonstrated for the determination of the following: the thermal conductivity of newspaper briquettes as a function of briquette density, the heat capacity of dry newspaper and the thermal diffusivity as a function of density. It provides a potentially versatile method useful for future studies in the determination of these different briquette thermal properties;

- an aluminium slab enveloped by a flame was allowed to heat up, and by numerical optimisation methods, a differential heat transfer equation was fitted to the temperature data to find the best values for the heat transfer parameters; the convective heat transfer coefficient and the flame emissivity were thus determined.

In the chapter which follows, the kinetic reaction parameters are obtained by numerical optimisation. The values of the thermal parameters and heat transfer coefficients identified in this chapter are then used in the evaluation of the model for briquettes burning in free air, and predictions compared with experimental data from Chapter 4.

Chapter 6

Evaluation of the Model

The material thermal constants and heat transfer coefficients for the model have been estimated in Chapter 5. In what follows, these constants are used in the model evaluation, with the objective of predicting the normalised burn rate of a briquette burning in free air, and understanding how this rate is affected by changes in the material properties and external environmental conditions. In the first section, values for the kinetic constants are optimised to reproduce as closely as possible the experimental data, and the sensitivity of the fit to changes in these parameters is evaluated. Following this, a parametric study on the model constants is carried out in order to establish their effect on the normalised burn rate. Finally, the limitations of the model are discussed and several improvements are considered. It is concluded that the simple model is sufficient for predicting the normalised burn rate of a single burning briquette in free air, and offers a numerically cheap model of briquette devolatisation. The chapter ends with a discussion of the limitations of the model and considers its improvement in order to better understand the complex physical processes involved in the devolatisation process.

6.1   Numerical Solution of The Model Equations

Each slab was discretised into slices as illustrated in Figure 6.1. The set of simultaneous differential equations and boundary conditions given in Section 5.1.4 were written in matrix form and solved by the explicit Euler method. Figure 6.2 is a flow chart showing each of the steps implemented in the code, in order to obtain the output of briquette mass decrease as a function of time; the parameters required for the evaluation of each part have been highlighted.
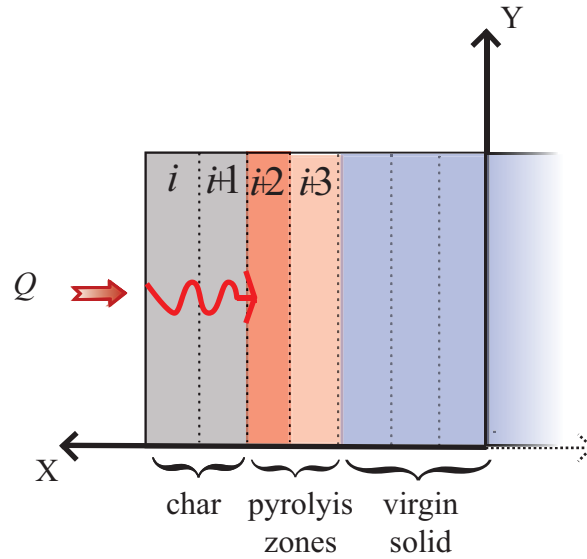
Figure 6.1: A slab briquette descritised into N zones. Half of the briquette is shown, the second half is symmetrical about the y-axis, where the boundary conditions are given by Equation 5.11.

A given thickness of slab was assumed, and using the boundary conditions described (see 5.1.4), the one-dimensional model was then numerically solved to find the mass loss per unit volume occurring in each of the control volumes at any given time (see Figure 6.1). The actual total mass loss for a particular control volume within the slab was determined by multiplying, at each time step, the mass loss per unit volume by the control volume (determined by the briquette height and width and the thickness of a slice). A summation of all the control volumes was then calculated to find the total mass loss for each time step. The thickness of the slab was changed, the model re-evaluated, and this process repeated[1]. The equivalent A/V ratio for each thin slab was found from its thickness, height and width. This modelling approach, it would appear, is only valid for samples that are much thinner than their height and widths (this is discussed further in Section 6.6). For particles where the dimensions are approximately equal, multi-dimensional models should be considered, for example modelling decomposition based on spherical geometry. Such models are not considered by this study and further work should be carried out in this area, comparing the behaviour of multidimensional models with one-dimensional models for modelling the same situation.

---

[1]For slabs that are thin, relative to their height and width, changing the slab thickness has a significant effect on its overall A/V ratio (compared to changing any of its other dimensions).
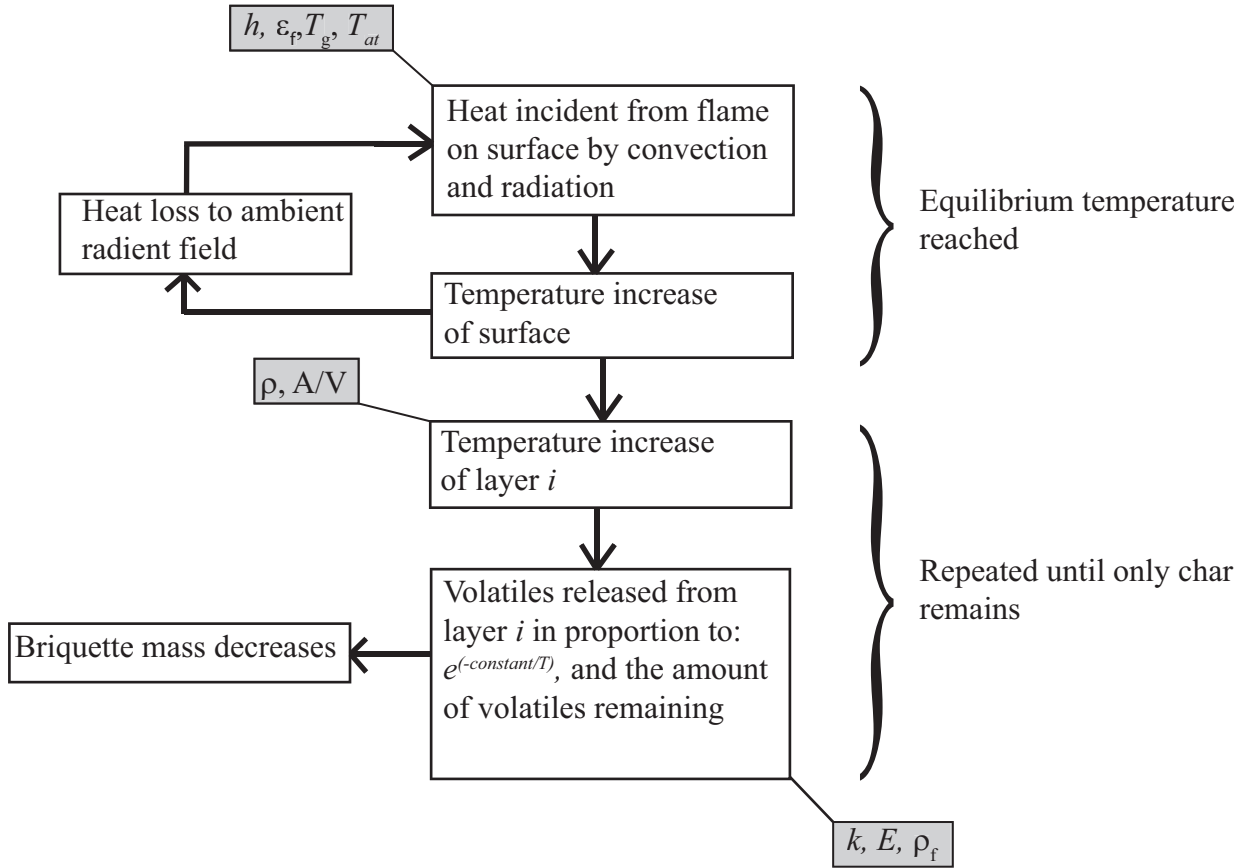
Figure 6.2: A flow diagram showing the stages in the execution of the model.

Time step and slice thickness

The maximum time step possible in order to achieve a physically realistic solution is given by:

$$\delta t < \frac{(\delta x)^2}{2\alpha} \tag{6.1}$$

Figure 6.3 shows how the predicted normalised burn rate from the model tends to a constant value as a function of the number of slices, N, of thickness $\delta x = R/N$, where $2R$ is the thickness of the slab. A slice thickness δx of 0.2×10^{-3} was used in the solution of the model in this chapter; it can be seen from the graph that there is less that a 4% change in normalised burn rate between N=25 and N=100. A time step of 0.08 s was chosen (it was found that a lower time step of $0.01s$ resulted in less than a 2% change in predicted normalised burn rate compared to 0.08 s, but led to a considerable increase in the computational processing time). The values for N and dt chosen gave a good balance between computational accuracy and the

total model run time; the resulting uncertainty from this choice of values is much less than the experimental uncertainty in the normalised burn rate estimated in Chapter 4.
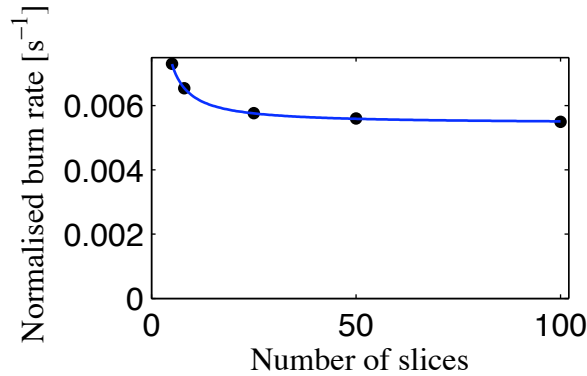
Figure 6.3: The change in predicted NBR with an increasing number of slices for a slab width of 1cm, and density of 250 kgm^{-3}. The width of a slice (control zones) can be found from: $(\delta x = R/N)$.

6.2 Fuel Properties

6.2.1 Thermal properties

Table 6.1 gives a summary of the values determined in Chapter 5 for the fuel heat transfer parameters and briquette thermal properties. They have been quoted with estimates of their associated uncertainties, and these are used in establishing the sensitivity and uncertainty in the model output caused by these factors. To evaluate the model, all the elements in the briquette were initially assumed to be at room temperature, 293K. One particular limitation in this thesis is, however, the lack of thermal property data obtained for partially pyrolysised biomass briquettes [83]. The heat-probe method could provide a potential means to obtain data to fill this gap in the literature. But for now in this study, solving the model equations would be significantly simplified if the thermal parameters could be assumed constant throughout the briquette's thermal decomposition process.

Roberts [82] argues that the balance between the increase of specific heat capacity with increasing temperature, with its decrease as biomass material thermally decomposes, will cause there to be very little change in the specific heat capacity throughout the pyrolysis. Furthermore, Bamford [83], and later, Roberts assume that the thermal conductivity is proportional to the local density, thus making the

Parameter	Value	Uncertainty
Flame temperature	750 K	$\pm$ 50 K
Flame Emissivity, ϵ_f	0.54	$\pm$ 0.07
Heat convection coefficient, h	102 W/m^2K	$\pm$ 26 W/m^2K
Thermal conductivity, virgin briquette	$\lambda = (0.000121\rho + 0.0526)\ W/mK$	$\pm$ 7%
Heat capacity, virgin briquette	1612 J/kgK	$\pm$ 400 J/kgK
Density, virgin briquette	between 200 and 600 kg/m^3	see Section 5.2.6
Volatile fraction	mean from literature*: 85 %	$\pm$ 5%

Table 6.1: A table of the parameters used in the simple model for the determination of E and k_0 for dry paper briquettes. Apart from the volatile content of the paper briquettes, all the other quantities were determined by experiment. *([126], [127] cited in [128])

thermal diffusivity independent of the degree of pyrolysis [82]. If this is the case, the thermal diffusivity can be assumed to be approximately constant throughout the pyrolysis. Data available for wood suggest that the diffusivity of charcoal is very similar to the diffusivity of the original wood from which it was formed, although the values of the thermal conductivity, heat capacity and density may be significantly different [83]. The data do not, however, take into account the effects of temperature. Unfortunately, there are no direct experimental measurements of the change in the thermal diffusivity during densified biomass pyrolysis available in the literature (at different degrees of degradation and at combustion temperatures), to allow the validity of the constant thermal diffusivity assumption to be assessed more fully.

In the model developed in this work, the simplifying assumption was made of a constant thermal diffusivity throughout pyrolysis. In Section 6.3, the limitation of this assumption is considered by completing a sensitivity study on the relative affect of changes in the thermal diffusivity on the NBR predicted by the model.

6.2.2   Determination of the kinetic parameters (E and k_0)

The rate of mass decompositon was modelled by assuming a global one step reaction, where the rate is given by Equation 5.2. E and k_0 can effectively be considered as mean representative values for the overall more complex set of multiple reactions, which in fact are not fully understood in the literature [65]. The particular chosen value of E effectively defines the temperature at which the decomposition process begins, and coupled with k_0, allows a prediction of the rate at which the reaction proceeds as a function of the solid's temperature after

the critical pyrolysis temperature has been reached. Bamford et al. [83] attempt to determine these parameters by simply trying different values for k_0 and E to match their model predicted temperature-time curve (for the centre of the solid) with their experimental measurements. Values that gave a central temperature rise in close agreement with their experimental data were adopted, and used in the subsequent calculations [83]; numerical optimisation was not used. In a similar manner, Roberts et al. [91] chose parameters to try and fit their theoretical model prediction of the mass decrease as a function of time with experimental data. Neither of these methods uses numerical optimisation, but rather the values are chosen by the judgement of the individual researcher. Table 6.2 gives a summary of the range of kinetic parameters used in some previous studies. Although the specifics of the wood used in each study are not known, the large variation in these values, especially in the pre-exponential factor k_0, suggests that they have limited physical significance for the material alone, but also depend significantly on the specific conditions of the study.

An alternative numerical method for the determination of the kinetic parameters, by fitting to experimental study is proposed here. One major objective of this model was to predict the measured normalised-burn-rate (NBR) of briquettes burning in free air, which was measured for briquettes of different sizes, geometries and densities as outlined in Chapter 4. Optimisation of E and k_0 using the NBR parameter will, therefore, be considered (rather than the behaviour of the temperature profile in the slab, for example). In this study, constant values of E and k_0 were assumed for the entire range of briquettes burnt in free air (see Chapter 4). In order to find values for these kinetic parameters, rather than only look at the goodness of fit of a single mass decrease curve, the NBR model prediction for particular pair of kinetic parameter values, was compared over the entire A/V ratio versus NBR curve.

The objective of optimisation is thus to identify pairs of values for E and k_0 that give a prediction agreeing closely with this curve. To achieve this, rather than judging by eye how good a fit is and choosing values for E and k_0 that give a fit that appears as though it is good, it was considered better to use an analytical technique to identify optimum values.

Before using an optimisation algorithm, in order to assess possible optimum values for E and k_0, the model was systematically run for a large range of different values: with k_0 taking values between 0 and $10 \times 10^5 s^{-1}$, and E taking values between 0.6×10^5 and $1.4 \times 10^5 Jmol^{-1}$. For each pair of kinetic parameter values, a comparison was made with the experimentally determined NBR versus A/V curve,
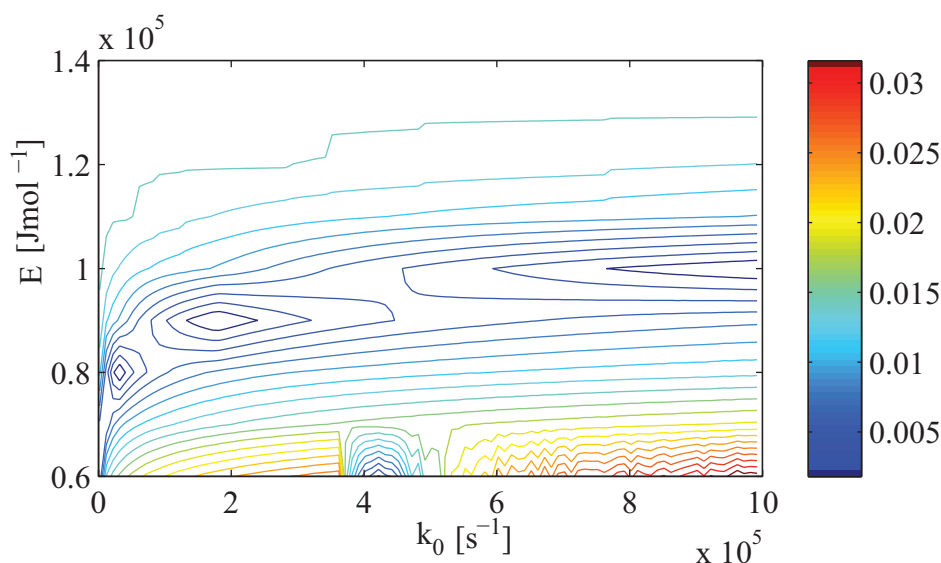
Figure 6.4: A contour plot of the sum of the residual of the the model predictions compared to the experimentally determined NBR. There is a valley running left-to-right through the centre of the range investigated, with two local minima visible, and a third appearing at the limit of the range, at the right hand edge of the figure.

by finding the sum of the residuals of the numerical model prediction compared with the experimentally determined results (see Section 6.2.3 below). A contour plot of the result is given in Figure 6.4, where values of the contour 0.0145 and above represent the case where the values for the kinetic constants have not yielded a mass-decrease curve in the numerical model, or one that was nonsensical. Two pairs of E and k_0 can been seen to give a minimum in the residuals in the range tested, with other minima appearing to be formed on the right hand edge of the plot. The fact that there is more than one pair of optimum values for kinetic parameters possible, suggests that there are several combinations of values that are possible for constant environmental conditions. Indeed, the existence of multiple minima may well explain the range of experimental values of the kinetic parameters presented in the literature. It was shown that by choosing values for k_0 and E in the vicinity of the minima, and then using a simplex optimisation algorithm, the two minima shown in Figure 6.4 could be be found: $k_0 = 1.8328 \times 10^5 s^{-1}$, $E = 0.8644 \times 10^5 Jmol^{-1}$ and $k_0 = 3.312374 \times 10^4 s^{-1}$, $E = 7.6949912 \times 10^4 Jmol^{-1}$. Figure 6.4 shows that the optimum values appear to lie in a valley. Choosing values outside this valley often resulted in nonconvergent behaviour.

6.2.3   A description of the optimisation procedure

The optimisation worked by using the model described in Section 5.1 to produce a series of curves of the mass decrease as a function of time for briquettes with different A/V ratios. The gradient of each of the predicted normalised mass decrease curves was then found, by drawing a line between the times when the normalised mass was equal to 0.9 and 0.3, and finding the resulting gradient. The normalised burn rate was recorded and the residual of each fit calculated. A curve of A/V ratio versus NBR was then drawn. This was compared to the experimentally measured curve, shown in Figure 4.6, and the residual of the fit calculated. This procedure was iterated, with the simplex algorithm being used to select new values for E and k_0 (the kinetic parameters), with the objective of minimising the residuals of both the mass decrease and the A/V versus NBR curve.

Figure 6.5 shows three experimental mass decrease curves compared with model predictions for optimised values of k_0 and E. Figure 6.6 shows the corresponding A/V versus NBR curve plotted against the experimental results for newspaper briquettes at a density of 250 kgm^{-3}. It is clear that the optimum values of k_0 and E found using this procedure give values for the NBR as a function A/V that are a good fit with the experimentally measured data. It is therefore reasonable to use these values in the model to make further predictions.
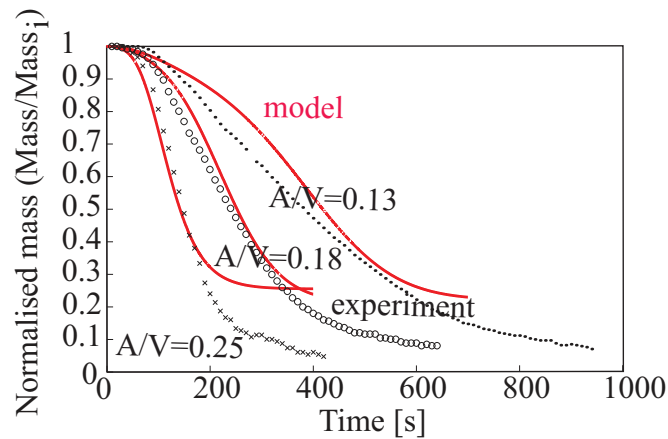
Figure 6.5: The mass decrease as a function of time for three briquette samples with different A/V ratios, compared with model predictions. Model predictions are given by the solid lines (−).
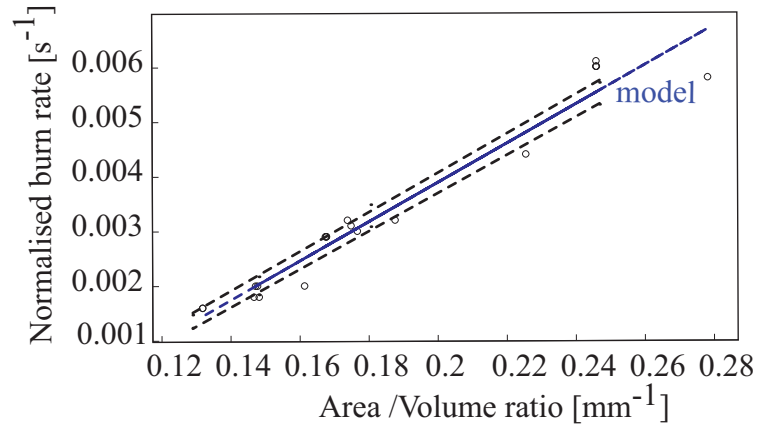
Figure 6.6: The NBR rate predicted by the model as a function of A/V ratio compared with experimentally measured data ($\circ$); the density of the briquettes was 250 kgm^{-3}.

6.2.4   Discussion of the kinetic parameters

This study has provided suitable values for the kinetic parameters. They have been determined using an optimisation procedure over a large range of samples with different A/V ratios, rather than only a single mass decrease curve. The resulting values are thus an average, suitable for making predictions over the entire size range considered in this study. A more comprehensive study of kinetic parameters under different experimental conditions, and over a greater range of values, would allow the experimental values found in other literature studies to be plotted on the same graph.

It is interesting to note the range of values for E and k_0 used in the literature for wood combustion modelling, and a selection have been given in Table 6.2 below. It can be observed that the values for k_0 span a much greater magnitude range than the values for E. This is consistent with the results observed in the contour plot, which show the optimum values for the kinetic parameters lie in a valley, in which the rate of change E is decreasing as k_0 increases (see Figure 6.4).

As discussed in Section 6.2.2, the values of E and k_0 describe the point at which pyrolysis begins, and the rate at which it occurs. Typical pyrolysis temperatures of biomass samples are recorded in the literature: Yaman et al. [130] show that the devolatisation of paper mill waste occurs between about 500K and 700K. It is interesting, therefore, to compare the predicted pyrolysis temperature range resulting from the above optimisation. This can be done by simulating the pyrolysis of a small sample of the material in which temperature gradients are negligible, and the decomposition is primarily kinetically controlled. This was

$k_0[s^{-1}]$	$E[kJmol^{-1}]$	Ref
$2 \times 10^3 - 3 \times 10^3$	66-69	[86]
1.35×10^3	62.76	[91]
4.33×10^7	104.6	[91]
7.00×10^7	126	[82]
5.30×10^8	139	[83, 129]

Table 6.2: A summary of some kinetic parameters used in theoretical models of wood pyrolysis, where a single Arrhenius expression is assumed to account for the decomposition. The specifics of the type of wood used in the above investigations were not given in the references. A further review of thermal parameters used by other authors is given in [103].

achieved by reducing the slab thickness parameter in the model, and recording the predicted temperature within the sample as a function of the mass decrease per unit time. As the sample thickness was reduced and the temperature gradients became negligible, convergence was reached for a sample thickness of 1mm. The heating rate of the surface of the sample has been kept the same as for the modelling of the larger slab briquettes[2]. The resulting curve is shown in Figure 6.7. The pyrolysis can be seen to begin at around 500K and is complete by around 690K, which agrees well with the literature values given above. This suggests that the values for k_0 and E found are physically sensible, and that the method of optimisation described might be a useful method for their estimation.

An indication of the sensitivity in the optimum values for k_0 and E, when there are variations in the model input parameters, needed to be assessed. This was done by using the simplex optimisation method to find optimum values for k_0 and E when input values of the model constants had been varied according to the uncertainties given in Table 6.1.

The sensitivity in k_0 and E was can then be defined respectively as [64]:

$$\varphi_k = \frac{\delta k_0/k_0}{\delta \chi/\chi} : \varphi_E = \frac{\delta E/E}{\delta \chi/\chi} \tag{6.2}$$

where χ is any one of the input parameters in the model, as given in Table 6.1. $\delta\chi$ is the uncertainty in the parameter, δk_0 and δE are the change in the optimum value for k_0 and E, respectively. The relative sensitivity calculated for each parameter is shown in Figure 6.8. It is immediately clear that the optimised values of E and k_0 are most sensitive to changes in the flame temperature: a 1% change in the

---

[2]This is specified by the constants in Table 6.1 and the temperature difference between the sample surface and the gas phase (see Equation 5.4).
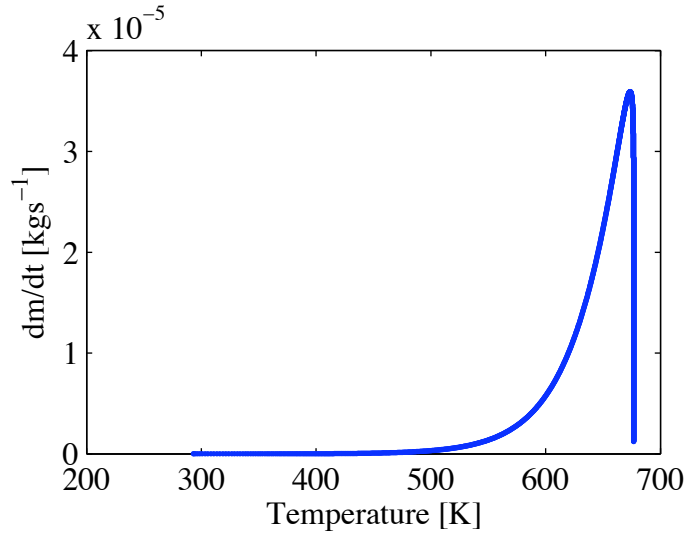
Figure 6.7: The reaction rate of a sample of newspaper as predicted by the model. The reaction is kinetically controlled and the temperature gradients are negligible. The heat transfer coefficients in the model are the same as those given in Table 6.1.

flame temperature would lead to an approximately 0.8% change in both E and k_0; whereas the thermal conductivity of the medium has a comparably insignificant effect with a 1% change in thermal conductivity leading to less than a 0.02% change in E and k_0. The effect of both material properties and environmental conditions on the determination of the kinetic parameters is significant, which suggests that unless specific conditions are know under which these parameters have been determined for a given material, values in the literature should be treated with caution.

6.3 Sensitivity analysis

Bamford [83], and later studies that use this model, do not address the degree to which the burn rate predicted by the conduction devolatisation model, is sensitive to the variation in each of the model input parameters. This, however, is important to assess as it will effectively determine the accuracy with which the normalised burn rate can be predicted. In the first part of this section, the sensitivity of the normalised burn rate on changes in the kinetic parameters, k_0 and E is estimated. Following this, the expected variation in the normalised burn rate caused by the uncertainty in each model parameter is individually evaluated.
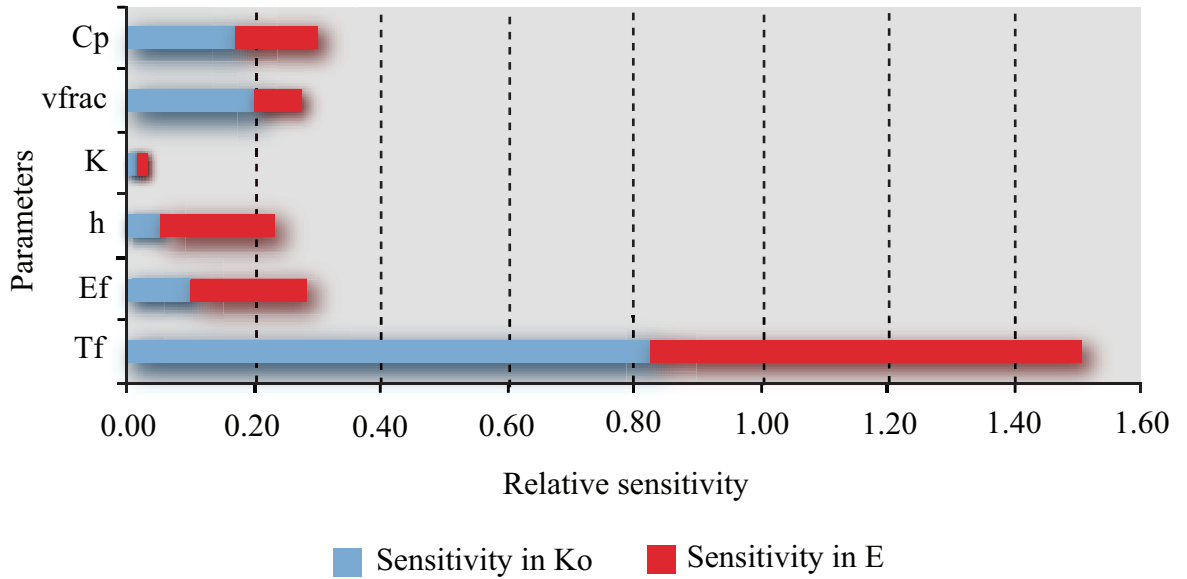
Figure 6.8: The relative sensitivity of the best fit values of E and k_0, found when each of the model parameters given in Table 6.1 is varied according to its maximum associated uncertainty (sensitivity calculated using Equation 6.7).

6.3.1 The effect of changing the kinetic parameters, E and k_0, on the normalised burn rate

Figure 6.9 and 6.10 show the effect of changing E and k_0 on the NBR respectively. Both E and k_0 are varied by $\pm$ 10% and the model results are overlaid on the experimental results. It is immediately clear that the samples with higher area-to-volume ratios are affected more significantly by variations in these parameters. This suggests that, as the area-to-volume ratio increases, the burn rate becomes increasingly kinetically controlled, as would be expected. The consequence of this for parameter determination is that for a particular material, the choice of E and k_0 should be calculated preferentially by fitting data to thinner slab samples. The accuracy in the determination of the kinetic parameters becomes less important the smaller the A/V ratio (thicker slab samples).
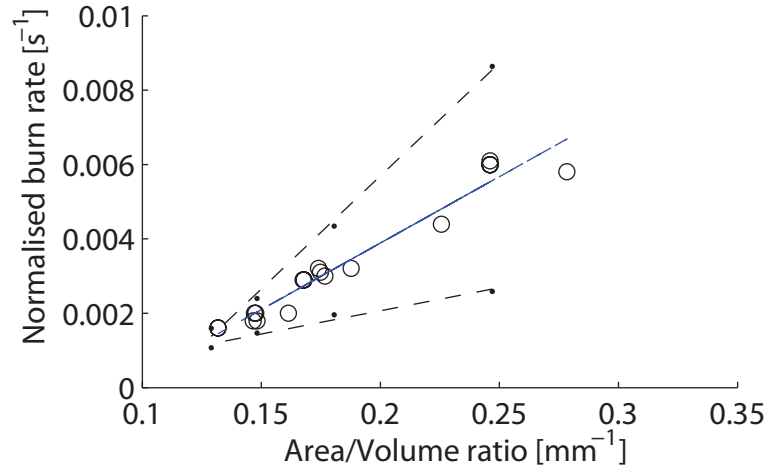
Figure 6.9: The effect of changing the kinetic activation energy E: the central line shows the model prediction using optimised values for E and k_0, while the two dotted lines either side show the effect on the model prediction of changing E by $\pm$ 10%.
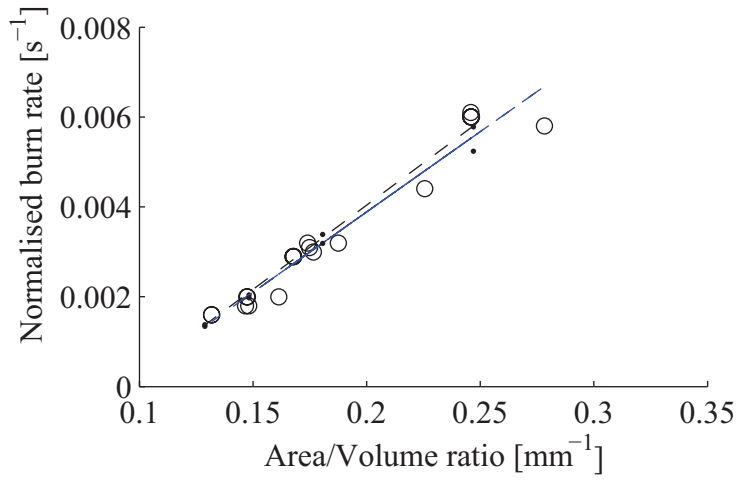
Figure 6.10: The effect of changing the kinetic parameter k_0 in the Arrhenius expression: the central line shows the model prediction using optimised values for E and k_0, while the dotted lines show the effect on the model predictions of varying k_0 by $\pm 10\%$.

6.4   The Effect of Changes in Model Parameters on the Normalised Burn Rate

6.4.1   The surface heat transfer parameters

Figure 6.11 shows how the NBR predicted by the model changes when each of the parameters associated with surface heat transfer is varied according to its expected experimental uncertainty, as given in Table 6.1. The uncertainty in the temperature of the gas can be seen to have the most pronounced affect on the predicted NBR, with sensitivity increasing for samples with larger A/V ratios. Consequently, the measurement uncertainty in the temperature significantly limits the certainty of predicting the NBR for thin briquette samples, however, the larger the sample, the greater the relative accuracy in the model prediction.

In Section 5.2.11 the effect of volatile transpiration from the surface or 'blowing' on the convection heat transfer coefficient was considered. It was estimated that this might lead to a modification in the convective heat transfer coefficient in the order of 20%. Figure 6.12 shows the effect of changing h $\pm 20\%$ of the experimentally determined value, on the predicted normalised burn rate, for three different A/V ratios. The relative change in NBR is small, compared to the effect of changes in the gas temperature (see Figure 6.11). It is only for the sample A/V=0.247 that a significant shift of $\pm 0.5 \times 10^{-3}$ (about 8%) in NBR is observed. In practice, however, briquettes with such a high A/V ratio would be too thin to be manufactured or to be useful. This study suggests that neglecting blowing might be considered legitimate in the case of modelling large briquettes (with A/V ratios less than around 0.18), but might need to be considered in the modelling of smaller briquettes (depending on the objective of the modelling and the accuracy required).

6.4.2   The effect of changes in material thermal parameters

Figure 6.13 shows the potential change in the NBR of a briquette at different A/V ratios due to variations in material thermal parameters, according to their associated uncertainty. However, the large variation in relative uncertainty between the different parameters, (see Table 6.1), means that Figure 6.13 does not provide a means to make relative comparisons between the sensitivity of parameters. In order to make a relative comparison between variations in material thermal parameters, the effect of changing heat capacity and thermal conductivity

Figure 6.11: The effect of uncertainty in the parameters associated with heat transfer on the normalised burn rate. The central line gives the experimentally expected trend, which corresponds to the trend predicted by the model with the values of the variables given in Table 6.1. The points either side of this line show the variation in normalised burn rate when each of the parameters, given in the legend, is varied by its associated uncertainty, also given in Table 6.1.

by $\pm 20\%$ was examined. Figure 6.14 shows the result. The relative effect of changes in both of these parameters on the predicted NBR is shown to be approximately the same. The larger uncertainty in the NBR caused by the uncertainty in the heat capacity (compared to thermal conductivity), observed in Figure 6.13, results from the greater experimental uncertainty in its determination using the heat probe method.

It is hard to experimentally investigate how NBR varies as a function of material thermal properties (heat capacity and thermal conductivity). It is made even more difficult because there is sparse data in the literature of values for the material thermal properties of compressed biomass. This is a problem that can be addressed in the future with further developments of the heat probe method (described in Chapter 5), but detailed studies of which have not been carried out in this work. Nevertheless, an idea of the expected spread in values of the thermal conductivity can be obtained by observing the variation in values for different
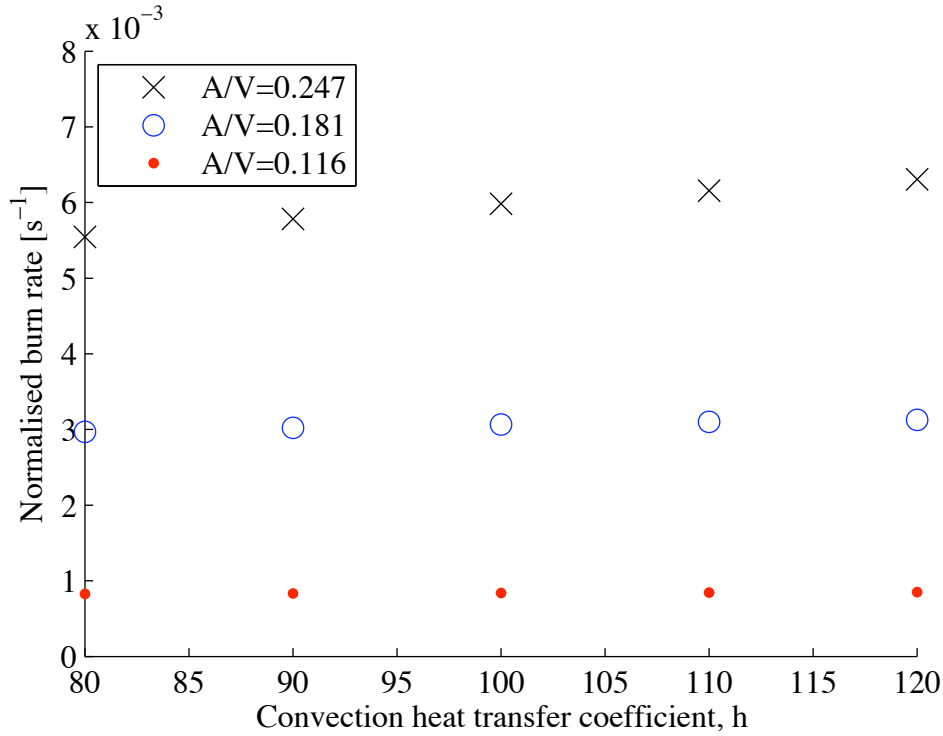
Figure 6.12: The effect of changes in the convective heat transfer parameter, h, on the normalised burn rate of briquettes, according to the model.

types of woody biomass, data for which are available in the literature. Simpson gives oven dry values that vary from 0.17 $Wm^{-1}K^{-1}$ for Mockernut Hickory and Shagbark Hickory, to 0.079 $Wm^{-1}K^{-1}$ for Northwhite Cedar [131], while Ravi gives measured values for sawdust in a packed bed of around 0.06 $Wm^{-1}K^{-1}$ [100]. In terms of the heat capacity, as far as the author is aware, data for dry compressed agricultural biomass is not available. However, it is interesting to note that for wood, Ragland et al. [66] state that the specific heat capacity 'can vary by as much as 100% depending on temperature and moisture content'.

Figure 6.15 gives the variation in normalised burn rate for changes in λ, predicted by the model over a range of different A/V ratios (each marked point is a model prediction). The range of values for λ were chosen on the basis of those suggested by wood data given above, and by the heat probe data given in Section 5.2.6 for dry newspaper briquettes[3]. Qualitatively speaking, it can be seen that as the thermal conductivity decreases, the NBR also declines, as would logically be expected; a lower thermal conductivity will reduce the rate of heat transfer into

[3]The thermal conductivity was shown to vary between about 0.07 to almost 0.1 $Wm^{-1}K^{-1}$ for a change in bulk density of about 180 to 375 kgm^{-3}.
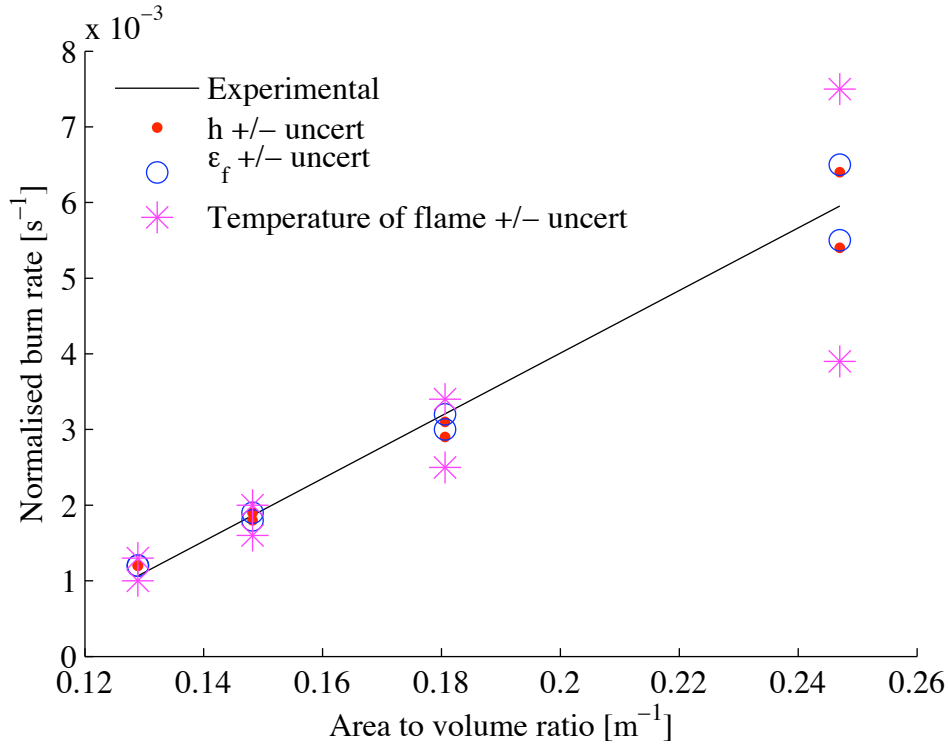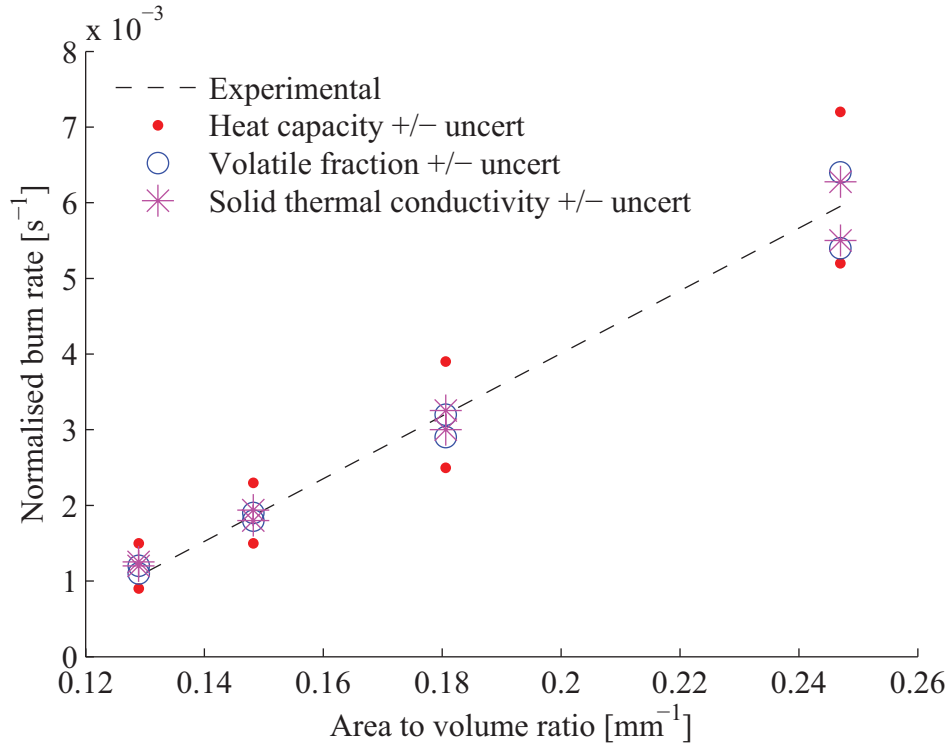
Figure 6.13: The effect of uncertainty in the material thermal parameters on the normalised burn rate. The central line gives the experimentally expected trend, which corresponds to the trend predicted by the model with the mean variable values given in Table 6.1. The points either side of this line show the variation in normalised burn rate when each of the parameters, given in the legend, is varied by its associated uncertainty, also given in Table 6.1.

the solid. The curves shown are the result of a least squares fit of the exponential function $Jexp(C_1/\lambda)$, where J is an empirical constant and C_1 is found to take a value of -0.068.). This (of course) suggests that the NBR can be considered to vary approximately as an exponential function of the thermal conductivity. It should be noted that with denser briquettes, varying moisture contents and many different types of residue available, it is quite likely that the range of variation of thermal conductivity will in fact be greater than the range investigated here, and future investigations should take these factors into account.

Figure 6.16 gives the change in NBR with c_p over a sensible range, where each point marked is a model prediction. It can be observed that as the heat capacity of briquette material increases, the NBR decreases. This is because the higher the heat capacity, the greater the amount of heat required to raise a unit mass of the briquette material to pyrolysis temperature. The solid lines show a least squares fit of the exponential expression $Gexp(C_2 * c_p)$, where G is an empirical constant
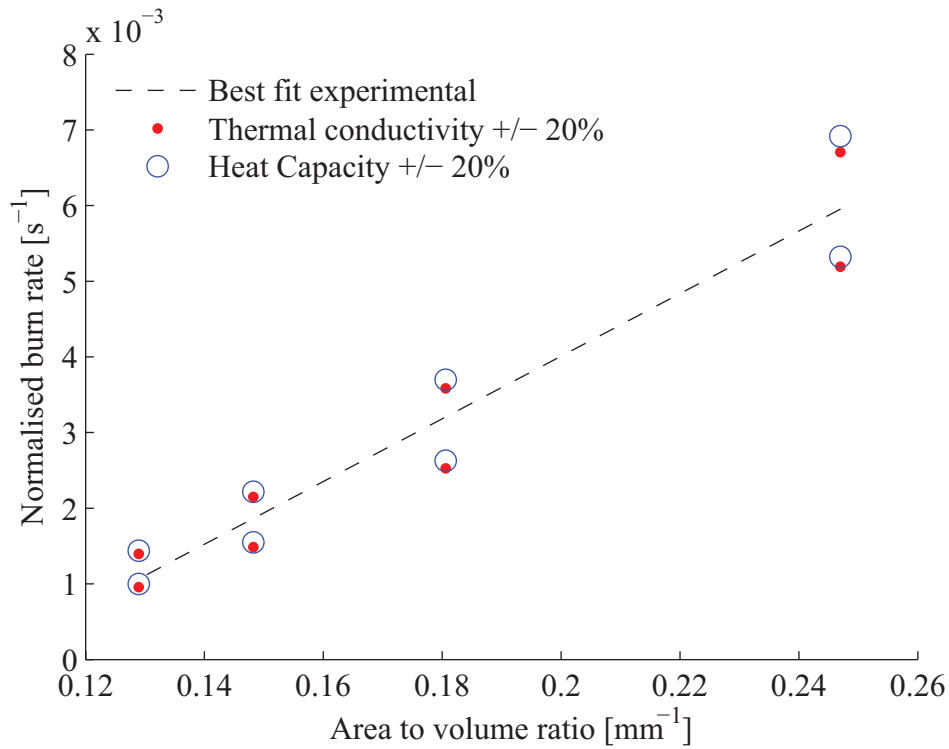
Figure 6.14: The heat capacity and thermal conductivity have been varied by $\pm 20\%$ in order to compare their relative effect on the normalised burn rate.

and C_2 is found to take a value of -0.0057). Further investigation is required of densifed biomass using the heat probe method, to find the heat capacity at different different degrees of degradation, temperatures and moisture contents. What is clear is that changes in the thermal parameters of the virgin fuel affect the normalised burn rate predicted by the model at all A/V ratios, suggesting the necessity of their determination in modelling the devolatisation of compressed biomass.
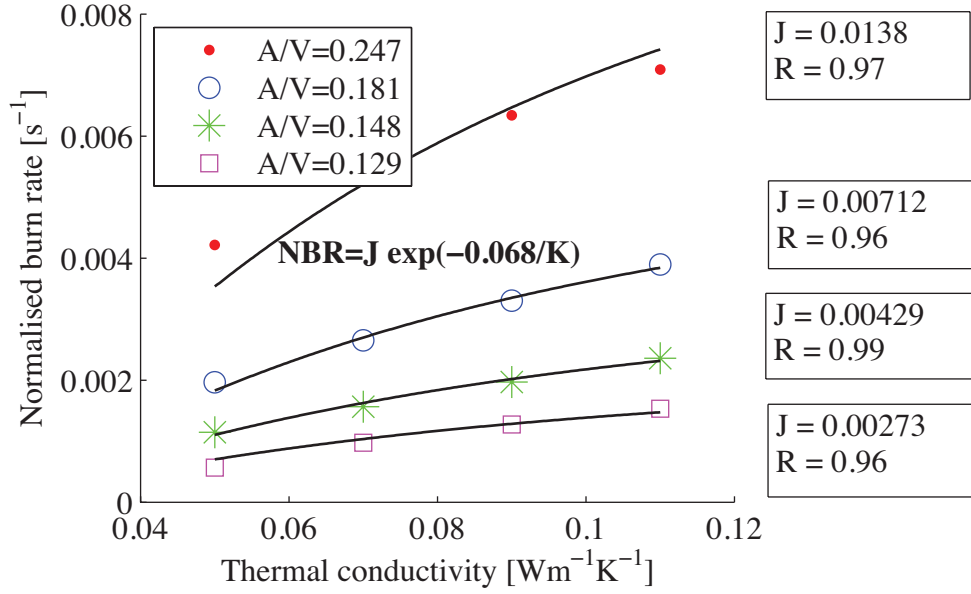
Figure 6.15: Model predictions of briquette thermal conductivity as a function of normalised burn-rate, for briquettes with different A/V ratios. The points are model predictions, and the solid lines are best curve fits of the exponential function: $Jexp(C_1/\lambda)$.

6.4.3 An analytical briquette equation

The above results of the numerical model can be used to extend the analytical equation describing the quai-steady state burn rate of a newspaper briquette in free air, given in Equation 4.5 in Chapter 4, from density and A/V ratio to include thermal conductivity and heat capacity, such that for dry newspaper briquettes burning in free air:

$$NBR_{\text{free air}} = \frac{(0.074 * \frac{A}{V} - 0.0076)e^{-0.0023\rho}e^{-0.0057c_p}e^{-0.068/\lambda}}{e^{-0.0057 \times 1612\rho}e^{-0.068/0.083}} \tag{6.3}$$

where the constants in the denominator are normalisation factors. This result can also be combined with the experimental result obtained for the effect of moisture on the normalised burn rate:

$$\frac{NBR_{wet}}{NBR_{dry}} = 1 - C_4[\%M] \tag{6.4}$$

where C_4 is a material constant, which for newspaper briquettes was found to take a value of 0.038 ± 0.01 (see Section 4.3 for more details). Calorific value can be taken into account using the approximation described in Section 4.4.2.
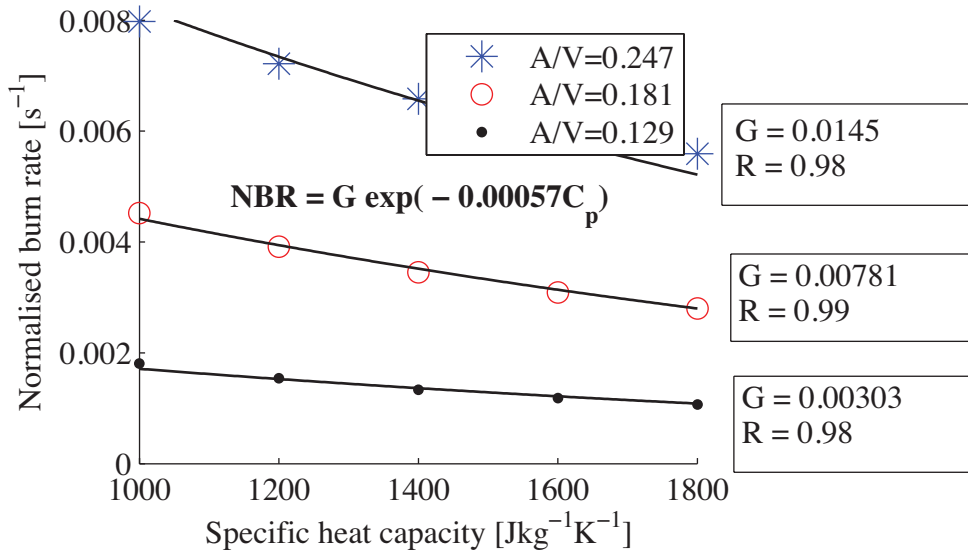
Figure 6.16: Model predictions of the effect of changing the briquette heat capacity on the normalised burn rate of briquettes with different A/V ratios. The points are model predictions, while the solid lines are best curve fits of the exponential function: $Gexp(C_2 * c_p)$.

6.4.4 The effect due to changes in the temperature of the gas phase

In comparison to the other parameters, the predicted NBR was shown in the sensitivity study to be particularly sensitive to the flame temperature used in the surface heat transfer function of the model (for example see Figure 6.11). Although this study does not deal directly with the gas phase, the relative importance of this factor suggests a necessity for it to be included in the analytical expression. This has been approached in the same way as the thermal conductivity and heat capacity in Section 6.4.2: by modelling the change in NBR as a function of A/V ratio, and numerically fitting an analytical expression to the results.

In order to achieve this, the flame emissivity and convective heat transfer coefficient are assumed to stay approximately constant, and then using the model the change in rate as a function of gas phase temperature can be obtained. For briquettes of small A/V ratios, it is found that the change in burn-rate as a function of temperature can be approximated to follow a logarithmic trend[4]:

$$NBR(T_g) = \frac{1}{\Gamma} ln(T_g/C_6) \tag{6.5}$$

---

[4]It is important to note here that this is an approximation that has been fitted to describe the change in normalised burn rate for analytical purposes and is not a trend that has been derived theoretically.

where the average value of C_6 was found to be 540 by least squares fitting this function to the model results. The physical meaning of this is the approximate temperature at which the gasification process begins, below which point pyrolysis will be negligible. This is in agreement with literature values for the temperature at which pyrolysis occurs (see Section 6.2.4). The constant Γ can be found from the NBR of a briquette burning in free air (Equation 6.3 above) and using:

$$\Gamma = \left(\frac{1}{NBR_{\text{free-air}}}\right) ln(T_g/C_6) \tag{6.6}$$

where T_g is taken as the free air measured value of 750 K (as given in Table 6.1).

This equation makes a direct connection between the gas phase and the solid phase. It could be used to estimate the rate of devolatisation for a briquette in a packed bed, when the gas phase temperature will be dependent on such factors such as airflow rate, oxygen availability, mixing and char combustion rate. In his study on numerical stove optimisation, Burham-Slipper suggests a similar approach of using the gas phase temperature in a lumped fuel model to estimate the pyrolysis rate [75]. Further work should be carried out to include the effects of the heat transfer coefficients, h and ϵ_f, and experimental studies of briquettes burning in packed beds should be carried out to provide validation.

6.4.5 The effect of material density on the NBR: comparing experimental results with the model prediction

One of the authors objectives, as described in this chapter, was to predict the effect of changes in material properties that are difficult to vary experimentally, on the rate of devolatisation of the briquette. This achievement is outlined in Section 6.2.1, which considered the effect of heat transfer parameters, briquette thermal conductivity and heat capacity on the normalised burn rate. In this section, the model is applied to make predictions of the effect of density on the normalised pyrolysis rate, a variable which was investigated experimentally (see Chapter 4). Model predictions are compared with experimental results in order to assess the model's robustness.

The investigations outlined in Chapter 4 into the effect of density on the rate of devolatisation of compressed paper briquettes revealed that the results could be correlated using an exponential function of the form $exp(C_7\rho)$ where C_7 is a constant. For the newspaper briquettes investigated, C_7 was found to take a value

of -0.0023. Figure 6.17 compares the model prediction of the NBR as a function of density with the experimentally measured values from Chapter 4. Error bars representing the expected experimental uncertainty are also plotted. It can be observed that, within the density range tested, the predicted results lie within these error bounds. Fitting an exponential function to the model predicted curve, gives an exponential factor constant C_7 of -0.0026. This is indeed close to the experimentally determined value.
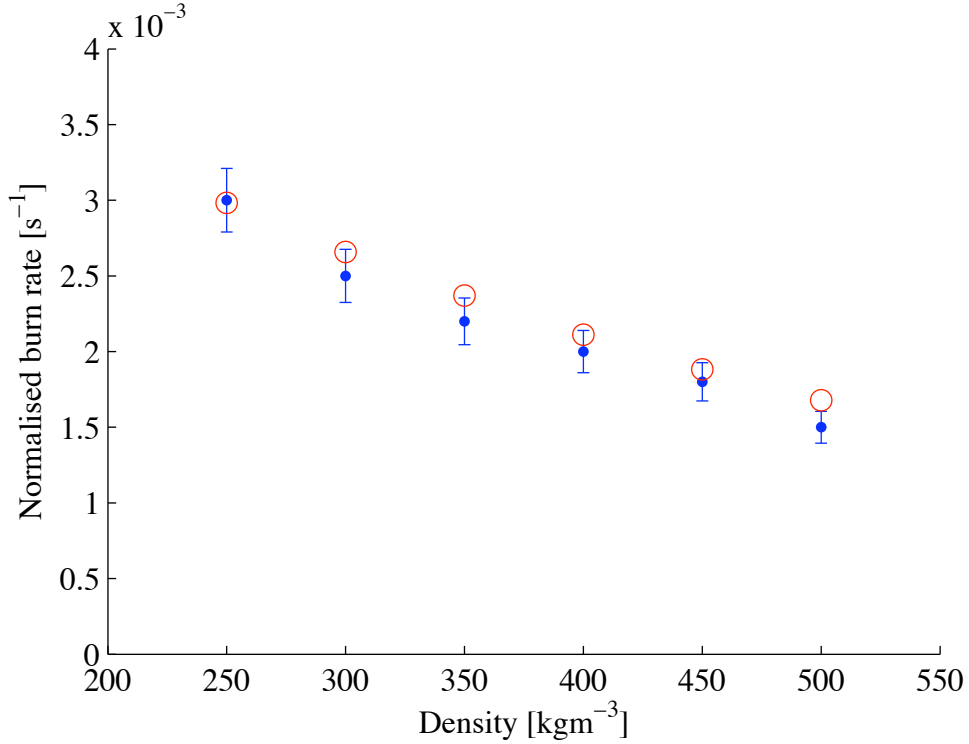
Figure 6.17: The effect of density on the normalised burn rate. The $\bullet$'s are experimental results for a briquette with an A/V ratio of $0.179mm^{-1}$; the error bars give an indication of the minimum expected experimental error. The $\circ$'s are the results of the normalised burn rate predicted with the simple model where the parameters used are given in Table 6.1.

The sensitivity of changes in the model parameters on this fitted value were estimated, by varying each of the parameters and using the following expression:

$$\varphi_{C_7} = \frac{\delta C_7 / C_7}{\delta \chi / \chi} \tag{6.7}$$

where χ is another model parameter.

Table 6.3 shows the resulting relative sensitivity of some key parameters. It is clear that a change in the value of the kinetic factor E will have the most pronounced effect on the predicted values for C_7, compared to changes in the values of the other parameters. This suggests that for different materials, the value of C_7 will be a function of the kinetic properties as well as material thermal properties. It is likely that this explains the different values for C_7 infered from the results of Chin et al. for different compressed biomass materials (see Section 4.1).

Parameter	Sensitivity*
λ	1.0
c_p	0.5
E	2.1
k_0	0.04

Table 6.3: The sensitivity of the exponential constant, C_7, to changes in the model parameters.

In terms of what is happening in the model code, changing the virgin density simply results in a change in the thermal diffusivity of the briquette. It is this parameter which controls the rate of heat transfer into the briquette and therefore the rate of pyrolysis. This is the primary variable in the model code influencing the calculation of heat transfer into the briquette. Changing the heat capacity and thermal conductivity, as considered in Section 6.4.2, also modifies the thermal diffusivity ($\alpha = \lambda/\rho c_p$). It has been shown in this section, by comparison with experimental data from Chapter 4, that the model is able to predict the effect of changes in the thermal diffusivity on the NBR, caused by changes in material density. Therefore, it is reasonable to assume that the predictions made in Section 6.4.2, where the thermal diffusivity is modified by changing the heat capacity and thermal conductivity, are at least of the correct order of magnitude.

6.4.6 Concluding remarks

In this section (6.4), a sensitivity study was carried out, looking at the effect of changes in the heat transfer parameters and material thermal properties on the normalised burn rate (pyrolysis rate) predicted by the model.

On considering the heat transfer parameters, it was found that fluctuations in the convective heat transfer coefficient due to blowing can be neglected as a first approximation, especially for large briquettes with an A/V ratio less than about $0.18mm^{-1}$. On the other hand, the predicted NBR is particulary sensitive to

the temperature of the gas phase, and so this needs to be measured or predicted carefully. An analytical expression was suggested, derived from application of the model, which approximately correlates the predicted change in NBR as a function of gas phase temperature.

The values for both the heat capacity and the thermal conductivity of a briquette used in the model were shown to have important effects on the predicted burn rate, making the determination of sensible values important. An analytical expression was suggested for the prediction of the NBR of a briquette in free air as a function of these parameters.

The effect of changes in NBR with briquette density was also investigated using the model. The agreement of model predictions with experimental measurements, from Chapter 4, suggest the appropriateness of a pure conduction model for pyrolysis rate predictions. This study, however, has been mainly limited to a focus on newspaper briquettes, and further studies are required to asscertain the limits of application of such a model in other circumstances. In particular, further experimental and modelling work is required involving other biomass materials and combustion conditions. For example, it is possible that, with such a diversity of biomass residues available, there may be cases where other factors become important and need to be taken into account in the pyrolysis modelling. In such a situation, a more complex approach to the modelling would be required.

One of the limits of this numerical study is that it has considered only the virgin material properties of a briquette, using a model that assumes a constant thermal diffusivity throughout the decomposition. The limitations of this assumption are examined in Section 6.5.1.

In conclusion, the suggested pyrolysis model is able provide a good prediction of the normalised burn rate for compressed newspaper briquettes. The analytical expression allows the relative importance of different factors on the pyrolysis rate of a briquette burning in free air to be assessed at different geometries and moisture contents. Its usefulness is in further investigations where an understanding of the effect of material properties on pyrolysis rate is important. For example, it could be applied in future briquette stove optimisation studies, which require a simple lumped fuel model that includes fuel properties, for example, in a study looking at the effect of fuel properties on stove efficiency.

This section has considered the application of a conduction based pyrolysis model. The literature review (Chapter 2) discussed more complex analytical models, which took into account other physicial factors, such as the outflow of volatiles and the fact that the thermal properties of a briquette change during the decomposition

(see Section 2.7). The relative importance of inclusion of these factors, which is hard to assess direcly by experiment is considered in Section 6.5, which follows.

6.5   Exploring the basis of some important model assumptions

In this section three important assumptions applied in the described model are further explored, by assessing their affect on the behaviour predicted by the model: the assumption of constant thermal diffusivity, no convective heat transfer by the volatile gases, and a zero enthalpy of pyrolysis.

In the first part of this section, the effect of assuming constant material properties is assessed. This is an assumption that greatly simplifies the model, and, in the case of a newspaper briquette burning in free air, it appears to be sufficient for making numerical predictions of NBR. However, a more complex model that includes the effect of changing parameters with degree of pyrolysis and temperature would allow the limitations and implications of this simplifying assumption on pyrolysis behaviour and NBR predictions to be assessed, and enable a better understanding of the thermal transformation processes taking place to be gained. Furthermore, the assumption of constant diffusivity appears only to be validated qualitatively with limited experimental data in the literature [82, 83]. In Section 6.5.1, a more complex model is developed, and some preliminary studies are carried out to investigate the implications of assuming a constant thermal diffusivity.

In the second part, the effect of the convective heat carried by volatiles is considered. This is included because different studies have reached different conclusions as to whether it is important to include this effect (for example Ravi et al. conclude that the effect of volatiles should be included [100] whereas Bamford assumes that they are not important [83]).

Finally, the effect of including an enthalpy term, to account for the energy changes during thermal decomposition and heat released through secondary chemical reactions of the volatiles, is considered. This was not originally treated in the study, because with the complex chemical reactions that are involved it is difficult to physically quantify. However, it is important to consider its effect, firstly, because in the literature it is considered a real physical effect, and secondly, because the inclusion of such a term was observed by the author to have a significant influence on the model prediction results.

6.5.1 Changing material properties with solid temperature and degree of decomposition

In the first instance, it was assumed that throughout the devolatisation process, although the density and thermal conductivity change, the thermal diffusivity could be considered to remain an approximately constant value. Many models, for example Di Blasi's model of devolatisation [99], jump to greater levels of sophistication without first assessing the necessity for this. In this section, the influence of the inclusion of this additional degree of complexity, that is the effect of varying thermal properties, is assessed.

In the first part of this section, estimates are given of how material properties vary as a function of temperature and degree of degradation, based on the limited available literature. These parameters were coded in the model, and the resulting behaviour was compared with that predicted by the simpler model, where a constant thermal diffusivity was assumed.

Properties of partly pyrolysised material

One approach to dealing with partly pyrolysised material is to assume that each briquette is made up of four components determined by its proximate analysis (volatile matter, moisture content, ash and fixed carbon; see Section 2.4.1 for more details), and then assuming that the proportion of each of these components varies as a function of degree of pyrolysis. In this preliminary study, ash content was considered negligible, and the moisture content was also considered to be zero (as has been done throughout this thesis); these factors were not included in the modelling.

The briquette was divided into zones (control volumes) in the same way as shown in Figure 6.1. The proportion of the constituents in each control volume was calculated as the pyrolysis proceeded, as the volatiles were released from each zone. The properties of the pyrolysising solid were calculated by interpolation between those of the virgin biomass and char. A method similar to this was employed by Ravi et al. [100]. Before pyrolysis began, the proportion of char and volatile matter was considered to be as that determined by the proximate analysis of the biomass; in this case literature values for newspaper were used, as in the initial model (see Table 6.1). The thermal properties of the virgin solid have been previously estimated with the heat probe method (see Section 5.2.6) and the properties of the char are discussed below.

Properties of the char

Ravi et al.'s semi-empirical model of sawdust took the thermal conductivity of the char to be that of graphite across the grain ($2.68\ Wm^{-1}K^{-1}$) [100]. However, this thermal conductivity is much greater than that of virgin wood, which is unlikely to occur physically, and in their model there is no clear basis presented for the choice of using the thermal conductivity of graphite across the grain, in contrast to along the grain. In addition, the density of graphite is significantly higher than that of a porous char layer ($2210\ kgm^{-3}$ compared to around $120\ kgm^{-3}$, respectively). Therefore, without experimental data, this assumption must be treated with caution. Kanury [84], however, suggests that assuming the properties of anthracite carbon might be more reasonable. Nevertheless, assumptions for wood char based on different forms of carbon are not really necessary, as data for some wood chars do appear in the literature. For example, in the CRC handbook of Chemistry and Physics [118] the thermal conductivity of maple, beech and birch char is reported to be $0.052\ Wm^{-1}K^{-1}$, at room temperature. However in reality, selecting an appropriate value is not so simple. Intuitively, it is clear that the thermal conductivity of char will depend on its density, and this in turn depends on the sample's heating rate [66]. Therefore, the particular combustion conditions in which a sample is burning will affect the final char density remaining. Helpfully, it has been reported that the thermal conductivity of char varies as a function of its specific gravity, S, as (cited in [66]):

$$\lambda = (0.67S - 0.071)Wm^{-1}K^{-1} \tag{6.8}$$

Therefore, if the final density of char is known, its thermal conductivity can be estimated.

In terms of the *specific heat* of char, Ragland et al. suggest that for wood char, this *can* in fact reasonably be assumed to be the same as graphite, which varies between $0.715\ kJkg^{-1}$ at $300\ K$ to $2.04\ kJkg^{-1}$ at $2000\ K$ (cited in [66]). This assumption has been successfully applied in a wood combustion model by Burham-Slipper [64].

Variation of properties with temperature

Properties of the dry briquettes were determined in Chapter 5 with the heat probe method. However, time and facilities did not permit properties to be found as a function of temperature. Ragland et al. [66] report that the thermal conductivity

of wood increases at a rate of approximately 0.2 % per degree K above room temperature. The same study gives an expression for the specific heat of dry wood, which suggests that it is a linear function of temperature, increasing by 0.39% per K. These trends are assumed valid for a pyrolysising solid, and used in the determination of the thermal conductivity and heat capacity of unpyrolysised material within control volumes of the dry briquette during pyrolysis. The initial (reference) values for the heat capacity and thermal conductivity were taken to be those determined by the heat probe method at room temperature (see Section 5.2.6).

In terms of the char, Alves et al.[132] found that for pine wood char, the thermal conductivity varied as a function of temperature in the range 220-493 K as:

$$\lambda_{char} = 0.0686 + 8.2 \times 10^{-5}T \tag{6.9}$$

In the same study, Alves et al. go on to apply this in a numerical pyrolysis model for temperatures *outside* of this experimental range. The same approach was applied in the present model, making use of Equation 6.9 to estimate the thermal conductivity of the char.

Discussion

The above equations were implemented in the model (given in Section 5.1), using the same iterative procedure described in Section 6.2.3 (this describes how the gradient of each mass decrease curve was found). Figure 6.18 compares the NBR behaviour of the original model, where a constant thermal diffusivity is assumed, with the enhanced model where the thermal parameters are allowed to vary with degree of degradation and temperature. The enhanced model shows a visible shift in the position of the mass decrease curve. Although there is insufficient data in the literature describing how the thermal properties of compressed biomass change with degree of pyrolysis, the magnitude of variation (assuming that the flow of volatiles does not alter the thermal properties) will not be greater than that determined by the properties of the virgin solid and that of the final char at the temperatures encountered. Thus, the curves in Figure 6.18 probably give a realistic indication of the change in predicted behaviour resulting from not taking into account this effect.

For large A/V ratios (thin samples), the mass-decrease curve predicted by the enhanced model appears to follow the form of the curve predicted by the orignial model, where a constant thermal diffusivity is assumed. However, as the A/V ratio

becomes smaller, there is an increased deviation from this curve, as can be seen for the curves on the right hand side of Figure 6.18. Taking into account changing thermal parameters, therefore, becomes more significant with larger samples, for example in modelling the devolatisation of large logs. Nevertheless, over the size range of samples tested in this study, there is negligible difference between the normalised burn rate predicted by the two models.

The degree to which taking into account the effect of changing parameters during pyrolysis is important, will depend on the parameters being studied and the purpose of the modelling. In the case of determining a briquette's NBR, as in this study, assuming a constant thermal diffusvity appears a reasonable assumption. However, a study of the ignition phase, for example, would need to take into account the effect of varying parameters, as the time for the sample to begin pyrolysising is markedly different between the two different model predictions.
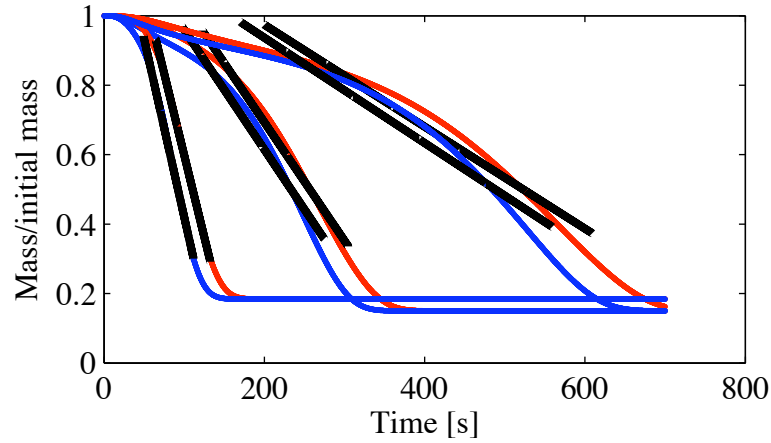
Figure 6.18: Comparision of model predictions with and without varying thermal parameters: the red curves are the predictions when the thermal diffusivity is held constant, and the blue curves are the prediction when material properties are allowed to vary with degree of degradation and temperature (see Section 6.5.1). From left to right the A/V ratios of the three curve sets are as follows: $0.220mm^{-1}$, $0.190mm^{-1}$ and $0.169mm^{-1}$. The density of briquette used in the model was $250kgm^{-3}$. An average NBR predicted for each curve was calculated by completing a linear best fit between 0.9 and 0.3 of the normalised mass, the black lines give the result for each curve (NB: this is the same method by which the NBR gradient was calculated in the experimental studies, see Section 3.3 in Chapter 3).

6.5.2   Convective heat transfer by the outflow of volatiles

As the volatiles flow out of the solid, they transfer energy by convection. In the model suggested in Section 5.1, this term was assumed to be negligible. However, it can be taken into account by including an additional term to account the flow of heat by convection carried by the volatiles as they pass out of the solid [82, 99]. If local thermal equilibrium between the solid matrix and the flowing gases is assumed then [84]:

$$(c_s\rho_s + c_g\rho_g)\frac{\partial T}{\partial t} = \lambda\frac{\partial^2 T}{\partial x^2} - u\rho_g c_g\frac{\partial T}{\partial x} \tag{6.10}$$

The magnitude of the effect of volatiles can be estimated by considering the ratio of the conductive heat transfer into the solid, to the convective heat transfer by volatile gases out of the solid. The ratio of these two terms can be written as:

$$\frac{\text{Convective energy flux by volatiles}}{\text{Heat transfer by conduction}} = \frac{Au\rho_g c_g(T_p - T_{at})}{(\lambda A/L)(T_p - T_{at})} \Rightarrow \frac{(u\rho_g c_g L)}{\lambda} \tag{6.11}$$

where c_g is the heat capacity of the volatile gases, assumed to take a constant value of $1.1 kJkg^{-1}K^{-1}$ [99] and $u\rho_g$ is equivalent to the mass flux of volatile gases leaving the surface. The characteristic length was taken as the approximate thickness of the pyrolysis front, which is the region from which the volatiles are being released[5] The whole of the solid does not decompose simultaneously, and therefore it is probably unrealistic to take the characteristic length as the thickness of the slab. For a typical NBR of 0.004 s^{-1} and a thermal conductivity of 0.08, where a pyrolysis front thickness of about $4mm$ is assumed (approximate reaction zone thickness calculated in a numerical study by Bamford [83]), the above ratio takes a value around 0.1. Neglecting the flow of volatiles, in this case, would lead to a 10% error in the predicted heat flow in the model. Equation 6.11 was implemented, and it was found that with the inclusion of the volatile term, there was, however, negligible difference in the predicted normalised burn rate for the size range of briquettes investigated in this study.

---

[5]Another approach would have been to take the characteristic length as the thickness of the solid, or the distance from the surface to the pyrolysis front. There is some doubt as to whether the ratio given in Equation 6.11 in fact gives a realistic picture of the physics with unsteady state heat flow in a pyrolysising solid. Further consideration is required. For example using the numerical volatile model (of Equation 6.10) to plot this ratio as a function of time throughout decomposition, and comparing the results with the value estimated here).

6.5.3   The enthalpy of formation of the volatiles

The enthalpy of decomposition is the difference between the heat of combustion of the biomass, and that of the products which are formed on decomposition [83]. The literature review revealed (see Section 2.7.1), however, that the energetics of pyrolysis is not straightforward to quantify for densified biomass because complex secondary reactions may occur as the volatiles pass out of the porous char layer generating heat, which will in turn drive the pyrolysis. In fact, there appears to be a disagreement in the literature regarding the energetic nature of this thermal decomposition for biomass materials, suggesting that it has a complex nature.

Logically speaking, it might be expected that to thermally decompose a material, that is to vaporise it into volatile gases, the reaction would be endothermic [84]. This is indeed what was found by Daugaard et al. [109] in an investigation of the enthalpy of pyrolysis of different biomass species using a fludised bed reactor (an average enthalpy for the pyrolysis of 1.5MJ/kg was found). The biomass samples in Daugaard et al.'s study are small such that temperature gradients within the solid are not important [109]. They attribute the difference in the enthalpy between materials as due to the variation in their lignocellulosic composition (cellulose, hemi-cellulose and lignin), which is further supported by Alves et al. [133].

Alves et al. also propose that particle size will affect the extent of secondary reactions with the solid. For larger biomass solids, such as within large logs, it has been suggested that the devolatisation is immediately followed by fast exothermic reactions within the solid, resulting in an apparent exothermic process. This is supported by Bamford who measured a sudden rise in temperature at the centre of wood during its decomposition [83]. Furthermore, Akita has suggested that there may be secondary reactions on the outflow of gases catalysed by the hot char residue in the outer char layers, resulting in a non-uniform release of heat within solid as the reaction proceeds (cited in [84]). Roberts argues that pyrolysis is first slightly endothermic and then exothermic (due to secondary reactions) so that the overall reaction can be considered thermally neutral [66].

What is clear is that the value for the enthalpy determined for loose biomass, might be markedly different to the effective value required to model the thermal decomposition of a compressed solid where secondary reactions of the outflowing volatiles could become important. Ultimately, all the energy will either be released, carried away as unburnt soot, or left as as unburnt char or residue. The importance of this discussion is that when the energy is released, *where* it is released has an effect on the overall rate of pyrolysis. If the release of heat occurs within the fuel/char through secondary reactions, then the heat available to further drive

the pyrolysis is greater than if it is released in the external environment through flaming combustion, for example. Furthermore, depending on the nature of the heat release, it is likely that the internal structure and thus thermal properties of the char will also be modified, affecting the heat transfer, making modelling potentially all the more complex.

Without a more detailed understanding of the kinetics of the secondary reactions caused by the interaction of the volatiles with the char structure of a particular solid, it is difficult to (theoretically) determine independently the enthalpy change for a material. In this study, the enthalpy of pyrolysis has been considered to take an effective value of zero. It is interesting to assess the effect that the addition of an enthalpy term has on the model predictions in order to understand the implications of this assumption. The following equation was used to model an enthalpy of pyrolysis [83]:

$$\frac{\partial(c_p\rho T)}{\partial t} = \lambda\left(\frac{\partial^2 T}{\partial r^2} + \frac{(a-1)}{r}\frac{\partial T}{\partial r}\right) - H_{solid}\frac{\partial m}{dt} \qquad (6.12)$$

where H_{solid} is the heat liberated at constant pressure per unit mass of volatile product evolved, and $\frac{\partial m}{dt}$ is the mass of volatiles evolved per second.

Figure 6.19 shows three curves: the central curve gives a model prediction when the enthalpy is considered zero, and curves to the left and right show the effect of the addition of an endothermic and exothermic enthalpy term, respectively. It is interesting to note that all of the curves appear to begin decreasing with the same gradient at time=0 seconds. They then pivot around approximately the same point at time≈350 seconds (in this case): the predicted gradient becomes steeper when an endothermic enthalpy term is assumed, but flattens out with an exothermic term. The fact that the addition of an endothermic enthalpy term tends to make the curve increasingly steep, indicates that the sudden decrease in gradient is related to limitations in the amount of heat being transferred to the inner parts of the solid and available for pyrolysis. The addition of an exothermic term effectively provides an additional heat source within the solid, flattening out the curve. An optimisation was carried out using a simplex algorithm where k_0, E and H_{solid} were fitted to experimental data of the normalised burn rate as a function of A/V ratio (as in Section 6.2.3). The fit gave the following values for these parameters: k_0=2.172×10^5 s^{-1}, E=0.582×10^5 $Jmol^{-1}$ and H_{solid}=4.004e5 Jkg^{-1}. Figure 6.20 shows a comparison of model predictions with and without the enthalpy term using the optimised parameters. The new parameters, which include the enthalpy term, are able to predict the trend in normalised burn rate as a function of A/V

ratio. However, there are clear differences between the mass decrease curves. One important difference is the predicted behaviour of the mass decrease at the ignition phase. Looking closely at the change in gradient as a function of time for each of the curves, the following can be observed: when the exothermic enthalpy term is used in the model, the large briquettes are predicted to ignite very rapidly, such that the mass decrease at the beginning of the burn appears faster than the steady state phase. This is not, however, what is observed in a typical mass decrease curve measured experimentally (see Figure 3.5 in Section 3.3), where the curve shape is characterised by an initial slower rate of mass decrease followed by a more rapid quasi-steady state phase. Nevertheless, these results do suggest that the linear mass decrease experimentally observed during the quasi-steady state burn phase (see Figure 3.5) might indeed be due to exothermic reactions occuring within the solid.

In the above treatment the exothermic reactions were considered to occur immediately at the place of production of the gases. This, however, might not be the case and heat could be released by secondary reactions of the volatile gases, as they pass out through the porous char matrix of the solid. Modelling secondary reactions is an area that requires further work.

The above behaviour suggests that the decomposition could be modelled in two phases. In the first phase, the rate can be thought of as controlled by conduction heat transfer into the solid alone, and the volatiles pass out with negligible secondary exothermic reactions. Then, after a critical solid thickness, as the volatiles have to pass a greater distance through a growing char layer, the heat from secondary reactions might become more significant. For this phase of the decomposition, a model including an exothermic enthalpy term might be more suitable. What becomes clear when using the optimisation procedure described above, is that the physical significance of the enthalpy term in the modelling parameters is not fully defined, especially as the nature and mechanism of the release of heat within the solid is not fully understood.

6.5.4   Conclusions

In the first part of this section, the effect of allowing material properties to vary as a function of degree of degradation and temperature was considered. It was concluded that taking into account changing material properties becomes more important the smaller the A/V ratio of the briquette. For predictions of the NBR of briquettes burning in free air, as treated in this study, it was found that it was sufficient to assume a constant diffusivity. However, for larger briquettes and more
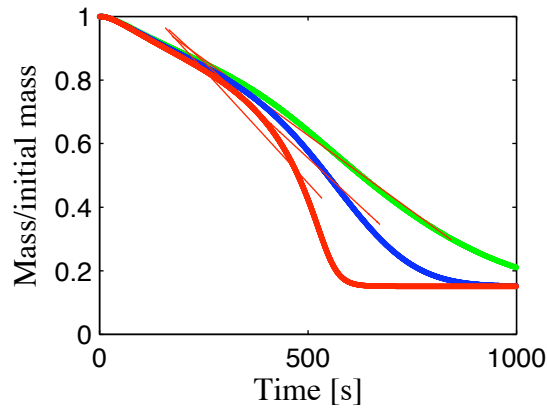
Figure 6.19: The effect of the addition of an enthalpy term on the mass decrease curve caused by the pyrolysis of a briquette burning in free air. The central (blue) curve is with no enthalpy term, the right hand (green) is with the addition of an exothermic enthalpy of magnitude 2×10^5 (while the other parameters remain unchanged). The left hand (red) curve is the result with an endothermic enthalpy term, of the same order of magnitude as the exothermic term.
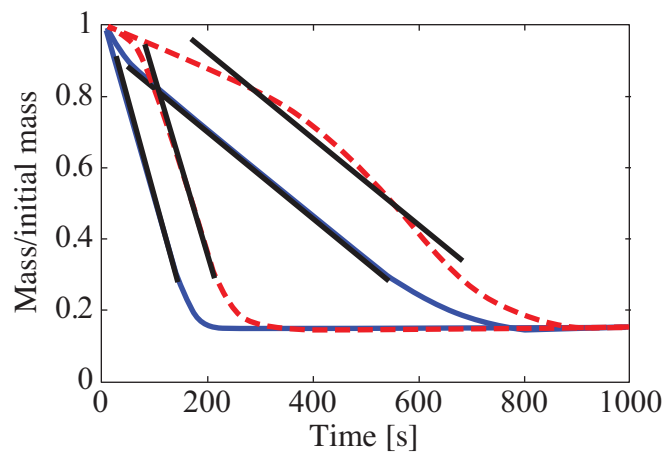
Figure 6.20: A comparison between the optimised model predictions for the cases when the enthalpy term is included (—)and excluded (- - -) in the model evaluation.

detailed studies on the decomposition process, the variation in material properties with degree of degradation and temperature would need to be considered.

The effect of volatiles was then investigated, and it was concluded that the heat that they transport by convection out of the solid could be around 10% of the heat transferred into the solid by conduction. However, this appears to have a negligible effect on the predicted NBR for the briquettes considered (it might be that this loss has been taken into account in the optimisation of k_0 and E). Further investigation into the effect of this variable is required, in order to understand more fully the conditions under which it becomes important to model.

In the final part, the assumption of zero enthalpy of formation of the volatiles was considered. Including an enthalpy term in the model was shown to have a significant influence on the form of the mass decrease curve. An exothermic enthalpy term was shown to flatten the curve and bring the shape closer to that observed experimentally, suggesting that there might be secondary heat releasing reactions occurring within the solid as the volatiles pass out through the char layer. This has not been included in the simple model for two reasons: firstly because it is difficult to understand the physical nature of this term. Secondly, the simple model is able to make adequate predictions of the normalised burn rate by taking the average gradient of the curve for larger samples, and therefore it is not necessary to add this extra level of sophistication (it is likely that it has been partly accounted for in the kinetic optimisation). However, its clear impact on the numerical simulation, and its non-trivial nature revealed by the literature suggest this variable cannot be ignored. Further work, looking for patterns in the optimised value for briquettes of different materials over different briquette sizes and with different combustion conditions, would lead to a deeper understanding of this variable and its relative importance in the study of densified biomass.

6.6   Summary and Conclusions

This chapter has considered the evaluation of the numerical model of pyrolysis presented in Section 5.1, using the material and heat transfer parameters found in Section 5.2. Possible values for k_0 and E were explored by running the model and comparing the predicted NBR result with experimental measurements. A contour map of the residuals was produced, showing that there are several combinations of optimum values for k_0 and E. A numerical minimisation algorithm (the simplex algorithm) was then used. This was shown to be effective in identifying minima. Moreover, the determined values for the kinetic parameters were shown to predict

a pyrolysis temperature in the range suggested by literature values, giving some confidence that the identified kinetic parameters are sensible. What is unique about the optimisation procedure used in this study is that it is done over a large range of different size briquettes simultaneously, rather than focusing on the behaviour of one mass decrease curve and attempting to fit to that. With the nature of the chemical kinetics being complex, this provides a simple means to determine representative values for the kinetic parameters suitable for a large range of briquettes. Further studies should be carried out comparing results predicted by this method with other independent techniques, in particular thermogravimetric analysis would be useful. However, it is difficult to ascertain how successful this would be because of the dependence of the kinetic parameters on combustion conditions, and because of the complex nature of the energetics of pyrolysis.

It was found that the model was able to predict the experimental data from Chapter 4 for newspaper briquettes within the error bounds. This suggests that the assumption of a primarily conduction based devolatisation model, where heat transfer is controlled by the material's thermal diffusivity, is sufficient in this case. A sensitivity study was carried out on the variation in the predicted NBR caused by changes in the kinetic and heat transfer parameters. A particular sensitivity was observed due changes in E and T_f. On the other hand, changes in the heat transfer coefficient, h, of 20% led to a maximum of approximately an 8% change in the predicted NBR, giving an indication of the upper limit of uncertainty associated with neglecting the modification of h by the transpiration of volatiles from the surface.

A study was carried out looking at the effect on the NBR of changing the material thermal parameters c_p and λ, and the trends predicted could be approximated as following exponential functions. This allowed the briquette equation derived in Chapter 4 to be expanded and written as a function of these material properties. Finally, the high sensitivity of the predicted NBR to changes in the gas phase temperature necessitates its inclusion in the briquette equation. Simulations were carried out to predict its behaviour, and an equation fitted to the results. The final derived expression allows the pyrolysis rate of densified biomass to be estimated. Some of the potential limitations of the model, which would directly lead to limitations in this equation, were then explored.

The validity of three important assumptions were explored: the assumption of constant thermal diffusivity, the assumption of no convective heat transfer by the volatile gases, and the assumption of a zero enthalpy of pyrolysis. It was concluded that modelling changing material properties (with degree of decomposition and

temperature), was not necessary for the determination of the NBR for the briquettes investigated in this study. However, for larger briquette samples than considered here, and in studies considering other aspects of the combustion, for example the ignition phase, this assumption would have to be reassessed. In terms of the convective outflow of heat with the volatiles, this did not appear to have a significant affect on the NBR, and so it was reasonable to assume it was negligible in this study. On the other hand, including an enthalpy term in the model, proved to have a significant effect on the shape of the predicted mass decrease curve. Indeed, it was possible to find optimised values for E and k_0, to correctly predict the NBR versus A/V trend with and without the enthalpy term. But, for thicker samples, including an enthalpy term appeared to flatten out the curve and give a better approximation to the form of the experimentally determined one. This indicates heat producing reactions may indeed be occurring within the char matrix of the briquette during devolatisation. Further work needs to be done with other biomass residues and sizes of briquettes to understand more fully the nature of this term.

In summary, Chapter 5 and the work completed in this chapter provides the analytical tools required to make predictions of the devolatisation rate of a biomass briquette as a function of its material properties. In the final chapter, a discussion is given of the relevance of these findings, and how they relate to the rest of the thesis.

Chapter 7

Conclusions and Recommendations

The first part of this chapter summarises and draws together some of the important findings of this thesis and reviews the objectives achieved. Following this is a brief discussion of the limitations and implications of the results, and recommendations for further work.

7.1 Summary and Conclusions

The overriding objective of this thesis was to understand how some of the key physical properties of compressed biomass fuel relate to the burn rate of briquettes. The approach adopted in exploring this research question involved experimental study of briquettes burning in free air and numerical modelling of their thermal decomposition. The result is an understanding of the relative change in burn rate as a function of key material properties. The derived briquette equation has the potential to be used as a pyrolysis sub-model for cookstove optimisation[1] with the added advantage over previous approaches of being able to vary material properties.

The key findings from this thesis that informed the research question and flow from its exploration are reviewed in the remainder of this section.

The problem has its origins in Chapter 1, which presented the social context of this briquette combustion study. In this chapter a case study on Ghana was carried

---

[1]A similar numerical approach to Burham-Slipper could be used; see Chapter 3 of [75].

out considering some key aspects relating to the use of biomass residues as a fuel substitute, including:

- woodfuel consumption in different sectors of the economy;

- deforestation and its impact;

- future projections of woodfuel use;

- the availability of biomass residues and advantages and disadvantages of using them as a fuel substitute.

The study suggested that briquettes could be a viable alternative to woodfuel in Ghana, a conclusion which probably applies to many parts of the developing world, especially those with large agricultural economies. The review set the scope of the combustion study to be constrained to briquettes that could be formed in rural areas of developing nations, using an appropriate low-pressure wet technique (described in Chapter 2).

It was concluded that low-pressure briquetting could provide a simple means for people with limited equipment and resources, of upgrading residues that might otherwise go to waste. One of the particular advantages over use of woodfuel is the control that the producer has during manufacture over certain key bulk properties: briquettes can be optimised in terms of their power output during combustion by varying their size, shape, density and moisture content. Furthermore, they can be manufactured consistently, ensuring a constant power output after stoking, while being of a regular shape and size to aid both storage and transport.

The literature review revealed in a general way that the bulk properties of a briquette will affect how it burns. However, a lack of knowledge was identified for quantifying how and to what extent these different properties affect the burns rate. There is a myriad of waste residues from which briquettes can be made, amongst which there will be a large range of different material properties (see Chapter 2). If briquettes are to provide an alternative solid fuel to wood for existing cookstoves, quantifying their combustion behaviour is important. It would allow briquettes to be designed to have a comparable burn rate and power output to existing woodfuels used, and ultimately would help in the optimisation of cookstoves for different biomass residues.

The literature review (Chapter 2) identified some important biomass fuel properties that have an influence on the combustion: in particular moisture content, fuel volatile content, ash content and calorific value. The effect on

the combustion of each of these properties was reviewed (see Section 2.4.1). One limitation of focusing on these properties alone, is that they do not fully describe how the biomass will behave in a densified state, and the rate at which the compressed biomass will thermally decompose. Section 2.5 highlighted some of the key bulk properties that would need to be considered for biomass briquettes: the bulk density of the compressed briquette, its size and shape, and its thermal-material properties that control heat transfer. The relative effect of these quantities on a briquette's burn rate is not documented in the literature in a format that can easily be exploited. It was therefore considered necessary to carry out systematic experiments in order to quantify the relative effect on the burn rate caused by changes in different bulk properties.

To date, most briquette related studies have focused on the manufacture of briquettes under high pressures, and journal publications on low-pressure briquetting for rural areas of developing countries are few. It was identified that experimental methodologies describing how to manufacture briquettes in a controlled fashion, but using processes appropriate for rural locations were not readily documented. Therefore in order to investigate the effect of bulk material properties on burn rate, it was concluded that a suitable methodology was required: the briquette manufacturing process should ideally resemble the method that might be used in a rural setting in a developing country, but allow much greater control over the pressures applied, compression speed, and hold time for the purposes of this study. This is addressed in Chapter 3. Once the briquettes had been manufactured, a suitable test method was needed to allow the study of the change in combustion behaviour as a function of material properties, and this is also described in Chapter 3.

Much of the previous work on combustion has concentrated on trying to understand behaviour through the development of numerical models, and indeed there are many complex models of combustion already available in the literature. Studying the background, the details of these models and their results, helped to develop an understanding of the processes occurring during combustion (see Section 2.7). However, it was noted that the models have not been applied to understanding the combustion behaviour of compressed biomass fuels, particularly in relation to the bulk material properties that have been discussed. This applies to those that can be explicitly varied during briquette manufacture (briquette bulk density, size, geometry and moisture content), and those that which the manufacturer has no direct control over (such as material thermal conductivity, heat capacity and thermal diffusivity, calorific value and ash content), which are of course interrelated with the aforementioned explicit quantities. The solid fuel

models available in the literature are often too computationally complex to readily allow relative comparisons to be made between the combustion behaviour that would result from different material properties. Furthermore, models are not in a format that can be easily exploited in a numerical cookstove optimisation process [41]. It was concluded, therefore, that it would be useful to develop a simple analytical model that would allow:

- the estimation of the relative change in briquette properties as a function of material properties;

- the potential numerical optimisation of cookstoves for different fuel types, allowing the study in greater detail of the effect of material properties on stove efficiency.

Chapter 3 considered the development of a suitable methodology for the manufacture of briquettes. Newspaper was chosen as the primary material for this investigation because it is readily available in the UK (which is where this study was carried out), and it is easy to break down and briquette. Encouragingly, the compressive behaviour observed when compacting pulped newspaper to different densities was found to be similar to the compressive behaviour of other biomass materials presented in the literature (Chapter 4). Furthermore, the trends observed in its combustion behaviour were shown to be similar to those for both compressed sawdust and rapeseed oil residue briquettes. These results suggest that newspaper is representative of a least a range of other biomass materials. An experiment was performed to investigate the effect of the pulp moisture content of the charge (loaded in the mould), on the final briquette dry density (Chapter 3). Within the pulp moisture content range tested (650 to 1300% dry basis), there was no significant effect observed. It was therefore concluded that charge moisture content did not need to be carefully controlled or monitored for the manufacture of repeatable briquettes of consistent density.

In order to explore the combustion behaviour of briquettes, a methodology for the systematic investigation of compressed biomass briquettes burning in free air was developed, where briquettes of different dimensions and geometry were placed on a mesh grid, and their mass decrease as a function of time was measured (Chapter 3). This methodology allows the systematic investigation of briquette burn rate as a function of different material properties.

In the first part of Chapter 4 the effect of process variables on the NBR (normalised burn rate) were investigated using the methodology described in Chapter 3. These are variables are that can be controlled during manufacturing process: the bulk

density of the compressed material, the briquettes' size and shape, and to some extent the briquettes' final moisture content. The effect of changing material density was investigated here for newspaper briquettes and a decaying exponential relationship between the normalised burn rate of a briquette and its density was found. For newspaper briquettes the exponential exponent factor was found to be -0.0023. In the size range of briquettes tested, this exponential exponent factor was shown not to be a function of briquette size and geometry. This suggests it is an empirical constant, which can be specified for different residues, and is some function of material properties. The exponential coefficient found here for newspaper was found to be of a similar order of magnitude to other values from another study (see Section 4.1), which was completed using much smaller briquettes (made from only 4g of material). This density behaviour for newspaper was successfully predicted in Chapter 6 using the numerical model, which assumed heat transfer to be the primary mechanism driving the pyrolysis. This is an encouraging result, and suggests that the rate of pyrolysis is fundamentally thermally driven, controlled by the rate of heat transfer into the solid (the kinetic decomposition behaviour of the material depends on the heat transfer).

The effect of moisture content on the NBR was also investigated experimentally in Chapter 4. An approximate trend was observed: a linear decrease in NBR with increasing percentage moisture content (dry basis).

In Chapter 4 it was observed that for briquettes burning in free air, the sample's area-to-volume ratio (A/V ratio) has a significant influence on its NBR. Plotting the A/V ratio against NBR was shown to provide a useful method to correlate results for briquettes of different sizes and dimensions, as a function of a single one-dimensional variable. For slab-shaped briquettes burning in free air (of constant density), this relationship was shown to be linear. As the A/V ratio decreases the normalised burn rate is found to decrease. This is interesting, because it suggests that it is possible to correlate briquettes with a range of different sizes and shapes, using a simple one-dimensional quantity (the unit of A/V ratio is mm^{-1}).

Further experiments were conducted investigating the relationship between A/V ratio and NBR for some other materials: sawdust, rapeseed oil and pinewood. The behaviour was also found to be linear, but the gradient for rapeseed oil residue briquettes was shown to be significantly different to that for newspaper briquettes. It was thus concluded that material properties indeed have a significant influence on the gradient of the A/V ratio versus NBR curve. An expression was proposed for predicting the relative change in NBR for two materials having

different net calorific values. This was used to predict the increase in the gradient of the A/V versus NBR curve for rapeseed oil residue briquettes, compared to newspaper briquettes. The result appears to be successful, but the method should be applied to other materials with significantly different calorific values for further validation. If it is assumed that the relationship between calorific value and NBR is correct, this clearly demonstrates that biomass calorific value has a very significant influence on briquette burn rate and cannot be ignored in approximations.

The effect of briquette geometry on the NBR was further investigated in Chapter 4 by considering a cylindrical briquette with a central hole. The central hole was found to increase the NBR compared to a slabs with the same A/V ratio. The increase in rate could be predicted by considering the view-factor from the inside of the hole to the atmosphere; the smaller the overall view factor (the taller the briquette), the higher the NBR. This suggests that the geometrical effect of the hole might be important, but this needs to be considered in conjunction with the increase in rate caused by an increased flow of air through the central hole supplying increased levels of oxygen to the reaction. This has not been considered in this study. The results from this analysis and the slab experiments imply that in free air, solid briquettes with a geometry that that has no internal angles (where any given surface cannot see any other) should burn at the rate predicted for slabs. Whereas, when part of the briquette surface can 'see' another part, radiative exchange means the NBR will be increased.

Biomass briquettes can be manufactured from a vast array of different residues, which can be compressed to different densities and have different moisture contents. This leads to a large range of bulk fuel properties between different briquettes. Understanding how changes in the thermal properties affect the burn rate of the material, is one important step in deriving a general expression to predict the rate of decomposition for any compressed biomass sample under different combustion conditions. It is, however, difficult to investigate these properties experimentally.

In order to better understand the observed experimental behaviour, a numerical model for the devolatisation of briquettes was developed. The first objective was to predict the NBR versus A/V behaviour observed experimentally. The second objective was to investigate how the thermal parameters (the thermal conductivity, heat capacity) of a material affect the NBR. The third objective was to use the model to develop an analytical expression for the burn rate of a briquette as a function of these material properties.

Chapter 5 presents this numerical model. It consists of a one-dimensional conduction model coupled with an Arrenheius equation describing the kinetics

of pyrolysis (assuming a global one step decomposition reaction). In order to determine the thermal parameters of the briquette required for the execution of the model, the use of a dynamic heat probe method was developed and tested that was able to determine both the thermal conductivity and heat capacity of a briquette simultaneously in a single measurement. The kinetic parameters (k_0 and E) were determined by numerically fitting the model to the experimental data. A contour plot was constructed of the difference between the model prediction and the experimental data for a range of different values of k_0 and E. It suggested that there are a number of different possible pairs of the kinetic parameters that produce a good fit. It was proposed that this might explain the large range of values (differing by orders of magnitude) for the kinetic parameters that are observed in the literature.

Chapter 6 describes how the model was used to predict the combustion behaviour of newspaper slabs. A linear correlation between NBR and A/V ratio was calculated, which gave a good fit with experimental data. The experimental trend is found to be valid not only for thick and thin slabs, but also for tall and short slabs. A suggested rationale behind the one-dimensional model result being applicable to the three-dimensional case is as follows (based on [134]): if it is assumed that there are isotropic external conditions, and that the briquette material properties are also isotropic, then, every point at a determined distance from the surface of the briquette will be approximately in the same state of decomposition. Therefore, control volumes can be defined at equal distances from the surface such that the distance from the surface is the same for each dimension. In this way, three-dimensional finite sized briquettes can be treated in a one-dimensional frame. This has not been validated in this study, and this is picked up on in the recommendations for further work.

Chapter 6 goes on to further apply the model to consider the effect of the material properties that control the heat transfer into a briquette. It was found that an increase in the specific heat capacity leads to an exponential decrease in the NBR, but that the magnitude of the decrease is a function of the A/V ratio of the solid. It was also found that as the thermal conductivity of a solid is increased, the NBR increases in an exponential fashion. The rate of the exponential increase, was also found to be dependent on the A/V ratio (in a similar way to heat capacity). The noticeable affect on predicted NBR caused by variation in these properties, consequently means that the choice of sensible values in a numerical model is important. By completing analytical fits to model predictions, the analytical briquette equation for free air developed in Chapter 4[2] was extended.

---

[2]See Equations 4.5, 4.22, 4.24, 4.29.

The analytical briquette equation provides a means to estimate the NBR of a newspaper briquette in free air as a function of the material's thermal conductivity, heat capacity, density, A/V ratio, moisture content and calorific value. If pyrolysis is indeed primarily thermally driven, and the behaviour expressed in this equation is valid for different environmental combustion conditions (for example in a cookstove packed combustion bed), then this equation provides a general means to find the relative change in NBR resulting from a change in the described properties. The equation was further developed to include gas-phase temperature. However, the approximation proposed has ignored an analysis on soot formation, which significantly contributes to the flame radiation to the briquette surface. But it does provide a (tentative) connection with the gas phase, so that by measuring or predicting the temperature in a stove and assuming a lumped fuel model, this equation could be used to give a rough estimate of the rate of *pyrolsis* in a stoked fire. This equation could potentially be used in combination with a char model (see Appendix B) to determine the approximate size and density of briquettes required to give the equivalent burn rate (or equivalent power output) of a wood fire. It essentially provides the basis for a pyrolysis submodel, which has the advantage of allowing certain key briquette fuel properties to be varied; it has potential to be used in numerically low-cost numerical cookstove optimisation, for designing improved cookstoves that perform well for different biomass residues.

At the end of Chapter 6, some of the limitations of the simple analytical model were considered. Firstly, the assumption of a constant thermal diffusivity was challenged, but it was concluded that this assumption was valid for making NBR predictions in this study. More detailed studies trying to understand the process of the decomposition and the ensuing changes in material structure, would however, need to take this into account. The effect on the predicted NBR of not including a term for the outflow of volatiles was investigated. The magnitude of the convective to conductive heat transfer was approximated, suggesting for a typical case a 10% uncertainty in the heat transferred. However, when an equation for the convective heat transfer by volatile gases was integrated into the analytical model, the effect on the predicted NBR for the range of samples investigated in this study was negligible. Because of its limited influence on the NBR, it was not considered necessary to include convective heat transfer in the model. Finally, the effect of including an enthalpy term to account for possible energy released (or used) *inside* the briquette as part of the devolatisation reaction, was investigated. It was shown to have a significant influence on the shape of the mass decrease curve, and thus the NBR predicted by the model. When an exothermic enthalpy term was included in modelling thick briquette samples, the predicted mass decrease

curve was found to more closely approximate the linear form of the experimental data in the steady state burn phase. It was suggested that this might be the result of secondary reactions of the volatile pyrolysis gases, releasing heat as they pass through the briquette char matrix. A preliminary optimisation was carried out using the Simplex algorithm, using a similar procedure to that described in Section 6.1, in order to find values for k_0, E and q (the enthalpy).

The consideration of the limitations above illustrates how complex a process combustion is. This is one aspect that makes detailed numerical cookstove optimisation difficult and time consuming. Burham-Slipper [75] suggested that 'stove optimisation programs should be based in the country of interest and only involve numerical modelling as a last resort or to resolve very precisely defined aspects'. However, although the processes are complex and many assumptions have to be made, numerical optimisation can be useful in a broader sense. It can provide (for a stove practitioner) an understanding of the key parameters affecting cookstove efficiency and levels of emissions that need to be taken into account. Even if all the details of the combustion are not resolved, knowing the trends in behaviour can help in the design process, allowing attention to be given to optimising the most important aspects to achieve good thermal performance, while keeping the important social aspects in mind. A simple model of a cookstove containing the essential physics and chemical kinetics, allows the key trends in and behaviour to be identified. The Appendices outline a char combustion model (Appendix B) and a simple analytical model for a rocket cookstove (Appendix C), which potentially could be developed and applied for this purpose. It is the vision of the author that in the future this might lead to the development of some simple appropriate software that would allow the cookstove practitioner to build up a cookstove design component by component (on a computer), then identify the key parameters affecting its performance as an aid to an on the field optimisation process.

7.2 Limitations and Recomendations for Further work

Due to restrictions of resources, equipment and time, there are aspects of this study that have been overlooked, questions that have not been explored and further validation that needs to be done. In this section, some of the limitations, and areas that need to be examined further are highlighted.

- Only the free air combustion environment was considered experimentally in this study. In suggesting its application as a pyrolysis submodel, an assumption has been made that the pyrolysis is thermally driven, which appears realistic from model fits in this work. Further work is, however, required to verify that this is the case under different combustion conditions. Indeed, one challenge will be calculating the heat transfer to the surface of a briquette as a function of the combustion conditions. It would be interesting to look into the effect of combustion environment on the empirical constants in the equation derived for the normalised burn rate of a briquette.

- This study has considered the bulk properties of compressed biomass, mainly focusing on the following aspects: process variables, bulk material thermal properties, and one material specific property (calorific value). But there are other aspects of the properties of biomass that influence the burn rate, discussed in Chapter 2. These include the volatile matter content, ash content, and material chemical composition, as well as considering the changes in structure that occur during the thermal decomposition, which can be different for different compressed residues [135]. Further studies are required to understand their relative effects and take them into consideration.

- The study was limited in the extent of biomass residues that it considered, and it is necessary to validate and develop this work for a larger range of different types of residues, and determine the constants for the equations derived. The behaviour of different blends of materials should also be examined. In particular, the method used to predict the change in rate due to the calorific value method should be applied to other materials with significantly different calorific values for further validation.

- In this work, the heat probe method was used to find the thermal properties of dry newspaper briquettes. This work should be expanded to include different moisture contents and residue materials. However, the heat probe method was shown to have many limitations in its current state (Chapter 5), and its accuracy was considered only sufficient to provide approximate values for the thermal properties (within specified uncertainties). Further development is thus needed to improve its accuracy. In particular the design of the probes should be improved and the technique developed in order to reduce the large measurement uncertainties that are occurring, primarily caused by uncertainties in the probe spacing. Further developments could also be made to allow the collection of data at different temperatures, and

at different degrees of thermal degradation. This would then allow the gap in the literature concerning the material properties of partly decomposed densified biomass to be addressed.

- The view-factor explanation developed to explain the NBR of cylindrical briquettes with a central hole as a function of briquette height, needs to be more rigourously tested for other geometry briquettes in free air, for example stars, in order to assess its generality. The limits of the view-factor theory should also be explored, looking at very tall briquettes for example. Furthermore, the numerical model should be developed and applied to attempt to predict the change in NBR caused by variations in the radiative heat flux at the surface of a briquette (caused by changes in surface view-factor). This it would provide further validation of the thermally driven nature of pyrolysis and enable the results for holey briquettes with changing heights to be modelled. A model of the airflow around and through the holey briquette should also be realised, and the relative influence of changing flow with briquette dimensions explored and compared with the discussed view-factor effects.

- One particular aspect that was not considered explicitly in the free air experimental studies was the critical limits for briquettes beyond which combustion ceases to be self-sustaining. This would be an interesting area for further study, both for free air and for other combustion conditions (i.e. in a stove), and should be examined in terms of briquette dimensions, geometry and the other material properties of densified briquettes.

- The simple global one-step kinetic reaction, used in this thesis to model the chemistry of biomass combustion, has been adequate, but it is likely that model behaviour and predictions could be improved by using a multi-step devolatisation model, which are available in the literature. Further tests should be done using the technique described in this work, to determine the kinetic parameters for a wide range of biomass residues and compare the results to values determined using thermogravimetric analysis.

- The effect of moisture content has not been investigated using the analytical model. Nevertheless, the foundation has been laid to make this possible: the heat probe method (see Section 5.2.1) would allow the change in material thermal properties with moisture content to be investigated, and the numerical model (see Section 5.1) provides a simple, and what has thus far been shown to be a robust method, of predicting the rate of heat transfer

into the solid. This could be further developed to take into account the latent heat of evaporation of moisture, and to attempt to predict the experimentally observed behaviour in Section 4.3.

- The briquette fuel model should be further developed and applied in analytical stove simulations, with the objective of establishing a better understanding of how to optimise existing woodburning cookstoves (and new biomass briquette specific stoves) for use with different residue briquettes.

References

[1] S. B. Atakora, "Biomass technologies in Ghana," tech. rep., Kumasi Institute of Technology and Environment, 1999?

[2] Ghana Statistical Service, "2000 Population and Housing Census," Accra, 2002.

[3] F. O. Akuffo, A. Brew-Hammond, E. A. Ankudey, E. B. Hagan, K. S. Nketia, and F. Nkrumah, "Strategic national energy plan - 2005-2020 Republic of Ghana: Indigenous energy resource catalogue," tech. rep., Kwame Nkrumah University of Science and Technology, School of Engineering, 2003.

[4] Energy Commission of Ghana, "Ghana energy statistics," 2004, available online: `www.energycom.gov.gh` (last checked March 2010).

[5] I. Edjekumhene, S. Bonsu, Atakora, R. Atta-Konadu, and A. Brew-Hammond, "Implementation of renewable energy technologies-opportunities and barriers," Ghana country study, Kumasi Institute of Technology and Environment, 2001.

[6] J. Chaney, "Interviews and observations concerning small businesses and farmers in Ghana." (unpublished), recorded interviews and notes from a field trip to Ghana, 2007.

[7] maps.com, *Political Map of Ghana showing its position in West Africa*. Available at `http://www.maps.com/ref_map.aspx?cid=694,720,730, 927&pid=12049` (last accessed 8th March 2010), 2009.

[8] Energy Commission of Ghana, "Strategic national energy plan 2006-2020: energy supply to the economy," report, 2005.

[9] E. Riegelhaupt, "Sustainable forest management programme in African ACP countries (GCP/RAF/354/EC) wood energy planning and policy development component: Ghana," final report, United Nations Food and Agriculture Organisation, Accra, Ghana, October 2001.

[10] Kumasi Institute of Technology and Environment, "Energy for poverty reduction action plan for Ghana: a targeted approach to delivery of modern energy services to the poor." Ghanaian Ministry of energy, 2006.

[11] N. Bruce, R. Perez-Padilla, and R. Albalak, "Indoor air pollution in developing countries: a major environmental and public health challenge," *Bulletin of the World Health Organisation*, vol. 78, no. 9, pp. 1078–1092, 2000.

[12] T. Agyarko, "Forestry outlook study for Africa [FOSA]: Ghana," tech. rep., Ministry of Lands and Forestry, 1999?

[13] Japan International Cooperation Agency, "Country profile on environment: Ghana," report, November 1999.

[14] D. E. K. A. Siaw, "State of genetic resources in Ghana," tech. rep., Forestry Resources Division, FAO, Italy, 2001.

[15] F. K. Odoom, "Chainsawing in the natural forests of ghana: An assessment of the socio-economic impacts of this practice," tech. rep., Food and Agriculture Organisation of the United Nations, 2005.

[16] Ministry of Food and Agriculture, "Annual sample survey of agriculture: Regional and district cropped, yield and production statistics," report, Statistics Research and Information Directorate (SRID), Ghana, 2007.

[17] S. Jekayinfa and O. Omisakin, "The energy potentials of some agricultural wastes as local fuel in Nigeria," *Agricultural Engineering International: the CIGR Ejournal*, vol. 7, 2005.

[18] B. M. Jenkins, *Biomass Handbook*, ch. Properties of biomass. Gordon and Breach, New York, 1989.

[19] S. Gaur, *An Atlas of Thermal Data For Biomass and Other Fuels*. National Renewable Energy Laboratory, U.S, 1995.

[20] Ministry of Food and Agriculture, "Production of major crops in Ghana," report, Statistics, Research and Information Directorate (SRID), 2000.

[21] P. Wilaipon, "The effects of briquetting pressure on banana-peel briquette and the banana waste in Northern Thailand," *American Journal of Applied Sciences*, vol. 6, no. 1, pp. 167–171, 2009.

[22] T. Nkurunziza and J. Ntaganda, "Laboratory scale biogas production from banana tree residues," in *3rd International Conference on Appropriate Technology: Proceedings of Oral Platform Presentations* (J. Tharakan and J. Trimble, eds.), 2008.

[23] B. Singh, D. R. M. Raj, K. E. Dashiell, and L. Jackai, *Advances in Cowpea Research*. International Institute of Tropical Agriculture (IITA) and Japan International Research Centre for Agricultural Sciences (JIRCAS), 1997.

[24] R. Oliver and E. Fripp, "Changing industrial markets for timber-what can African producers do," report, Timber Trade Federation, UK, 2005.

[25] Forest Products Inspection Bureau, "Log production statistics," tech. rep., 1993.

[26] K. Mason, *Fuel for Free: Waste Materials in Brickmaking*. Practical Action Publishing, 2007.

[27] G. Barnard and L. Kristoferson, *Agricultural Residues as Fuel in the Third World*. International Institute for Environment and Development, 1985.

[28] L. Wamukonya and B. Jenkins, "Durability and relaxation of sawdust and wheat-straw briquettes as possible fuels for Kenya," *Biomass and Bioenergy*, vol. 8, no. 3, pp. 175–179, 1995.

[29] Z. Husain, Z. Zainac, and Z. Abdullah, "Briquetting of palm fibre and shell from the processing of palm nuts to palm oil," *Biomass and Bioenergy*, vol. 22, pp. 505–509, 2002.

[30] Legacy Foundation, *Fuel Briquettes-Theory and applications from around the world*. Published Online: `http://www.legacyfound.org` (last accessed 5th March 2010), 2003.

[31] Legacy Foundation, "Fuel briquette press kit- a construction manual." Published Online: `http://www.legacyfound.org` (last accessed 5th March 2010), 2003.

[32] Legacy Foundation, *Fuel Briquettes- A trainers manual*. Published Online: `http://www.legacyfound.org` (last accessed 5th March 2010), 2003.

[33] Legacy Foundation, *Fuel Briquette making, A users Manual*. Published Online: `http://www.legacyfound.org` (last accessed 5th March 2010), 2003.

[34] J. Zhang, K. R. Smith, R. Uma, Y. Ma, V. V. N. Kishore, K. Lata, M. A. K. Khalil, R. A. Rasmussen, and S. T. Thorneloe, "Carbon monoxide from cookstoves in developing countries: 1. emission factors," *Chemosphere: Global Change Science*, vol. 1, no. 1-3, pp. 353–366, 1999.

[35] J. B. Kandpal and R. C. Maheshwai, "Combustion of biomass fuels in two cookstoves for their conservation," *Energy Conversion and Management*, vol. 36, no. 10, pp. 1015–1021, 1995.

[36] G. Ballard-Tremeer and H. H. Jawurek, "Comparison of five rural wood-burning cooking devices: efficiencies and emissions," *Biomass and Bioenergy*, vol. 11, no. 5, pp. 419–430, 1996.

[37] S. C. Bhattacharya, D. O. Albina, and A. M. Khaing, "Effects of selected parameters on performance and emission of biomass-fired cookstoves," *Biomass and Bioenergy*, vol. 23, no. 5, pp. 387–395, 2002.

[38] S. C. Bhattacharya, D. O. Albina, and P. A. Salam, "Emission factors of wood and charcoal-fired cookstove," *Biomass and Bioenergy*, vol. 23, no. 6, pp. 453–469, 2002.

[39] V. Joshi, C. Venkataraman, and D. R. Ahuja, "Emissions from burning biomass in metal cookstoves," *Environmental Management*, vol. 13, no. 6, pp. 763–772, 1989.

[40] V. Joshi, C. Venkataraman, and D. R. Ahuja, "Thermal performance and emission chacteristics of biomass-burning heavy stoves with flues," *Pacific and Asian Journal of Energy*, vol. 1, pp. 1–19, 1999.

[41] H. Burnham-Slipper, *Breeding a better stove: The use of Computational Fluid Dynamics and Genetic Algorithms to optimise a wood burning stove for Eritrea*. PhD thesis, School of Mechanical, Materials and Manufacturing Engineering, 2008.

[42] British Standards Institution, "Solid biofuels- terminology, definitions and descriptions." draft biomass standard, DD CEN/TS 14588, 2004.

[43] A. O. Olorunnisola, "Briquetting of rattan furniture waste," *Journal of Bamboo and Rattan*, vol. 3, no. 2, pp. 139–149, 2004.

[44] R. Stanley, "Fuelling development," *Boiling Point*, vol. 49, pp. 13–14, 2003.

[45] M. Cosgrove, "Understanding briquetting (ISBN: 0-86619-233-6)," Technical Paper 31, VITA, 1985.

[46] P. J. Svenningson, "Biomass briquettes in the Dominican Republic part ii: Technical analysis," *Biomass*, vol. 13, pp. 275–291, 1987.

[47] W. H. Engelleitner, "Binders: how they work and how to select one," *Powder and Bulk Engineering*, vol. 15, pp. 31–38, February 2001.

[48] M. O. Faborode and J. R. O'Callaghan, "Optimising the compression/briquetting of fibrous agricultural materials," *Journal of Agricultural Engineering Research*, vol. 38, pp. 245–262, 1987.

[49] R. S. rstanley@legacyfound.org. *Briquette Press Photos*, Unpublished [E-mail] Message to J. Chaney (joel.chaney@gmail.com), November 2009.

[50] O. C. Chin and K. M. Siddiqui, "Characteristics of some biomass briquettes prepared under modest die pressures," *Biomass and Bioenergy*, vol. 18, pp. 223–228, 2000.

[51] T. R. Marrero, "A review of binders for briquetting and pelletizing," in *Proceedings- Biennial Conference of the Institute for Briquetting and Agglomeration*, vol. 27, pp. 133–140, 2001.

[52] M. McGrath, "Going bananas for energy in africa." BBC news, available online: `http://news.bbc.co.uk/1/hi/world/africa/8044092.stm` (last accessed 9th March 2010), May 2009.

[53] The Glacier Trust, "Forest conservation and alternative fuel appeal." Available online: `http://www.theglaciertrust.org/2008/09/biomass-briquette-appeal.html` (last accessed 9th March 2010), 2009.

[54] M. J. O'Dogherty, "A review of the mechanical behaviour of straw when compressed to high densities," *Journal of Agricultural Engineering Research*, vol. 44, pp. 241–265, 1989.

[55] M. J. O'Dogherty and J. A. Wheeler, "Compaction of straw to high densities in closed cylindrical dies," *Journal of Agricultural Engineering Research*, vol. 29, pp. 61–72, 1984.

[56] B. J. Butler and H. F. McColly, "Factors affecting the pelleting of hay," *Agricultural Engineering*, vol. 40, no. 8, pp. 442–446, 1959.

[57] P. L. Bellinger and H. H. McColly, "Energy requirements for forming hay pellets," *Agricultural Engineering*, vol. 42, no. 5, pp. 244–247, 1961.

[58] G. F. Rehkugler and W. F. Buchele, "Biomechanics of forage wafering," *Transactions of the ASAE*, vol. 12, pp. 1–8, 1969.

[59] S. C. Cowin, "Mechanical modelling of the shrinking and swelling of porous elastic solids," *Journal of Rheology*, vol. 29, pp. 119–130, 1985.

[60] M. O. Faborode, "Moisture effects in the compaction of fibrous agricultural residues," *Biological Wastes*, vol. 28, pp. 61–71, 1989.

[61] K. Peleg, "A rheological model of nonlinear viscoplastic solids," *Journal of Rheology*, vol. 27, no. 5, pp. 411–431, 1983.

[62] S. V. Loo and J. Koppejan, *The Handbook of Biomass Combustion and Co-firing.* Earthscan, 2008.

[63] H.-C. Kung, "A mathematical model of wood pyrolysis," *Combustion and Flame*, vol. 18, pp. 185–195, 1972.

[64] H. Burnham-Slipper, M. J. Clifford, and S. J. Pickering, "A simplified wood combustion model for use in the simulation of cooking fires," in *5th International Conference on Heat Tranfer, Fluid Mechanics and Thermodynamics*, Sun City South Africa, 2007.

[65] B. M. Jenkins, L. L. Baxter, T. R. M. Jr, and T. R. Miles, "Combustion properties of biomass," *Fuel Processing Technology*, vol. 54, pp. 17–46, 1998.

[66] K. W. Ragland and D. J. Aerts, "Properties of wood for combustion analysis," *Bioresource Technology*, vol. 37, pp. 161–168, 1991.

[67] G. L. Borman and K. W. Ragland, *Combustion Engineering.* McGraw-Hill Science/Engineering/Math, 1998.

[68] B. S. Institution, "Soild biofuels-methods for the determination of moisture content-oven dry method." draft biomass standard, DD CEN/TS 14774-2, 2004.

[69] Y. B. Yang, C. Ryu, A. Khor, N. E. Yates, V. N. Sharifi, and J. Swithenbank, "Effect of fuel properties on biomass combustion. part ii. modelling approach-identification of controlling factors," *Fuel*, vol. 84, pp. 2116–2130, 2005.

[70] C. A. Zaror and P. D. Pyle, "The pyrolysis of biomass: A general review," *Sadhana Academy Proceedings in Engineering Sciences*, vol. 5, no. 4, pp. 269–285, 1982.

[71] Y. B. Yang, J. Yamauchi, V. N. Sharifi, and J. Swithenbank, "Effect of moisture content on the combustion of biomass and simulated solid waste in a packed bed," *Journal of Institute of Energy*, vol. 76, pp. 105–115, 2003.

[72] B. S. Institution, "Solid biofuels: method for the determination of the content of volatile matter." draft biomass standard, CEN/TS 15148, 2009.

[73] A. Demirbas, "Physical properties of briquettes from waste paper and wheat straw mixtures," *Energy Conversion and Management*, vol. 40, pp. 437–445, 1999.

[74] F. de Souza and D. Sandberg, "Mathematical model of a smoldering log," *Combustion and Flame*, vol. 139, pp. 227–238, 2004.

[75] H. Burnham-Slipper, *Breeding a better stove: The use of Computational Fluid Dynamics and Genetic Algorithms to optimise a wood burning stove for Eritrea.* PhD thesis, University of Nottingam, School of Mechanical, Materials and Manufacturing Engineering, 2008.

[76] B. M. Jenkins, R. R. Bakker, and J. B. Wei, "On the properties of washed straw," *Biomass and Bioenergy*, vol. 10, no. 4, pp. 177–200, 1996.

[77] H.-J. Kim, G.-Q. Lu, I. Naruse, J. Yuan, and K. Ohtake, "Modeling combustion characteristics of biocoalbriquettes," *Journal of Energy Resources Technology*, vol. 123, pp. 27–31, 2001.

[78] B. S. Institution, "Solid biomfuels-determination of total content of carbon, hydrogen and nitrogen- instumental methods." draft biomass standard, DD CEN/TS 15104, 2005.

[79] M. Dietenberger, "Update for combustion properties of wood components," *Fire and Materials*, vol. 26, pp. 255–267, 2002.

[80] British Standards Institution, "Solid biofuels- method for the determination of calorific value." draft biomass standard, DD CEN/TS 14918, 2005.

[81] T. J. Buckley, "Calculation of the higher heating values of biomass material and waste components from elemental analysis," *Resources, Concervation and Recycling*, vol. 5, pp. 329–341, 1991.

[82] A. F. Roberts, "Problems associated with the theoretical analysis of the burning of wood," in *13th International Symposium on Combustion*, The Combustion Institute, 1971.

[83] C. H. Bamford, J. Crank, and D. H. Malan, "The combustion of wood. part 1," *Proceedings of the Cambridge Philosophical Society*, pp. 166–182, 1946.

[84] A. M. Kanury, "Some considerations pertaining to the problem of wood-burning," *Combustion Science and Technology*, vol. 1, pp. 339–355, 1970.

[85] N. E. Altun, C. Hicyilmaz, and A. S. Bagci, "Influence of coal briquette size on combustion kinetics," *Fuel Processing Technology*, vol. 85, pp. 1345–1357, 2004.

[86] D. L. Pyle and C. A. Zaror, "Heat transfer and kinetics in the low temperature pyrolysis of solids," *Chemical Engineering Science*, vol. 39, no. 1, pp. 147–158, 1984.

[87] F. P. Incropera and D. P. DeWitt, *Fundamentals of Heat and Mass Transfer*. John Wily and Sons, 1996.

[88] T. R. Rao and A. Sharma, "Pyrolysis rates of biomass materials," *Energy*, vol. 23, no. 11, 1998.

[89] C. Alfredo, *Studies of the Pyrolysis of wood at low temperatures*. PhD thesis, London University, 1982.

[90] F. Winter, *Single fuel particle and NOx/N2O- Emission Characteristics Under (Circulating) Fluidized Bed Conditions*. PhD thesis, University of Technolgy, Vienna, 1995.

[91] A. F. Roberts and G. Clough, "Thermal decomposition of wood in an inert atmosphere," in *9th International Symposium on Combustion*, pp. 158–165, The Combustion Institute, 1963.

[92] E. R. Tinney, "The combustion of wooden dowels in heated air," in *Tenth Symposium (International) on Combustion*, pp. 925–930, The Combustion Institute, 1965.

[93] T. Liliedahl and K. Sjostrom, "Heat transfer controlled pyrolysis kinetics of a biomass slab, rod or sphere," *Biomass and Bioenergy*, vol. 15, no. 6, pp. 503–509, 1998.

[94] F. Thurner and U. Mann, "Kinetic investigation of wood pyrolysis," *Industrial and Engineering Chemistry Process Design and Development*, vol. 20, pp. 482–488, 1981.

[95] R. Radmanesh, Y. Courbariaux, J. Chaouki, and C. Guy, "A unified lumped approach in kinetic modeling of biomass pyrolysis," *Fuel*, vol. 85, pp. 1211–1220, 2006.

[96] L. T. Fan, L.-S. Fan, K. Miyanami, T. Y. Chen, and W. P. Walawender, "A mathematical model for pyrolysis of a solid particle," *The Canadian Journal of Chemical Engineering*, vol. 55, pp. 47–53, 1977.

[97] E. J. Kansa, H. E. Perlee, and R. F. Chaiken, "Mathematical model of wood pyrolysis including internal forced convection," *Combustion and Flame*, vol. 29, pp. 311–324, 1977.

[98] P. S. Maa and R. C. Bailie, "Influence of particle sizes and environmental conditions on high temperature pyrolysis of cellulosic material-I (theoretical)," *Combustion Science and Technology*, vol. 7, pp. 257–269, 1973.

[99] C. D. Blasi, "Influences of physical properties on biomass devolatisation characteristics," *Fuel*, vol. 76, no. 10, pp. 957–964, 1997.

[100] M. R. Ravi, A. Jhalani, S. Sinha, and A. Ray, "Development of a semi-empirical model for pyrolysis of an annular sawdust bed," *Journal of Analytical and Applied Pyrolysis*, vol. 71, pp. 353–374, 2003.

[101] J. Saastamoinen, "Simultaneous drying and pyrolysis of solid fuel particles," *Combustion and Flame*, vol. 106, pp. 288–300, 1996.

[102] H. Thunman and B. Leckner, "Thermal conductivity of wood-models for different stages of combustion," *Biomass and Bioenergy*, vol. 23, pp. 47–54, 2002.

[103] H. Y. Y. B. Yang, V. Nasserzadeh, and J. Swithenbank, "Effects of fuel devolatisation on combustion of wood chips and incineration of simulated municiple solid wastes in packed bed," *Fuel*, vol. 82, pp. 2205–2221, 2003.

[104] O. Levenspiel, *Chemical Reaction Engineering*. John Wily and Sons, 1972.

[105] F. Rabier, M. Temmerman, T. Bohm, H. Hartmann, P. D. Jensen, J. Rathbauer, J. Carrasco, and M. Fernandez, "Particale density determination of pellets and briquettes," *Biomass and Bioenergy*, vol. 30, pp. 954–963, 2006.

[106] S. Amous, "The role of wood energy in Africa," tech. rep., FAO, 1999.

[107] G. Ballard-Tremeer and H. H. Jawurek, "The hood method of measuring emissions of rural cooking devices," *Biomass and Bioenergy*, vol. 16, pp. 341–345, 1999.

[108] H. R. N. Jones, *Radiation Heat Tranfer*. Oxford University Press, 2000.

[109] D. E. Daugaard and R. C. Brown, "Enthalpy for pyrolysis for several types of biomass," *Energy and Fuels*, vol. 17, pp. 934–939, 2003.

[110] S. P. Ketkar, *Numerical Thermal Analysis*. ASME Press, 1999.

[111] G. S. Campbell, C. Calissendorff, and J. H. Williams, "Probe for measuring soil specific heat using a heat-pulse method," *Soil Science of America Journal*, vol. 55, pp. 291–293, 1991.

[112] K. L. Bristow, G. J. Kluitenberg, and R. Horton, "Measurement of soild thermal properties with a dual-probe heat-pulse technique," *Soil Science Society of America Journal*, vol. 58, pp. 1288–1294, 1994.

[113] K. L. Bristow, "Measurement of thermal properties and water content of unsaturated sandy soil using dual-probe heat-pulse probes," *Agriculatural and Forest Meteorology*, pp. 75–78, 1997.

[114] A. J. Fontana, J. Varith, J. Ikediala, J. Reyes, and B. Wacker, "Thermal properties of selected foods using a dual needle heat-pulse sensor," in *ASAE Annual International Meeting*, no. 996063, 1999.

[115] K. L. Bristow, R. D. White, and G. J. Kluitenberg, "Comparison of single and dual probes for measuring soil thermal properties with transient heating," *Australian Journal of Soil Research*, vol. 32, pp. 447–464, 1994.

[116] K. L. Bristow, G. S. Campbell, and K. Calissendorff, "Test of a heat-pulse probe for measuring changes in soil water content," *Soil Science of America Journal*, vol. 57, pp. 930–934, 1993.

[117] T. E. Ochsner, R. Horton, and T. Ren, "Use of the dual-pulse technique to monitor soil water content in the vadose zone," *Vadose Zone Journal*, vol. 2, pp. 572–579, 2003.

[118] D. R. Lide, ed., *CRC Handbook of Chemistry and Physics*. CRC Press, 89th edition ed., 2008.

[119] G. J. Kluitenberg, J. M. Ham, and K. L. Bristow, "Error analysis of the heat pulse method for measuring soil volumetric heat capacity," *Soil Science Society of America Journal*, vol. 57, pp. 1444–1451, 1993.

[120] G. J. Kluitenberg, K. L. Bristow, and B. S. Das, "Error analysis of heat pulse method for measuring soil heat capacity, diffusivity, and conductivity," *Soil Science Society of America Journal*, vol. 59, pp. 719–726, 1995.

[121] N. H. Abu-Hamdeh and R. C. Reeder, "Soil thermal conductivity: Effects of density, moisture, salt concentration, and organic matter," *Soil Science Society of America Journal*, vol. 64, pp. 1285–1290, 2000.

[122] D. R. Lide, ed., *Handbook of Chemistry and Physics*. CRC Press, 90th edition ed., 2009.

[123] D. Drysdale, *An Introduction to Fire Dynamics*. Wiley, 1998.

[124] W. M. Kays and M. E. Crawford, *Convective Heat and Mass Transfer*. McGraw-Hill, 1993.

[125] B. Karlsson and J. G. Quintiere, *Enclosure Fire Dynamics*. CRC Press, 2000.

[126] L. Sorum, M. G. Gronli, and J. E. Hustad, "Pyrolysis characteristics and kinetics of municiple solid wastes," *Fuel*, vol. 80, pp. 1217–1227, 2001.

[127] T. A. Moe, "Wastepaper pellets as a source of fuel for auxiliary home heating," Tech. Rep. 21, University of North Dakota, 1995.

[128] Energy Research Centre of the Netherlands, *Phyllis, database for biomass and waste*. Published online: `http://www.ecn.nl/phyllis` (last accessed 4th March 2010).

[129] W. D. Weatherford, J. Sheppard, and D. M. Sheppard, "Basic studies of the mechanism of ignition of cellulosic materials," in *Tenth Symposium (international) on Combustion*, The Combustion Institute, 1965.

[130] S. Yaman, M. Sahan, H. Haykiri-acma, K. Sesen, and S. Kucukayrak, "Production of fuel briquettes from olive refuse and paper mill waste," *Fuel Processing Technology*, vol. 68, pp. 23–31, 2000.

[131] W. Simpson and A. TenWolde, *The Encyclopedia of Wood*, ch. Physical Properties and Moisture Relations of Wood. Skyhorse Publishing, 2007.

[132] T. A. Moe, "Wastepaper pellets as a source of fuel for auxiliary home heating," tech. rep., University of North Dakota, 1995.

[133] S. S. Alves and J. L. Figueiredo, "A model for the pyrolysis of wet wood," *Chemical Engineering Science*, vol. 44, no. 12, pp. 2861–2869, 1989.

[134] J. Porteiro, J. L. Miguez, E. Granada, and J. C. Moran, "Mathematical modelling of the combustion of a single wood particle," *Fuel Processing Technology*, vol. 87, pp. 169–175, 2006.

[135] A. Williams, M. Pourkashanian, and J. M. Jones, "The combustion of coal and some other solid fuels," *Proceedings of the Combustion Institute*, vol. 28, pp. 2141–2162, 2000.

[136] A. Ouedraogo, J. C. Mulligan, and J. G. Cleland, "A quasi-steady shrinking core analysis of wood combustion," *Combustion and Flame*, vol. 114, pp. 1–12, 1998.

Appendix A

Experimental data

This appendix gives tables of experimental data of the normalised burn rate of briquettes made from newspaper, sawdust, pinewood and rapeseed oil (tables have been arranged to minimise printing, and are not in the order referred to in the text).

Code	ρ $[kgm^{-3}]$	H $[mm]$	Th $[mm]$	W $[mm]$	A/V ratio $[mm^{-1}]$	NBR $[s^{-1}]$
G1	983.3	54.10	2.40	69.72	0.898	0.0095
G2	1003.7	53.60	2.53	104.99	0.847	0.0093
G3	1047.5	52.32	2.53	76.09	0.856	0.0087
G4	975.3	53.89	2.06	100.92	1.030	0.0111
G5	1000.2	53.58	2.03	100.99	1.041	0.0105
G6	1011.9	53.67	2.20	101.33	0.968	0.0110
G7	971.8	53.61	2.26	101.16	0.942	0.0115
G8	1062.1	36.76	4.14	88.77	0.561	0.0061
G10	1082.1	35.63	3.55	101.42	0.640	0.0070
G11	1052.6	35.54	3.75	101.51	0.609	0.0069
G13	1046.8	53.84	3.63	101.16	0.608	0.0064
G14	1081.2	53.60	3.59	101.13	0.614	0.0056
G15	1051.2	53.75	3.80	101.29	0.584	0.0059
G17	1073.4	35.69	6.30	101.19	0.393	0.0033
G18	1105.8	41.45	6.45	101.18	0.378	0.0029
G19	1096.7	53.73	6.34	101.43	0.373	0.0031
G20	1118.2	54.01	6.10	101.46	0.384	0.0030
G21	1100.5	53.93	6.26	100.95	0.377	0.0022

Table A.1: A table giving the raw data for the rapeseed oil briquette slab experiments.

Exp No.	Code	ρ $[kgm^{-3}]$	H $[mm]$	Th $[mm]$	W $[mm]$	A/V ratio $[mm^{-1}]$	NBR $[s^{-1}]$
1	C-1	250.3	33.00	10.30	85.00	0.278	0.0058
	D-1	407.6	33.00	10.30	85.00	0.278	0.0051
	A-2	402.0	34.00	14.20	90.00	0.222	0.0036
	B-2	251.8	33.00	14.20	83.00	0.226	0.0044
	C-2	250.3	33.00	14.20	84.00	0.225	
	D-2	407.6	32.00	14.20	80.10	0.228	0.0037
	E-2	192.6	33.00	14.20	80.00	0.226	0.0056
	A-3	402.0	33.30	19.00	83.00	0.189	0.0028
	B-3	251.8	33.00	19.00	83.00	0.190	0.0046
	C-3	250.3	34.00	19.00	85.00	0.188	0.0032
	D-3	407.6	34.00	19.00	87.00	0.187	0.0027
	E-3	192.6	33.00	19.00	81.00	0.191	0.0042
	A-4	402.0	35.00	25.50	88.00	0.158	0.0011
	B-4	251.8	33.00	25.50	83.00	0.163	0.0022
	C-4	250.3	34.00	25.50	83.00	0.161	0.0020
	D-4	407.6	32.00	25.50	87.00	0.164	0.0015
	E-4	192.6	32.00	25.50	81.50	0.165	0.0029
2	F1	276.1	33.86	25.93	85.08	0.160	0.0020
	F2	276.1	32.87	18.11	85.37	0.195	0.0032
	F3	276.1	33.58	14.26	85.95	0.223	0.0047
	F4	276.1	32.42	10.71	85.84	0.272	0.0068
	G1	184.5	33.94	25.82	76.31	0.163	0.0029
	G2	184.5	33.28	17.62	76.77	0.200	0.0044
	G3	184.5	33.02	14.21	76.73	0.227	0.0054
	G4	184.5	32.83	10.45	76.73	0.278	0.0087
	I1	197.5	33.82	25.98	76.32	0.162	0.0026
	I2	197.5	33.89	17.95	76.77	0.197	0.0047
	I3	197.5	33.68	14.49	76.87	0.223	0.0057
	I4	197.5	33.69	10.48	76.76	0.276	0.0089
3	c1-A	252.1	70.87	10.35	81.13	0.246	0.0060
	c1-D	245.9	70.93	10.35	81.43	0.246	0.0061
	c1-E	251.4	70.67	17.43	81.07	0.168	0.0029
	c1-F	246.5	71.20	17.43	81.43	0.167	0.0029
	C3-G	249.5	55.50	17.50	85.00	0.174	0.0032
	C3-H	250.7	54.80	17.43	84.80	0.175	0.0031
	C3-I	260.1	54.37	17.20	84.70	0.177	0.0030
	C2-J	263.7	42.27	26.43	82.83	0.147	0.0020
	C2-K	263.7	42.07	26.20	82.23	0.148	0.0018
	C2-L	250.0	41.77	26.45	82.57	0.148	0.0020
	C4-M	260.3	41.50	26.78	84.00	0.147	0.0018
	C5-O	284.3	40.53	26.20	87.10	0.149	0.0020
	C5-P	312.4	40.90	26.65	87.23	0.147	0.0019
	C5-Q	358.6	40.60	26.23	87.73	0.148	0.0017
	C6-R	386.7	40.03	26.23	87.43	0.149	0.0015
	C4-S	238.5	61.03	26.68	85.00	0.131	0.0016
	C4-T	244.0	61.87	26.43	83.97	0.132	0.0016
	C7-U	335.3	43.70	14.23	85.40	0.210	0.0039
	C7-V	346.3	43.97	14.25	85.27	0.209	0.0039

Table A.2: Briquette slab data: a table giving the raw data for the paper briquette slab experiments. The results have been divided up into the three independent experimental runs that were completed.

Code	ρ [kgm^{-3}]	H [mm]	Th [mm]	W [mm]	A/V ratio [mm^{-1}]	NBR [s^{-1}]
s1	265.1	53.975	10.13	91.29	0.256	0.0067
s2	280.8	47.935	10.0325	93.62	0.178	0.0029
s3	253.7	33.275	16.5125	90.385	0.203	0.0040
s4	286.8	53.18	15.0325	92.075	0.192	0.0038
s5	280.1	51.47	15.065	92.36	0.193	0.0039
s6	273.5	53.935	10.595	91.83	0.248	0.0060
s7	281.8	50.11	13.86	90.065	0.206	0.0040
s8	266.3	50.55	13.9975	90.425	0.205	0.0041
s9	266.1	49.31	16.9775	89.46	0.181	0.0033

Table A.3: A table giving the raw data for the sawdust experiments. An average density was used in the analysis of 272 kgm^{-3}; the difference in density in these samples will lead to a variation of approximately 7% in the predicted normalised burn rate between the highest and the lowest density sample; this is small compared to the change in rate due to changes in the A/V ratio, and is equivalent to the expected uncertainty in the NBR. It is therefore difficult to use this data to identify trends relating to changes in the density for sawdust.

Code	ρ [kgm^{-3}]	H [mm]	Th [mm]	W [mm]	A/V ratio [mm^{-1}]	NBR [s^{-1}]
P1	436.1	64.16	7.15	113.95	0.328	0.0079
P2	473.4	63.56	2.28	109.61	0.927	0.0205
P3	517.1	63.76	7.87	113.81	0.303	0.0055
P4	474.4	63.37	2.58	110.10	0.825	0.0173
P5	472.6	64.04	7.41	113.89	0.319	0.0067
P6	450.3	63.42	6.15	110.43	0.375	0.0080
P7	458.9	63.30	2.41	114.26	0.879	0.0188
P8	503.8	63.77	3.90	113.98	0.561	0.0110
P9	461.6	63.51	2.48	113.97	0.857	0.0203
P10	452.5	63.55	6.35	114.12	0.364	0.0083
P11	513.6	63.65	3.97	113.95	0.553	0.0108
P12	522.9	63.53	4.13	113.70	0.533	0.0104
P13	456.7	42.04	4.76	114.30	0.485	0.0123
P14	451.8	63.59	6.42	113.89	0.361	0.0082
P15	435.8	41.89	5.16	113.80	0.453	0.0109
P16	460.1	33.42	6.31	113.66	0.395	0.0101
P17	463.8	41.92	4.42	113.81	0.518	0.0114

Table A.4: A table giving the raw data for the pine wood slab experiments.

	code (my ref)	H [mm]	ED [mm]	ID [mm]	ρ [kgm^{-3}]	A/V ratio [mm^{-1}]	NBR/exp(-0.0023*ρ)
1	HB1	18.86	61.94	22.20	341.5	0.213	0.0077
	HB2	40.4	61.74	21.84	344.8	0.139	0.0049
	HB3	47.19	61.07	22.13	350.9	0.127	0.0052
	HB4	61.03	61.15	22.15	326.4	0.113	0.0049
	HB5	67.29	61.50	21.65	333.7	0.107	0.0047
2	H1	18.62	63.40	22.40	348.5	0.208	0.0070
	H2	35.39	63.40	22.40	353.4	0.154	0.0050
	H3	43.59	63.40	22.40	339.8	0.142	0.0054
	H4	29.48	63.40	22.40	344.8	0.166	0.0057
	H5	35.56	63.40	22.40	360.7	0.153	0.0052
	H6	43.62	63.40	22.40	356.0	0.142	0.0049
	H7	13.26	63.40	22.40	350.5	0.255	0.0093
	H8	18.07	63.40	22.40	337.6	0.212	0.0075
	H9	27.49	63.40	22.40	354.1	0.171	0.0061
3	L1	28.925	80.03	22.10	309.5	0.124	0.0035
	L3	30.975	72.16	22.15	305.9	0.134	0.0044
	L4	29.0025	61.81	22.01	349.1	0.165	0.0060
	L5	37.095	42.21	22.13	332.6	0.267	0.0150
	L6	37.1675	42.64	22.48	314.1	0.267	0.0152
4	ch1	31.8575	59.14	22.39	306.8	0.140	0.0061
	ch2	29.7925	59.44	22.19	319.8	0.141	0.0063
	ch3	28.98	68.99	33.12	309.0	0.150	0.0067
	ch4	29.72	70.14	33.26	309.4	0.145	0.0065
	ch5	31.865	79.92	44.29	302.3	0.150	0.0066
	ch6	33.0175	79.40	44.12	315.4	0.148	0.0062
5	D1	39.4525	63.31	21.59	508.4	0.147	0.0057
	D2	38.48	63.07	21.69	516.2	0.149	0.0060
	D3	36.7025	62.40	21.71	400.3	0.153	0.0056
	D4	38.825	62.29	22.00	394.8	0.151	0.0055
	D5	60.11	59.84	21.57	217.0	0.138	0.0063
	D6	61.28	59.70	20.93	211.5	0.136	0.0052

Table A.5: Cylindrical briquette data: details of the holey briquette data plotted in Figure 4.10 is given here.

Appendix B

Char combustion model

This study has yielded the potential basis for a pyrolysis sub-model. For completeness a char combustion model has been included here.

For a block burning in free-air it was observed that char combustion was not significant until towards the end of devolatisation, this has also been noted by other authors (for example [64, 90]. This is because the outward blowing of the volatiles during this process inhibits the diffusion of oxygen to the surface char layer. In a stoked packed-bed fire there will a mixture of new virgin fuel, which has been added to the top of the bed, and fuel which has completely devolatised, now in the form of char. Therefore both devolatisation and char combustion will occur simultaneously and the later cannot be ignored. A good review of char combustion is provided by Winter [90]. In this apprendix a simple model of char combustion based on a model presented by Burham-Slipper [41] is presented. It allows the modelling the burning of the char particles in a packed bed and can be implemented the analytical stove model.

In char combustion oxygen from the bulk stream is transferred by diffusion to the surface of the char layer, where it reacts to form the primary products of CO_2 and CO. The following reaction has been applied by Yang et al. in modelling the combustion of wood-chips in a packed bed [103]:

$$C(s) + \alpha O_2 \longrightarrow 2(1 - \alpha)CO + (2\alpha - 1)CO_2 \qquad \text{(B.1)}$$
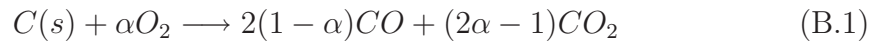
where the ratio of production rate of carbon dioxide depends on the surface temperature of the fuel and is given by the following correlation for natural graphite and coal char at atmospheric conditions in the temperature range 730 to $1170K$ (cited in [103] and [90]):

$$\frac{CO}{CO_2} = 2500 exp(-6420/T_s) \tag{B.2}$$

The mass flux of oxygen to the char surface by diffusion can be written as:

$$(\dot{m})_{O_2} = A_S h_D (\rho_{O_2\infty} - \rho O_{2S}) \tag{B.3}$$

where A_S is the surface area of the fuel, h_D is the mass transfer coefficient and $\rho_{O_2\infty}$ and ρO_{2S} is the density of O_2 in the bulk flow and at the surface respectively. At the surface of the char layer the reaction rate can be assumed to be a function of the concentration of the oxidiser [136], that is the rate at which oxygen is diffused to the surface. This reaction is assumed to be first order and the rate of oxygen consumption at the surface can be written as:

$$(\dot{m})_{O_2} = \phi \rho_{O_2 S} \tag{B.4}$$

where ϕ is the rate of the chemical reaction. Combining equations B.3 and B.4 the concentration of oxygen at the surface can be eliminated [41]:

$$(\dot{m}) = \frac{\phi A_S h_D}{\phi + A_S h_D} \rho_{O_2\infty} \tag{B.5}$$

If it is assumed that the kinetic rate is significantly greater than the diffusion rate, so that the reaction is diffusion controlled, then $\phi >> A_S h_D$ [41, 136] and therefore B.5 can be written as:

$$(\dot{m}) = A_S h_D \rho_{O_2\infty} \tag{B.6}$$

The mass transfer coefficient, h_D, for flow through a packed bed is given by Cussler and applied by Burham-Slipper in a combustion model used in a rocket stove [41]:

$$\frac{h_D}{v_0} = 1.17(\frac{dv_0}{v})^{-0.42}(\frac{D}{v})^{0.66} \tag{B.7}$$

As noted by Burham-Slipper [41], from equation B.7, the mass transfer coefficient is approximately proportional to the superficial velocity. This is also in agreement with other expressions given in the literature, where the mass transfer coefficient is suggested to be approximately proportional to $Re^{0.5}$ (see [90]). For example, Ragland gives the mass transfer coefficient as:

$$h_D = \frac{D(2 + 0.6Re^{(1/2)}Sc^{(1/3)})}{d} \tag{B.8}$$

Equation B.6 can therefore be approximately written in the form [41]:

$$(\dot{m}) = -A_S \xi v_0^{0.5} \rho_{O_2 \infty} \tag{B.9}$$

where ξ is a constant of proportionality. A negative sign has been introduced to indicate that the oxygen is being removed from the bulk flow of gas. The rate of char consumption by char combustion can therefore be found by considering the mass of carbon consumed per kg of oxygen:

$$(\dot{x})_C = -\frac{12}{32 \times \alpha} A_S \xi v_0^{0.5} \rho_{O_2 \infty} \tag{B.10}$$

and thus the heat released by char combustion is given by

$$(\dot{q})_{char} = H_{char} \frac{12}{32 \times \alpha} A_S \xi v_0^{0.5} \rho_{O_2 \infty} \tag{B.11}$$

Appendix C

Simple stove radiation model

It was stated in the conclusions that the pyrolysis model could be used in combination with a char combustion model (see Appendix B). For completeness, a simple model of heat transfer in a rocket cookstove is presented here, which could be used for initial simulations. It is based on work completed by Burham-Slipper [75].

C.1 Analytical model of the heat transfer

The analytical model of a stove makes the following simplifying assumptions:

- The gases in the combustion chamber of the rocket stove were well mixed, and can be considered to have a constant (average) temperature[75].

- Air flows into the stove by buoyancy driven flow [75], and the resistance to flow for the bed can be considered constant throughout the devolatisation. The resistance to flow is a result of a pressure drop at the inlet and outlet and due to the flow resistance caused by the briquette fuel in the stove.

- The mixture of gases in the combustion chamber, behave as an ideal gas and maintained the properties of air [75].

- the fire is stoked such that fuel is added at regular intervals to balance the mass of fuel which has burnt;

- once ignited the fire the fire burns at a quasi-steady state rate, as has been observed in experiment;

- after an equilibrium has been reached the proportion of virgin fuel to char remains approximately constant

- ash is is continually removed from the stove, resulting in an roughly constant resistance to air flow through the stove.

The velocity of the hot gases in the combustion region were calculated based on the equation for chimney draft, assuming, as stated above, that the gases behave as an ideal gas:

$$u = \sqrt{\frac{2gh}{Res}(\frac{T_g}{T_{at}} - 1)} \tag{C.1}$$

where u is the gas velocity, Res is the resistance to flow and the other symbols have their means as defined earlier.

C.1.1   The heat fluxes in the stove

It is assumed that the hot gas within the stove and surrounding the fuel elements is well mixed. The emissivity of the flame is assumed to take a constant value equal to 0.54, as was found for a flame in chapter. The six main heat fluxes were thus given as [75]:

Convection to the pot:
$$Q_{c-p} = h_p A_p (Tf - Tp) \tag{C.2}$$

where the Nussult number was assumed to be according to the expression for jet impinging heat transfer to a flate plate from a nozzle, as suggested by Burham-Slipper[41], which was developed to evaluate the convective heat transfer to a cooking plate in a rocket stove, and is being considered in this study:

$$Nu_p = 2.60 Re_p^{0.40}(z/d)^{-0.22})(R/d)^{-0.1} \tag{C.3}$$

Radiation to the pot:
$$Q_{r-p} = E_f V F_p A_p \sigma (T_f^4 - T_p^4) \tag{C.4}$$

Radiation to the stove walls:

$$Q_{r-w} = E_f V F_w A_w \sigma (T_f^4 - T_w^4) \tag{C.5}$$

Convective heat transfer at the stove walls:

$$Q_{c-w} = h_w(T_f - T_w);$$ (C.6)

where the Nusselt number is given by Drysdale [123]:

$$Nu_w = 0.66 * (Re^{0.5})$$ (C.7)

Radiation from the combustion gases to the ground:

$$Q_{r-gr} = E_f A_c \sigma(T_g^4 - T_f^4)$$ (C.8)

Radiation from the combustion gases to the atmosphere:

$$Q_{r-at} = V F_{at} E_f A_c \sigma(T_{gr}^4 - T_f^4)$$ (C.9)

The advection heat loss, when cold air entering the bottom of the stove replaces hot air leaving the top.

$$Q_{advec} = \rho A_c u_c c_p(T_f - T_{at})$$ (C.10)

The temperature of the combustion gas can be found by considering the energy balance within the stove:

$$mc_p\frac{dT}{dt} = Q_{combust} - (Q_{advec} + Q_{c-p} + Q_{r-p} + Q_{r-w} + Q_{c-w} + Q_{r-gr} + Q_{r-at} + Q_{advec})$$
(C.11)

Appendix D

Additional notes on volatile gases in the pore structure

The porosity of char can be estimated by the equation [84]:

$$\phi_{char} = (1 - \frac{\rho_{char}}{\rho_{carbon}}) \times 100\% \qquad \text{(D.1)}$$

If the mean density of carbon $\phi = 0$ is 1957 kgm^{-3} [84] and the porous density of wood char is approximately 120 kgm^{-3} then the porosity of char by equation D.1 is estimated to be about 94%. This gives suggests some validity to to assumption that on the volatile gases pass out though the char layer with little resistance to flow, being dispersed rapidly on formation [64]. However, this large porosity could mean that presence of pyrolysis gases within this porous char structure, with different thermal properties to air, could have an affect on both the thermal conductivity and the volumetric heat capacity of the char layer. In order to estimate the effect of the presence of gases, Kanury et al.[84]applied a very simple model in which the pyrolysis gases were assumed to have a very low-velocity through the porous char, such that the char material could be considered a composite of the solid char filled with a fluid. The gases were assumed equivalent to carbon dioxide in their thermal properties, and the resulting thermal conductivity calculated was found to be in excellent agreement with experiment, and it demonstrated that the contribution due to the gases is negligibly small. For this reason their effect on the thermal conductivity and heat capacity of the char layer were neglected in this work.

Burn fuel briquette
burn away
through the night
and through the day
cook and burn
until the people say,
O, that was a scrumptious steak
burn with a flame
that lights the room
burn with delight
and with voom
burn until the people say
no charcoal, no wood
needed here today
(A briquette poem, by the Author)